UNIVERSITÉ DE MONTRÉAL

INFLUENCE OF HIGHER MODES OF VIBRATION ON THE BEHAVIOUR OF REINFORCED CONCRETE SHEAR WALLS STRUCTURES

NIKOLAY NIKOLOV VELEV

DÉPARTEMENT DES GÉNIES CIVIL, GÉOLOGIQUE ET DES MINES
ÉCOLE POYTECHNIQUE DE MONTRÉAL

MÉMOIRE PRÉSENTÉ EN VUE DE L'OBTENTION
DU DIPLÔME DE MAÎTRISE ÈS SCIENCES APPLIQUÉES
(GÉNIE CIVIL)
MARS 2007

Your file Votre référence
ISBN: 978-0-494-29259-4
Our file Notre référence
ISBN: 978-0-494-29259-4

UNIVERSITÉ DE MONTRÉAL

ÉCOLE POLYTECHNIQUE DE MONTRÉAL

Ce mémoire intitulé:

INFLUENCE OF HIGHER MODES OF VIBRATION ON THE BEHAVIOUR OF REINFORCED CONCRETE SHEAR WALLS STRUCTURES

présenté par: VELEV Nikolay Nikolov

en vue de l'obtention du diplôme de: Maîtrise ès sciences appliquées

a été dûment accepté par le jury d'examen constitué de:

Mme KOBOEVIC Sanda, Ph.D., présidente

M. TREMBLAY Robert, Ph.D., membre et directeur de recherche

M. MASSICOTTE Bruno, Ph.D., membre et codirecteur de recherche

M. LÉGER Pierre, Ph.D. membre

ACKNOWLEDGEMENTS

I would like to express my profound gratitude and deepest indebtedness to my research director Professor ROBERT TREMBLAY for his valuable advises, constructive suggestions, tireless guidance, and enduring patience throughout this study. He has been a limitless source of guidance, patience, and inspiration during the course of this research. It has been a great honour for me to work with a researcher of his calibre, and this will remain as an unforgettable experience in my memory.

I would like to express my deepest gratitude to Professor BRUNO MASSICOTTE, co-director, for his sharp suggestions, valuable guidance and kindness through out this research work. Infinite thanks and deepest feelings of gratitude for his assistance and good advices.

I want to thank also all professors at Research Group in Structural Engineering at Ecole Polytechnique of Montreal for the many useful discussions I have had with them, for always offering help and advice during the course of my studies.

I would like to thank my wife and my son for their infinite patience, and for their continuing love and support. I realise that you went through a lot just for me, I love you so much as well.

At last but not least I want to thank my parents for teaching me the most beautiful things in life, for always believing, and for all unconditional support. Thanks for always be there.

Just a final word to my father: I know you would have been very proud.

RESUMÉ

Une étude paramétrique a été réalisée pour étudier le comportement sismique inélastique des murs de refend en béton armé conçus selon le Code National du Bâtiment du Canada 2005 (CNBC 2005) et la norme CSA-A23.3-04. Les murs étudiés font partie de bâtiments de 5, 10, 15, 20, et 25 étages situés à l'Est (Montréal, QC) et à l'Ouest (Vancouver, BC) du Canada. Les murs des bâtiments situés à Montréal ont ét conçus comme des murs avec ductilité modérée, avec un facteur de modification des forces sismiques R_d = 2.0, alors que les murs situés à Vancouver étaient des murs ductiles, avec un facteur R_d = 3.5.

Le comportement sismique de ces murs a été étudié au moyen d'analyses non-linéaires temporelles réalisées avec le logiciel Ruaumoko pour des ensembles de séismes historiques et artificiels représentatifs pour chacun des sites considérés. Une étude comparative des différents modèles utilisés pour représenter le comportement inélastique cyclique des murs de refend a été réalisée. Deux types d'éléments ont été examinés: le modèle «Bar», faits d'éléments poteau-poutre avec rotules plastiques concentrées aux extrémités, et le modèle «Mur» permettant une représentation de la section par des fibres représentant le comportement cyclique inélastique des matériaux.

Les résultats obtenus avec les deux éléments montrent que les déplacements inter-étages rencontrent la limite spécifiée dans le CNBC 2005 pour tous les bâtiments. Les efforts tranchants déterminés des analyses dépassent largement ceux correspondant au développement des rotules plastiques à la base des murs. Des équations sont proposées pour un coefficient d'amplification permettant d'obtenir les efforts tranchants prédits par les analyses à partir de ceux obtenus de la méthode dynamique spectrale du CNBC 2005.

Un modèle à l'échelle réduite d'un spécimen a été proposé, conçu et vérifié pour la réalisation d'essais dynamiques sur le simulateur sismique de Laboratoire de Structures de l'École Polytechnique de Montréal. Une nouvelle loi de similitude, appelée similitude d'accélération modifiée, a été développée pour l'étude des murs de refend en béton armé.

ABSTRACT

A parametric analytical study was carried out to examine the inelastic seismic response of reinforced concrete shear walls designed according to the provisions of the 2005 National Building Code of Canada (NBCC) and the CSA-A23.3-04 Standard. The studied walls were assumed to be part of 5-, 10-, 15-, 20-, and 25-storey office buildings located in Montreal, QC, and Vancouver, BC. Moderately ductile shear walls qualifying for a ductility-related force modification factor, R_d, of 2.0 were considered for the Montreal site whereas the walls in Vancouver were of the Ductile shear wall category ($R_d = 3.5$).

Nonlinear time history analyses of the walls were performed under site-specific ground motion ensembles using the Ruaumoko computer program. Two different wall models were used: frame elements with concentrated plastic hinges at their ends and wall elements with fiber discretization of the cross-section.

For both models, the results indicate that the deformation demand of all walls remain below the limits specified in the 2005 NBCC for buildings of the normal importance category. The shear force demand in all structures was found to exceed the values predicted by the capacity design procedures implemented in the CSA-A23.3 Standard. Correction factors are proposed to adequately predict the maximum shear forces in walls for both sites.

A reduced-scale model specimen to study the inelastic seismic response of shear walls by shaking table test in Structural Laboratory at Ecole Polytechnique of Montreal was proposed, designed and verified, as well a modified scaling similitude procedure.

CONDENSÉ EN FRANÇAIS

Les études récentes qui ont été publiées partout dans le monde sur l'impact des séismes sur la vie sociale et économique des gens ont résulté en une augmentation de la prise de conscience des populations, des institutions et des gouvernements pour ce type de catastrophe.

Les recherches récentes ont aussi démontré que les murs de refend en béton armé sont très efficaces pour résister adéquatement aux séismes. Les murs de refend absorbent les secousses sismiques importantes en fléchissant dans le domaine plastique à leur base, permettant ainsi de dissiper une grande quantité d'énergie en limitant les forces dans la structure. Ils se caractérisent aussi par la possibilité d'une rupture en cisaillement plutôt fragile. Lors de la conception, on doit donc s'assurer que le mur pourra résister aux efforts de cisaillement maximum anticipés. Les dernières études ont démontré que les méthodes de superposition multimodales et la "conception par capacité" sont non-conservatrices pour prédire la distribution des efforts sur la hauteur du mur. De plus, même avec l'introduction du coefficient d'amplification dynamique M_v dans le nouveau code du bâtiment du Canada (CNBC) 2005, la prise en compte de l'amplification dynamique des efforts est insuffisante. Les modes supérieurs de vibration peuvent provoquer des efforts de cisaillements très élevés dans les murs élancés.

Dans les zones de forte sismicité, on adopte de plus en plus des systèmes structuraux dans lesquels les charges sismiques sont reprises par des murs de refend et où les charges de gravité sont supportées par des colonnes, poutres et dalles. Récemment, on porte plus d'attention lors de la conception parasismique sur les limites de déformation inter-étages et le contrôle des déplacements. Étant donné que les murs de refend possèdent une rigidité supérieure à celle de la plupart des autres systèmes structuraux, ils permettent un meilleur contrôle des déplacements et une réduction des dommages aux autres éléments constructifs et non-structuraux.

Les codes modernes de conception prescrivent les détails de construction et les règles d'application visant à contrôler les réponses inélastiques des éléments résistants aux forces sismiques. Ces principes et règles sont développés et améliorés grâce aux nombreuses études numériques et expérimentales réalisées dans le cadre de projets de recherche visant à mieux comprendre le comportement sismique inélastique des structures.

L'objectif principal de ce projet de recherche était d'étudier le comportement des bâtiments multi-étagés contreventés par des murs de refend élancés en béton armé. L'intérêt particulier était d'examiner l'effet des modes supérieurs de vibration sur la distribution verticale des efforts dus au séisme et de proposer un facteur d'amplification dynamique qui s'appliquera à l'effort tranchant dans les murs de refend qui est obtenu de la méthode dynamique spectrale du CNBC 2005.

Le deuxième objectif consistait à développer un modèle à échelle réduite pour la réalisation d'essais sur murs de refends sur le simulateur sismique à l'École Polytechnique de Montréal. Ces tests permettront de valider des différents aspects du comportement sismique des murs de refend incluant les effets des modes supérieurs, la distribution verticale des forces sismiques, la longueur de la zone critique et le développement et les locations des rotules plastiques.

La méthodologie utilisée comprend tout d'abord une revue des codes de conception modernes dont le CNBC 2005, NZ3101, EC8 et UBC97, de même qu'une revue des publications et recherches scientifiques sur l'influence des modes supérieurs de vibration sur le comportement des murs de refend et sur les essais réalisés sur les murs de refend.

La deuxième étape comprend la conception selon le CNBC 2005 et la norme CSA-A23.3-04 des murs de refend pour des bâtiments de 5, 10, 15, 20, et 25 étages situés

dans l'Est (Montréal) et l'Ouest (Vancouver) du Canada. Le comportement sismique de ces murs a été étudiée par des analyses non-linéaires temporelles réalisées avec le logiciel Ruaumoko sous des ensembles de séismes historiques et artificiels représentatifs pour chacun des sites considérés. Une étude comparative des différents modèles représentatifs du comportement des murs de refend a d'abord été réalisée. À partir des résultats des analyses, on a ensuite calculé et proposé un facteur d'amplification dynamique pour l'effort tranchant.

On a vérifié la faisabilité des essais sur simulateur sismique sur modèle à échelle réduite pour un mur de refend similaire à l'un des murs étudiés dans la première partie du projet. Le modèle proposé fera environ 9 m de hauteur et reproduira un bâtiment de 10 étages contreventé avec des murs de refend ductiles. Les lois de similitude applicables à ce type d'essais sont prises en compte dans le dimensionnement du modèle.

Dans toutes les normes de conception qui ont été examinées, on fait l'hypothèse que sous un fort séisme, les murs vont dissiper l'énergie induite sous forme de rotation inélastique dans des rotules plastique qui se formeront uniquement à leur base et que le reste du mur demeurera élastique. Pour s'assurer que la rotule plastique se forme à la base du mur, et pour protéger le mur contre une rupture fragile en cisaillement, toutes les normes examinées ont adopté la philosophie de «conception par capacité». On distingue trois classes de mur, selon le comportement inélastique qui est visé: les murs ordinaires, les murs avec ductilité modérée et les murs ductiles. Les charges de conception de chaque classe de mur telles que prescrites dans le CNBC 2005 se comparent très bien avec celles spécifiées dans les autres normes. Le CNBC 2005 prescrit les charges les plus faibles pour les murs ordinaires. Par contre, pour les murs de ductilité modérée, les charges calculées avec le CNBC 2005 sont les plus élevées. Les murs ductiles au Canada sont conçus pour des charges intermédiaires entre celles requises par les codes de Nouvelle-Zélande et l'Eurocode EC8.

Tous les codes, y compris le CNBC 2005, recommandent l'utilisation de la méthode dynamique spectrale pour le calcul des forces sismiques et rendent cette méthode obligatoire pour des bâtiments irréguliers à l'exception des bâtiments de faible hauteur situés dans des régions de faible sismicité. Quand la méthode statique équivalente est utilisée, les forces sismiques calculées avec CNBC 2005 sont d'abord amplifiées pour tenir compte des effets dynamiques des modes supérieurs de vibration, puis modifiés à nouveau pour obtenir le diagramme des moments. L'enveloppe des moments de conception est obtenue en réduisant les moments de flexion dans la moitié inférieure des murs avec le facteur de réduction J. Ce facteur dépend du premier mode de vibration du bâtiment et de la pente du spectre d'accélération au site. Par la suite, les efforts de cisaillement sont calculés en respectant la procédure du calcul par capacité. On utilise une autre approche dans l'EC8 et le code de la Nouvelle Zélande. Les moments de conception sont calculés avec des forces non-amplifiées. Les forces de cisaillement de conception sont ensuite obtenues en appliquant la méthode de conception par capacité avec un facteur d'amplification dynamique, ce dernier tenant compte des effets des modes supérieurs.

Le chapitre 3 décrit la procédure de conception des 10 murs de refends qui ont été considérés dans l'étude. Ces murs ont été conçus avec le CNBC 2005 et la norme CSA-A23.3-04. Cet échantillon de bâtiments représente les types des bâtiments les plus courants dans les zones de haute sismicité au Canada. Tel que recommandé dans le CNBC 2005, on a utilisé la méthode dynamique spectrale pour déterminer les efforts dans les murs de refend. La méthode des forces statiques équivalentes été également appliquée pour des fins de comparaison et pour étalonner les force sismiques de l'analyse spectrale. La quantité et les détails d'armature des murs ont été déterminés à partir des exigences de la norme A23.3-04.

La section des murs de refends a été déterminée pour obtenir une période fondamentale de vibration qui soit un multiple de la période obtenue de l'équation empirique du CNBC 2005 : 2.0 fois pour les bâtiments situés à Vancouver et 2.5 fois pour les structures localisées à Montréal. On a ensuite effectué une conception préliminaire des structures afin de déterminer lequel des deux types de murs de refend, murs ductiles ou murs à ductilité modérée, était le plus approprié à chacun des deux sites. Le facteur de modification de la force sismique lié à la ductilité, R_d, est égal à 3.5 pour le premier système et à 2.0 pour le second. De cette conception préliminaire, on a tiré les conclusions suivantes :

- Pour les bâtiments situés à Montréal et conçus comme des murs ductiles, le choix de l'armature longitudinale était gouverné par l'exigence d'armature minimale. Cette exigence, combinée à l'application de la conception par capacité, a résulté en une augmentation significative de l'armature en cisaillement, donc à une utilisation non efficiente des matériaux et surtout de l'armature.

- Pour les bâtiments situés à Vancouver, la conclusion inverse a pu être tirée. On a observé que les murs conçus avec un facteur de modification des forces $R_d = 2.0$, les sections des murs étaient de dimensions insuffisantes pour obtenir une résistance en cisaillement dépassant les efforts de conception, ce qui exigerait une augmentation des sections en béton.

Basé sur ces conclusions, on a procédé au choix final des catégories de ductilité pour les murs de l'étude : murs ductiles ($R_d = 3.5$) pour Vancouver et murs avec ductilité modérée ($R_d = 2.0$) pour Montréal.

Lors de la conception finales des murs, on a observé les points suivants dans l'application des dispositions du CNBC 2005 et de la norme A23.3-04:

• Un changement important apporté dans la nouvelle version de la norme CSA-A23.3-04 est la vérification de la ductilité des murs qui se fait au niveau de la rotation plastique du mur à sa base. La capacité inélastique en rotation est calculée en fonction du déplacement anticipé du sommet du bâtiment et des propriétés géométriques du mur. Dans ce calcul, on suppose implicitement un profil des déformations qui est similaire à celui du premier mode de vibration et on admet que la hauteur de la rotule plastique est égale à la moitié de la longueur du mur. Cette méthode donne une estimation conservatrice de la rotation inélastique.

• Pour tous les bâtiments étudiés, la capacité en rotation plastique dépassait la rotation inélastique prévue sauf pour le bâtiment de 5-étages à Vancouver. Pour rencontrer cette exigence, les dimensions du mur ont été changées et la période fondamental T_1 est passée de 2.0 T_a à 1.7 T_a. On a noté que la rotation inélastique anticipée a tendance à diminuer avec la hauteur des murs pour les bâtiments situés à Vancouver. Pour tous les bâtiments, la capacité en rotation inélastique diminue avec l'augmentation de la hauteur des murs. Pour les plus hauts bâtiments, elle est presque 3 fois plus grande que la rotation prévue. Pour les murs à Montréal conçus avec R_d= 2.0 la rotation anticipée correspond à la valeur minimale qui est spécifiée dans la norme A23.3-04.

• L'effort tranchant à la base des murs calculé avec la méthode spectrale multimodale était supérieur à 80% de l'effort calculé avec la méthode statique équivalente pour tous les bâtiments sauf ceux de 20 et 25 étages situés à Montréal pour lesquel la force minimale de conception requise par le CNBC 2005 contrôlait. En plus, pour les bâtiments possédant des périodes plus longues à Vancouver (20 et 25 étages), la force sismique dynamique V_d est même plus grande que 100% de la force statique V.

• Un autre changement important dans la norme A23.3-04 est la hauteur de la zone crique pour les murs ductiles (1.5 la longueur du mur) et le calcul des efforts au-dessus de la zone critique. Au-dessus de la zone critique, les efforts de conception doivent être multipliés par un coefficient égal au rapport entre la résistance

pondérée en flexion et le moment pondéré de l'analyse spectrale au sommet de la zone critique. Cette exigence donne une valeur de moment de conception juste au-dessus de la zone critique qui est similaire à la résistance au sommet de la zone critique. Comme l'effort axial dans le mur au-dessus de la zone critique est plus faible, on doit augmenter l'armature de flexion au-dessus de la zone critique. Cette exigence n'a aucune justification pratique et on a maintenu la même quantité d'armature en dessous et au dessus de la limite supérieure de la zone critique.

Au chapitre 4, on présente les résultats des analyses temporelles non linéaires obtenus avec le logiciel Ruaumoko. Deux types d'éléments ont été utilisés pour la modélisation des murs: le modèle « Bar » et le modèle «Mur». Le premier modèle, plus simple et utilisé abondamment dans les études passées, reproduit le comportement flexionnel du mur par des éléments poteau-poutre à chaque niveau avec rotules plastiques concentrées à chacune des deux extrémités. Le deuxième modèle est un modèle multi-fibres qui permet de représenter la section du mur par plusieurs fibres représentant les barres d'armature et la section de béton. Dans cet élément, le comportement mécanique des deux matériaux, le béton et l'armature, sont caractérisés par leurs diagrammes de contrainte-déformation, ce qui permet de reproduire plus précisément le comportement flexionnel de la section. Une étude approfondie des paramètres caractérisant cet élément a été réalisée et valeurs spécifiques de ces paramètres ont été proposées. La validation des résultats a été effectuée en comparant le comportement de cet élément avec les résultats d'un essai réalisé par Adebar et Ibrahim (2000) sur un mur ductile.

Les déplacements horizontaux des structures, les efforts tranchants et les niveaux de ductilité à la base des murs obtenus avec les deux éléments ont été comparés. On a constaté que les deux éléments ont donné des résultats très similaires. Suite à ces comparaisons, toutes les informations sur le comportement sismique inélastique des

murs ont été basées sur les résultats obtenus avec le modèle «Mur» et les conclusions suivantes ont pu être tirées :

- Les déplacements inter-étage maximum rencontrent la limite de 2.5% h_s (h_s = hauteur de l'étage) spécifiée dans le CNBC 2005. Les déplacements inter-étage maximum sont plus grands pour les bâtiments moins élevés comparés à ceux observés pour les bâtiments plus hauts. Les rapports du déplacement inter-étage maximal à la limite de 2.5% h_s sont de de trois à quatre fois plus grands pour les bâtiments situés à Vancouver que pour ceux localisés à Montréal. Les déplacements maximum des murs de Vancouver sont proches des déplacements élastiques calculés avec la Méthode Dynamique Spectrale du CNBC 2005. Pour les bâtiments siutés à Montréal, les déplacements sont entre 50% et 88% des valeurs prédites par l'analyse.
- Les niveaux maximum de ductilité à la base des murs sont plus faibles que ceux calculés en suivant la méthode prescrite dans la norme CSA-A23.3. Pour les bâtiments de 5, 10 et 15 étages à Vancouver, les valeurs sont entre 60% et 70% de celles calculées avec la norme. Pour les bâtiments élevés, ce rapport diminue à environ 10%. Pour les murs de faible hauteur à Montréal, les niveaux de ductilité sont de 10% à 30% ceux prédits par la norme. Ils sont près de zéro pour les murs plus élevés. Ces résultats montrent que les calculs de la rotation inélastique dans la norme CSA-A23.3-04 donnent une estimation très conservatrice, surtout pour les bâtiments conçus avec $R_d = 2.0$ situés à Montréal. Dans tous les cas, la ductilité est cependant concentrée à la base des murs, comme prévu dans la norme. Pour les deux sites, les bâtiments de 5-étages ont des niveaux de ductilité plus élevés comparés aux autres bâtiments et ces niveaux diminuent avec l'augmentation de la hauteur du mur. Les résultats ont permis une autre trouvaille intéressante : tous les bâtiments à Montréal et les deux structures les plus élevées à Vancouver demeurent pratiquement élastiques sous les séismes de conception et ne subissent le niveau de plastification anticipé par le CNBC 2005 et la norme A23.3-04.

• Pour les bâtiments localisés à Vancouver, les moments maximum à la base des murs obtenus des analyses non linéaires sont proches de la capacité probable des sections. Dans certains cas, ils excèdent cette valeur. Pour les murs situés à Montréal, les moments obtenus sont plus faibles que la capacité nominale des murs calculée selon la norme A23.3, sauf pour le bâtiment de 5 étages.

• Les efforts tranchants déterminés dans les analyses temporelles dépassent largement ceux qui correspondent au développement des rotules plastique à la base des murs. Pour Vancouver, le rapport de l'effort tranchant inélastique à l'effort tranchant de conception à la base des murs augmente avec l'augmentation de la hauteur des murs. Ce rapport varie de 1.61 à 2.08. La tendance inverse est remarquée à Montréal où le rapport varie de 1.37 pour le bâtiment de 5 étages à 1.1 pour le bâtiment le plus haut. Pour chacun des deux sites, deux équations ont été proposés pour un coefficient d'amplification dynamique, γ_V, à appliquer aux efforts tranchants déterminés de la méthode dynamique spectrale du CNBC 2005 pour obtenir les valeurs observées dans les analyses. Dans une équation, on propose une variation linéaire du coefficient d'amplification avec le nombre d'étage, n, alors qu'une variation du deuxième ordre est suggérée dans la seconde. Pour des murs ductiles situés à Vancouver:

$$\gamma_V = 1.5 + n/40 \qquad \textit{Éq.1}$$

$$\gamma_V = 1.5 + n/50 + (n/50)^2 \qquad \textit{Éq.2}$$

Pour des murs avec ductilité modérée situés à Montréal:

$$\gamma_V = 1.4 - n/100 \qquad \textit{Éq.3}$$

$$\gamma_V = 1.4 - n/140 - (n/140)^2 \qquad \textit{Éq.4}$$

• L'influence du confinement du béton dans les zones comprimées des murs sur le comportement des murs a également été étudiée. Différents modèles de confinement du béton ont été comparés pour les murs des bâtiments à 5, 10 et 15 étages et un modèle représentantif de l,ensemble de ces modèles a été retenu. Les

résultats obtenus avec le modèle de béton confiné retenu ont été comparés avec ceux obtenus avec le modèle de béton non confiné. Les déplacements inter-étages calculés avec le béton confiné sont légèrement supérieurs, moins de 10% d'augmentation, mais demeurent inférieurs à la limite du CNBC. Les différences dans les moments de flexion sont plus petites, environ 2 à 3%, ce qui est logique car l'amplitude des moments dépend plus des caractéristiques de l'armature flexionnelle que des propriétés du béton. L'augmentation des efforts tranchants est similaire à celle observée pour les moments. En général, on peut donc conclure que la prise en compte du confinement du béton a très peu d'influence sur le comportement sismique global des murs de refend et peu être négligée.

On présente au chapitre 5 la théorie de la modélisation de même que les différentes approches concernant les essais sur des modèles réduits. On a aussi fait revue des lois de similitude utilisées pour les tests en génie civil et des points importants relativement à la modélisation du béton et des barres d'armature ont été soulevés.

Un programme a été proposé pour la réalisation de tests dynamiques sur le simulateur sismique du Laboratoire de Structures de l'École Polytechnique de Montréal. Un spécimen d'un mur de refend correspondant d'une structure réaliste a été conçu en tenant compte des contraintes géométriques, de la capacité des équipements et de la constructibilité du spécimen. Les deux lois de similitude les plus utilisées dans le génie civil, celle de similitude de la vitesse et celle de similitude d'accélération, ont été examinées pour en identifier les points positifs et les inconvenants. Malheureusement, aucune de ces deux méthodes ne permettait la réalisation de ce programme d'essais et une nouvelle loi de similitude, appelée similitude d'accélération modifiée, a été développée pour surmonter cet inconvenant et permettre des essais sur des murs de refend en béton armé représentatifs de la réalité. Cette méthode fait appel à deux facteurs d'échelle, l'un pour l'étalonnage de la géométrie et l'autre pour l'amplification de l'accélération,

Pour valider la loi proposée, les comportements sismiques inélastiques du mur réel (Prototype) et du modèle réduit correspondant (Modèle) ont été étudiés avec le logiciel Ruaumoko et comparés. Des valeurs pratiquement identiques ont été obtenues pour les paramètres du comportement global du Prototype et du Modèle, incluant les valeurs de pointe des déplacements, des moments de flexion et des efforts tranchants. La différence maximum observée entre les deux structures était de 0.6%. La réponse dans le temps pour les deux structures ont été également comparées et la différence maximum calculé était du même ordre, 0.6%, ce qui est pratiquement négligeable.

Le deuxième volet de validation a consisté à vérifier que la capacité du simulateur sismique n'était pas excédée: la capacité en service du vérin, résistance vertical des appuis du simulateur, et accélération maximale appliquée. Tous ces paramètres ont ét vérifiés, ce qui a permis de confirmer la faisabilité du modèle de mur proposé. Les résultats des analyses ont aussi permis de faire trois conclusions générales :

- Malgré que le modèle proposé ne prends pas totalement en compte les effets des charges de gravité (effets P-delta), la loi de similitude d'accélération modifiée donne des réponses réalistes et pratiquement identiques pour des systèmes qui ne sont pas très sensibles aux effets de deuxième ordre, comme c'est le cas des murs de refend étudiés.
- Le spécimen proposé et le programme de tests sont réalisables. Les forces et accélérations induites dans le système n'excèdent pas la capacité du simulateur sismique.
- En employant deux facteurs d'étalonnage, l'un pour la géométrie et l'autre pour l'accélération, la loi de similitude d'accélération modifiée permet plus de flexibilité et donne un choix plus vaste pour les essais à échelle réduite de grands spécimens de mur de refend, tout en permettant de rencontrer les limites géométriques et de capacité des équipements.

À la fin de cette mémoire, on propose trois recommandations pour de futures études. Sur la base des résultats obtenus dans ce projet, les normes en vigueur devraient être modifiées pour correctement représenter l'amplification de l'effort tranchant dans les murs de refend en béton armé due aux modes supérieurs de vibration. En deuxième lieu, il est important d'élargir cette étude pour inclure un plus grand éventail des murs de refend. En effet, les constats présentés dans le présent document doivent être validés en étudiant un plus grand spectre de bâtiments ayant des périodes différentes et conçus avec différents facteurs de modification des forces sismiques pour les deux sites étudiés. Des analyses supplémentaires avec des logiciels des éléments finis devraient aussi être réalisées pour confirmer l'amplification dynamique des efforts tranchants trouvée dans cette étude. Finalement, des tests sur simulateur sismique devraient être exécutées pour valider les résultats de cette étude analytique, en particulier en ce qui a trait à l'amortissement, aux effets des modes supérieurs, la fissuration du béton et à l'effort tranchant inélastique.

TABLE OF CONTENTS

ACKNOWLEDGMENTS iv

RESUMÉ v

ABSTRACT vii

CONDENSÉ EN FRANÇAIS viii

TABLE OF CONTENTS xx

LIST OF TABLES xxiii

LIST OF FIGURES xxvi

LIST OF NOTATIONS AND ABBREVIATIONS xxxiv

LIST OF APPENDICES xl

CHAPTER 1 INTRODUCTION 1

1.1 Studied problem 1

1.2 Objectives 2

1.3 Methodology 3

1.4 Organization of the thesis 4

CHAPTER 2 DESIGN CODES AND LITERATURE REVIEW 6

2.1 Introduction 6

2-2 Design codes 7

2.2.1 Seismic design approach in Canada - NBCC 2005, CSA A23.3-04 7

2.2.2 Seismic design approach in Europe - EUROCODE 8 17

2.2.3 Seismic design approach in USA – UBC and NEHRP 23

2.2.4 Seismic design approach in New Zealand and Australia ... 30

2-3 Code comparison 35

2-4 Revue of the scientific literature 39

CHAPTER 3 DESIGN OF THE BUILDINGS ACCORDING TO NBCC 05 AND CSA – A23-04 47

3.1 Studied problem 47

3.2 Design of the buildings 51

3.3 Design example 53

3.4 Summary 67

CHAPTER 4 NONLINEAR DYNAMIC ANALYSIS 83

4.1 Model choice 83

4.2 Studied models 87

4.3 Properties and parameters used for nonlinear analysis 112

4.3.1 Bar element 113

4.3.2 Wall element 115

4.4 Choice of earthquake ground motions 117

4.5 Analytical results 122

4.5.1 Comparison between elements "Wall" and "Bar" 128

4.5.2 Results for Element "Wall" 136

CHAPTER 5 DESIGN OF A WALL SPECIMEN FOR A SHAKING TABLE TEST PROGRAM 157

5.1 Introduction 157

5.2 Similitude laws 158

5.3 Studied building and application of the similitude law 160

5.4 Analytical verification of the proposed model 164

5.5 Concluding remarks and recommendations 170

CHAPTER 6 CONCLUSIONS AND RECOMMENDATIONS 172

6.1 Codes comparison 173

6.2 Seismic loading, design forces and detailing requirements according to NBCC 05 and CAN/CSA A23.3-04 174

6.3 Nonlinear dynamic analysis 177
6.4 Design of wall specimen for shaking table test program 180
6.5 Recommendations 182
CHAPTER 7 BIBLIOGRAPHY 183
APPENDICES 190

LIST OF TABLES

Table 2.1	Base overturning reduction factors for shear wall buildings	11
Table 2.2	CSA A23.3-04 minimum reinforcement requirements for shear walls	15
Table 2.3	Amplification factor for Equivalent static and Modal Response Procedures according to NBCC05	45
Table 3.1	Natural fundamental periods of the buildings and geometry of the walls	49
Table 3.2	Design spectral ordinates, S	51
Table 3.3	Results of the preliminary design at the base of the buildings (ratios in %)	52
Table 3.4	Reduction factors for moments - Equivalent Static Force Procedure	56
Table 3.5	Design forces - Equivalent Static Force Procedure	57
Table 3.6	Calculation of the effective wall flexural properties.....	58
Table 3.7	Calculation of the design forces	60
Table 3.8	Inter- storey drifts – 10-storey building in Vancouver	62
Table 3.9	Summary of the periods, parameters and lateral earthquake forces for Equivalent Static Procedure and Modal Response Spectrum Method	68
Table 3.10	Summary of the Lateral earthquake forces for Equivalent Static Procedure and Modal Response Spectrum Method and the controlling method for Base shear	68
Table 3.11	Summary of the coefficients used for calculation of the design forces for Vancouver	70
Table 3.12	Summary of the coefficients used for the calculation of the design forces for Montreal	70
Table 3.13	Calculations of inelastic rotational capacity and demand	78

Table 3.14	Summary of parameters used for calculations of shear reinforcement in plastic hinge region in the walls	79
Table 3.15	Summary of design forces, factored resistances and flexural and shear reinforcement in plastic hinge region (base) at the walls	80
Table 3.16	Summary of the calculation of the interface shear resistance at the wall bases	81
Table 4.1	10-storey building Vancouver	115
Table 4.2	10-storey building – Vancouver	117
Table 4.3	Characteristics of the selected ground motions for Montreal	119
Table 4.4	Characteristics of the selected ground motions for Vancouver	120
Table 4.5	Computed building period (s) in the first four modes of vibration	123
Table 4.6	50th percentile for Curvature ductility above the plastic hinge	141
Table 4.7	50th percentile for V_{EQ} / V_r at the base of walls	147
Table 4.8	Base Shears Ratio - $V_{EQ} / \gamma_p . V_{spectral}$ and $V_{EQ} / \gamma_n . V_{spectral}$	150
Table 4.9	Base Shears Correction Factors	151
Table 5.1	Modeling parameters for Acceleration and Velocity similitude	160
Table 5.2	Design forces, reinforcement and yielding moment approximation for Prototype	163
Table 5.3	Modeling parameters for the proposed "Modified Acceleration Similitude"	164
Table B.1	5-storey building in Vancouver "Bar" model properties	193
Table B.2	10-storey building in Vancouver "Bar" model properties	193
Table B.3	15-storey building in Vancouver "Bar" model properties	193
Table B.4	20-storey building in Vancouver "Bar" model properties	194
Table B.5	25-storey building in Vancouver "Bar" model properties	194
Table B.6	5-storey building in Montreal "Bar" model properties	195
Table B.7	10-storey building in Montreal "Bar" model properties	195
Table B.8	15-storey building in Montreal "Bar" model properties	196

Table B.9	20-storey building in Montreal "Bar" model properties	196
Table B.10	25-storey building in Montreal "Bar" model properties	197
Table B.11	5-storey building in Vancouver "Wall" model properties	198
Table B.12	10-storey building in Vancouver "Wall" model properties	198
Table B.13	15-storey building in Vancouver "Wall" model properties	198
Table B.14	20-storey building in Vancouver "Wall" model properties	199
Table B.15	25-storey building in Vancouver "Wall" model properties	199
Table B.16	5-storey building in Montreal "Wall" model properties	200
Table B.17	10-storey building in Montreal "Wall" model properties	200
Table B.18	15-storey building in Montreal "Wall" model properties	200
Table B.19	20-storey building in Montreal "Wall" model properties	200
Table B.20	25-storey building in Montreal "Wall" model properties	201
Table F.1	Summary of the wall properties	236

LIST OF FIGURES

Figure 2.1	Design loads: NBCC05; NZS4203, 1992; UBC 97; and EC8	36
Figure 2.2	Equivalent lateral force procedure: NBCC05; NZS4203, 1992; UBC 97; NEHRP 2000; and EC8	37
Figure 3.1	Geometrical properties of the walls studied	48
Figure 3.2	Computed fundamental periods of the buildings and NBCC 2005 empirical fundamental period T_a for shear wall structures	49
Figure 3.3	Typical 30x 30 m storey layout	50
Figure 3.4	Analytical model: 10-storey building	57
Figure 3.5	Comparisons of the ESFP and the MRSM	61
Figure 3.6	5-storey building in Vancouver: Dynamic and Design forces	72
Figure 3.7	10-storey building in Vancouver: Dynamic and Design forces	72
Figure 3.8	15-storey building in Vancouver: Dynamic and Design forces	73
Figure 3.9	20-storey building in Vancouver: Dynamic and Design forces	73
Figure 3.10	25-storey building in Vancouver: Dynamic and Design forces	74
Figure 3.11	5-storey building in Montreal: Dynamic and Design forces	74
Figure 3.12	10-storey building in Montreal: Dynamic and Design forces	75
Figure 3.13	15-storey building in Montreal: Dynamic and Design forces	75
Figure 3.14	20-storey building in Montreal: Dynamic and Design forces	76
Figure 3.15	25-storey building in Montreal: Dynamic and Design forces	76
Figure 4.1	Rate of shear strength degradation due to the increase of rotational ductility, adopted from NZNSEE 1996	84
Figure 4.2	Hysteresis curves for a shear wall	85
Figure 4.3	Analytical models for shear walls	86
Figure 4.4	Moment-curvature: Montreal - level 1	89
Figure 4.5	Moment-curvature: Montreal - level 10.....	89
Figure 4.6	Moment-curvature: Vancouver - level 1	90

Figure 4.7	Moment-curvature: Vancouver - level 10	90
Figure 4.8	Moment-curvature: Montreal - level 1	91
Figure 4.9	Moment-curvature: Montreal - level 10	91
Figure 4.10	Moment-curvature: Vancouver - level 1	92
Figure 4.11	Moment-curvature: Vancouver - level 10	92
Figure 4.12	Structural-Wall element	94
Figure 4.13	Schematic of the test setup	96
Figure 4.14	Sequence of imposed reverse cyclic lateral displacement at tip of the wall. (Adebar, P; Ibrahim, A.M.M.; 2000)	96
Figure 4.15	Influence of NIP on the lateral load-displacement response of the wall	98
Figure 4.16	Sensitivity of the lateral load-displacement response of the wall to the number of members	99
Figure 4.17	Influence of NIP on the lateral load-displacement response of the wall	100
Figure 4.18	Influence of the axial load on the cyclic behaviour of RC walls	101
Figure 4.19	Available concrete models in Ruaumoko programme for Wall element	102
Figure 4.20	Available concrete models in Ruaumoko programme for Wall element	103
Figure 4.21	Comparison of the Taylor and K&P concrete models with Response 2000	104
Figure 4.22	Story shear at 17th story in 25-story building located in Vancouver, W65302	105
Figure 4.23	Maximum storey shear forces for different values of F_{cr} for the 25-storey building in Vancouver under the W65302 ground motion	106
Figure 4.24	Base shear force time history for different values of F_{cr} for the 25-storey building in Vancouver under the W65302 ground motion	106

Figure 4.25 Base shear force time history for different values of F_{cr} for the 25-storey building in Vancouver under the W72701 ground motion 107

Figure 4.26 Storey shear force time history at 17th storey for different values of F_{cr} for the 25-storey building in Vancouver under the W72701 ground motion 108

Figure 4.27 Base shear time history for different values of F_{cr} for the 10-storey building in Vancouver under the W65302 ground motion 109

Figure 4.28 Story shear force time history at 7th storey for different values of F_{cr} for the 10-storey building in Vancouver under the W65302 ground motion 110

Figure 4.29 Base shear time history for different values of F_{cr} for the 10-storey building in Vancouver under the W72701 ground motion 110

Figure 4.30 Story shear force time history at 7th storey for different values of F_{cr} for the 10-storey building in Vancouver under the W72701 ground motion 111

Figure 4.31 Analytical Bar Model models for shear walls 113

Figure 4.32 Takeda hysteretic model 114

Figure 4.33 10-storey building – Vancouver 116

Figure 4.34 5% damped response spectra for Montreal 121

Figure 4.35 5% damped response spectra for Vancouver – NBCC 2005 and simulated earthquakes W1 to W8 121

Figure 4.36 5% damped response spectra for Vancouver – NBCC 2005 and Historical Earthquakes W9 to W15 122

Figure 4.37 Modal shapes of vibration: 5-storey building in Vancouver 124

Figure 4.38 Modal shapes of vibration: 10- storey building in Vancouver 124

Figure 4.39 Modal shapes of vibration: 15- storey building in Vancouver 125

Figure 4.40 Modal shapes of vibration: 20- storey building in Vancouver 126

Figure 4.41 Modal shapes of vibration: 25- storey building in Vancouver 127

Figure 4.42 Modal shapes of vibration: 5- storey building in Montreal 124

Figure 4.43 Modal shapes of vibration: 10- storey building in Montreal 124

Figure 4.44 Modal shapes of vibration: 15- storey building in Montreal 124

Figure 4.45 Modal shapes of vibration: 20- storey building in Montreal 125

Figure 4.46 Modal shapes of vibration: 25- storey building in Montreal 125

Figure 4.47 Comparison of peak storey horizontal displacement from "Wall" and "Bar" elements (50^{th} Δ_{wall} / 50^{th} Δ_{bar}) for Vancouver buildings 128

Figure 4.48 Comparison "Wall"-"Bar" Vancouver: V_{wall} / V_{bar} 131

Figure 4.49 Comparison "Wall"-"Bar" Montreal: V_{wall} / V_{bar} 131

Figure 4.50 Definition of maximum permitted curvature and elastic curvature 132

Figure 4.51 Comparison "Wall"-"Bar": Δ_{top} / h_s; $\varphi_{max} / \varphi_{code}$; $\varphi_{inel.} / \varphi_{code}$ 135

Figure 4.52 Maximum storey displacement: $\Delta_{wall} / \Delta_{code,max}$ 137

Figure 4.53 Maximum storey displacement: $\Delta_{wall} / \Delta_{spectral}$ 139

Figure 4.54 Curvature ductility at the base and above the plastic hinge 141

Figure 4.55 Base moments ratio for the Vancouver buildings: $M_{EQ} / M_{spectral}$ 143

Figure 4.56 Base moments ratio for the Vancouver buildings: M_{EQ} / M_p 143

Figure 4.57 Base moments ratio - Montreal: $M_{EQ} / M_{spectral}$ 144

Figure 4.58 Base moments ratio - Montreal: M_{EQ} / M_n 144

Figure 4.59 Shear forces: $V_{EQ} / V_{spectral}$ 145

Figure 4.60 Shear forces: V_{EQ} / V_{design} 146

Figure 4.61 Shear forces: V_{EQ} / V_r 147

Figure 4.62 Base shear ratio - Vancouver: $V_{EQ} / V_{spectral}$ 148

Figure 4.63 Base shear ratio - Vancouver: $V_{EQ} / \gamma_p . V_{spectral}$ 148

Figure 4.64 Base shear ratio - Montreal: $V_{EQ} / V_{spectral}$ 149

Figure 4.65 Base shear ratio - Montreal: $V_{EQ} / \gamma_n . V_{spectral}$ 149

Figure 4.66 Correction base shear factors for Vancouver compared to $V_{EQ} / \gamma_p . V_{spectral}$ 151

Figure 4.67 Correction base shear factors for Montreal compared to $V_{EQ} / \gamma_n . V_{spectral}$ 152

Figure 4.68 Concrete models – Montreal 153

Figure 4.69 Comparison between confined and unconfined concrete models: $\Delta_{conf.} / \Delta_{unconf.}$ 154

Figure 4.70 Comparison Confined and unconfined model of concrete: $M_{conf.} / M_{unconf}$ 155

Figure 4.71 Comparison Confined and unconfined model of concrete: $V_{conf.} / V_{unconf}$ 156

Figure 5.1 Structural Engineering Laboratory at Ecole Polytechnique of Montreal 161

Figure 5.2 Suggested test set-up 161

Figure 5.3 Proposed set-up and mathematical modeling of Model Wall specimen 165

Figure 5.4 Comparison: Prototype – Model 166

Figure 5.5 Input ground acceleration W72701: Prototype – Model 167

Figure 5.6 Top displacement: Prototype – Model 167

Figure 5.7 Base moment: Prototype - Model 168

Figure 5.8 Base shear: Prototype - Model 168

Figure 5.9 Actuator axial force 169

Figure 5.10 Vertical reactions in the left and right supports 170

Figure C.1.1 Maximum storey responses for the 5-storey building in Vancouver - "Bar" 203

Figure C.1.2 Maximum storey responses for the 10-storey building in Vancouver - "Bar" 204

Figure C.1.3 Maximum storey responses of the 15-storey building in Vancouver - "Bar" 205

Figure C.1.4 Maximum storey responses for the 20-storey building in Vancouver - "Bar" 206
Figure C.1.5 Maximum storey responses for the 25-storey building in Vancouver - "Bar" 207
Figure C.1.6 Maximum storey responses for the 5-storey building in Montreal - "Bar" 208
Figure C.1.7 Maximum storey responses for the 10-storey building in Montreal - "Bar" 209
Figure C.1.8 Maximum storey responses for the 15-storey building in Montreal - "Bar" 210
Figure C.1.9 Maximum storey responses for the 20-storey building in Montreal - "Bar" 211
Figure C.1.10 Maximum storey responses for the 25-storey building in Montreal - "Bar" 212
Figure C.2.1 Maximum storey responses for the 5-storey building in Vancouver - "Wall" 213
Figure C.2.2 Maximum storey responses for the 10-storey building in Vancouver - "Wall" 214
Figure C.2.3 Maximum storey responses for the 15-storey building in Vancouver - "Wall" 215
Figure C.2.4 Maximum storey responses for the 20-storey building in Vancouver - "Wall" 216
Figure C.2.5 Maximum storey responses for the 25-storey building in Vancouver - "Wall" 217
Figure C.2.6 Maximum storey responses for the 5-storey building in Montreal - "Wall" 218
Figure C.2.7 Maximum storey responses for the 10-storey building in Montreal - "Wall" 219

Figure C.2.8 Maximum storey responses for the 15-storey building in Montreal - "Wall" 220
Figure C.2.9 Maximum storey responses for the 20-storey building in Montreal - "Wall" 221
Figure C.2.10 Maximum storey responses for the 25-storey building in Montreal - "Wall" 222
Figure D.1 Maximum storey shear responses for the 5-storey building in Vancouver 223
Figure D.2 Maximum storey shear responses for the 10-storey building in Vancouver 224
Figure D.3 Maximum storey shear responses for the 15-storey building in Vancouver 224
Figure D.4 Maximum storey shear responses for the 20-storey building in Vancouver 225
Figure D.5 Maximum storey shear responses for the 25-storey building in Vancouver 225
Figure D.6 Maximum storey shear responses for the 5-storey building in Montreal 226
Figure D.7 Maximum storey shear responses for the 10-storey building in Montreal 226
Figure D.8 Maximum storey shear responses for the 15-storey building in Montreal 227
Figure D.9 Maximum storey shear responses for the 20-storey building in Montreal 227
Figure D.10 Maximum storey shear responses for the 25-storey building in Montreal 228
Figure F.1 "Studied Wall" concept 233
Figure F.2 Comparison between different wall configurations 235
Figure F.3 "Prototype" and "Model" walls concept 237

Figure F.4 Normalized force-displacement for Studied, Prototype and Model walls 238
Figure F.5 Load-displacement response for Prototype wall 238
Figure F.6 Cracking pattern and displacements at the onset of failure for Prototype wall 239
Figure F.7 Load-displacement response for Model wall 240
Figure F.8 Cracking pattern and displacements at the onset of failure for Model wall 240

LIST OF NOTATIONS AND ABBREVIATIONS

A_B	floor area of the diaphragm level immediately above the storey,
A_g	gross area of wall cross-section,
b_{col}	wall flange length,
b_w	wall web width,
c	distance from the extreme fibre in compression to the neutral axis of the wall, cohesion stress,
$C_h\ (T_1, \mu)$	spectral coefficient based on 5% damped elastic response,
C_s	seismic response coefficient,
C_v	seismic coefficient that depends on the soil profile type and the seismic zone factor,
C_u	coefficient for the upper limit on the calculated period,
d_b	reinforcing bar diameter,
E	seismic load; earthquake design load,
E_c	elastic modulus of concrete,
E_s	elastic modulus of steel reinforcement,
ESFP	equivalent static force procedure,
f_1	factor for live load UBC97,
f_2	factor for snow load UBC 97,
f'_c	maximum compressive stress of concrete,
f_y	yielding stress of steel reinforcement,
F_a	acceleration-based site coefficient,
F_b	seismic base shear,
F_{cr}	tensile strength of the concrete,
F_t	concentrated force at the top of the structure accounting for the higher, mode effects,
F_i	horizontal force acting on storey i, equivalent static horizontal force at each level i,

F_v	velocity-based site coefficient,
F_x	lateral force applied to Level x, total lateral force,
G_c	shear modulus of concrete,
G_k	permanent gravity loads,
h_i, h_n, h_x	height above the base (i = 0) to level i, n, or x respectively, where the base of the structure is that level at which horizontal earthquake motions are considered to be imparted to the structure,
h_s	storey height (h_i - h_{i-1}),
I, I_E	importance factor of the structure, occupancy importance factor,
J	reduction coefficient for base overturning moment,
J_x	reduction coefficient for overturning moment at level x,
k	minimum number of modes, exponent related to the structure period,
k_d	ratio of the factored moment resistance to the applied factored moment both calculated at the top of the plastic hinge region,
k_s	factor that defines the squatness of the wall,
K_o	initial stiffness,
l_u	nominal height of the wall section under consideration,
L_w	length of shear walls,
M, m_i, m_j	total mass of the building, above the foundation or above the top of a rigid basement, storey masses,
M_E	seismic design moment,
$M_{o,w}$	nominal moment capacity,
M_p	probable moment capacity,
M_{1i}	inelastic first mode moment at level i.
M_{Rd}	actual flexural resistance at the base of the wall,
M_{Sd}	design bending moment at the base,
M_u	ultimate moment capacity,
M_v	factor to account for higher mode effect on base shear,
M_x	overturning moment at level x,

M_y	yielding moment,
n	number of storeys above the foundation,
N	total number of storeys above exterior grade to level n, axial load,
P_D	average constant axial force due to dead loads,
PGA	peak ground acceleration expressed as a ratio to gravitational acceleration,
q	behaviour factor,
Q_{Ej}	internal forces,
Q_{ki}	variable gravity loads;
r	bilinear factor for the simplified bi-linear response representation of wall responses,
R	response modification factor, risk factor;
R_d	ductility related force modification factor,
R_o	overstrength related force modification factor,
s_i, s_j	displacements of masses m_i, m_j in the fundamental mode shape,
$SFRS$	seismic force resisting system,
$S(T)$	design spectral response acceleration for a period T,
$S_a(T)$	5% damped spectral response acceleration for a period T,
S_{DS}	design spectral response acceleration in the short period range,
S_{D1}	design spectral acceleration at a period of 1.0 s,
$S_d(T_1)$	ordinate of the design spectrum at period T_1,
$S_e(T)$	the ordinate of the elastic response spectrum for the period T,
S_p	structural performance factor,
T, T_a, T_1	period of vibration, fundamental lateral period of vibration of buildings, elastic fundamental period of vibration of buildings for lateral motion in the direction considered,
V	lateral earthquake design force at the base of the structure, shear force,
V_{2Ei}	second mode elastic shear force at level i.
V_{2Ei}	second mode elastic bending moment at level i,

V_c	factored concrete shear resistance,
V_d	lateral earthquake design force at the base of the structure as determined by the dynamic analysis procedures,
V_e	elastic lateral earthquake force at the base of the structure as determined by dynamic analysis procedures,
V_E	design base shear reduced for ductility,
V_{Ii}	inelastic first mode shear force at level i,
V_p	lateral force on a part of the structure,
V_r	factored shear resistance,
V'_{Sd}	shear force,
V_s	factored transverse steel reinforcement shear resistance,
V_t	design value for the modal base shear,
w	wall thickness,
W, W_i, W_x	seismic weight, dead load, portion of W which is located at or is assigned to level i or x respectively,
z_i, z_j	heights of the masses m_i, m_j,
α	unloading stiffness parameter for Takeda model, geometrical scale factor,
α_f	angle between the shear friction reinforcement and the shear plane,
α_w	effective property factor for reinforced concrete shear wall,
β	reloading stiffness parameter for Takeda model, acceleration scale factor,
δ_{max}	maximum displacement of the structure at Level x,
Δ_i	storey drift at level i,
$\Delta_{fi,i}$	inelastic storey drift at level i,
$\Delta_{max,i}$	maximum permitted inelastic storey drift at level i,
ε_c	peak strain of concrete at maximum compressive stress,
ε_{cu}	ultimate compressive strain of concrete,
ε_x	longitudinal strain at mid-depth of the cross-section,
ϕ_c	concrete resistance factor,

ϕ_o	flexural overstrength factor,
ϕ_s	reinforced steel resistance factor,
φ	coefficient that depends of the building category and the number of storeys,
φ'_y	point of first-yield curvature, where the extreme bar starts to yield,
φ_y	yielding curvature,
γ_I	importance factor assigned in EC8,
γ_p	probable overstrength factor,
γ_{Rd}	factor accounting for the overstrength,
γ_w	nominal overstrength factor,
λ	correction factor in EC8 to account for the concrete density,
θ	angle between the shear reinforcement and the shear plane,
μ	structural ductility factor, structural displacement ductility factor, coefficient of friction,
θ_{ic}	inelastic rotational capacity of the wall,
θ_{id}	inelastic rotational demand on the wall,
ρ	redundancy factor,
ρ_{max}	ratio of the design storey shear resisted by the single element carrying the most shear force in the storey to the total storey shear for a given direction of loading,
ρ_v	reinforcement ratio for the steel reinforcement in tension,
σ	effective normal stress in the section,
Ω_o	seismic force overstrength factor for concrete shear walls,
ψ	reduction factor for ULS live load in NZS,
$\psi_{E,i}$	combination coefficient for a variable action i to be considered when determining the effects of the design seismic action,
$\psi_{2,i}$	combination coefficient for the quasi-permanent value of a variable action i,

ω_v	dynamic shear magnification factor.

LIST OF APPENDICES

APPENDIX A	SHEAR WALL BUILDING DATA REPORTED IN SCIENTIFIC LITERATURE	190
APPENDIX B	ELEMENT PROPERTIES FOR NONLINEAR ANALYSIS	193
APPENDIX C	RESULTS FROM NONLINEAR ANALYSIS	202
APPENDIX D	RATIOS OF THE SHEAR FORCES FROM NONLINEAR DYNAMIC ANALYSIS TO THE SHEAR RESISTANCE FOR THE "BAR" AND "WALL" ELEMENTS	223
APPENDIX E	DEVELOPMENT OF "MODIFIED ACCELERATION SIMILITUDE" LAW	229
APPENDIX F	DESIGN OF THE SPECIMENS FOR SEISMIC TESTING OF SHEAR WALL STRUCTURES	230

CHAPTER 1

INTRODUCTION

1.1 STUDIED PROBLEM

Recent developments across the world relating to examples of the devastating impacts of modern earthquakes on both social and economic areas have resulted in an increased awareness amongst populations, institutions, and governments of the potential hazard and vulnerability of buildings located in a precarious environment. Greater interest has thus been taken in the research of methods with which the potential risk of this hazard can be assessed, allowing also for mitigating measures to be adopted.

Based on elastic behaviour, structures subjected to a major earthquake would be required to undergo large displacements and sustain high forces. However, modern practices allow structures to be designed to withstand only a fraction of the forces associated with those displacements. The relatively low force designs forces are justified by the observations that buildings designed to withstand reduced forces can behave satisfactorily and can dissipate significant energy through yielding and inelastic response of the building material provided they are properly designed and detailed. In Canada, this approach has been adopted in the National Building Code of Canada (NBCC 2005) and the CSA A23.3 Standard for the design of concrete structures (CSA 2004). Details are given in Mitchell et al. (2003).

In routine seismic design practice, and particularly when using the equivalent static force procedure, it is usually assumed that the bending moments and shear forces over the height of the building can be obtained from the same lateral force distribution. Also, the lateral storey shear forces in multi-storey reinforced concrete (RC) wall structures with rigid floor diaphragms are usually distributed to the resisting walls on the basis of

their relative lateral stiffness. It is well known now, that higher modes of vibration magnify the seismic base shear demand on flexural walls relative to that consistent with the lateral force distribution generating the base moment. The shear forces in walls increase above those corresponding to the maximum base moments due to higher modes of vibration in the elastic range as well as higher mode response following the formation of base plastic hinges.

Modern seismic design codes prescribe detailed principles and application rules to control the inelastic response of RC structures to ground motions at the design level and beyond. Extensive numerical and experimental studies are typically performed in order to calibrate the code provisions so that the desired inelastic structural response is obtained. Some of these code provisions and studies of this type are presented in this work.

1.2 OBJECTIVES

The main objective of this work is to improve our knowledge on the nonlinear seismic behaviour of high-rise concrete walls with particular interest in the higher mode effects on the distribution of the seismic shear forces and the dynamic amplification of shear and flexure in cantilevered wall structures designed using the Modal Response Spectrum Method described in the 2005 National Building Code of Canada (NBCC 2005) and the detailing requirements prescribed in the CSA A23.3-04 Standard.

The second objective is to propose and preliminarily design a shaking table test reduced-scale model in order to study and better understand the inelastic seismic response of shear walls including higher mode effects along with, the vertical distribution of seismic forces, critical zone lengths, and plastic hinge locations.

The study presented herein is limited to the two-dimensional response of wall structures above ground level, thus ignoring the influence of soil-structure interaction.

1.3 METHODOLOGY

To achieve the objectives as they are described in the previous paragraph,, the methodology used in this study is as follows:

1. To study the code provisions related to reinforced concrete shear walls of modern building codes including NBCC 2005, UBC97, NEHRP 2000, New Zealand NZS3101, and EC8.

2. To assess the current state of the research work conducted on the seismic response of shear wall structures concerning the determination of the fundamental period of vibration, higher modes effects, the amplification of shear forces due to dynamic response, location of the plastic hinges, and the length of the critical zones.

3. To design typical wall structures for 5-, 10-, 15-, 20-, and 25-story buildings located in Vancouver and Montreal, using the provisions of NBCC 2005 and CSA Standard A23.3-04.

4. To examine the dynamic inelastic response of the designed shear walls using the Ruaumoko computer software for nonlinear dynamic seismic analysis. The buildings were subjected to several time history ground motions typical for Vancouver in western Canada and for Montreal in eastern Canada. The ground motions will be scaled to match the design spectrum at each site.

5. To propose and study the response of a reduced-scale RC shear wall model to be used in a shaking table test program. The model will be developed to further investigate through shake table tests the above-mentioned problems for slender reinforced shear walls.

6. To provide a summary of the findings and conclusions of the study.

1.4 ORGANISATION OF THE THESIS

This thesis is divided into six chapters. Chapter 2 presents the review of the seismic provisions of EC8, UBC97, NEHRP 2000, NZS4203, and NBCC 2005 as well as a comparison between these codes. This chapter contains also the review of past research on aspects of the shear wall behaviour related to the objectives of this work.

Chapter 3 illustrates the procedures involved in the seismic design of shear walls for 5-, 10-, 15-, 20- and 25-storey reinforced concrete buildings located in Montreal and Vancouver. This building sample was chosen to cover the range of the common shear wall buildings used in Canadian seismic active regions. The seismic analysis is done in accordance with NBCC 2005. That code recommends the Dynamic Analysis Procedure, and particularly the Modal response spectrum method, as the preferred method of analysis. The Equivalent Static Force Procedure was also applied for comparison and scaling purposes. The design of the walls was done applying the special seismic requirements for the design and construction of reinforced concrete walls of CSA Standard A23.3-04.

Chapter 4 discusses the nonlinear earthquake response analysis of the buildings studied with the nonlinear analysis program Ruaumoko. Two types of models were used:

1) the most popular and common frame element representation with end plastic hinges exhibiting the flexural bi-linear Takeda hysteresis rule, and 2) a more complex "Wall" element with fibre representation of the cross-section that accounts for the interaction of axial loads and bending moments, the opening and closing of the cracks, and the variation of the position of the neutral axis.

Chapter 5 contains the proposal for the shaking table test model. Similitude scaling rules are presented and a specific proposal is made for the testing of a scaled model of a 10-storey slender concrete structural wall. The characteristics of the shaking table at Ecole Polytechnique and the description of the test procedure are presented. The design of the laboratory model was done at a 1:3.25 scale of the 10-storey prototype wall studied in Chapter 3.

Chapter 6 summarizes the work, presents the conclusions of the study, and includes recommendations for future research.

CHAPTER 2

DESIGN CODES AND LITERATURE REVUE

2.1 Introduction

The new 2005 edition of the National Building Code of Canada (NBCC 2005) contains very significant changes in the provisions for seismic loading and design, of which: updated seismic hazard data presented in a uniform hazard spectral format, change in the return period (475 to 2500 years), period-dependent site factors, delineation of the effects of overstrength and ductility, modified period calculation formulas, explicit recognition of higher mode effects on base shear forces, rational determination of irregularities, and specification of the dynamic analysis as the preferred method of analysis for use in seismic design.

There are several major reasons for updating the seismic provisions. The first reason is the information obtained by studying and learning from damages due to major earthquakes around the world. The second reason comes from the results of the earthquake engineering research conducted in Canada and around the world. Another major reason for changing the Canadian provisions is the comparison of these provisions with those being adopted in codes in other countries. The last two points are the object of this chapter.

First, a short review of several code provisions for earthquake loads, effects and procedures is presented. Secondly, past research work concerning the higher modes effects and the dynamic amplification of shear forces reported in the literature is presented, with particular emphasis on research carried out by the Canadian earthquake engineering research community.

2.2 Design codes

2.2.1 Seismic design approach in Canada - NBCC 2005, CSA A23.3-04

Introduction

The 2005 edition of the National Building Code of Canada (NBCC) recognizes dynamic analysis as the preferred procedure for obtaining the design forces and, in fact, makes such analysis mandatory for all irregular structures except those of low height or located in zones of low seismicity. Dynamic analysis is also mandatory for tall regular structures that are located in zones of high seismicity.

Design seismic action

The design seismic load combination is as follows:

$$1.0D + 1.0E + 0.5L + 0.25S \qquad (2.1)$$

D Dead load;

E Earthquake load E includes horizontal earth pressure due to earthquakes;

L Live load, except roof live load;

S Snow load.

Structural analysis

Structural modeling must be representative of the magnitude and spatial distribution of the mass of the building and stiffness of all elements of the SFRS, which includes stiff elements that are not separated, and must account for the effect of cracked sections in reinforced concrete and reinforced masonry elements, the effect of the finite size of members and joints, sway effects arising from the interaction of gravity loads with the displaced configuration of the structure and other effects which influence the buildings lateral stiffness.

Analysis for design earthquake actions must be carried out in accordance with the Dynamic Analysis Procedure, except that the Equivalent Static Force Procedure may be used for structures that meet any of the following criteria: (a) for cases where $I_E.F_a.S_a(0.2)$ is less than 0.35; (b) regular structures that are less than 60 m in height and have a fundamental lateral period, T_a, less than 2 s in each of two orthogonal directions; and (c) structures with structural irregularity, except structural irregularity Type 7 (torsion), as defined in the code, that are less than 20 m in height and have a fundamental lateral period, T_a, less than 0.5 seconds in each of two orthogonal directions. In the first criteria, I_E is the earthquake importance factor, F_a is the acceleration-based site coefficient and S_a is the uniform hazard spectrum ordinate at the site. These parameters are discussed further below.

Seismic Base Shear

The seismic design base shear for use in an equivalent static force procedure of design, V, is obtained from the uniform hazard spectrum for the site corresponding to the first mode period of the building. The base shear so computed is adjusted to account for effects of higher modes. The procedure for deriving these base shear adjustment factors, and the values proposed in NBCC 2005 for these factors, will be presented later for different types of structural systems. The adjusted base shear is distributed along the height of the building in accordance with the seismic weight and height of each level. In the equivalent static force procedure, the code-specified distribution is primarily based on the first mode vibration shape. This method leads to an overestimation of the overturning moments, which should therefore be suitably adjusted. The NBCC 2005 therefore includes an adjustment factor J for the overturning moments at the base and along the building height. This factor need not be applied to bending moments obtained from a dynamic analysis method.

The minimum lateral earthquake force, V, shall be calculated in accordance with the following formula:

$$V = S(T_a) \cdot M_v \cdot I_E \cdot W / (R_d \cdot R_o), \qquad (2.2)$$

except that V shall not be taken less than $S(2.0) \cdot M_v \cdot I_E \cdot W / (R_d \cdot R_o)$ and, for an SFRS with an R_d equal to or greater than 1.5 V, need not be taken greater than $\frac{2}{3} S(0.2) \cdot I_E \cdot W / (R_d R_o)$. In these equations, R_d is the ductility-related force modification factor that reflects the capability of a structure to dissipate energy through inelastic behaviour (R_d = *3.5* for Ductile reinforced concrete shear walls, R_d = *2.0* for Moderately Ductile reinforced concrete shear walls, and R_d = *1.5* for conventional constructions); R_o is the overstrength-related force modification factor that accounts for the dependable portion of reserve strength in a structure designed according to the provisions (R_o = *1.6* for Ductile reinforced concrete shear walls, R_o = *1.4* for Moderately Ductile reinforced concrete shear walls, and R_o = *1.3* for conventional constructions); $S(T_a)$ is the design spectral response acceleration, W is the seismic weight, and M_v is a factor that accounts for the amplification of the shear forces related to higher mode effects. The values for M_v are given in Table 2.1 for periods $T_a \leq 1.0$ s and $T_a \geq 2.0$ s. For values between these fundamental lateral periods, T_a, of 1.0 and 2.0 s, the product $S(T_a) \cdot M_V$ must be obtained by linear interpolation. It must be noticed that for sites characterized with earthquakes with predominant higher frequency content, as is the case in eastern Canada, and structures with long first period of vibration, the M_v factor is much higher compared to similar structures located at sites with predominant low frequency content, as in the western part of Canada. The values for the M_v factor are obtained by comparing the spectral elastic responses of equivalent single degree of freedom systems with those from multi degree of freedom systems (Humar et al. 2003).

The seismic weight W includes the dead load, except that the minimum partition load need not exceed 0.5 kPa, plus 25% of the design snow load, plus 60% of the storage load for areas used for storage except that parking garages need not be considered as storage areas, and the full contents of any tanks.

The design spectral response acceleration is expressed as a ratio to gravitational acceleration for a period $T = T_a$, and it is determined by using linear interpolation for intermediate values of T: $S(T)$ is equal to $F_a S_a(0.2)$ for $T < 0.2$ s; minimum of $F_v S_a(0.5)$ and $F_a S_a(0.2)$, for $T = 0.5$ s; $F_v S_a(1.0)$ for $T = 1.0$ s; $F_v S_a(2.0)$ for $T = 2.0$ s; and $F_v S_a$ $(2.0)/2$ for $T \geq 4.0$ s, where F_a is the acceleration-based site coefficient, F_v is the velocity-based site coefficient and $S_a(T)$ is the 5% damped spectral response acceleration for a Class C site. The values of F_a and F_v are given for the different site classes A to E. The factor F_a depends of the response spectral acceleration for $T = 0.2$ s whereas F_v depends on S_a for $T = 1.0$ s.

The design fundamental lateral period for shear walls, T_a, is determined as $T_a = 0.05\ (h_n)^{3/4}$, where h_n is the building height in metres. Alternatively, T_a can be obtained from other established methods of mechanics using a structural model that complies with the code requirements, except that T_a for shear wall structures must not be greater than 2.0 times the value determined with the empirical formula. For the purpose of calculating the deflections, the period with other established methods without the upper limit may be used.

In the equivalent static force procedure, the total lateral seismic force, V, is distributed such that a portion, F_t, is assumed to be concentrated at the top of the building. This concentrated force F_t accounts for the higher mode effects and is calculated as follows:

$$F_t = 0.07\ T_a V \leq 0.25\ V \qquad (2.3)$$

and may be considered as zero when T_a is less than 0.7 s. The remainder, $(V - F_t)$, must be distributed along the height of the building, including the top level, in accordance with the formula:

$$F_x = (V - F_t) W_x h_x / (\sum_{i=1}^{n} W_i h_i) \qquad (2.4)$$

The structure must be designed to resist overturning effects caused by the earthquake forces determined with equation 2.4. The overturning moment at level x, M_x, must be determined from the following equation:

$$M_x = J_x \sum_{i=x}^{n} F_i (h_i - h_x) \qquad (2.5)$$

where $J_x = 1.0$ for $h_x \geq 0.6\ h_n$ and $J_x = J + (1 - J)(h_x / 0.6\ h_n)$ for $h_x < 0.6\ h_n$, where J is the base overturning moment reduction factor. That factor depends on the site properties and the fundamental period of the building. The values of the J factor for shear walls are summarised in Table 2.1. The factor decreases with the increase of the period of the building and decreases faster for sites characterized by earthquakes with high frequency content.

Table 2.1 Base overturning reduction factors for shear wall buildings.

$S_a(0.2)/S_a(2.0)$	Mv for $T_a \leq 1.0$	Mv for $T_a \geq 2.0$	J for $T_a \leq 0.5$	J for $T_a \geq 2.0$
< 8.0	1.0	1.2	1.0	0.7
≥ 8.0	1.0	2.5	1.0	0.4

Modal response spectrum analysis

The modal response spectrum analysis consists of the analysis of a linear mathematical model reflecting the dynamic properties (stiffness, mass, and damping) of the structure. The seismic hazard in NBCC 2005 is specified in terms of spectral acceleration for 5% damped design spectral response acceleration values $S_a(T)$

multiplied by the site amplification factors for periods T of 0.2, 0.5, 1.0, and 2.0 s. The spectral acceleration values used in the modal response spectrum method are the design spectral acceleration values $S(T)$ used to determine the minimum lateral seismic force V in the equivalent static force procedure. Although the 2005 NBCC makes dynamic analysis the preferred procedure, there is a concern that the resulting seismic forces may be too low because the assumptions made in the analysis. To overcome this and to provide some protection against inappropriate choices of analytical parameters, the 2005 NBCC provisions require that the dynamically determined base shear for regular structures must not be less than 80% of that determined using the static method. In the case of irregular structures for which dynamic analysis is required, the minimum dynamic base shear must be equal to 100% of the statically determined value.

Elastic Time History Analysis

Linear response history analysis, also commonly known as time history analysis, is a numerically involved technique in which the response of a structural model is calculated at each time increment under a specific ground motion. When a numerical integration linear time history method of dynamic analysis is used, the ground motion histories must be compatible with the design response spectrum. The ground shaking accelerogram, or record, is digitized into a series of small time steps, typically on the order of $1/100^{-th}$ of a second or smaller. Starting at the initial time step, a finite difference solution, or other numerical integration algorithm is followed to allow the calculation of the displacements of each node in the model and the forces in each element of model for each time step of the record.

The main advantage of response history analysis is that it provides a time history of the response of the structure to a specific time history motion. Conversely, a response spectrum analysis indicates only the maximum response quantities and does not indicate when these maximums occur during the earthquake, or how the response of a specific portion of the structure is phased relative to that of another portion. Response history

analyses are highly dependent on the characteristics of the individual ground shaking records and subtle changes in these records can lead to significant differences with regards to the predicted response of the structure. This is why it is necessary to consider a suite of ground motion records when response history analysis is used in the design process. The ground motion histories used in the Numerical Integration Linear Time History Method shall be compatible with a response spectrum constructed from the design spectral acceleration values. When the numerical integration time history method is used, the building must be subjected to appropriate ground motion records scaled to match the design level earthquake for the limit state and location of the building. Unfortunately, no indication is given for the number of records but reference is made to other codes or provisions such as UBC or NEHRP documents (see section 2.2.3). However, the use of multiple records in the analyses allows observation of the differences in response resulting from differences in record characteristics. The requirements for the scaling of the analysis results with respect to the base shear force as specified for the modal response spectrum analysis also apply to the time history analysis procedure.

Nonlinear Dynamic Analysis Method

This method of analysis is very similar to the linear response history analysis. Nonlinear time history analysis involves the computation of the dynamic response at each time increment with due consideration to the inelasticity in the structural members. Nonlinear analysis allows for flexural yielding (or other inelastic actions) and accounts for subsequent changes in strength and stiffness. Hysteretic behaviour under cyclic loading is evaluated. Softening caused by inelasticity of deformations during loading, unloading, and reloading is computed. This method accounts the changes of the dynamic characteristics of structures due to inelasticity, such as lengthening of the period and the exiting cracks. It also permits the evaluation of nonlinear behaviour as foundation rocking, opening and closing of gaps, and nonlinear viscous and hysteretic damping. Potentially, this ability to directly account for these various nonlinearities can permit

nonlinear response history analysis to provide very accurate evaluations of the response of the structure to strong ground motions. However, this accuracy can seldom be achieved in practice. This is partially because currently available nonlinear models for different elements can only approximate the behaviour of real structural elements. Another limit on the accuracy of this approach is the fact that minor deviations in ground motion, or even in element hysteretic behaviour, can result in significant differences in the predicted response. For these reasons, it is critical that suites of ground motion time histories be considered when nonlinear response history analysis is used in the design process. It may also be appropriate to perform sensitivity studies, in which the assumed hysteretic properties of the elements are varied within expected ranges, to evaluate the effects of such uncertainties on the predicted response. Application of nonlinear response history analysis to even the simplest structures requires complex computer software that has been specifically developed for this purpose and an experienced engineering team. This type of analysis was used in this study, as described Chapter 4.

Ductility detailing and capacity design of reinforced concrete shear walls

The walls must be designed and detailed according to CSA A23.3-04. These requirements are discussed in details in Chapter 3. Herein we will only present the philosophy of the code provisions, the main principles and the required design steps. The shear walls are classified in three ductility classes: Conventional construction (low ductility class), designed with a force modification factor $R_d = 1.5$, Moderate ductility class with $R_d = 2.0$, and Ductile walls with $R_d = 3.5$.

The Ductile and Moderately ductile shear walls must be designed by employing the capacity design approach. For walls that do not contain irregularity types 1, 3, 4, 5 or 6 as defined in NBCC 2005, the method assumes that a flexural plastic hinge will form at the base of the wall. That portion must therefore be detailed to achieve ductile rotational response whereas the rest of the wall must be protected against plastic hinging

by considering design forces that correspond to the attainment of the maximum expected bending moment in the base hinge: probable maximum resistance for Ductile walls and nominal moment resistance for Moderately ductile walls.

Special confinement requirements are prescribed for the flexural reinforcement in the compression zones in the base plastic hinge region. Minimum reinforcement ratios are also specified for the distributed and concentrated longitudinal reinforcement as well as for the horizontal distributed shear and confinement reinforcement. These requirements are summarized in Table 2.2. In addition, the lap splice length must be increased to at least 1.5 times the value required for Conventional construction walls and no more than 50% of the tension reinforcement can be spliced at a given horizontal section along the wall height.

Table 2.2 CSA A23.3-04 minimum reinforcement ratios (%) and maximum reinforcement spacing (s) for shear walls.

	Plastic hinge zone			Above the plastic hinge		
Ductility Class	Longitudinal		Horizontal	Longitudinal		Horizontal
	Distributed	Concentrated		Distributed	Concentrated	
Conventional Construction $R_d = 1.5$	0.20% $s \leq (3b_w;500$ mm)	-	0.15% $s \leq (3b_w;500$ mm)	0.20%	-	0.15%
Moderately Ductile $R_d = 2.0$	0.25% $s \leq (3b_w;500$ mm)	0.15%	0.25% $s \leq (3b_w;500$ mm)	0.25% $s \leq 450$ mm	0.10%	0.25% $s \leq 450$ mm
Ductile $R_d = 3.5$	0.25% $s \leq 300$ mm	0.15%	0.25% $s \leq 300$ mm	0.25% $s \leq 450$ mm	0.10%	0.25% $s \leq 450$ mm

Note: b_w is the thickness of the wall element.

The concentrated flexural reinforcement must be made of a minimum of four bars placed in two layers and must it be tied as specified for columns with buckling

prevention ties in the critical (base hinge) zone location. The height of the critical zone for Ductile walls is set to 1.5 times the length of the longest individual wall element in the direction under consideration. For Moderately ductile walls, no indication is given for the plastic hinge height, and the choice is left to the design engineer.

At the base of the plastic hinge zone of Ductile walls, the factored moment resistance of the wall must exceed the design bending moment and the shear resistance must be equal to or exceed the minimum of the elastic base shear calculated using $R_d R_o$ = 1.0 and the base shear corresponding to the development of the probable flexural moment capacity at base of the wall. The design shear forces above the critical zone must also correspond to the values corresponding to the probable moment capacity at the base of the wall. The same rules apply for the Moderately ductile walls except that the design shear forces need not exceed those corresponding to the wall nominal moment capacity. In addition to this requirement, the design overturning moments and shear forces at any elevation above the plastic hinge region in Ductile walls must be increased by the ratio of the factored bending moment resistance to the factored bending moment, both calculated at the top of the plastic hinge region.

In CSA A23.3, the shear strength in the plastic zone depends on two factors: the anticipated inelastic rotational demand on the wall, θ_{id}, for the contribution of concrete to the shear resistance, V_c, and the average axial stress in the section under consideration for the contribution of the horizontal steel to the shear resistance, V_s. Excessive flexural ductility demand in the base hinge region of the wall is prevented by verifying that the inelastic rotational demand at the base of the wall is equal to or less than the inelastic rotational capacity of the wall, θ_{ic}. The inelastic rotational demand is associated to the anticipated plastic roof displacement and the height and length of the wall. In this calculation, it is assumed that the displacement profile is similar to that of the first vibration mode and that the height of the plastic hinge is equal to half the length of the

wall. The code imposes also a minimum inelastic rotational demand of 0.004 radians for Ductile walls and 0.003 radians for Moderately ductile walls.

The low ductility (Conventional construction) class walls must be designed according to Clause 14 of CSA A23.3-04 and no reduction of lap splice length is allowed. Walls must have a factored shear resistance greater than the smaller of the shear force corresponding to the development of the factored moment capacity of the wall system at its base and the elastic shear force calculated using $R_d R_o$ equal to 1.0.

2.2.2 Seismic design approach in Europe - EUROCODE 8

Introduction

The main concept assumed in the drafting of EC8 (ECS 2001) is that different combinations of strength and ductility can yield the same required safety level. The code allows the designer to choose among three ductility classes: Low, Medium, and High. Each class is expected to correspond to structures having the same safety against earthquakes. The choice of the ductility class corresponds to the definition, by means of the q factor, of the forces to be adopted in the design. Exploitation of the ductility is different for the three ductility classes, however, and capacity design provisions are not the same either as their severity decreases with the lowering of the ductility demand.

The balance between resistance and energy-dissipation capacity is characterized by the values of the behaviour factor q and the associated ductility classification. As a limiting case, for the design of structures classified as non-dissipative, i.e. Low Ductility class structures, no account is taken of any hysteretic energy dissipation and the behaviour factor may not be taken greater than the value of 1.5, which is considered to account for overstrength. For dissipative structures, the behaviour factor is taken greater than 1.5 accounting for the hysteretic energy dissipation that mainly occurs in specifically designed zones of the structures, called dissipative zones or critical regions.

Medium Ductility class structures must comply with a set of specific detailing rules to ensure that the behaviour is sufficiently ductile. High Ductility class structures must respect more demanding detailing rules to ensure that a stable and efficient dissipative mechanism is developed when the structure enters into the nonlinear regime.

Design seismic action

The design seismic load combination is as follows:

$\Sigma G_k + \gamma_I E + \Sigma \psi_{E,i} Q_{ki}$, where: (2.6)

G_k : permanent gravity loads;

Q_{ki} : variable gravity loads;

E seismic load;

$\psi_{E,i}$: combination coefficient for a variable action *i*, to be considered when determining the effects of the design seismic action :

$\psi_{E,i} = \varphi \cdot \psi_{2,i}$

$\psi_{2,i}$: combination coefficient for the quasi-permanent value of a variable action *i*;

φ : coefficient that depends on the building category and the number of storeys;

γ_I : importance factor assigned to each importance class and that corresponds to a selected return period. For ordinary buildings (class III) and a reference probability of exceedance of 10% in 50 years, γ_I is set equal to 1.0.

Structural analysis

The model of the building must adequately represent the distribution of stiffness and mass so that all significant deformation shapes and inertia forces are properly accounted for. In the case of non-linear analysis, the model must also represent adequately the distribution of strength. In concrete buildings, the stiffness of the elements should take into accounts the effect of cracking. The elastic flexural and shear

stiffness properties of concrete elements may be taken equal to one-half of the corresponding stiffness of the uncracked elements.

The reference method for determining the seismic effects is the modal response spectrum analysis, using a linear-elastic model of the structure and the design spectrum. Depending on the structural characteristics of the building, one of the following two types of linear-elastic analysis may be used: a simplified response spectrum analysis (lateral force procedure) or a modal analysis. The behaviour factor for coupled walls structures of High Ductility class have q = 5.0, and uncoupled concrete walls structures have q = 4.0. The seismic motions may also be represented in terms of ground acceleration time-histories and related quantities (velocity and displacement). As an alternative to a linear method, a non-linear method may also be used, such as a non-linear static (pushover) analysis and a non-linear time history (dynamic) analysis.

Lateral force method of analysis

This type of analysis may be applied to buildings whose response is not significantly affected by contributions from higher modes of vibration. These buildings must fulfil the two following conditions: a) they have fundamental periods of vibration T_1 in the two main directions smaller than $4\ T_c$ or 2.0 s; b) they meet the criteria for regularity in elevation. The seismic base shear force F_b, as follows:

$$F_b = S_d\,(T1)\ \lambda\ m \qquad (2.7)$$

where:

$S_d\,(T_1)$ ordinate of the design spectrum at period T_1;

T_1 fundamental period of vibration of the building for lateral motion in the direction considered;

m total mass of the building, above the foundation or above the top of a rigid basement;

λ correction factor, the value of which is equal to 0.85 if $T_1 < 2\ T_c$ and the building has more than two storeys, or $\lambda = 1.0$ otherwise.

For the determination of the fundamental period of vibration T_1 of the building, expressions based on methods of structural dynamics (e.g. Rayleigh method) may be used. For buildings with heights up to 40 m the value of T_1 may be approximated by $T_1 = C_t H^{3/4}$, where $C_t = 0.050$ for shear wall structures and H is the height of the building, in m, from the foundation or from the top of a rigid basement. Alternatively, the estimation of T_1 may be made by the following expression: $T_1 = 2\ d^{1/2}$, where d is the lateral elastic displacement of the top of the building, in m, due to the gravity loads applied in the horizontal direction.

The fundamental mode shapes in the horizontal directions of analysis of the building may be calculated using methods of structural dynamics or may be approximated by assuming horizontal displacements increasing linearly along the height of the building. The seismic load effects must be determined by applying, to the two planar models, horizontal forces F_i to all storeys:

$$F_i = F_b \,.\, (s_i \,.\, m_i) \,/\, \Sigma\,(s_j \,.\, m_j) \qquad (2.8)$$

F_i horizontal force acting on storey i;

F_b seismic base shear according to equation (2.6),

s_i, s_j displacements of masses m_i, m_j in the fundamental mode shape;

m_i, m_j storey masses. When the fundamental mode shape is approximated by horizontal displacements increasing linearly along the height, the horizontal forces F_i are given by:

$$F_i = F_b \,.\, (z_i \,.\, m_i) \,/\, \Sigma\,(z_j \,.\, m_j) \qquad (2.9)$$

where z_i, z_j are the heights of the masses m_i, m_j above the level of application of the seismic action (foundation or top of a rigid basement). The calculation of the moments

must be based on the vertical distribution of shear forces above the level and no correction factor needs to be applied.

Modal response spectrum analysis

This type of analysis shall be applied to buildings that do not satisfy the conditions for applying the lateral force method of analysis. The response of all modes of vibration contributing significantly to the global response shall be taken into account: the sum of the effective modal masses for the modes included in the analysis must amount to at least 90% of the total mass of the structure and all modes with effective modal masses greater than 5% of the total mass are considered. Another requirement is the minimum number of modes, k, to be included in the analysis which must comply with the two following conditions: k is larger than $3n^{1/2}$ and $T_k < 0.20\ s$, where n is the number of storeys above the foundation and T_k is the period of vibration of mode k.

Non-linear methods

The mathematical model used for inelastic analysis must include the strength of the structural elements and their post-elastic behaviour. As a minimum, bilinear force-deformation envelopes should be used at the element level. In reinforced concrete and masonry buildings, the elastic stiffness of a bilinear force-deformation relation should correspond to cracked sections with axial forces due to gravity loads considered. In ductile elements expected to exhibit post-yield excursions during the response, the elastic stiffness of a bilinear relation should be the secant stiffness to the yield-point. The seismic action must be applied in both directions and the envelope of seismic effects must be used.

Capacity design for wall structures

The design value of the bending moment at the wall base is the one obtained from the analysis of the structure under the respective seismic load combination. To account

for a possible overstrength at the base section, which would increase the wall moment with respect to those from the analysis, as well as to account for inelastic higher mode effects for slender walls, the design bending moment diagram is a linear envelope of the calculated one, displaced vertically by a distance equal to the "critical region" of the wall: h_{cr}. The value of h_{cr} is the maximum between the width of the wall and 1/6 of its height. This procedure is meant to ensure that the plastic rotation are restricted to the base region only, which has the advantages of not requiring ductile detailing in the upper part and producing a linear drift distribution along the height.

The design values for the shear forces are meant to take into account a possible increase due to the onset of higher vibration modes, after yielding of the base. The design shear force is therefore given by the expression:

$$V_{Sd} = \varepsilon V'_{Sd} \qquad (2.10)$$

where V'_{Sd} is the shear force along the wall, obtained from the analysis, and ε is:

$$\varepsilon = q \{ (\gamma_{Rd} / q \,.\, M_{Rd} / M_{Sd})^2 + 0.1 [S_e (T_c) / S_e(T_1)]^2 \}^{1/2} \leq q \qquad (2.11)$$

where γ_{Rd} is a factor accounting for the overstrength due to steel strain-hardening. In absence of more precise data, this factor may be taken equal to 1.25 for structures with high ductility capacity and 1.15 for medium ductility class structures. M_{Rd} is the actual flexural resistance at the base of the wall and M_{Sd} is the design bending moment at the base. $S_e(T)$ is the ordinate of the elastic response spectrum for the period T_1 of the fundamental mode of the building and T_c is the corner period of the constant acceleration branch of the design response spectrum. In this equation, the first term accounts for the probable overstrength, according to capacity design assumptions. The second expression accounts for the influence of the higher modes of vibration, the longer the period, the larger the amplification required for shear. The behaviour factor q accounts for the

structural type of the system, ductility class, structural regularity and prevailing failure mode specified for each type of retaining structure. The factor reflecting the prevailing failure mode in structural systems with walls, k_w, is equal to 3.0 for the Moderate Ductility class and 4.0 α_u/α_1 for the High Ductility class. The ratio α_u/α_1 is equal to 1.0 for wall systems with only two uncoupled walls per horizontal direction and 1.1 for other uncoupled wall systems.

2.2.3 Seismic design approach in USA - UBC and NEHRP

Introduction

At the time of writing, there were four codes dealing with seismic provisions for buildings in the USA. These were the Council for American Building Officials (CABO) code for dwellings, the Building Officials and Code Administrators (BOCA) National Building Code, the Southern Building Code Congress International (SBCCI) Standard Building Code and the International Conference of Building Officials (ICBO) Uniform Building Code. The first three codes have adopted, to a greater or lesser degree, the provisions of the National Earthquake Hazard Reduction Program (NEHRP) guidelines, and UBC is traditionally lined to the guidelines produced by the Structural Engineers Association of California (SEAOC). Therefore, the UBC 1997 and NEHRP 2000 will be presented herein. It should be noted that the seismic provisions in UBC are similar to those in NEHRP.

Uniform Building Code (UBC) and NEHRP 2000

Design seismic action

The design seismic load combination is as follows:

$$1.2D + 1.0E + (f_1 L + f_2 S), \qquad (2.12)$$

where:

D Dead load;

E Earthquake load;

L Live load, except roof live load;

S Snow load

f_1 1.0 for floor in places of public assembly, for live loads in excess of 4.9 kN/m^2, and for the garage live load;

f_2 0.7 for roof configurations that do not shed snow off the structure; 0.2 for other roof configurations.

$$E = \rho E_h + E_v \qquad (2.13a)$$

$$E_m = \Omega_o E_h \qquad (2.13b)$$

$\rho = 2 - 6.1/(\rho_{max} A_B^{1/2})$ redundancy factor

ρ_{max} the ratio of the design story shear resisted by the single element carrying the most shear force in the storey to the total storey shear for a given direction of loading.

A_B the floor area of the diaphragm level immediately above the storey

Ωo seismic force overstrength factor, for concrete shear walls, it is equal to 2.8 (UBC) and 2.5 (NEHRP);

The values of E_h and E_v must be obtained by employing one of the permitted types of structural analysis described in the next paragraph.

Structural analysis

The mathematical model must include all elements of the lateral force-resisting system. The model must also include the stiffness and strength of the elements, which are significant to the distribution of the forces, and must represent the spatial distribution of the mass and stiffness of the structure. The model and the stiffness properties of

reinforced concrete must consider the effects of cracked sections. NEHRP prescribes to use 50% of the gross moment of inertia while UBC requires 35% of the gross stiffness.

Drifts predicted by the analysis must be within the specified limits for the specific seismic group and P-delta effects must be included. The structural analysis must consist of one of the following types: Index Force Analysis, Equivalent Lateral Force Analysis, Modal Response Spectrum Analysis, Linear and Nonlinear Response History Analysis. The choice of the method of analysis is based on the structure seismic design category, the structural system, the dynamic properties, and the structure regularity.

Equivalent lateral force procedure

In the equivalent lateral force analysis method, equivalent static lateral forces are applied to a linear mathematical model of the structure and the lateral forces must be applied in each direction.

Seismic Base Shear

In the NEHRP document, the seismic base shear V, equal to E_h, in a given direction shall be determined in accordance with the following equation:

$$V = C_s W \qquad (2.14)$$

In this equation C_s is seismic response coefficient equal to $S_{DS}/(R/I)$, where S_{DS} is the design spectral response acceleration in the short period range, R is the response modification factor, equal to 4.0 for ordinary reinforced concrete shear walls and 5.0 for the special reinforced concrete walls, and I is the occupancy importance factor. However, the base shear needs not to exceed $S_{D1}/(T\,R/I)$, where S_{D1} is the design spectral acceleration at a period of 1.0 second. A lower limit is set to 0.044 IS_{DS}, except for seismic design categories E and F in which case the limit is equal to $0.5S_1/(R/I)$, where

S_1 is the mapped maximum considered earthquake spectral response acceleration at 1.0 second.

The UBC97 approach is similar. The seismic design force is given by:

$$V = C_v \; W / (T \, R/I) \qquad (2.15)$$

where C_v is seismic coefficient depended from the soil profile type and seismic zone factor, and T is the elastic fundamental period of vibration.

For concrete shear wall building the value of T may by approximated as $T = 0.0488 \; h_n^{3/4}$ or $T = 0.0743/A_c^{1/2}$, where A_c is equal to $\Sigma(A_e.(0.2+D_e/h_n))$. Alternatively, the fundamental period may by calculated using the structural properties and the deformation characteristics of the resisting elements using Rayleigh's method. However, the fundamental period of the structure must not exceed the coefficient for the upper limit on the calculated period, C_u, times the approximate fundamental period of the structure, T_a. Cu varies from 1.4 for site with S_{D1} greater than or equal to $0.3g$ to 1.7 for S_{D1} equal to $0.1g$ or less. This period value ($C_u T_a$) can be used as an alternative to performing an analysis to determine the fundamental period of vibration of the building.

Distribution of the horizontal seismic forces

In NEHRP 2000, the total force shall be distributed over the height of the structure according to the following equation:

$$F_x = [(w_x \, . \, h_x^k) / \Sigma w_i \, . \, h_i^k \,] \, . \, V \qquad (2.16)$$

where k is an exponent related to the structure period. It is equal to 1.0 for structures having a period of 0.5 seconds or less and 2.0 for structures having a period of 2.5 seconds or more. For structures having a period between 0.5 and 2.5 seconds, k can be

determined by linear interpolation between 1.0 and 2.0. UBC97 prescribes a force distribution along the building height similar to the one specified in NBCC:

$$F_x = [(V - F_t)\, w_x .\, h_x\,] / \Sigma w_i .\, h_i \qquad (2.17)$$

where F_t accounts for the effects of the higher modes and is equal to:

$$F_t = 0.07\, T\, V \qquad (2.18)$$

The main difference between the UBC97 and NEHRP provisions is related on how the effects of higher modes are accounted for: UBC97 uses F_t while NEHRP uses the coefficient k.

In the 1997 and earlier editions of the NEHRP provisions, the overturning moment was modified by a factor $\hat{o}$ to account, in an approximate manner, for the effects of the higher mode response in taller structures. In the 2000 edition of NEHRP, the equivalent lateral force procedure was limited to structures that do not have significant higher mode participation and have no vertical stiffness irregularity. The design category is a classification assigned to the structure based on its seismic use and the severity of the design earthquake motion. As a result, it was possible to simplify the design procedure by eliminating the ô factor. According to this new approach, tall structures in Seismic Design Categories B and C designed using the equivalent lateral force procedure need to be designed for somewhat larger overturning demand than under past editions of the provisions. This conservatism is acceptable and encourages design engineers to use a more appropriate dynamic analysis procedure for such tall structures.

Modal response spectrum analysis

The modal response spectrum analysis requirements in UBC and NEHRP are almost identical, and no distinction between the two documents is made herein. A modal

response spectrum analysis must consist of the analysis of a linear mathematical model of the structure to determine the maximum accelerations, forces, and displacements resulting from the dynamic response to ground shaking represented by the design response spectrum. For purposes of analysis, it is permitted to consider the structure fixed at the base or, alternatively, it is permitted to use realistic assumptions with regards to the stiffness of the foundations. A mathematical model of the structure must be constructed to represent the spatial distribution of mass and stiffness throughout the structure. Where the diaphragms are not rigid compared to the vertical elements of the lateral-force-resisting system, the model must include a representation of the diaphragm flexibility and such additional dynamic degrees of freedom as are required to account for the participation of the diaphragm in the structure dynamic response. In addition, the effects of cracked sections must be considered in the stiffness properties of concrete elements the model.

An analysis must be conducted to determine the natural modes of vibration for the structure including the period of each mode, the modal shape vector N, the modal participation factor, and modal mass. It must include a sufficient number of modes to obtain a combined modal mass participation of at least 90% of the actual mass in each of two orthogonal directions. The required periods, mode shapes, and participation factors of the structure must be calculated by established methods of structural analysis for the fixed-base condition using the masses and elastic stiffness of the seismic-force-resisting system. The peak number forces, displacements, story shears, and base reactions for each mode must be combined by recognized methods.

A base shear, V, must also be calculated using the equivalent lateral force procedure. Where the design value for the modal base shear, V_t, is less than 85% of the calculated base shear, V, using the equivalent lateral force procedure, the design story shears, bending moments, drifts, and floor deflections shall be multiplied by the following modification factor: $0.85\ (V / V_t)$.

Elastic, Non-linear time-history and static analysis

A linear response history analysis must consist of an analysis of a linear mathematical model of the structure to determine its response, through methods of numerical integration, to suites of ground motion acceleration histories compatible with the design response spectrum for the site. A mathematical model of the structure must be constructed to represent the spatial distribution of mass throughout the structure. For the purposes of analysis, it is permitted that the structure be considered as fixed at the base or, alternatively, to use realistic assumptions with regard to the stiffness of the foundations. At least three appropriate ground motions shall be used in the analysis. If three time-history analyses are performed, then the maximum response of the parameter of interest shall be used for design. If seven or more time-history analyses are performed, then the average value of the response parameter may be used for design.

When a nonlinear response history analysis is used, the mathematical model of the structure must account for the nonlinear hysteretic behaviour of the structure components. The hysteretic behaviour of elements must be consistent with suitable laboratory test data and must account for all significant yielding, strength degradation, stiffness degradation, and hysteretic pinching indicated by such test data. Strength of elements must be based on expected values considering material overstrength, strain hardening, and hysteretic strength degradation.

In the nonlinear static analysis, the mathematical model of the structure directly accounts for the nonlinear behaviour of the structure's components under an incrementally increased pattern of lateral forces. In this procedure, a mathematical model of the structure is incrementally displaced to a target displacement through application of a series of lateral forces or until the structure collapses and the resulting internal forces, Q_{Ej}, and member deformations at each increment of loading are determined. At the target displacement for the structure, the resulting internal forces and

deflections should be less than the capacity of each element calculated according to the applicable acceptance criteria

Capacity design for wall structures

The overturning moment to be resisted shall be determined using those seismic forces that act on levels above the level under consideration. The height of the plastic hinge above the critical section shall be established on the basis of substantiated test data or may be alternatively taken at $0.5\ l_w$ (one half of the wall length). For structures in high seismic risk areas, the design shear force is evaluated not from applied design loads but from the probable flexural strength of the member under consideration.

2.2.4 ***Seismic design approach in New Zealand and Australia***

Introduction

The New Zealand Building Code (NZS 4203), as well as The Building Code of Australia (AS1170.4), prescribes that the building is to retain its amenity when subjected to frequent events of moderate intensity, and that it is to remain stable and avoid collapse during rare events of high intensity. It is left to the Loadings Standards of New Zealand and Australia to interpret 'moderate' and 'high' loading intensities. This they do by equating the 'amenity' retention as the Serviceability Limit State and collapse avoidance as the Ultimate Limit State loads and combinations of loads. The New Zealand capacity design principles for ductile structural walls and coupled walls involve a requirement for a dependable inelastic mechanism based on wall base flexural hinges and coupling-beam hinges, together with a capacity approach to avoid shear failures.

Design seismic action

In seismic design to the ultimate state, there is only one load combination:

$$U = 1.0\,G + 1.0\,\Psi\,Q + 1.0\,E \qquad (2.19)$$

where:

G dead load;

Ψ reduction factor for ULS live load, usually taken 0.3 (or 0.4);

E earthquake design load, as defined below.

Structural analysis

In the design of a structure, action effects such as bending moments, shear forces and axial forces must be determined at critical sections under the load combinations for both the ultimate and serviceability limit states. Various methods of structural analysis can be used in structural design. The most frequently used method of analysis, based on elastic concepts, is the elastic modal spectrum analysis. Plastic collapse methods of analysis are included as well as more-accurate non-linear methods of analysis based on computer simulation.

The engineer must consider carefully the design implications of all the simplifications and idealizations that are inevitably made in any structural analysis. It is allowed to use linear elastic methods to determine the moments, shears, etc. at both the serviceability and ultimate limit states. While overall elastic behaviour is assumed in the structural analysis to determine moments in the structure as the basis for ultimate strength design, local inelastic action is at the same time assumed in undertaking the strength design of individual cross-sections.

Several empirical formulas are available as the basis for determining the fundamental period of buildings. It is generally preferable to assess the building response based on a realistic distribution of seismic mass at each level up the building and appropriate inter-level structure stiffness. For concrete, a cracked section is appropriate. It is required that reasonable assumptions be made to represent the limit state being considered, and that these assumptions be applied consistently throughout the structure. Within these limits, the designer is free to choose appropriate stiffness values. For walls, the effective moment of inertia depends on concrete strength, steel strength and axial load. Indicative values are given in table C6.4 of New Zealand Standard, Concrete Structures Standard, Draft Number: DZ 3101.2 rel. 1, March 2004, for $N/A_g f'_c$ varying from 0 to 0.2, where N is the axial load and A_g is the gross area section. For ductile shear walls it varies from 0.25 to 0.48 times the value based on gross section geometry and it can be taken equal to 0.7 for moderate ductile walls.

Seismic Base Shear

Capacity design with respect to wall structures relates primarily to the estimation of maximum shear forces that could be generated when the chosen flexural energy dissipating mechanisms are operating at overstrength. The potential plastic hinge will generally be located at the base of the walls. Several studies have indicated that the shear forces induced during the dynamic response of cantilever walls may be considerably higher than the values obtained from the equivalent lateral static forces even when these are scaled up to correspond with the flexural overstrength of the base hinge. Increased shear forces are generated during higher modes of vibration of the entire height of a wall above the plastic hinge at the base, a part of the structure that is intended to remain elastic. It is therefore recommended, when an equivalent static method or first mode spectral method is used, that design shear forces at all levels of structural walls be obtained from:

$$V^*_{wall} = \omega_v \, \phi_o \, V_E < \mu V_E \qquad (2.20)$$

$\phi_o V_E < \mu V_E$, where the value of the dynamic shear magnification factor is equal to $\omega_v = 0.9 + N/10$ for buildings up to 6 stories, and $\omega_v = 1.3 + N/30$, but not larger than 1.8 for buildings over 6 stories, where N is the total number of stories. The flexural overstrength factor $\phi_o = M_{o,w} / M_E$. For calculation of ϕ_o no strength reduction factors must be assumed and longitudinal reinforcement is provided to ensure that the nominal moment is equal to M_E and the reinforcement reaches the strain hardening. The design shear force cannot exceed the value of the elastic base shear, μV_E, where μ is the structural ductility factor and V_E is the design base shear reduced for ductility. The structural ductility factor μ is equal to 2.0 for moderate ductile walls. For a single ductile concrete shear walls μ is equal to $4/k_s$ and $5/k_s$ for two or more structural shear walls. The factor k_s defines the squatness of the wall and $k_s = 2.5 - 0.5A_t$, where A_t is the aspect ratio of the wall. In all cases k_s must taken not less than 1.0 and not larger than 2.0.

It is also recommended that the vertical flexural reinforcement in cantilever wall structures be curtailed so as to give not less than a linear variation of nominal moment of resistance with height. Once the critical section at the base has been detailed, its nominal flexural strength, developed in the presence of the appropriate axial load, can be evaluated. It could conservatively assume that the moment at the base is maintained constant to a height equal to L_w and is varying linearly after to the top of the wall. When a dynamic spectrum method is employed no additional dynamic magnification of shear forces is specified.

Equivalent static method of analysis

The equivalent static method of analysis shall be used only when one of the following criteria is satisfied: the height between the base and the top does not exceed 15 m; the fundamental period of the structure does not exceed 0.40 s or 2.0 s for structures that satisfy the horizontal and vertical regularity requirements. The loading code specifies the following equation for the base shear:

$$V = C_h\,(T_1,\,\mu)\,.\,S_p\,.\,R\,.\,Z\,.\,W, \qquad (2.21)$$

where:

$C_h\,(T_1, \mu)$	spectral coefficient. The spectrum is based on 5% damped elastic response, corresponding to a 459-year return period;
S_p	structural performance factor; S_p = 1.0 for μ less than 1.25 and S_p = 0.67 for μ greater than or equal to 1.25
μ	structural displacement ductility factor;
T_1	first mode of vibration calculated with Rayleigh's method;
R	risk factor;
W	seismic weight.

As an alternative to Rayleigh's method, an empirical equation for calculating the first period can be used. At the service limit state, the fundamental period T_1 for shear wall structures can be approximated as $T_1 = 0.05\ h^{3/4}$. At the ultimate limit state, a longer period can be assumed: $T_1 = 0.0625\ h^{3/4}$.

The equivalent static horizontal force, F_i at each level i is obtained from:

$$F_i = F_t + 0.92V\frac{W_i h_i}{\sum_{i=1}^{n}(W_i h_i)}, \qquad (2.22)$$

where $F_t = 0.08V$ at the top level and 0 elsewhere.

Modal response spectrum

A dynamic analysis of the structure by the response spectrum method must be used to obtain the peak response of the modes. A sufficient number of modes must be

included in the analysis to ensure that at least 90% of the mass of the structure is participating for the direction under the consideration.

Numerical integration time history method

When the numerical integration time history method is used, the building must be subjected to a family of not less than three appropriate ground motion records each of which has been scaled to match the design level earthquake for the limit state and location of the building. The sectional properties assigned to the elements for the time history analysis must be those that result in the most adverse response of the parameter under the consideration with the constraint that they remain within a range appropriate for the limit state under consideration.

2.3 Codes comparison

It is difficult to compare design codes from three different places in the world, Europe, Australia and New Zealand, and North America (USA and Canada), mainly because each code prescribes provisions that address specific characteristics at each site and that are related to the local experience and traditions. However, all codes are based on the assumption that shear walls will respond in the inelastic range during a strong ground motion, dissipating energy through the formation of plastic hinges, generally at their bases, with the rest of the walls assumed to remain elastic. To prevent the formation of plastic hinges elsewhere in a wall and that the wall will not have brittle shear failure, a capacity design approach has been adopted in all modern codes.

The relative design loads for each ductility class shear walls are first compared in Fig. 2.1. The characteristic values were obtained by comparing the modification factor used by each code, $R_d R_o$ in NBCC 2005, q in EC8, R and Ω in UBC97 and NEHRP 2000 and μ in NZS.

As shown, the Canadian code generally compares well with the other codes. NBCC 2005 prescribes the smallest design loads for the low ductility class, corresponding to the conventional construction category. It must be noticed that this type of construction is prohibited in zones with high seismic risk in UBC97 and NEHRP. For the moderate ductile shear walls, NBCC 05 is less permissive with the highest relative design loads compared to all other codes. For the ductile shear walls, NBCC 2005 prescribes design values that are similar to the UBC 97 loads with the redundancy factor equal to one, and that correspond to the average value between the NZS and EC8 forces.

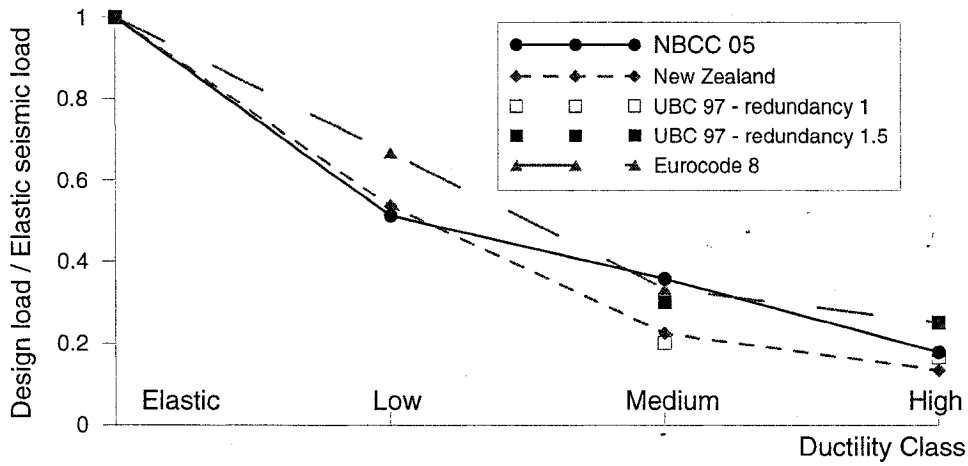

Figure 2.1: Design loads: NBCC05; NZS4203, 1992; UBC 97; EC8.

Next we compare the vertical distribution of the earthquake-induced forces. For this purpose, a Moderately ductile shear wall was designed as a part of a 10-story building located on a firm ground (Site Class C) in Montreal, Qc. The fundamental period of vibration was taken equal to 1.48 s. In order to compare the vertical seismic force profiles, the equivalent lateral procedure of each code was applied assuming the same base shear. Figures 2.2a and 22.b respectively give the resulting horizontal shear force and bending moment values along the height of the structure.

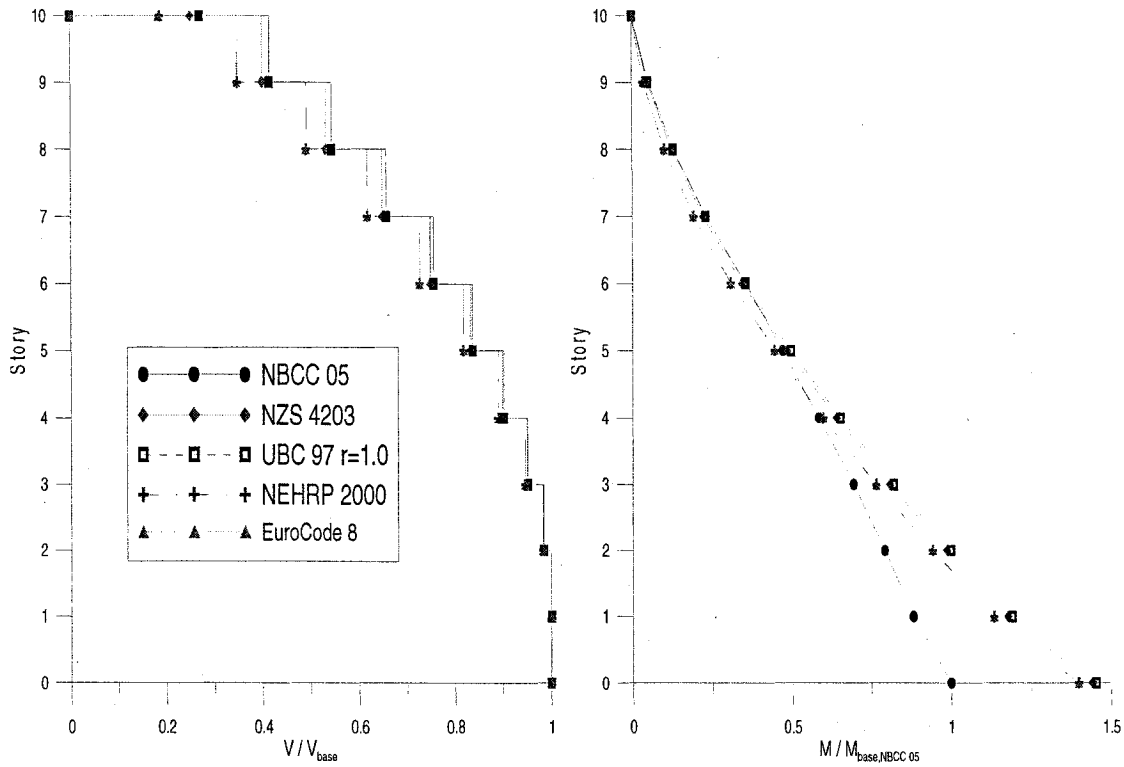

a) Shear force distribution **b) Moment Distribution**

Figure 2.2: Equivalent lateral force procedure: NBCC05; NZS4203, 1992; UBC 97; NEHRP 2000; EC8.

It should be underlined that the values presented do not correspond to actual design forces, but only give the vertical distribution of the lateral seismic force effects. The story shears are nearly the same for all codes over the bottom half portion of the building. The main difference is at the upper floors, where the influence of the various approaches to account for higher mode effects is more pronounced. In NBCC 2005, UBC 97 and NZS, a concentrated force is applied at the top of the building. An exponent related to the structure period is used in the equation for the force distribution in NEHRP 2000 (see *2.2.4*), while nothing is specified in EC8. However, the impact on the resulting flexural moment in Fig. 2.2b is very small. Contrary to the shear distribution, the resulting moments are similar in the upper half of the building. The main difference is in the lower half part and exists only between NBCC 2005 and all other codes. This is attributed to the application of the reduction factor *J* for bending moments. That factor

accounts for higher mode response already included with M_v factor in calculation of shear forces. For this specific wall, the J factor resulted in a 30% reduction of the base moment.

Based on this example, it can be concluded that the equivalent lateral force procedure in all four codes and NEHRP give similar shear forces and vertical distribution. In the four codes, the higher mode effects are taken into account by adding a concentrated force at the top on the building (NBCC 2005, UBC, and NZS) or by distributing the story forces according to the first mode shape. When the equivalent lateral force method is employed according to NBCC 2005, the shear forces are first magnified to account for dynamic amplification for shears due to higher mode effects (factor M_v) and are then used to calculate the moment distribution. To obtain the final moment envelope, the resulting moment at the bottom half of the wall is reduced with a reduction factor J, which depends on the period in the first mode of vibration. Then the design shear is calculated according to capacity design philosophy. The EC8 and New Zealand code use a slightly different approach: the moment envelopes are calculated with non-magnified storey shear forces. The design forces are calculated by combing the capacity design approach with dynamic magnification for shear to account for higher modes effects. In UBC the capacity design approach is also mandatory but no additional amplification for higher modes effects on shear forces is proposed.

However, the equivalent lateral force procedure has a limited application in all codes, and the application of the modal response analysis is the preferred and recommended method for design of earthquake resisting structures. That method would give the same values in all countries, except for the differences that exist between the scaling procedures that must be applied to the results of the dynamic analysis in each country.

2.4 Revue of the scientific literature

Introduction

In the past few years, extensive analytical studies and experimental results were performed on the behaviour of shear walls with different slenderness ratios and subjected to various loading conditions. Studies and findings concerning the vertical distribution and dynamic amplification of the shear forces are presented herein.

It has been shown that the inelastic seismic response of slender walls, characterized by height-over-width ratios equal to or larger than 2.0 is generally controlled by flexural deformations in a plastic hinge at the base of the wall. Numerous studies (Hidalgo et al. 2002, Tu et al. 2000, Kuenzli et al. 2002, Lee et al. 2003, Nilson et al. 2004, Tremblay et al 2006, Pauley 2001, Priestley et al. 2002, Reinhorn et al. 1996, Smith et al. 2002) have also demonstrated the sensitivity of the base shear response in flexural walls to higher vibration modes. Some of these studies offered alternative numerical formulations for the assessment of shear forces. It may not be correct to assume, as is usually done in practice on the basis of elastic analysis, that the shear force demand is proportional to the bending moment demand, even in cases where the effects of higher modes of vibration are considered in the analysis (Priestley et al. 2002, Reinhorn et al. 1996).

Blakeley et al. (1975), studied the response of 12-, 24- and 30-storey shear wall buildings designed according to New Zealand concrete design code. As in all other codes, that code requires structural walls to be capacity designed to ensure that they do not fail in a shear mode if advantage is to be taken of ductile flexural yielding to substantially reduce the seismic design loads. However, their study indicated that higher mode and other dynamic effects would make most of the inelastic seismic deformations of the wall to occur in shear rather than in the expected flexural mode. They concluded

that relatively large reserves of shear strength are required in a shear wall to ensure that inelastic shear deformations are kept to a small proportion of the inelastic demand.

The amplification of the shear forces, as was first quantified in the New Zealand concrete code through a height-dependent shear force amplifier ω_o, is based on the work of Blakeley et al. (1975). Further research works performed by Pauley and Priestley (Pauley, T and Priestley, N. 1992) led to the formulas included in the current design code of New Zealand (NZS 4203), as described in the previous section. Those equations were considered in the determination of the design shear forces and resulted in a dynamic base shear magnification factor reaching a maximum value of 1.8.

In the work by Hassan and Sherif El-Tawil (El-Tawil S., & Hassan, M 2004) on the inelastic dynamic behaviour of hybrid coupled and uncoupled walls as a part of 12-storey building, a base shear magnification computed with the equation proposed in New Zealand Code, $\omega_v = 1.3 + N/30$, which, in this case, is equal to 1.7 was found inadequate. Static pushover analyses indicate that total base shears for both coupled and uncoupled systems are almost identical and equal. However time history analyses for both systems showed that the base shears do increase well beyond this value under dynamic loading. It was shown that the median base shear reached for the uncoupled system is larger than the base shear for the coupled system. When compared to pushover results, dynamic base shear magnification reaches 44% for the coupled system and 87% for the uncoupled one. This indicates that higher mode effects are somewhat more prominent in the uncoupled walls versus the coupled walls. Furthermore, it appears that the equation *for* w_v is rather inaccurate and needs to be refined to more accurately pick up differences in structural characteristics.

Recent studies (Tu et al. 2000, Tremblay et al 2006, Priestley et al. 2002) on the behaviour of cantilever walls showed that both multi-mode analysis and conventional capacity design methods are non conservative in predicting the distribution of bending

moments and shear forces along the height of cantilever walls. In fact, all studies showed that the current dynamic amplification for moments and shears, especially in cantilever walls, is inadequate. Dynamic amplification was found to be highly dependent on higher mode effects, with second mode response dominating.

In an analytical research project carried out by Amaris and Priestley (2002), the influence of seismic intensity on the higher mode response of cantilever structural walls and, indirectly, the validity of the design forces determined by multi-mode analysis, are investigated. Six walls, varying from 2 to 20 storeys, were designed to the Eurocode 8 elastic acceleration response spectrum compatible with a peak ground acceleration of 0.4 g, and a medium soil condition (subsoil class B, deposits of medium dense sand, gravel, or medium stiff clays). They found an important amplification for the shear forces, varying from 1.0 to 1.8, through the entire height of the walls. They found that the dynamic amplification was highly dependent on the higher mode effects, with second mode response dominating. To account for the influence of the higher modes, Priestley and Amaris proposed a modification to the multi-mode analysis method. In this model, higher mode effects are not reduced by the effective behaviour factor for ductility. The method was found to give a good representation of both moment and shear envelopes at seismic intensities up to twice the design intensity. This Modified Modal Superposition method (MMS) extends and modifies an approach originally developed by Eibl and Kreintzel (1988) for the base shear force of cantilever walls. As a result of further work on this method, Priestley (Priestley et al. 2002) proposed to use the following formulas for the calculation of the design values for shear forces and bending moments:

$$V_i = \sqrt{V_{1i}^2 + V_{2Ei}^2 + V_{3Ei}^2 + ... + V_{nEi}^2} \qquad (2.23)$$

where:

V_{1i} = inelastic first mode shear force at level *i*. (elastic shear force divided by the applicable ductility-related force modification factor)

V_{2Ei} = elastic second second and higher mode shear force at level *i*.

$M_i = 1.1 * \sqrt{M_{1i}^2 + M_{2Ei}^2 + M_{3Ei}^2 + ... + M_{nEi}^2}$ where:

M_{1i} = inelastic moment in the first mode at level *i*.

V_{2Ei} = elastic second and higher mode moment at level *i*.

As shown, the force reduction for ductility is only applied to the first mode quantities. The equation for the bending moment calculation applies only over the top half of the wall and has a linear profile from mid-height to the wall base.

An equivalent simplified procedure was presented as well, where an amplification factor for shear that depends on the period T and the displacement ductility factor μ, but not the number of storeys: $\omega_v = 1 + \mu B_{(T)}$, where $0.067 \leq B_{(T)} = 0.067 + 0.4\ (T - 0.5\ ) \leq 1.15$. The design values for shear must be calculated from the equation $V_R = \phi_o\ \omega_v\ V$. For a design moment profile, he proposed a bilinear model, with a moment at mid-height equal to 0.75 times the base moment, which accounts for a higher ductility demand in the upper storeys of the wall.

Humar and Mahgoub (2003) carried out an extensive study on the distribution of the base shear over the height of a structure in the context of the equivalent static force procedure of the 2005 NBCC. The lateral seismic force distribution in NBCC is primarily in the form of the first mode shape, however, the resulting overturning moments generally overestimate the true moments, which arise from a combination of various modes. The distributions of shear forces and the adjustment factor J to be applied to the overturning moments has been determined by comparing the values obtained from the equivalent static force procedure and the modal response analysis method. The calculations were performed for various structural systems and for both

eastern and western Canada. The following conclusions concerning cantilever shear wall structures are drawn from their study:

- "The base shear adjustment factor M_v and the overturning moment reduction factor J are both dependent on the characteristics of the lateral force resisting system. The factor M_v is largest for a flexural wall system and smallest for a moment-resisting frame. On the other hand, J is smallest for a flexural wall and largest for a moment-resisting frame.
- The factors M_v and J also depend on the first mode period T_a. Thus M_v increases with an increase in T_a, whereas J decreases with an increase in T_a.
- The factors M_v and J strongly depend on the shape of the response spectrum. Compared with the western regions of Canada, the UHS for the eastern regions drops more rapidly with an increase in period. Thus the higher mode contribution is more predominant in the east; as a consequence, M_v values are larger ($M_v \approx 3.75$ for $T_1 = 3.0$ sec) and J values smaller for the eastern region."

In the last few years, research studies were conducted at Ecole Polytechnique of Montreal on cantilever reinforced concrete shear walls [10, 23, 32, 35, 47]. In all of those works, it was found that inelastic demand was not constrained only to the bottom of the walls, as assumed by current design provisions. At levels above the base, and particularly at wall mid-height, the moments were found to increase very significantly. The magnitude and distribution of the storey shear forces are different from those implied by the NBCC static design procedure. The modal analysis procedure provided a better distribution of the shear resulting from time-history analysis. A dynamic shear force amplification factor accounting for higher mode effects was found inadequate generally for the high-rise shear wall buildings, which usually have long first mode period. It was found that plastic hinging, which would be the consequence of designing to the multi-modal moment envelopes at levels above the base is possible and

undesirable, some limited ductility demand should be sustainable without failure. The consequences of the imposed shear demand exceeding the shear capacity could be catastrophic shear failure.

Filiatrault et al. (1993) conducted an extensive study on the behaviour of RC shear walls designed according to NBCC 1990 and CSA-A23.3-84. They studied the dynamic response of 3, 6, 10, 15, and 25-storey buildings located in three different seismic zones in Canada: Montreal, Vancouver, and Prince Rupert. They found an important amplification for shear forces for Montreal and Vancouver, between 1.0 and 1.93, and negligible for Prince Rupert 0.86 to 1.21. They also found a negative correlation between the dynamic amplification and the number of storeys, thus contrary to the New Zealand Code amplification factor. The good correlation of code provisions and the results from nonlinear analysis for Prince Rupert is explained by differences in the frequency content of the ground motions: the buildings at that site responded primarily in their fundamental model of vibration. Conversely, the buildings located in Montreal and Vancouver responded primarily in higher modes of vibration with significant influence of the second and third modes.

Tremblay et al. (2000), examined the P-delta effects on 12-storey shear wall buildings located in Montreal and Vancouver. The structures were designed according to NBCC 1995 and CSA-A23-3-94. They found that formation of plastic hinges can occur not only at the base, where a special confining is provided, but also in the upper part of the wall. The NBCC static design procedure was found to underestimate the shear forces in the wall. When the dynamic amplification factor from New Zealand Code is applied to NBCC modal analysis procedure, the distribution of story shears compares better to the shears resulting from the application of ground motion records. A dynamic shear force amplification factor accounting for higher mode effects must be considered to prevent shear modes of failure in ductile RC shear walls.

In his study of the behaviour of RC shear walls, Personeni (2004) found an average amplification factor for the shear force $M_{v,stat,avg.} = \frac{V_{epp}}{V_{stat}} \approx 3.0$, where V_{epp} is the base shear obtained from nonlinear analysis. For the seismic action in the west of Canada for buildings in the range of 5 to 25 floors, it was found that $M_v \approx (1.8 - 2.0)$. For the east, M_v ranged between 3.0 and 3.50. He proposed the formulas presented in Table 2.3, for magnification factors to be applied to shear forces obtained from the equivalent static force procedure, $M_{v,stat}$, and from the response spectrum modal analysis $M_{v,modal}$:

Table 2.3: Amplification factor for Equivalent static and Modal Response Procedures according to NBCC05.

Factor	East Canada	West Canada
$M_{v,stat} = \frac{V_{epp}}{V_{stat}}$	$\frac{n}{25} + 2.3$	1.8
$M_{v,mod} = \frac{V_{epp}}{V_{stat}}$	$\frac{n}{5} + 1.3$	$\frac{n}{50} + 1.8$

Pannenton et al. (2006) studied the inelastic behaviour of an 8-story shear wall building located in Montreal and designed according to NBCC 1995 and CSA-A23-3-94. He conducted the equivalent static and modal procedures according to NBCC 2005 (draft 2003) and CSA-A23-3-04 and three-dimensional dynamic inelastic time-history analysis to evaluate the impact of the new design requirements for shear wall structures. He found a large ductility demand in the upper part of the building and the formation of plastic hinges above the protected zone defined by the code, even when the capacity design approach was used. When the modal spectrum analysis is used, the mean dynamic amplification for shear was evaluated equal to 2.1 at the base of the walls and

2.57 in the upper stories, much higher than the 1.57 value computed according to New Zealand provisions.

It can be stated in summary that a significant amplification of the shear forces throughout the wall height and the possibility of formation of plastic hinges in the unprotected upper half of shear wall structures was observed in all studies examined. These problems are studied in detail in Chapter 4 and conclusions and correction factors are proposed to address these issues.

CHAPTER 3

DESIGN OF THE BUILDINGS ACCORDING TO NBCC 05 AND CSA – A23.3-04

3.1 Studied problem

A parametrical study was undertaken to achieve a better understanding of the seismic behaviour of reinforced concrete shear wall buildings. The parameters taken into consideration were the site and the height of the buildings (hence the fundamental period of vibration). The choice of the geometry and the floor seismic weight for the studied buildings was based on an extensive literature review. The data for sixty buildings braced with shear walls reported in the scientific literature was collected. The location of the buildings (most of them were located in California), the geometrical properties, the seismic weights, the moment of inertia of the walls, and the theoretical and measured fundamental periods are summarized in Appendix A. As a result, a total of ten buildings were chosen to be studied: five situated in Montreal, Quebec, and five located in Vancouver, British Columbia. The buildings at both sites have the same geometrical properties with 30 m x 30 m plan dimensions and a total height ranging from 15 to 75 m (five, ten, fifteen, twenty and twenty-five storey buildings).

In view of the fact that the empirical formula for the fundamental lateral period for shear wall structures in NBCC 2005 was developed for buildings located in California and that the seismicity for Vancouver and Montreal is lower than in California, the fundamental periods of the buildings studied were set longer than the values given by the NBCC 2005 empirical period equation, $T_a = 0.05 h_n^{0.75}$: 2.0 times for the Vancouver buildings and 2.5 times for the structures in Montreal. For instance, the 0.2 s spectral acceleration for 2% exceedence in 50 years for different regions in California varies between 0.8 g to 2.0 g, while it is equal to 0.94 g for Vancouver and 0.69 g for Montreal.

The difference between Vancouver and Montreal is also justified by the lower seismicity in Montreal. The geometrical properties of the walls were chosen to meet these target fundamental periods applying the NBCC 05, when considering the effective flexural stiffness properties specified in Clause 21.2.5.2.1 of CSA A23.3-04 requirements. The design of the walls was based on these fundamental periods while complying with the minimum lateral seismic force requirements of NBCC 2005. In the calculation of the wall properties, only the wall axial load due to dead load was considered. The final building fundamental periods, T_1, and the geometrical properties of the walls are given in Table 3.1. The different types of sections were chosen to obtain the target fundamental periods with practical wall dimensions. The I-wall type is a wall section with square columns at both ends, where b_w is the web width, b_{col} is the column dimension and L_w is the total length of the wall. The C-wall type is a channel type section where b_w is the web width, b_{col} is the length of the flange wall, and L_w is the total length of the wall (web wall). The wall fundamental periods are shown in figure 3.1.

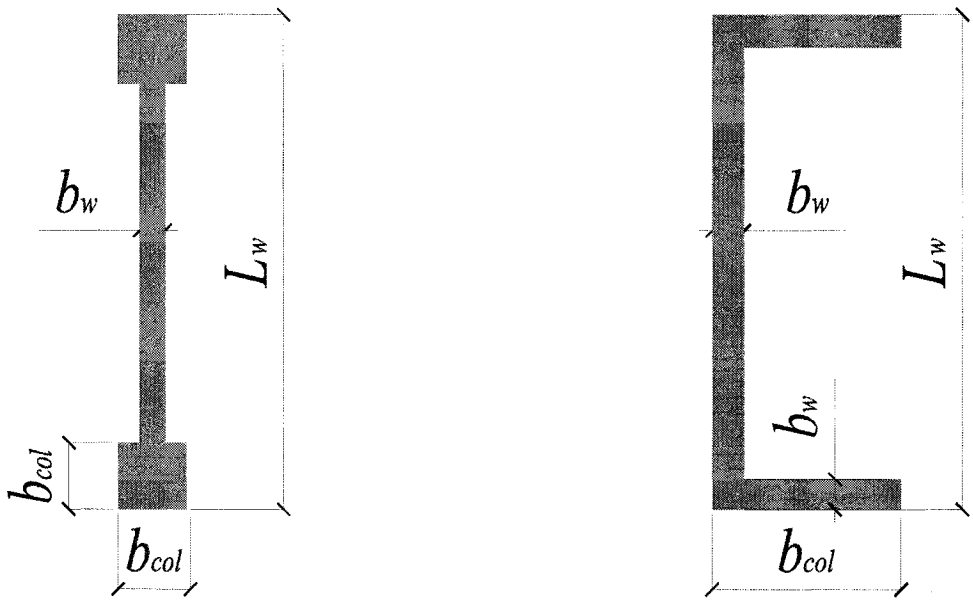

a) I section **b) ⊏ Section**

Figure 3.1 Geometrical properties of the walls studied: a) 5-, 10- and 15-story building; b) 20- and 25-story building.

Table 3.1 Natural fundamental periods of the buildings and geometry of the walls

h_n	T_a	Wall	Vancouver				Montreal			
(m)	(s)	type	T_1 (s)	b_w (m)	b_{col} (m)	L_w (m)	T_1 (s)	b_w (m)	b_{col} (m)	L_w (m)
15	0.38	I	0.645	0.250	0.400	5.200	0.943	0.200	0.400	4.000
30	0.64	I	1.320	0.250	0.450	7.450	1.605	0.200	0.450	6.650
45	0.87	I	1.733	0.250	0.450	10.500	2.148	0.200	0.500	9.200
60	1.08	C	2.131	0.300	3.000	10.500	2.675	0.300	3.000	8.000
75	1.27	C	2.577	0.300	4.000	11.000	3.190	0.300	3.500	9.500

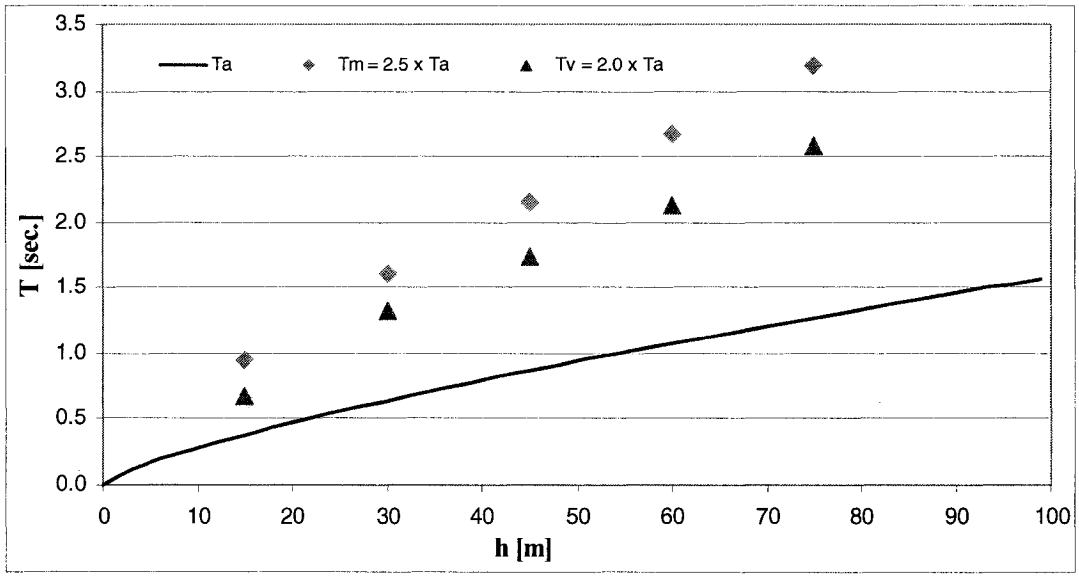

Figure 3.2 Computed fundamental periods of the buildings and NBCC 2005 empirical fundamental period T_a for shear wall structures.

Some generalizations and simplifications were assumed in the design process. First, the buildings were assumed to have uniform plan dimensions of 30 m x 30 m and a uniform storey height of 3.0 meters at all floors, as typically found for office buildings built with reinforced concrete. A typical floor plan lay-out is shown in figure 3.3. The lateral resistance was assumed to be entirely provided by two cantilevered shear walls

per direction that were symmetrically located in plan with respect to the centre of the buildings.

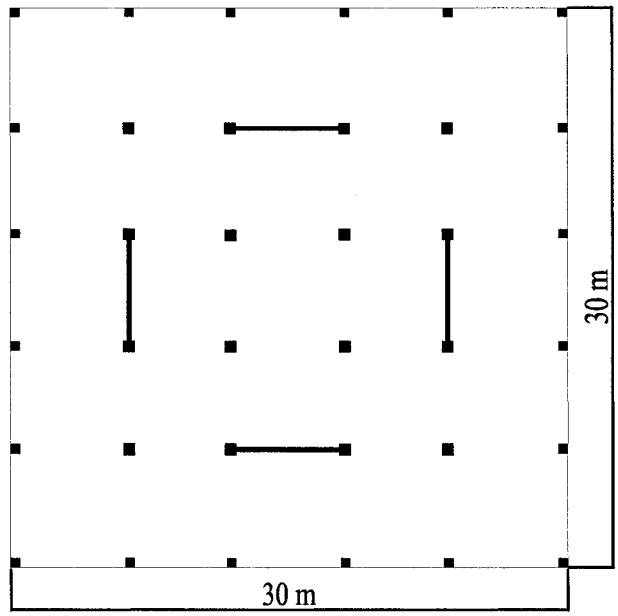

Figure 3.3 Typical 30x 30 m storey layout.

Secondly, based on available data for buildings listed in Appendix A, an average uniform seismic weight of 6000 kN per floor was selected for all structures. An average constant axial force due to dead loads acting on the walls, P_D , was taken equal to 504 kN per floor, which gives values of $P/[f'_c.A_g]$ ranging between 0.07 to 0.095 at the base of all buildings (f'_c = 30 MPa).

Site class C was chosen for the ground conditions, corresponding to very dense soil and soft rock with shear wave average velocity between 360 and 760 m/s. The acceleration- and velocity-based site coefficients, F_a and F_v, are then equal to 1.0 for all segments of the response spectrum. The importance factor I_E was set equal to 1.0 for all buildings. The design spectrum at both sites is given in Table 3.2.

The torsional effects were taken into account by magnifying the lateral seismic forces considered in the design of the walls. The torsional sensitivity of the buildings due to accidental eccentricities was evaluated by varying the geometrical position of the lateral load resisting system in the plan lay-out. The amplification of the lateral forces due to torsion was found to vary from 10% to 50% with an average value of 40%. The average value of 40% for this magnification factor was found realistic and was assumed for all buildings. As discussed later, the amplitude of the ground motions used in the seismic analyses were increased accordingly.

3.2 Design of the buildings

All the buildings were designed using the seismic provisions of NBCC 2005 and CSA-A23.3-04. The design for flexure was done with the computer programme W-SECT 6.02 and the design for shear resistance was performed with with a dedicated Excel spreadsheet. As was mentioned before, the analysis for design earthquake actions was carried out in accordance with the dynamic analysis procedure described in NBCC 2005. The equivalent static force procedure (ESFP) could have been used, but the structures had to meet any of the following criteria:

a) $I_E F_a S_a(0.2)$ is less than 0.35;
b) Regular structures must be less than 60 m in height and have a fundamental period, T_a, less than 2 s in each direction, or
c) Structures with structural irregularities Type 1, 2, 3, 4, 5, 6 or 8 as defined in Table 4.1.8.6 must be less than 20 m in height and have a fundamental lateral period, T_a, less than 0.5 s in each of two orthogonal directions.

Table 3.2 Design spectral ordinates, S

T (s)	≤ 0.2	0.5	1.0	2.0	≥ 4.0
Vancouver	0.94	0.64	0.33	0.17	0.085
Montreal	0.69	0.34	0.14	0.048	0.024

The buildings with 15, 20 and 25 floors in Montreal and the buildings with 20 and 25 floors in Vancouver do not meet the second criteria, which makes the ESFP non applicable for these cases. To ensure consistency in design, the dynamic analysis method was selected for all structures. However, the ESFP was carried out for seismic force scaling purposes as well as for comparison of the two methods.

To make a final choice for the design of the studied buildings, all buildings were analyzed and designed for force modification factors R_d of 3.5 and 2.0, corresponding to the Ductile and Moderately Ductile categories of shear walls. In NBCC 2005, there is only one load combination that includes earthquake loads, as given in Table 4.1.3.2 of NBCC. The principal load combination is given by *(1.0D + 1.0E)*, and companion loads of *(0.5L+0.25S)*, where *D*, *L* and *S* are respectively the dead, floor live, and roof snow loads. During the design, it was found that the participation of the principal loads alone gives the most critical condition for the quantity of wall flexural reinforcement. The resulting moment and shear factored demand to capacity ratios for the section at the base of walls are given in Table 3.3.

Table 3.3 Results of the preliminary design at the base of the buildings (ratios in %)

Site	Montreal T= 2.5 x Ta				Vancouver T= 2.0 x Ta			
Mod. factor	R_d = 2.0		R_d = 3.5		R_d = 2.0		R_d = 3.5	
Storey	M_f/M_r	V_f/V_r	M_f/M_r	V_f/V_r	M_f/M_r	V_f/V_r	M_f/M_r	V_f/V_r
5	99.3	96.5	75	98.6	162	140	99.0	99.9
10	97.9	99.8	45.7	97.4	134.5	120	97.6	97.2
15	79.6	98.5	31.5	104	117.8	108.5	86.7	99.5
20	76.2	96.7	31.02	97.7	98.5	131.4	84.8	99.5
25	82.2	94.5	28.7	96.4	99.5	95.7	77.9	93.75

In this table the values of M_f and V_f correspond to design values obtained with the dynamic (response spectrum) analysis method and scaled, when necessary, to the forces corresponding to 80% of the base shear calculated with the ESFP, as described in Clause

4.1.8.12.6 of NBCC 05. It should also be noticed that V_f is the shear force based on capacity design provisions. Details on how these calculations are performed are presented later for the 10-storey structure located in Vancouver.

For the buildings located in Montreal and designed with the ductility-related force modification factor of 3.5, the minimum requirements governed the choice of the flexural reinforcement, together with capacity design principles, led to a significant increase in the required amount of shear reinforcement, thus an ineffective utilization of the material, especially for the steel reinforcement. The opposite conclusion could be made for the buildings located in Vancouver. It was found that the shear area of the walls designed with $R_d = 2.0$ was not sufficient and the shear stresses exceeded the maximum allowed values, which required an increase of the wall thickness.

Based on those conclusions, the final choice of the sample buildings for complete design and the subsequent seismic analysis phase was made: buildings designed with ductile shear walls ($R_d = 3.5$) for Vancouver, and shear walls with moderate ductility ($R_d = 2.0$) for Montreal.

3.3 Design example

As a design example, we will use the ten storey building located in Vancouver with ductile shear walls designed with a force modification factor $R_d = 3.5$. The reinforced concrete office building has a seismic force resisting system made of four simple shear walls, two in each direction, as illustrated in figure 3.3. Each floor consists of a 200 mm thick flat plate with 6 m spans. All exterior columns are 450x450 mm throughout the height and the interior columns have cross sections varying from 550x550 mm to 450x450 mm along the building height. The shear walls are located along interior bays of the building and have a uniform thickness of 250 mm, with

450x450 mm end columns and a total length of 7450 mm. The design data can be summarised as follows:

1. Material properties

Concrete: normal density concrete (24 kN/m^3) with $f_c' = 30$ MPa

Reinforcement: $f_y = 400$ MPa.

2. Gravity loads

As gravity loads we assumed floor live loads of 2.4 kN/m^2 on typical office floors and 4.8 kN/m^2 on 12 m by 12 m corridor area. For the floor dead loads we assumed a 24 kN/m^3 density for the reinforced concrete members, 1.0 kN/m^2 for partition loading on all floors, 0.5 kN/m^2 for ceiling and mechanical services loading on all floors and 0.5 kN/m^2 for the roof insulation, which gives a total dead load of 6.67 kN/m^2, or a total seismic weight per floor of 6000 kN, assumed in the calculations. The total seismic weight per wall used for analysis is 3000 kN. The building has no structural irregularities. Dimensional limitations for the wall: $w \leq l_u$ / 10 = 2800/10 = 280 mm within a plastic hinge or $b_w \leq l_u / 14$ = 2800/14 = 200 mm within a plastic hinge (Clause 21.6.3.3 to 21.6.3.5), where b_w is the wall thickness within a plastic hinge and l_u is the nominal height of the wall section under consideration.

3. Seismic loading

The NBCC 2005 stipulates that the analysis for design earthquake actions shall be carried out in accordance with the dynamic analysis method, except that the ESFP Procedure may be used for structures that meet any of the criteria described in Clause 4.1.8.7.1, as explained earlier.

3.1 Equivalent Static Force Procedure (ESFP)

The procedure is applied to obtain the base shear value that will be used subsequently for scaling of the dynamic lateral earthquake design force V_d. The static

value is also computed for the sake of comparing base shear forces and bending moments obtained from both methods of analysis. For the buildings located in Vancouver, the 5% damped spectral response accelerations at 0.2 s and 2.0 s are respectively equal to: $S_a(0.2) = 0.94g$ and $S_a(2.0) = 0.17g$ (Table 3.2). For Site Class C, the acceleration-based site coefficient F_a and the velocity-based site coefficient F_v are both equal to 1.0. The lateral earthquake force V depends on the fundamental period T_a of the structure. For shear wall structures, $T_a = 0.05\ h_n^{3/4}$, where h_n is in meters. For the building, $T_a = 0.05(30)^{3/4} = 0.64$ s. Since, it is expected that the fundamental period will be much longer than 0.64 s, we will take advantage of the NBCC Clause 4.1.8.11.3.d.iii) which allows the use of the upper limit of 2.0 T_a for the determination of V. This gives a fundamental period $T_a = 1.28\ s$. The minimum lateral force V is:

$$V = \frac{S(T_a)\ M_V\ I_E\ W}{R_d\ R_o} \qquad (3.1)$$

In addition, $V \geq S(2.0)\ M_v\ I_E\ W\ /\ (R_d\ R_o)$ and, for R_d equal or greater than *1.5*, V need not to be taken greater than $2/3S(0.2)I_E\ W/(R_d\ R_o)$. In these equations, M_v is the higher mode effect factor, I_E is the earthquake importance factor of the structure, W is the seismic weight of the building, R_d is the ductility related force modification factor and R_o is the overstrength related force modification factor.

- Determination of M_v ($T_a = 1.28$ *sec.)*

-$S_a(0.2\text{ s})/S_a(2.0\text{ s}) = 0.94/0.17 = 5.53 < 8.0$

Using table 4.1.8.11

-$S(1.0\text{ s}) * M_v(1.0\text{ s}) = 0.33 * 1.0 = 0.330$

-$S(2.0\text{ s}) * M_v(2.0\text{ s}) = 0.17 * 1.2 = 0.204$,

$S_a(1.28\text{ s}) * M_v(1.28\text{ s}) = 0.2947$

As indicated, the designs for Vancouver are carried out with force modification factors $R_d = 3.5$ and $R_o = 1.6$, and the importance factor I_E is taken equal to 1.0.

$V = [S(T_a) * M_v] * I_E * W / (R_d * R_o)$

$V = 0.2947 * 1.0 * W / (3.5 * 1.6) = 0.05263 * W$

$V_{min} = 0.204 * 1.0 * W / (3.5 * 1.6) = 0.03643 * W$

$V_{max} = 2/3 * 0.94 * 1.0 * W / (3.5 * 1.6) = 0.1119 * W$

$V = 0.05263 * W = 1578.75$ kN

After including the torsional effects by multiplying V with 1.4, we obtain: $V =$ 2210 kN.

- The calculations of the seismic lateral forces at each level are summarized in Table 3.3.3. The concentrated force at the top F_t is equal to:

$F_t = 0.07 * T * V = 0.07 * 1.28 * 0.05263 * W = 0.00472 * W$

- The total lateral seismic force is distributed along the height of the building in accordance with the formula:

$F_x = (V - F_t) * W_x * h_x / (\Sigma W_i * h_i)$

- The structure must be designed to resist the overturning moment determined from the following equation:

$M_x = J_x S F_t (h_i - h_x)$, where

$J_x = 1.0$ for $h_x \geq 0.6 h_n$

$J_x = J + (1 - J) (h_x / 0.6h_n)$ for $h_x < 0.6 h_n$

To calculate J we interpolate for T_a=1.28 s. between $J = 1.0$ for $T = 1.0$ s and $J =$ 0.7 for $T = 2.0$ s. In our case, it is found that $J = 0.84$. Applying the equation for J_x we calculate the reduction factor for moments at each level, reported in Table 3.4.

Table 3.4 Reduction factors for moments - Equivalent Static Force Procedure

Story	1	2	3	4	5	6	7	8	9	10
J_x	0.844	0.870	0.896	0.948	0.974	1.0	1.0	1.0	1.0	1.0

The computed values for F_x, J, J_x, and the bending moments are given in Table 3.5.

Table 3.5 Design forces - Equivalent Static Force Procedure

Floor	h_x	W_i	h_x*W_i	F_x	h_i	V_d	$M_d \cdot J$	$V_{f,d}$*	$M_{f,d}$*
No	m	kN	kN-m	kN	m	kN	kN-m	kN	kN-m
1	3	3000	9000	26.13	3.00	1578.75	29057.83	2210.25	40680.96
2	6	3000	18000	52.26	3.00	1552.62	25832.44	2173.67	36165.41
3	9	3000	27000	78.39	3.00	1500.36	22430.99	2100.51	31403.39
4	12	3000	36000	104.52	3.00	1421.98	18931.89	1990.77	26504.64
5	15	3000	45000	130.64	3.00	1317.46	15421.66	1844.45	21590.32
6	18	3000	54000	156.77	3.00	1186.82	11994.99	1661.54	16792.99
7	21	3000	63000	182.90	3.00	1030.04	8754.74	1442.06	12256.63
8	24	3000	72000	209.03	3.00	847.14	5664.61	1186.00	7930.45
9	27	3000	81000	235.16	3.00	638.11	3123.18	893.35	4372.46
10	30	3000	90000	402.95	3.00	402.95	1208.85	564.13	1692.39

* $V_{f,d}$ and $M_{f,d}$ – Design forces including torsional effects

3.2 Dynamic Analysis Procedure – Modal Response Spectrum Method (MRSM)

The structure was analyzed with the structural program SAP2000 using a cantilever beam model as shown in figure 3.4.

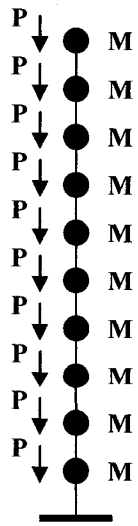

Figure 3.4 Computational model – 10-storey building

As discussed earlier, torsional effects in the analysis were accounted by multiplying the lateral forces by a factor of 1.4. The effective properties were calculated at every level of the wall in accordance with Clause 21.2.52.2 and Table 21.1 of CSA A23.3. For walls: $A_{xe} = \alpha_w A_g$ and $I_e = \alpha_w I_g$, where $\alpha_w = 0.6 + P_s/f'_c A_g \leq 1.0$. The resulting cross sections and stiffness are shown in Table 3.6.

Table 3.6 Calculation of the effective wall flexural properties

Storey	Axial force, P_s (kN)	$\alpha_w = I_{eff} / I_g$
1	5040	0.682
2	4536	0.674
3	4032	0.666
4	3528	0.658
5	3024	0.649
6	2520	0.641
7	2016	0.633
8	1512	0.625
9	1008	0.616
10	504	0.608

Clause 4.1.8.12

- The modal superposition analysis was performed using all possible modes, i.e. 5 modes for the 5-storey buildings to 25 modes for the 25-storey buildings, assuming 5% damping in each mode, and using the SRSS combination rule with the design spectrum values given in Table 3.1.
- The elastic base shear V_e from modal analysis was multiplied by the factor I_E (= 1.0) and divided by $R_d R_o$ (= 3.5*1.6 = 5.6) to obtain the earthquake design base shear, V_d.
- The lateral deflections obtained from the modal analysis were multiplied by $R_d R_o / I_E$ to give realistic values of the anticipated deflections.

V_e = 8269 kN

$V_d = V_e * I_E / (R_d * R_o)$

$V_d = 8269 * 1.0 / (3.5 * 1.6) = 1476$ kN

By adding the torsional effects, it is found that:

$V_d = V^*_d * 1.4 = 1476 * 1.4 = 2067$ kN

Clause 4.1.8.12.6 specifies that V_d must not be less than 80% of the lateral earthquake design force V, of article 4.1.8.11 for regular structures. In this case, V_d = $2067 \geq 0.80 * 2210 = 1768$ kN, and there is no need for scaling the design forces. For consistency, the design forces obtained from the Modal Response Method were however multiplied by 1.4 to account for the accidental torsional effects. The resulting shears and bending moments are given in Table 3.7.

As required in Clause 21.6.2.2, ductile walls must be detailed for plastic hinging over a critical zone, or plastic hinge region, having a height equal to at least 1.5 times the length of the longest wall above the design critical section, i.e. 1.5 L_w above the wall bases for the structures studied herein. The flexural and shear reinforcement required at the critical section must be maintained over the height of the critical zone. Above the critical zone, the design overturning moment and shear forces, M_d^{**} and V_d^{**}, respectively, must be increased by the ratio of the factored moment resistance to the applied factored moment, k_d, both calculated at the top of the plastic hinge region.

Clause 21.6.9.1 requires that walls have a factored shear resistance greater than the shear due to the effects of factored loads, accounting for the magnification of the shear due to the inelastic effects of higher modes. In addition, the factored shear resistance must not be less than the smaller or the shear forces corresponding to the development of the probable moment capacity of the wall system at its plastic hinge location, M_p, or the shear force calculated using $R_d R_o$ equal to 1.0. The design shear above the plastic hinge zone was assumed equal to the higher value of V^{**} and $\gamma_p V_{f,d}$. Calculating the design shear using Clauses 21.6.2.2 and 21.6.9.1:

Plastic hinge height: $l_p \geq 1.5\, L_w = 1.5 * 7.45$ m = 11.18 m

thus, assume l_p = 12.0 m (four storeys)

In the plastic hinge zone, $\gamma_p = M_p / M_f = 43540 / 32365 = 1.34$;

For levels 1 to 4, $V_d = \gamma_p * V_{f,d}$

Above the plastic hinge $k_d = M_{r,4}^{top} / M_{f,5}^{bottom} = 29360 / 16022 = 1.83$.

It is noted that $M_{f,4}^{top} = M_{f,5}^{bottom}$ and that the factor k_d is therefore computed at the same height.

For storeys 5 to 10: $M_d = k_d\, M_{f,d}$

$V_d = k_d\, V_{f,d}$

The values of M_p and M_r were calculated with W-SECT programme. All dynamic and design forces are summarized in Table 3.7.

Table 3.7 Calculation of the design forces

No	h_x	P	V_{dyn}	M_{dyn}	$V_{f,d}$*	$M_{f,d}$*	M_d **	V_d **
	m	kN	kN	kNm	kN	kNm	kNm	kN
1	3.00	-5040.00	1476.66	23118.44	2067.32	32365.82	**43370.19**	**2770.21**
2	6.00	-4536.00	1398.91	19551.20	1958.47	27371.68	**36678.05**	**2624.36**
3	9.00	-4032.00	1263.82	16397.94	1769.35	22957.12	**30762.54**	**2370.93**
4	12.00	-3528.00	1102.53	13718.94	1543.54	19206.52	**25736.73**	**2068.35**
5	15.00	-3024.00	950.64	11444.33	1330.90	16022.06	**29360.00**	**2438.83**
6	18.00	-2520.00	840.09	9403.02	1176.13	13164.23	**24123.10**	**2155.22**
7	21.00	-2016.00	779.67	7406.34	1091.54	10368.88	**19000.69**	**2000.21**
8	24.00	-1512.00	739.37	5343.84	1035.12	7481.38	**13709.42**	**1896.83**
9	27.00	-1008.00	653.58	3244.10	915.01	4541.74	**8322.62**	**1676.74**
10	30.00	-504.00	438.76	1316.29	614.26	1842.81	**3376.89**	**1125.62**

*** $V_{f,d}$ and $M_{f,d}$ – Design forces including torsional effects**

**** Final design forces, except that the moment M_{fd} at the base was used for the reinforcement steel of the first 4 storeys.**

Comparing the design values obtained with the NBCC 2005 Equivalent Static Force Procedure and the Modal Response Spectral Method, we found a good match between both methods. Both sets of values are plotted in figure 3.5. The dynamic base design shear is equal to 94% of the static base shear, so there is no need for scaling the dynamic forces. The dynamic shear forces are even larger at the top floors of the building: 102% of the static force at the 9th floor and 109% at the 10th floor. The base moment from dynamic analysis is 80% of the static one at the base. As shown, it is smaller than the static value over the entire building height except in the top two storeys.

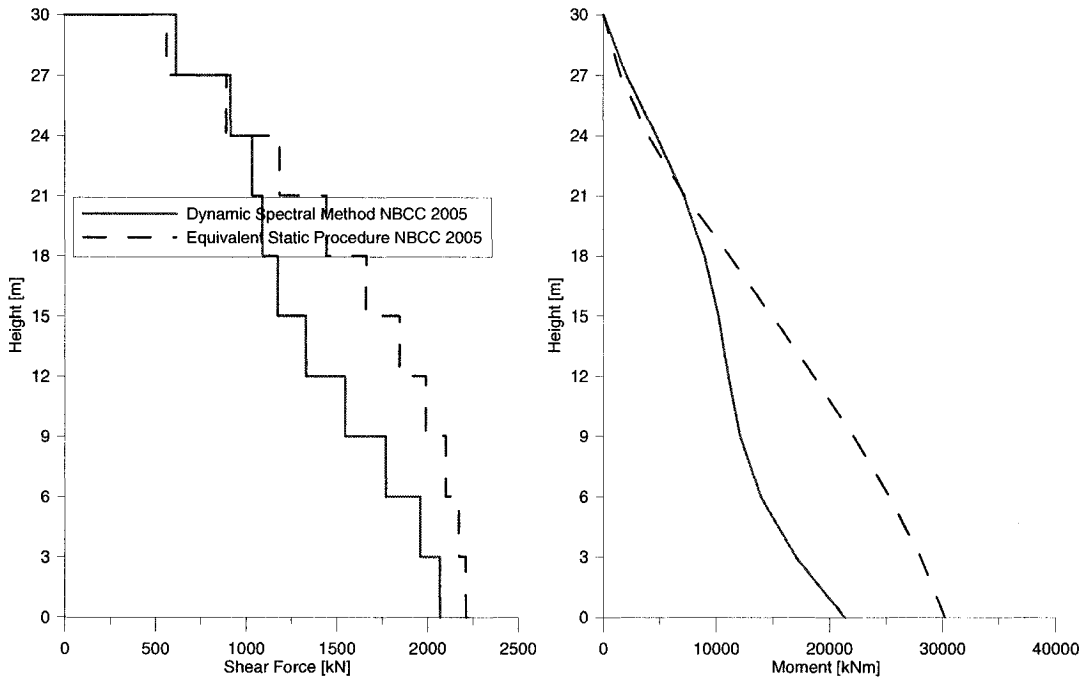

a) Shear Forces **b) Flexural Moments**

Figure 3.5 Comparisons of the ESFP and the MRSM

4. Design of the reinforcement and verifications

4.1 Dimension limitations (Clause 21.6.3)

The wall thickness within a plastic hinge shall be not less than $l_u/10$, except as permitted in clause 21.6.3.3 to 21.6.3.5, but shall not be less than $l_u/14$. In our case, l_u =

2800 mm (equal to 3000 – 200) and b_w = 250 mm. Hence, $l_u/14$ = 200 mm and $l_u/10$ = 280 mm. In this particular wall, we have boundary elements that provide stability in the highly stressed region of the wall. The limit of $l_u/10$ applies to those parts of the wall that are located more than halfway from the neutral axis "c" to the compression face of the wall section (clause 21.6.3.3) under factored vertical and lateral loads. The position of the neutral axis, c, was determined by plane section analysis using the computer program RESPONSE 2000. In the calculation of c, the material resistance factors ϕ_c = 0.65 and ϕ_s = 0.85 were used together with a compressive stress-strain curve of concrete with a maximum concrete stress of $0.9f'_c$. The length c was evaluated to be 1452 mm. The length of the web needed to be at least 280 mm was calculated to be 276 mm, 1452 / 2 - 450, from the column towards the middle of the wall. In view of the fact that the actual wall web thickness b_w = 250 mm was very close to the minimum value of 280 mm and that the critical region over which that minimum thickness was needed was very short (276 mm), the final thickness of 250 mm was assumed to satisfy the prevention of instability in the plastic hinge zone.

4.2 Deflections and Drift limits

The lateral deflections obtained from the linear dynamic analysis and incorporating the effects of torsion, including accidental torsional moments, were multiplied by R_dR_o/I_E to give realistic values of anticipated deflections. In NBCC, the largest interstorey deflection at any level is limited to 0.01 h_s for post-disaster buildings, 0.02 h_s for schools, and 0.025 h_s for all other buildings. The third limit corresponds to our case:

$$\Delta_i = \Delta_{f,i}\, R_d\, R_o / I_E < \Delta_{max,i} = 2.5\%\, h_s$$

Table 3.8 Interstorey drifts – 10-storey building in Vancouver

Storey	1	2	3	4	5	6	7	8	9	10
Drift	0.12%	0.29%	0.44%	0.56%	0.66%	0.73%	0.78%	0.81%	0.83%	0.83%

The interstorey drifts computed with the seismic loads amplified by 1.4 for torsional effects are reported in Table 3.8. All values met the imposed criteria ($\Delta_{i,max}$ = 0.83% $< \Delta_{max,i}$ = 2.5%). It is noted that storey drifts should have been checked along the exterior walls, where torsional effects are maximum. This calculation was not done here in view of the simplified approach that was adopted to account for torsional effects (forces multiplied by 1.4).

4.3 Ductility check (Clause 21.6.7)

To ensure ductility in the plastic hinge region, the inelastic rotational capacity of the wall, θ_{ic}, must be greater than the inelastic rotational demand, θ_{id}. The inelastic rotational demand, θ_{id} is calculated from:

$\theta_{id} = (\Delta_f R_d R_o - \Delta_f \gamma_w) / (h_w - l_w/2) \geq 0.004$

θ_{id} = (44 * 3.5 * 1.6 – 44 * 1.19) / (30000 – 7450/2) = 0.0074 ≥ 0.004, where Δ_f is the horizontal displacement at the roof level under factored loads and $\gamma_w = M_n/M_f$, and M_n is the nominal moment resistance at the wall base. For this wall, M_n = 38480 kN-m and γ_w = 1.19.

The inelastic rotational capacity is taken as:

$\theta_{ic} = (\varepsilon_{cu} l_w / 2 - 0.002) \leq 0.025$

$\theta_{ic} = (3.5*10^{-6} * 7450 / 2 - 0.002) = 0.011 \leq 0.025$

In this case, θ_{id} = 0.0074 ≤ θ_{ic} = 0.011, so the minimum ductility capacity at the base of the wall was verified.

4.4 Calculation of moment resistance M_r at the base of wall

For the calculation of M_r, the commercial computer program W-SECT V.6 was used. M_r was calculated using the stress block factors of clause 10.1.7, strain compatibility and a maximum concrete compressive strain of 0.0035. The concentrated and distributed reinforcement met the code criteria for minimum diameter, minimum

and maximum reinforcement ratios and ductility design requirements. All data for the final choice of the reinforcement are reported in Table 3.4.5. The wall is detailed for plastic hinging over a height equal to 1.5 times the length of the wall above the design critical section. The flexural and shear reinforcement at the critical section is maintained over that height.

According to Clause 21.6.2.2.c, the design overturning moments and shear forces above the plastic hinge region must be increased by the ratio of the factored moment resistance to the factored moment, both calculated at the top of the plastic hinge region. This requirement led to a factored design moment just above the 5th floor slab equal to the factored moment resistance below that same floor slab. Since the axial load in the wall above the floor slab is less than the one acting below the slab, an increase of the flexural reinforcement in the section just above the critical region was theoretically needed. This requirement for an increase of the flexural reinforcement was omitted in the design because it was found impractical and not supported by physical evidences. This discrepancy should be examined in the next edition of CSA A23.3 to provide a more practical solution to this situation.

4.5 Calculation of shear strength V_r at the base of wall

The effective shear depth, d_v, of the wall needs not to be taken as less than 0.8 l_w, so d_v = 0.8 l_w = 0.8 * 7450 = 5960 mm. Clause 21.6.9.6 stipulates the following additional requirements for regions of plastic hinging:

1) The factored shear demand of the wall shall not exceed $0.10\phi_c f'_c b_w d_v$, unless the inelastic rotational demand on the wall θ_{id} is less than 0.015.

$V_{f,max} = 0.10\phi_c f'_c b_w d_v = 0.10*0.65*0.030*250*5960 = 2906$ kN

$V_{f,max} = 2906$ kN > 2770 kN = V_f

2) Calculation of V_c

The contribution of the concrete to the factored shear resistance, V_c, is given by:

$$V_c = \phi_c \lambda \beta f'^{0.5}_c s$$

For the calculation of β, the general method as described in Clause 11.3.6.4 was employed. The value of the longitudinal strain, ε_x, at mid-depth of the cross-section that was obtained with Response 2000 assuming the development of the probable moment at the base M_p, and the value of β was equal to 0.059. In plastic hinge regions, the parameter β must be taken equal to zero unless it is shown that θ_{id} is less than 0.015. When $\theta_{id} \leq 0.005$, β is limited to 0.18. Linear interpolation can be used for intermediate values of θ_{id}. In our case, the inelastic rotational demand was calculated to be θ_{id} = 0.0074 < 0.015, and β was obtained by interpolation between 0.059 and 0: β = 0.0445. Hence:

$$V_c = \phi_c \lambda \beta f'^{0.5}_c b_w d_v = 0.65*1.0*0.0445*30^{0.5}*250*5960 = 236 \text{ kN}$$

3) Calculation of V_s

For this wall, horizontal steel consisting of 15M bars on each face of the wall (A_v = 400 mm^2) and vertically spaced 300 mm o/c (s = 300 mm) was assumed. Clause 21.6.9.6(c) stipulates that the value of θ in Clause 11.3.5 must be taken as 45° unless the axial compression (P_s+P_p) acting on the wall is greater than $0.1 f'_c A_g$.

P = 5040 kN < 6127.5 = $0.1 f'_c A_g$ = 0.1 * 0.030 * 2042.5*10^3, which gives θ = 45°.

$V_s = \phi_s A_v f_y d_v \cot\theta / s$ = 0.85 * 400 * 0.400 * 5960 * cot 45° / 300 = 2702 kN

The total factored shear resistance, V_r, is then equal to:

$V_r = V_c + V_s$ = 236 + 2702 = 2938 kN > 2770 = V_f

4.6 Checking Sliding Shear Resistance at Construction Joints

In accordance with Clause 21.6.9.4, all construction joints in walls must meet the requirements for sliding shear specified in Clause 11.5. Since the vertical uniformly distributed reinforcement is almost constant over the height of the wall, the most critical situation is at the wall base. If the construction joint is clean and intentionally roughened, the factored shear strength resistance from Clause 11.5 is given by:

$v_r = \lambda \phi_c (c + \mu\sigma) + \phi_s \rho_v f_y \cos\alpha_f$

where:

$\lambda\phi_c(c+\mu (P/A_g+\rho_v f_y \sin\alpha_f)) = 1.0*0.65*(0.50+1.0*(5040/2042500+0.00827*400*1.0)$

$= 2.48 \text{ MPa} < 0.25 \phi_c f'_c = 4.87 \text{ MPa}$

In this equation λ is equal to 1.0 for normal concrete density, c is the cohesion stress taken equal to 0.5 MPa for concrete placed monolithically, and μ is the friction coefficient (μ = 1.0 for concrete placed monolithically), ρ_v is the reinforcement ratio for the web reinforcement in tension (ρ_v = 15400/(250*7450) = 0.00827), and α_f is the angle between the shear friction reinforcement and the shear plane and is equal to 90°. The second term in the equation for v_r is equal to:

$\phi_s \rho_v f_y \cos\alpha_f = 0.85 * 0.00827 * 400 * \cos 90 = 0 \text{ MPa}$

Hence, the factored sliding shear resistance is $(2.48+0)*250*7450*10^{-3}$ = 4620kN, which exceeds the shear force corresponding to the attainment of the probable moment resistance in the wall plastic hinge. Hence, sliding shear is prevented.

4.7 Confinement of concentrated reinforcement

The concentrated reinforcement must be confined as in a column in accordance with Clause 7.6, and the ties shall be detailed as hoops. In regions of plastic hinging, the concentrated reinforcement must be tied with buckling prevention ties and the tie spacing shall not exceed the smallest of:

a) $6\ d_b = 6 * 29.9 = 179.4\ mm;$

b) $24\ d_b = 24 * 11.3 = 271.2\ mm;$

c) one half of the wall thickness = *200 / 2 = 100 mm;*

Hence, 10M hoops spaced at 100 mm were selected.

3.4 Summary

The design of the ten different buildings, five situated in Vancouver and five in Montreal, was done according to NBCC 2005 and CSA A23.3-04. The first dynamic period was fixed to be a multiple of the period T_a determined by the empirical equation from CSA A23.3. As discussed at the beginning of the Chapter, the dimensions of the walls were set such that the computed dynamic fundamental period was approximately equal to 2.0 times the empirical value for the buildings situated in Vancouver and 2.5 times the empirical value for those in Montreal. All the buildings met the ductility requirement that the inelastic rotational capacity exceeds the inelastic rotational demand, except for the 5-storey building situated in Vancouver. To meet that requirement, the dimensions of the walls were changed and the resulting dynamic period T_1 became equal to 1.70 T_a, instead of 2.0 T_a.

In NBCC 2005, the Modal Response Method is pointed as the preferred method of analysis. The Equivalent Static Force Procedure had to be carried out for the purpose of determining the minimum lateral earthquake design force for scaling purposes. The periods, parameters and lateral earthquake forces for Equivalent Static Procedure and Modal Response Spectrum Method are summarised in table 3.9. It is noted that the 1.4 factor for torsion is not included in tables 3.9 and 3.10.

Table 3.9 Summary of the periods, parameters and lateral earthquake forces for Equivalent Static Procedure and Modal Response Spectrum Method

Site	R_d	R_o	H [m]	$T_{a,code}$ [s]	T_a [s]	S_a [g]	M_v	J	V [kN]	T_1 [s]	T_2 [s]	T_1 / T_a	V_e [kN]
Vancouver	3.5	1.6	15	0.38	0.68	0.550	1.000	0.948	1473.21	0.645	0.131	1.70	6632.14
			30	0.64	1.28	0.285	1.035	0.844	1578.75	1.320	0.278	2.06	8269.22
			45	0.87	1.74	0.212	1.117	0.753	1902.86	1.737	0.322	2.00	10497.40
			60	1.08	2.16	0.163	1.200	0.700	2142.86	2.131	0.401	1.97	12179.05
			75	1.27	2.54	0.147	1.200	0.700	2390.63	2.577	0.480	2.03	13728.95
Montréal	2.0	1.4	15	0.38	0.76	0.236	1.000	0.896	1285.71	0.943	0.183	2.48	2929.46
			30	0.64	1.28	0.114	1.178	0.688	1440.00	1.605	0.298	2.51	3991.87
			45	0.87	1.74	0.072	1.736	0.504	2012.14	2.148	0.396	2.47	4716.97
			60	1.08	2.16	0.047	2.500	0.400	2520.00	2.675	0.486	2.48	5730.39
			75	1.27	2.54	0.042	2.500	0.400	3214.29	3.196	0.578	2.52	6443.12

Comparing the design base shear V_d obtained from Modal Response Spectrum Method with the limit of 80% of lateral earthquake design force from Equivalent Static Procedure (Table 3.10), the Modal Response Spectrum Method governed in all cases except for 20- and 25-storey buildings in Montreal where the value of total lateral force is the minimum required.

Table 3.10 Summary of the Lateral earthquake forces for Equivalent Static Procedure and Modal Response Spectrum Method and the controlling method for Base shear

Site	Height [m]	V [kN]	$0.8\,V$ [kN]	V_e [kN]	V_d [kN]	$V_{d,final}$* [0.8 V<Vd]	Controlling method
Vancouver	15	1473.21	1178.57	6632.10	1184.30	1184.30	spectral
	30	1578.75	1263.00	8269.22	1476.65	1476.65	spectral
	45	1902.86	1522.29	10497.40	1874.54	1874.54	spectral
	60	2142.86	1714.29	12179.05	2174.83	2174.83	spectral
	75	2390.63	1912.50	13728.95	2451.60	2451.60	spectral
Montreal	15	1285.71	1028.57	2929.46	1046.24	1046.24	spectral
	30	1440.00	1152.00	3991.87	1425.67	1425.67	spectral
	45	2012.14	1609.71	4716.97	1684.63	1684.63	spectral
	60	2571.43	2057.14	5730.39	2046.57	2057.14	ESP
	75	3214.29	2571.43	6443.12	2301.11	2571.43	ESP

*** Torsional effects are not included**

It must be mentioned that there are some significant changes in the design procedures of walls in the new edition of CSA A23.3-04. The first one is the specification for the length of the critical plastic hinge zone for ductile walls. The value of 1.5 times the length of the longest individual element in the direction under consideration seems to be appropriate for preventing yielding of the flexural reinforcement above the critical zone. However, the code does not prescribe a value for the height of the critical plastic zone for shear walls designed for moderate ductility (buildings in Montreal). In this work, the value proposed by Paulay and Priestley [1992] was adopted. The height of the critical wall section was assumed to be equal to length of the longest wall, which was found realistic because of the smaller ductility demand on the wall.

Another important change is that the design overturning moments and shear forces above the plastic hinge zone must be increased by the ratio of the factored moment resistance to the factored moment, both calculated at the top of the plastic hinge zone. This requirement was found to give a very important discrepancy in the design for flexural resistance. The value of the design overturning moment just above the top of the plastic zone is very close to the base design moment for some cases, especially for the more flexible buildings, even the larger ones. For these cases, the moment resistance is less than the flexural demand if the flexural reinforcement is kept the same as the one provided in the critical region because of the lower axial compression force. To compensate the missing resistance associated with the reduction in axial compression, the flexural reinforcement must be increased above the critical region, although typical engineering vision and experience would tell to maintain the same reinforcement as in the plastic hinge region.

In addition to those requirements for calculation of the factored shear, the factored shear resistance shall not be less than the smaller of the shear resistance corresponding to the development of the probable moment capacity of the wall at its plastic hinge

location and the shear resulting from design load combinations that include earthquake, with load effects calculated using R_dR_o equal to *1.0*. For the buildings located in Vancouver the values used in the design of the walls are reported in Table 3.11.

Table 3.11 Summary of the coefficients used for calculation of the design forces for Vancouver

Height	Period	In a plastic hinge zone	Above the plastic hinge zone
[m]	[sec]	γ_p	M_r^{top}/M_f^{top}
15	0.645	1.38	1.91
30	1.320	1.35	1.83
45	1.737	1.45	1.80
60	2.131	1.44	1.64
75	2.577	1.36	1.64

For Vancouver the design shear forces in the plastic hinge zone corresponded to the development of the probable moment M_p at the wall base and the probable overstrength ratio $\gamma_p = M_p / M_f$. Above the critical zone, the design overturning moments and shear forces were increased by the ratio of the factored moment resistance to the applied factored moment, both calculated at the top of the plastic hinge region. As can be noticed in Table 3.11, the difference between the two ratios is more important for the short period buildings, i.e. the structures that are less sensitive to the influence of the higher modes and that respond more in their first mode of vibration.

Table 3.12 Summary of the coefficients used for the calculation of the design forces for Montreal.

Height	Period	In a plastic hinge zone and above
[m]	[sec]	γ_w
15	0.645	1.16
30	1.320	1.19
45	1.737	1.50
60	2.131	1.40
75	2.577	1.29

For Montreal, the design shear forces in the plastic hinge zone correspond to the development of the nominal moment, M_n, and the nominal overstrength $\gamma_w = M_n / M_f$ at the wall base. The values of γ_w are given in Table 3.12. As discussed, there is no specification for the height of the plastic hinge region in CSA-A23.3-04 and we assumed a height equal to the length of the wall. Although not explicitly required in CSA-A23.3-04, the reinforcement required at the critical section was maintained over the height of the plastic region. Above this protected zone, CSA-A23.3-04 requires that the design shear forces be obtained by multiplying the shear forces due to the factored loads by the nominal overstrength factor γ_w of Table 3.12, without exceeding the elastic forces, i.e., the forces corresponding to $R_o R_d = 1.0$. There is no explicit requirement in CSA-A23.3-04 to prevent the formation of plastic hinges in the upper part of the wall. In order to achieve a controlled response and generally follow the principles developed for ductile walls, the design overturning moments above the base plastic hinge region were obtained by multiplying the moments from analysis by the nominal overstrength factor γ_w of Table 3.12.

The forces from response spectrum analysis and the forces used in design are plotted in figures 3.6 to 3.15 for all buildings. The factor 1.4 for torsion has been included in these graphs. The influence of the higher modes is more pronounced for the buildings located in Montreal where the earthquakes have predominant higher frequency content. It is also more pronounced for the high-rise buildings, which respond mainly in their second and third modes of vibration.

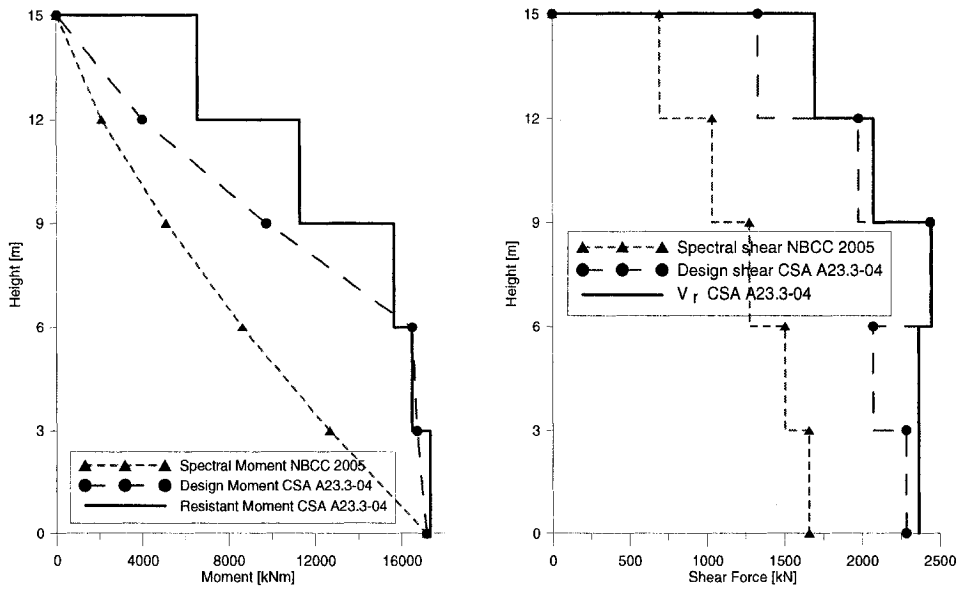

a) Moments **b) Shear forces**

Figure 3.6 5-storey building in Vancouver: Dynamic and Design forces

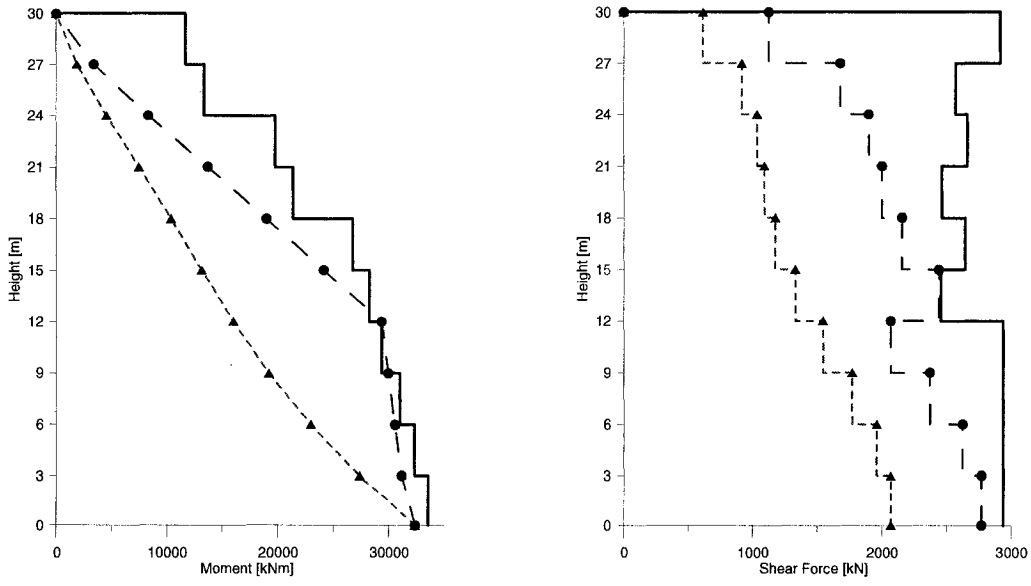

a) Moments **b) Shear forces**

Figure 3.7 10-storey building in Vancouver: Dynamic and Design forces

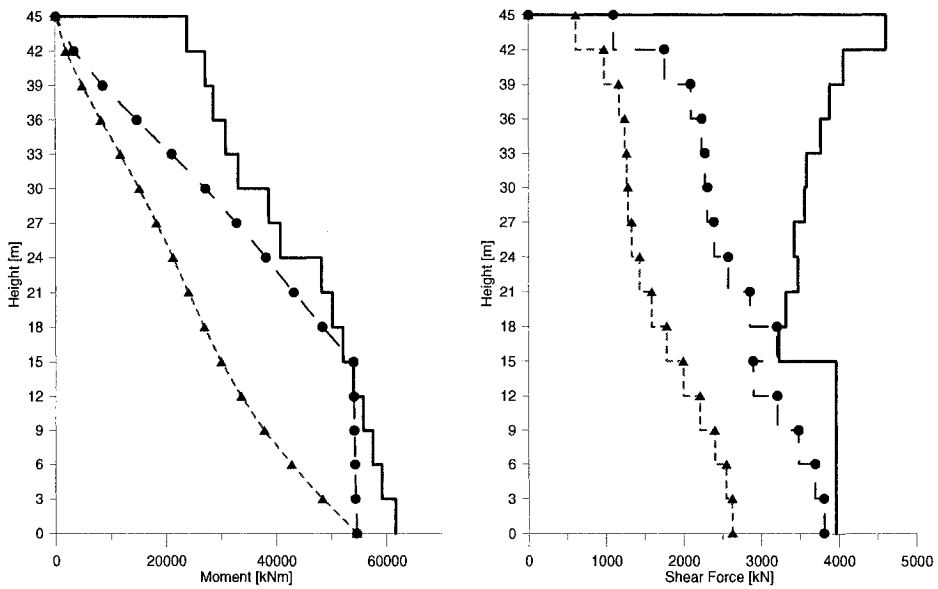

a) Moments **b) Shear forces**

Figure 3.8 15-storey building in Vancouver: Dynamic and Design forces

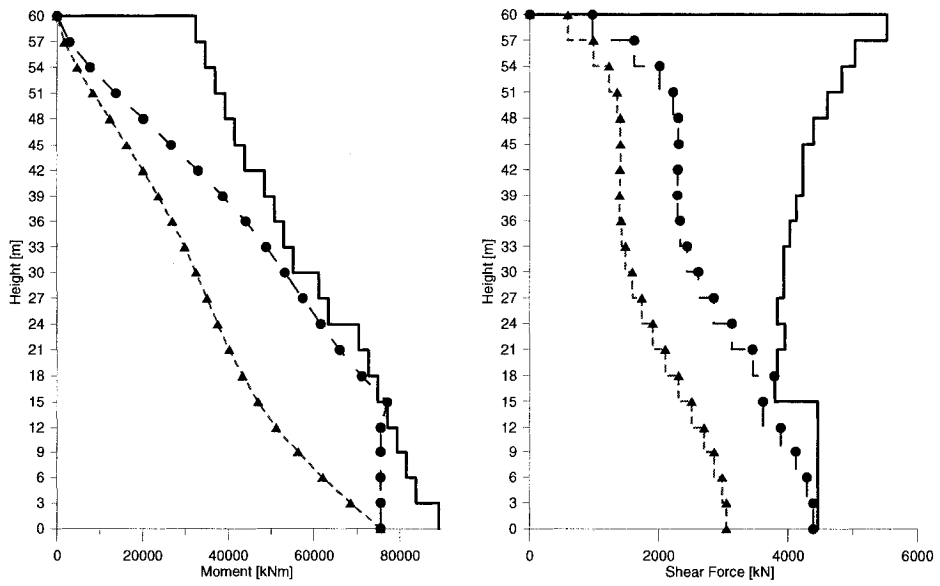

a) Moments **b) Shear forces**

Figure 3.9 20-storey building in Vancouver: Dynamic and Design forces

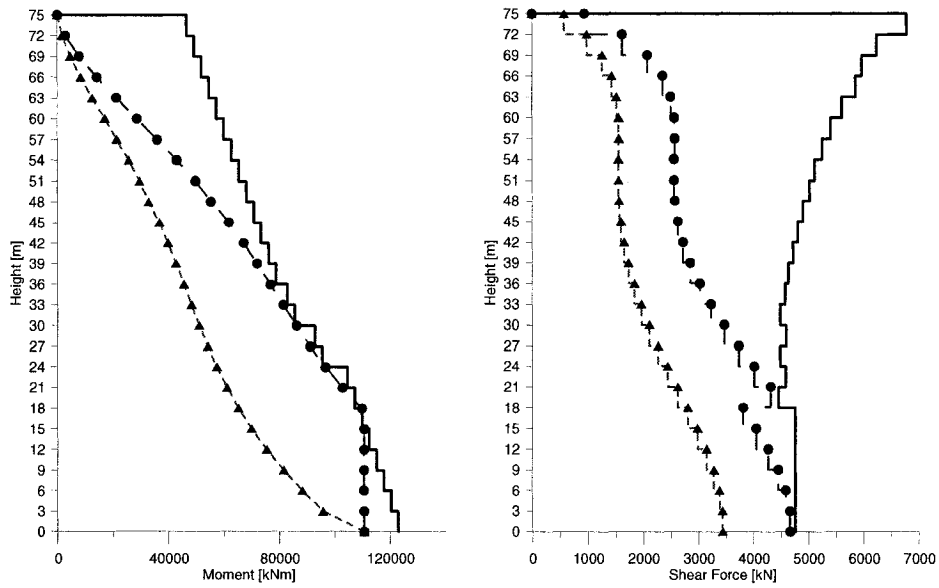

a) Moments **b) Shear forces**

Figure 3.10 25-storey building in Vancouver: Dynamic and Design forces

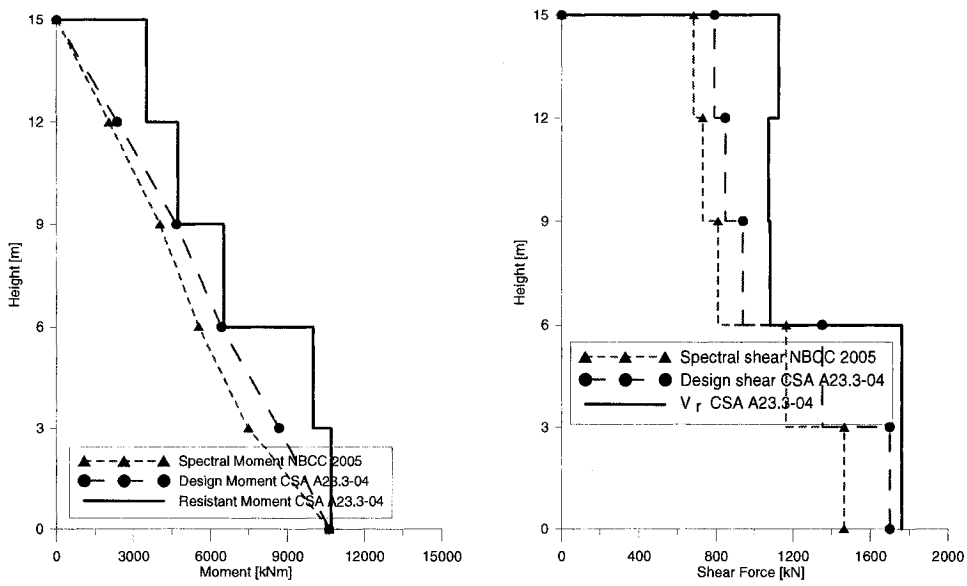

a) Moments **b) Shear forces**

Figure 3.11 5-storey building in Montreal: Dynamic and Design forces

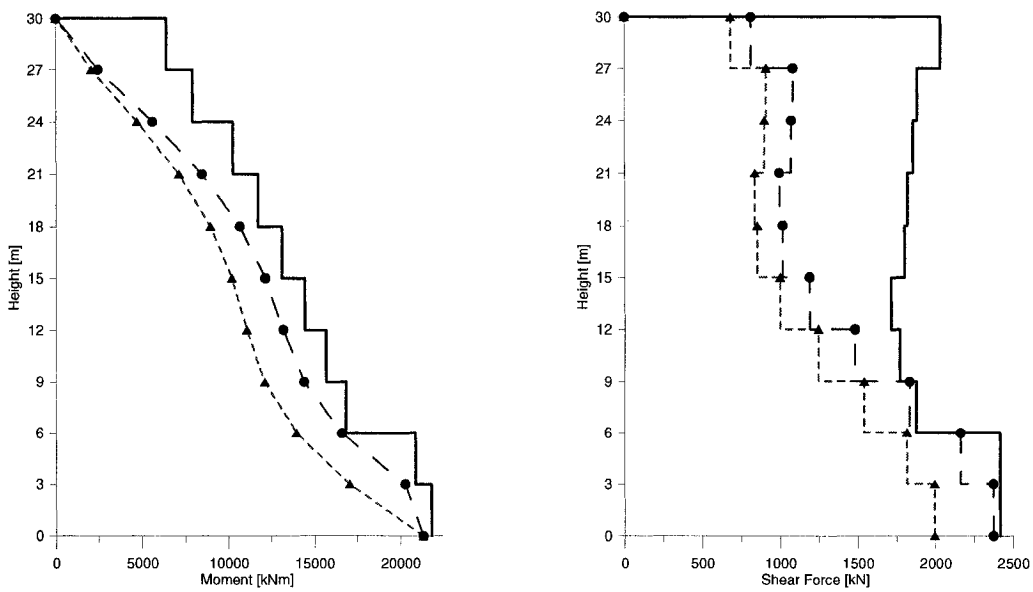

a) Moments **b) Shear forces**

Figure 3.12 10-storey building in Montreal: Dynamic and Design forces

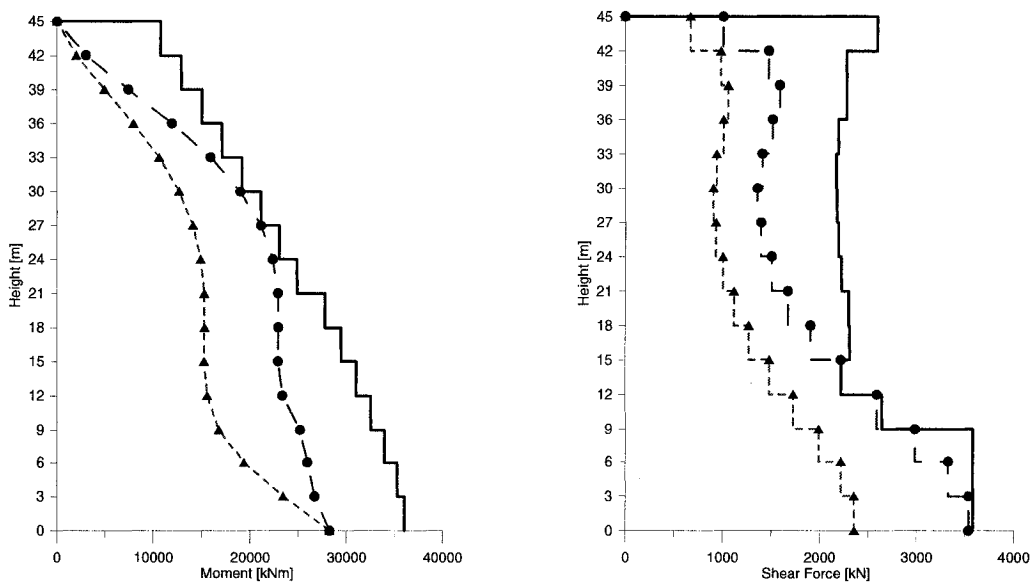

a) Moments **b) Shear forces**

Figure 3.13 15-storey building in Montreal: Dynamic and Design forces

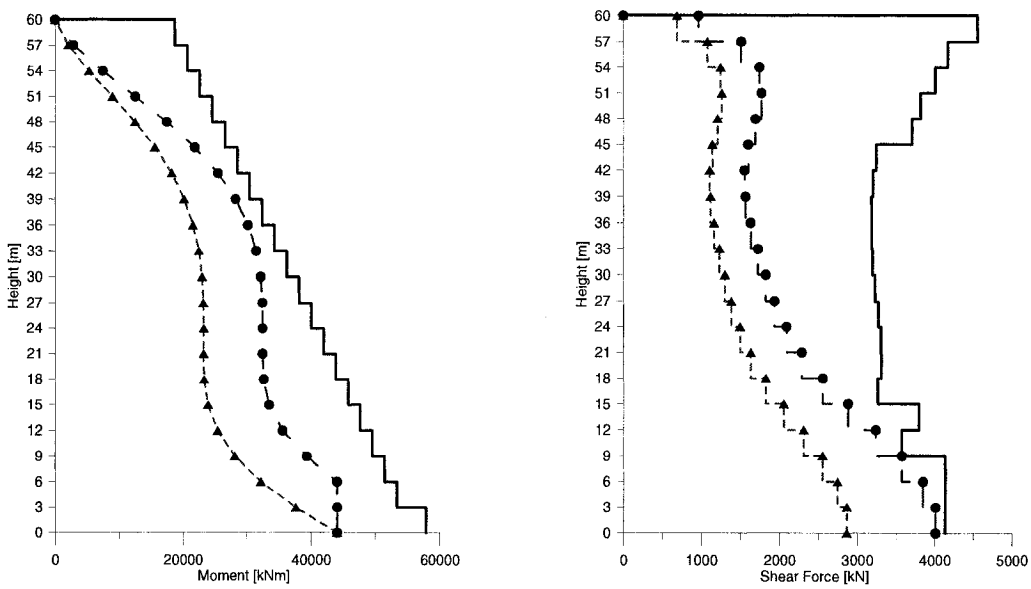

a) Moments **b) Shear forces**

Figure 3.14 20-storey building in Montreal: Dynamic and Design forces

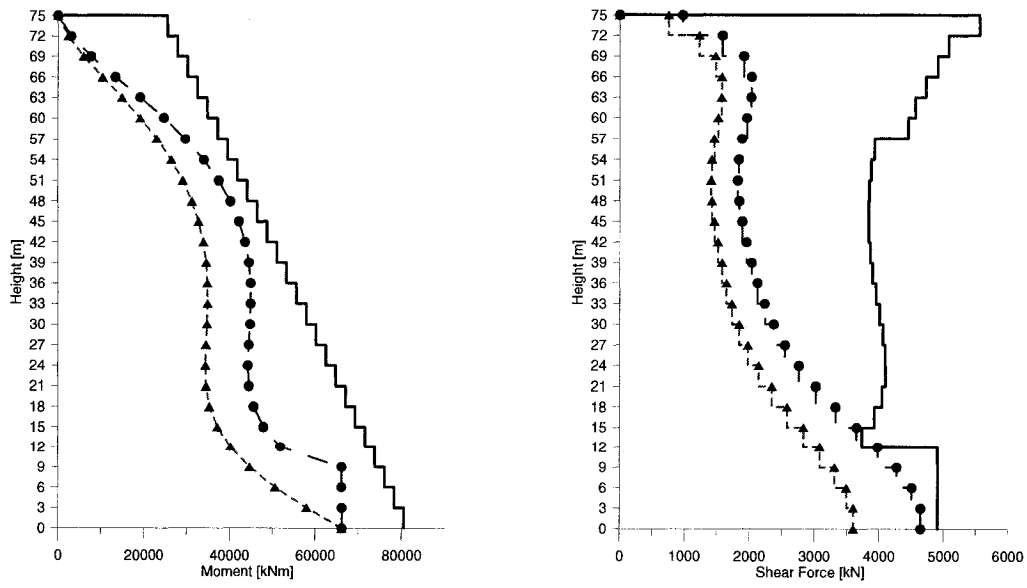

a) Moments **b) Shear forces**

Figure 3.15 25-storey building in Montreal: Dynamic and Design forces

As shown, the factored resistance provided at the wall base was nearly equal to the the overturning from analysis in all walls except for the 15-, 20-, and 25-storey buildings in Montreal for which minimum steel requirements governed. Above the plastic hinge region, the ductile walls in Vancouver possess sufficient flexural resistance against the formation of plastic hinges if the base moment reaches the probable wall moment capacity. Due to minimum requirements, walls of the 15-storey and taller buildings have additional protection against his response in their upper half. In Montreal, the anticipated flexural strength-to-demand ratio is uniform over the building height for the 5- and 10-storey walls. For the taller structures in Montreal, the variation of the demand due to higher mode effects and the effects of the minimum steel requirements on the capacity resulted in highly variable bending strength-to-supply ratios along the height with a minimum value located approximately at 2/3 of the wall height.

As shown in the figures, the shear resistance V_r generally increases towards the height of the taller buildings. Even if this looks counter-intuitive, it can be simply explained with the new general method for the calculation of the shear resistance of CAN/CSA A23.3-04. Briefly, the factored shear resistance depends mainly of two factors: shear reinforcement and flexural demand. In high-rise buildings the shear reinforcement design in the upper storeys is governed by the minimum reinforcement requirements, which have significant influence on the shear resistance at those parts of the walls. On other hand, the flexural demand decreases with the height. The angle of inclination of the diagonal compressive stresses then increases, which lead to an increase of the shear resistance from the shear reinforcement and an increase of the contribution of the concrete for shear resistance. So, both factors contribute to an increase in shear capacity of the walls towards the top of the buildings.

The most important change in CSA-A23.3-04 requirements is in the explicit verification of the ductility capacity of the wall. In the previous code editions, the only

requirement was that the compression region of the wall needed to be confined in a way similar to columns. In the last edition of CSA-A23.3, the inelastic rotational capacity of the wall must be equal to or greater than the inelastic rotational demand to avoid premature failure in the hinge region. In this case, the inelastic rotational capacity is associated to the design roof displacement and the properties of the wall. In the equation for the calculation of the inelastic rotational demand, it is assumed that the displacement profile will be similar to that of the first vibration mode and that the height of the plastic hinge is equal to half the length of the wall. This gives a conservative estimate of the inelastic rotational demand. The calculations of the inelastic rotational capacity and the inelastic rotational demand for all buildings are summarised in table 3.13.

Table 3.13 Calculations of inelastic rotational capacity and demand

Site	H (m)	R_d	R_o	d_v (m)	Δ (mm)	Δ_f* (mm)	γ_w	θ_{id} (rad)	θ_{ic} (rad)	$\theta_{ic} < \theta_{id}$
Vancouver	15	3.5	1.6	4.160	14.1	19.7	1.19	0.0069	0.0071	OK
	30	3.5	1.6	5.960	31.6	44.2	1.19	0.0074	0.0110	OK
	45	3.5	1.6	8.400	42.6	59.6	1.30	0.0065	0.0164	OK
	60	3.5	1.6	8.400	50.3	70.4	1.29	0.0055	0.0164	OK
	75	3.5	1.6	8.800	65.5	91.7	1.21	0.0058	0.0173	OK
Montreal	15	2.0	1.4	3.200	17.8	24.9	1.16	0.0031	0.0050	OK
	30	2.0	1.4	5.320	28.4	39.8	1.19	0.0030	0.0096	OK
	45	2.0	1.4	7.360	28.6	40.0	1.50	0.0030	0.0141	OK
	60	2.0	1.4	6.400	38.7	54.2	1.40	0.0030	0.0120	OK
	75	2.0	1.4	7.600	47.0	65.8	1.29	0.0030	0.0146	OK

* $\Delta_f = 1.4\,\Delta$ **(includes torsional effects)**

For the ductile walls designed with $R_d = 3.5$ in Vancouver, the inelastic rotational demand tends to decrease when the height of the buildings is increased. For all structures, the inelastic rotational capacity shows the opposite trend, with an increase with the building height. For the taller buildings, the capacity is approximately three times the demand. The ductility requirements of Clause 21.6.7 was met for all walls except for the 5-storey building in Vancouver. The geometry of the wall for tha building had to be modified to meet the code limits on plastic rotations. For the buildings located

in Montreal and designed with R_d = *2.0*, it is noticed that the rotational demand is generally governed by the minimum requirements specified in Clause 21.7.3.2 ($\theta_{id} \geq$ 0.003 rad). All walls at that site had sufficient rotational capacity.

A new simplified procedure is proposed in CSA-A23.3-04 for the calculation of the shear resistance of the wall. The calculation of V_c is directly related to the inelastic rotational demand, and the determination of the angle θ for the calculation of V_s is related to the normalised axial stress $(P_s+P_p)/f'_cA_g$. Table 3.14 presents the detail of the computation of V_r in the plastic hinge region of all walls. Table 3.15 gives the factored resistances in shear and flexure as well as the vertical and horizontal reinforcement of the critical region.

Table 3.14 Summary of parameters used for calculations of shear reinforcement in plastic hinge region in the walls.

Site	h_n (m)	d_v (m)	V_f (kN)	ε_x (mm/m)	β	β_{design}	$V_{f,design}$ (kN)	V_c (kN)	θ	s (mm)	V_s (kN)	V_r (kN)	V_f/V_r
Vancouver	5	4.160	2293	4.03	0.057	0.046	2775	169	45°	265	2135	2304	0.995
	10	5.960	2783	3.87	0.059	0.045	3885	236	45°	300	2702	2938	0.947
	15	8.400	3813	5.87	0.041	0.035	5316	261	45°	160	3570	3831	0.995
	20	7.440	4394	14.7	0.017	0.017	5036	131	45°	235	4306	4437	0.990
	25	8.800	4661	9.5	0.026	0.024	6293	227	45°	260	4603	4830	0.965
Montreal	5	3.200	1699	6.17	0.039	0.039	2281	89	45°	270	1612	1723	0.999
	10	5.320	2373	4.98	0.047	0.047	4063	179	45°	160	2192	2416	0.972
	15	7.360	3525	3.79	0.060	0.060	4931	314	45°	155	3229	3542	0.995
	20	6.400	3996	30	0.009	0.009	4135	59	45°	220	3956	4016	0.995
	25	7.600	4643	30	0.009	0.009	4910	71	45°	210	4922	4992	0.937

In table 3.14, the values for the design shear demand at the base, V_f, were obtained by multiplying the values of $V^*_{d,final}$ from Table 3.9 by 1.4 to account for torsional effects, as was explained earlier. The values so obtained were then multiplied by the corresponding values of γ_p for the Vancouver buildings and by γ_n for the Montreal located buildings to account for shear forces corresponding to the development of the probable moment capacity at the base of the ductile walls in Vancouver and the nominal

moment capacity at the base of the moderately ductile walls in Montreal. This procedure was explained in detail in Section 3.3. For example, for the 5-storey building located in Vancouver:

$$V_f = 1.4 * V^*_{d,final} * \gamma_p = 1.4 * 1184 * 1.383 = 2293 \text{ kN}$$

For the walls designed with $R_d = 3.5$ in Vancouver, ε_x was calculated with the Response 2000 program with the axial force at the base of wall and the bending moment corresponding to development of the probable moment, as in the design example. For the buildings in Montreal ($R_d = 2.0$), the same calculation was performed except that M_n was used instead of M_p. The contribution of the concrete to the factored shear resistance ranged between 6% and 9% of V_r for the 5-, 10- and 15-storey buildings at both sites. It decreased by almost a factor of 2.0, between 3% and 4.7% of V_r, for the 20- and 25-storey buildings in Vancouver and even less, 1.5% and 1.4% of V_r, respectively, for the Montreal high-rise 20- and 25-storey buildings. Therefore, the wall shear resistance was nearly entirely provided by the shear reinforcement, with reinforcement ratios varying between 0.0042 and 0.0063 in plastic hinge regions. Table 3.15 gives the details of the reinforcing steel.

Table 3.15 Summary of design forces, factored resistances and flexural and shear reinforcement in plastic hinge region (base) at the walls.

Site	R_d	R_o	Height [m]	L_p [m]	M_f [kNm]	M_r [kNm]	A_s [mm^2]	A_s two layer vertical distributed	V_f [kN]	V_r [kN]	A_{sv} horizontal distributed
Vancouver	3.5	1.6	15	6.0	17156	17322	4000	15M @ 230	1658	2304	15M @ 275
			30	12.0	32366	33532	5600	10M @ 300	2067	2938	15M @ 300
			45	15.0	54559	61558	5600	10M @ 300	2624	3830	10M @ 160
			60	15.0	75495	88990	10200	10M @ 260	3045	4430	15M @ 235
			75	18.0	110599	122883	11800	10M @ 260	3432	4711	15M @ 260
Montreal	2.0	1.4	15	6.0	10620	10675	4000	15M @ 420	1465	1701	15M @ 270
			30	6.0	21337	21807	2000	10M @ 250	1994	2440	10M @ 160
			45	9.0	28241	36522	1200	10M @ 400	2356	3542	10M @ 155
			60	9.0	44049	57843	3400	10M @ 260	2862	4016	15M @ 220
			75	12.0	59131	84469	3800	10M @ 260	3599	4992	15M @ 210

In the plastic hinge location, the concentrated flexural reinforcement for the 5-, 10-, 15- and 20-storey buildings in Vancouver was limited by the requirement for maximum permitted reinforcing ratio. For the 25-storey building, it was governed by the minimum required concentrated flexural zone reinforcement. For the 5-storey building, the maximum concentrated reinforcement was not sufficient to attain the required minimum moment resistance, and a larger quantity of distributed reinforcement was provided. That reinforcement provided approximately a 35% of the total moment resistance of the section. Similarly, for Montreal the minimum reinforcement requirements governed the reinforcement choice for the 15-, 20- and 25-story buildings. For these structures, nearly all of the flexural resistance is provided by the distributed reinforcement.

The verification for interface shear transfer was performed at the base of the walls. It was assumed that the fresh concrete was placed against hardened concrete with clean surface and intentionally roughened to full amplitude of at least 5 mm. The calculation is made according to clause 11.5 of CAN/CSA-A23.3-04 and the results are reported in table 3.16. A detailed example was presented in Section 3.3 (Item 4.7).

Table 3.16 Summary of the calculation of the interface shear resistance at the wall bases.

Site	H	w	L_w	N_f	V_f	A_g	A_{vf}	A_{cv}	r	σ	V_{rs}	V_f/V_{rs}
	m	mm	mm	kN	kN	mm^2	mm^2	mm^2	A_{vf}/A_{cv}	MPa	kN	
Vancouver	15	250	5200	2520	2293	1420000	15600	8.000E+05	1.95%	9.57	5239	44%
	30	250	7450	5040	2783	2042500	15400	1.863E+06	0.83%	5.77	7597	37%
	45	250	10500	7560	3813	2805000	17600	2.625E+06	0.67%	5.38	10028	38%
	60	300	9300	10080	4394	4710000	17200	2.790E+06	0.62%	4.61	9260	47%
	75	300	11000	12600	4661	5520000	20800	3.300E+06	0.63%	4.80	11377	41%
Montreal	15	200	4000	2520	1699	960000	10800	8.000E+05	1.35%	8.03	4433	38%
	30	200	6650	5040	2373	1555000	8600	1.330E+06	0.65%	5.83	5470	43%
	45	200	9200	7560	3525	2140000	6400	1.840E+06	0.35%	4.92	6487	54%
	60	300	8000	10080	3996	4020000	7200	2.400E+06	0.30%	3.71	6564	61%
	75	300	9500	12600	4679	4770000	8400	2.850E+06	0.29%	3.82	8004	58%

The ratio of the shear demand to the interface shear resistance for all buildings varies from 37% to 61%. It does not depend on the ductility class or the shape of the walls. It mostly depends on the effective normal stress in the section, σ, a larger stress resulting in a larger shear resistance.

CHAPTER 4

NONLINEAR DYNAMIC ANALYSIS

4.1 Model choice

To predict the inelastic response of a slender reinforced concrete walls and wall systems an accurate, an effective, and a robust model is required and analysis tools that account for the important material characteristics and behavioural response features as a variation of the position of neutral axis, tension-stiffening, progressive gap closure, and nonlinear shear.

The first of the parameters studied herein was the influence of the modeling on the inelastic response of the structure. The most commonly used model is the "stick-cantilever" or "Bar" model - "M1" (figure 4.3.a). This is a macro-model based on capturing overall behaviour with reasonable accuracy. In this model each storey is represented with a bar element and the first floor is restrained at the base. The seismic weight is concentrated as a lumped weight at each floor. The rotations of a beam-column element occur about the centroidal axis of the wall, the plastic rotation is concentrated at both ends of the bar, with a height of the plastic hinge formulated (calculated) in advance, and the response to shear forces is assumed to be elastic. The flexural behaviour is usually represented with a bi-linear Takeda hysteresis rule. The advantage of using this model is its simplicity and the fact that this element has been well studied and proven in past research. Although this analytical model has been proposed for realistic and practical prediction of the hysteretic behaviour of reinforced concrete members, the model is based on a simplified idealization and its validity is restricted to the conditions upon which the derivation of the model is based.

Recent developments in the seismic design of ductile reinforced concrete walls and knowledge of the behaviour of shear walls during cyclic loading show that there could be significant shear strength degradation and that the response of the wall to shear forces is nonlinear. The correlation between shear strength degradation due to increase of curvature ductility has been studied in past research (Sezzen & Moehle, 2004; Elwood, 2004; Greifenhagen, 2006). It was found, as shown in figure 4.1, that the shear strength degrades with an increase of flexural rotation.

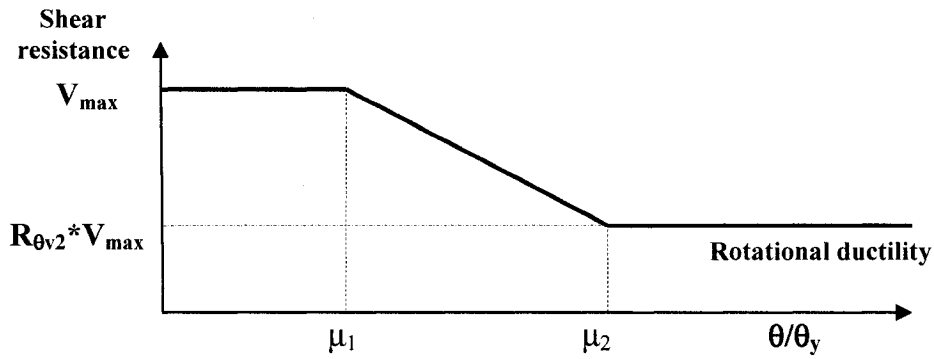

Figure 4.1: Rate of shear strength degradation due to the increase of rotational ductility, adopted from NZNSEE 1996.

Different models have been proposed in the literature to represent this phenomenon, such as the Three-Vertical-Line-Element-Model or the Macro-Element Model for RC Wall Member (Chen and Kabeyasawa, 2000; Elwood, 2004; Wallace and Orakcal, 2004), but most of those models have been developed for finite element analysis programmes. To account for this effect, an inelastic shear spring can be added to each member of model M1 to form model M2 in figure 4.3.b. This spring works in series with the bar that has only axial and flexural stiffness. Even if this spring is not coupled with the flexural one (no interaction between flexure and shear), it can give a better representation of the actual behaviour of the wall when the response is likely to depend on the shear capacity of the wall, which is not the case with the first model.

Another phenomenon, which cannot be well simulated, is the influence of the axial compression force on the flexural response of the wall under cyclic loading. (wall rocking). This effect is represented in figure 4.2. When axial load is present, part of the resitance to flexure is contributed by to the axial load acting at some distance from the neutral axis. Upon unloading, the energy associated to this additional resistance is not dissipated, as is the case with inelastic strain energy, and is returned to the system, resulting in a pinched hysteretic response. However, the axial load contributes to re-centring the wall to its original un-deformed position at each cycle.

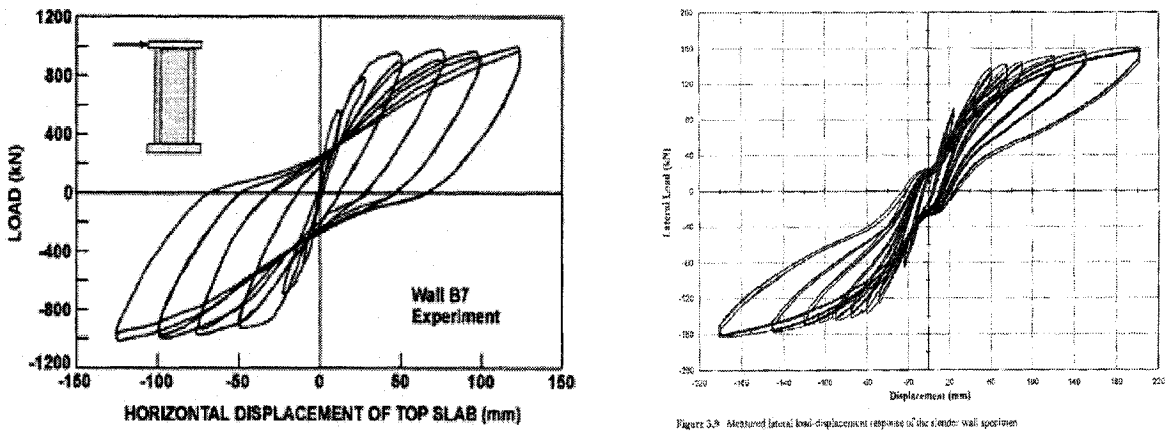

a) Without axial compression force; **b) With axial compression force**

Figure 4.2: Hysteresis curves for a shear wall: a) taken from Palermo and Vecchio (2004); b) taken from Adebar and Ibrahim (2000).

As can be observed in figure 4.2, in spite of the fact that the second specimen dissipates less energy than the first one, the axial force provides for re-centring behaviour that will contribute in reducing residual displacements. With the assumption that this effect is most important at the base of the wall, a third model, model M3 in figure 4.3, is proposed. This model is obtained by adding to Model 1 an infinitely rigid horizontal beam supported on uniformly distributed vertical springs (figure 4.3.c). The rigid beam has the length of the wall and the springs represent the behaviour of the wall section under cyclic tension-compression loading. The spring model is presently under

development at Ecole Polytechnique of Montreal. As a simplification of this complex behaviour of the series of springs, a simplified model can be used with a combination of two springs working in parallel: the first spring represents the behaviour on the concrete in compression while the second spring mimics the behaviour of the reinforcement steel in tension.

One main limitation of models M1 and M2 lies in the assumption that rotations occur about the centroida axis of the wall. Thus, important features of the observed behaviour as a variation of the neutral axis along the wall cross-section during lateral loading and unloading, rocking of the wall and inelastic shear are disregarded and the resulting effects on the structural system are not properly considered. Various macroscopic models have been proposed to capture these experimentally observed features when predicting the inelastic response of reinforced concrete structural walls. As a result of extensive studies, the Multi-Component-in-Parallel Model, MCPM, also referred to as Multiple-Vertical-Line-Element Model, MVLEM (Volcano et al., 1988) was proposed in the literature. A similar representation is the "WALL" element available in the computer program Ruaumoko (figure 4.3.d).

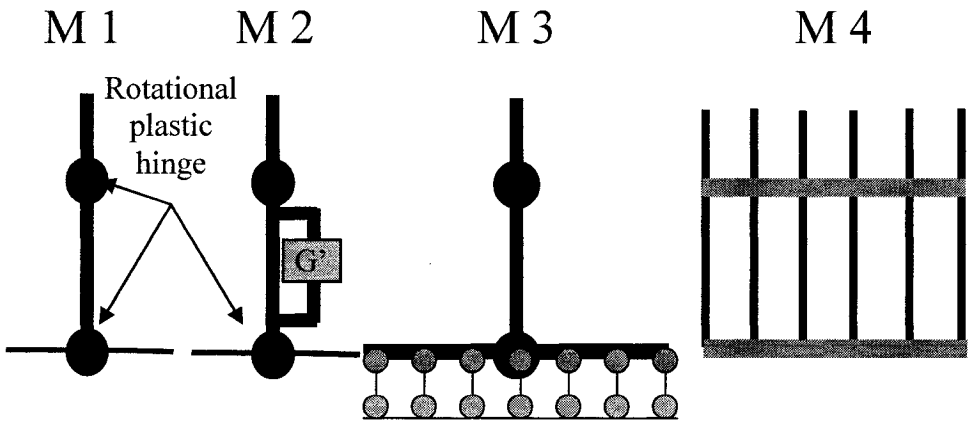

a) Model 1 **b) Model 2** **c) Model 3** **d) Model 4**

Figure 4.3: Analytical models for shear walls: a) Bar model – M1; b) Bar model with inelastic shear springs in parallel – M2; c) Bar model on the spring supports – M3; d) Model – element "WALL" – M4.

This model captures several important features including refined material behaviour, shifting of the neutral axis, rocking of the wall, and the effects of a fluctuating axial force, which are commonly ignored in simple beam models. The structural-wall member was developed as the Taylor Wall-A element (Taylor 1977) to represent the behaviour of reinforced concrete walls. The member cross-sectional area and second moment of area are numerically integrated across the section using the current steel and concrete modulii. As a result, the model allows for the shift of the neutral axis position due to the changing axial load and bending moment. The initial position of the neutral axis is determined assuming uncracked section properties.

4.2 Studied models

Based on the above discussion, it was decided to use "Model 1", the "Bar" model, and "Model 4", the "Structural-Wall" element in Ruaumoko, for the analytical nonlinear analysis.

A) Bar element

The choice of "Model 1" was based on the understanding that an effective analytical model for analysis and design of the systems should be relatively simple to use and should predict reasonably accurately the hysteretic response of RC wall systems.

Modeling of the hysteretic response

In the literature, the most commonly used model for the flexural response of reinforced concrete structure is the bilinear approximation of the "actual" moment-curvature response derived using the yield, nominal, and ultimate conditions given by Paulay and Priestley (1992). The secant stiffness is given by the straight line passing by the origin and the point of the first-yield curvature φ'_y, which is the point where the extreme bar starts to yield ($\varepsilon_s = f_y/E$) under a moment M'_y. The yielding moment M_y corresponds to the point where strain hardening in the extreme bar reinforcement starts,

at approximately $\varepsilon_s = 15\ mm/m$ for reinforcing steel complying to CSA G30.12 400MPa. Extrapolating linearly to the yielding moment, the yield curvature φ_y is given by:

$$\varphi_y = \frac{M_y}{M_y'} \varphi_y' \qquad [4.1]$$

The moment M_u is governed by the maximum attainable curvature of a section, or ultimate curvature, which is normally controlled by the maximum compression strain ε_{cu} at the extreme fiber of the concrete, since steel strain ductility capacity is typically high. The maximum concrete compression strain in the extreme fiber of unconfined wall section is assumed to be 0.0035, when normal-strength concrete is used. As an addition to this condition, the maximum curvature was selected at the point where the strain in the reinforcement on the tension side of the wall reached to 0.060 mm/mm, which approximately corresponded to the point of maximum moment when concrete strain did not govern.

When the tensile stress in a reinforced concrete section exceeds the tensile strength of the concrete, the reinforced concrete member starts cracking and this results in an increase of the tensile stresses in the steel reinforcement. However, at sections between successive cracks, due to the bond between the concrete and the reinforcement, the concrete can still carry some tensile stresses and contribute to the member resistance. This is called the "tension stiffening effect". This effect is influenced by the bond force acting at the interface between the steel bars and the surrounding concrete. The tension stiffening factor represent this bond stress: it is equal to 1.0 when a perfect bond is assumed and equal to 0.0, when this effect is neglected.

Using the above parameters with the stiffening factor equal to 1.0, the actual moment-curvature response for wall cross-sections can be computed using the computer program RESPONSE 2000. This curve is then used to determine the initial stiffness K_o and the bilinear factor r for the simplified bi-linear response representation of wall responses. This approach is illustrated in Figs. 4.4 to 4.7 for the first and top levels of the

10 storey buildings situated in Montreal (designed with R_d = 2.0) and in Vancouver (R_d = 3.5).

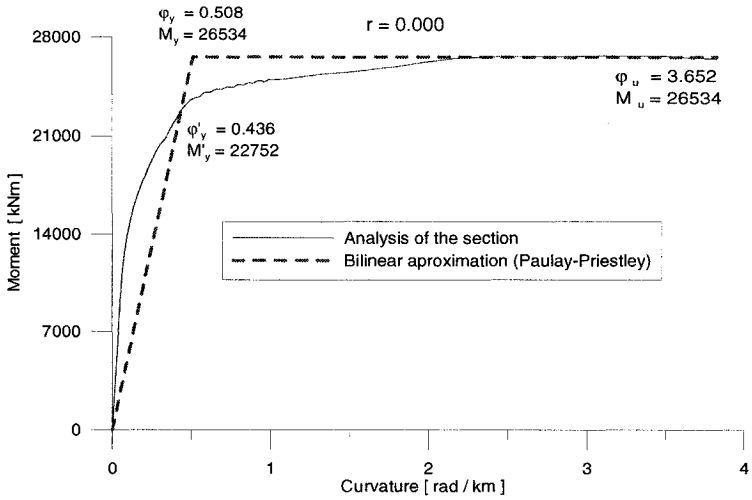

Figure 4.4: Moment-curvature: Montreal - level 1

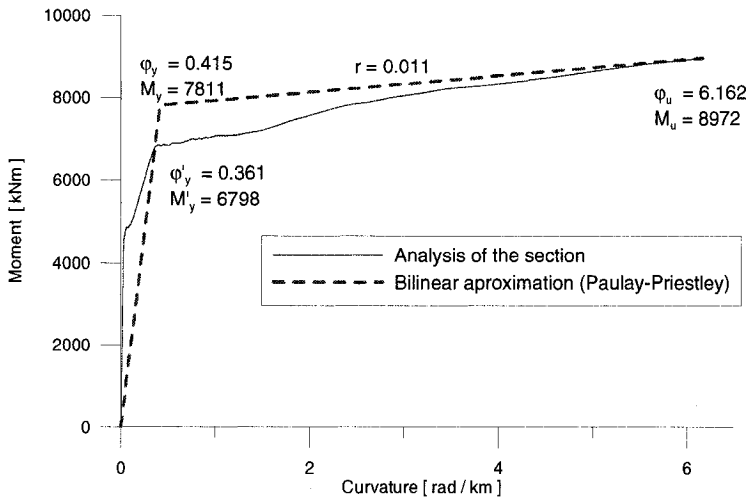

Figure 4.5: Moment-curvature: Montreal - level 10

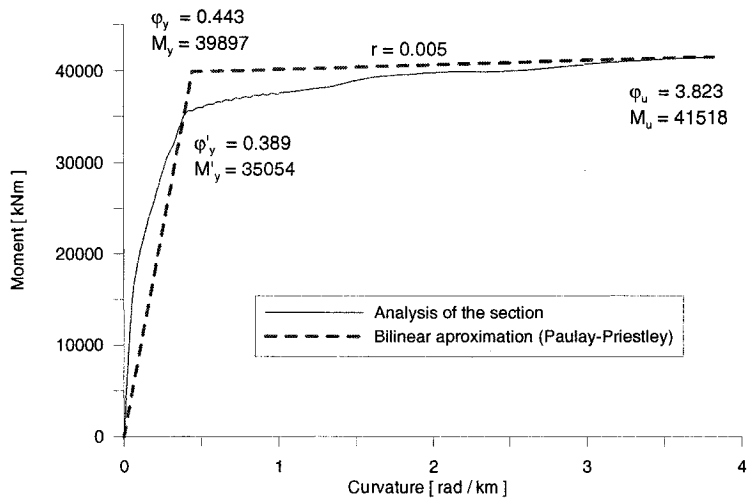

Figure 4.6: Moment-curvature: Vancouver - level 1

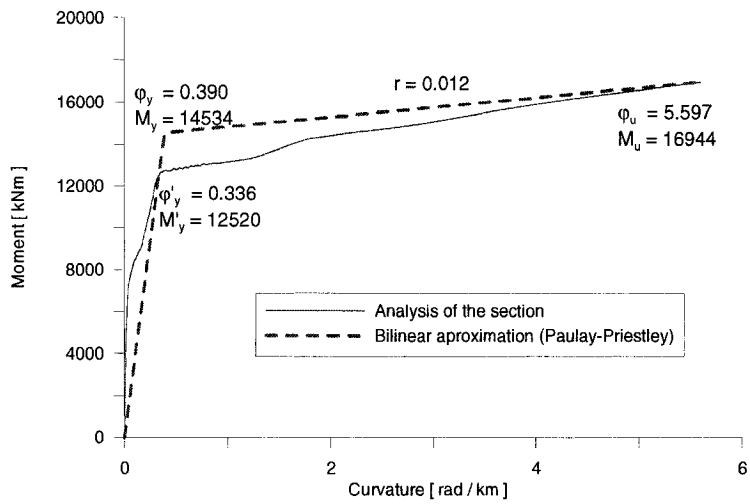

Figure 4.7: Moment-curvature: Vancouver - level 10

The agreement seems to be less consistent for sections located at the base of the buildings, i.e. where most of the inelastic rotation is likely to develop according to the seismic design assumptions. As illustrated in figures 4.5 and 4.7, this approach also overestimates the capacity of sections with low reinforcement ratio and low axial forces, as those located in the upper storeys.

To achieve a better representation of the inelastic behaviour of wall cross-sections, an alternative approach is proposed herein. In this approach, the secant stiffness is

calculated at the base as being equal to the average stiffness of the uncracked and cracked sections.

The values of the ultimate curvature and ultimate bending moment are obtained using the procedure by Paulay-Priestley. Then, the yielding curvature and moment are calculated using the equal energy principle to determine M_y by having the same total area below the force-deformation curve up to M_u, with the condition that the yielding moment M_y is not smaller than the moment at first yielding. The results for the same four sections are plotted in figures 4.8 to 4.11.

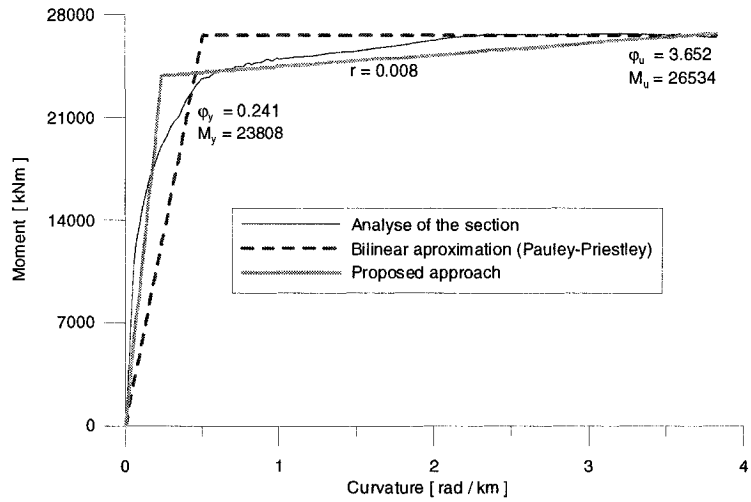

Figure 4.8: Moment-curvature: Montreal - level 1

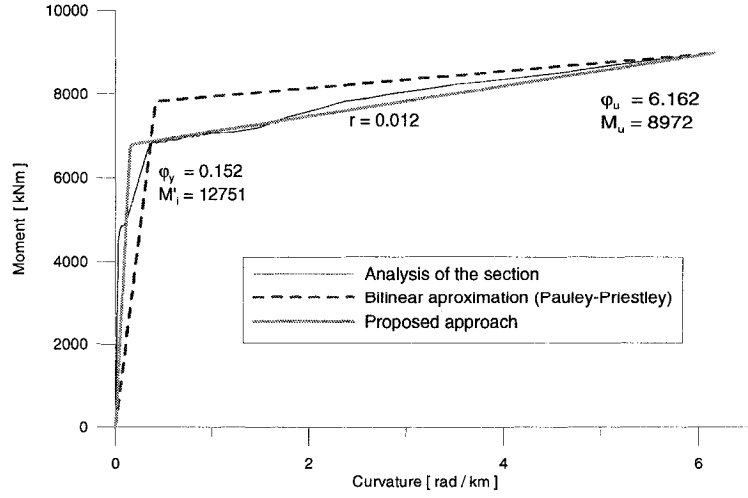

Figure 4.9: Moment-curvature: Montreal - level 10

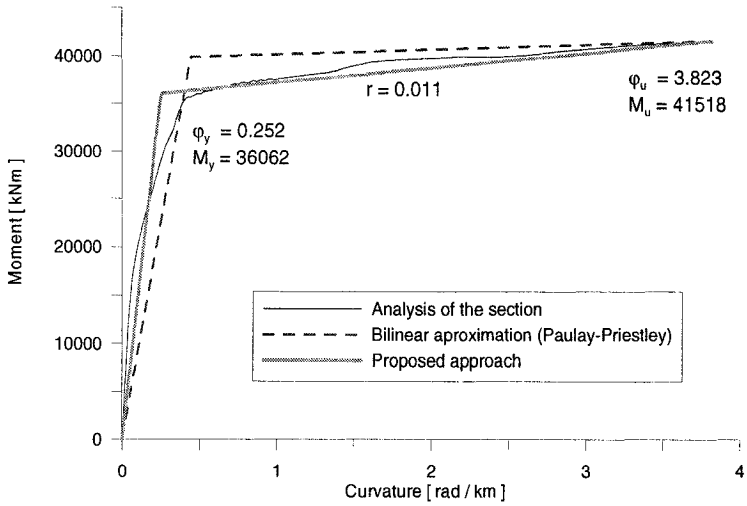

Figure 4.10: Moment-curvature: Vancouver - level 1

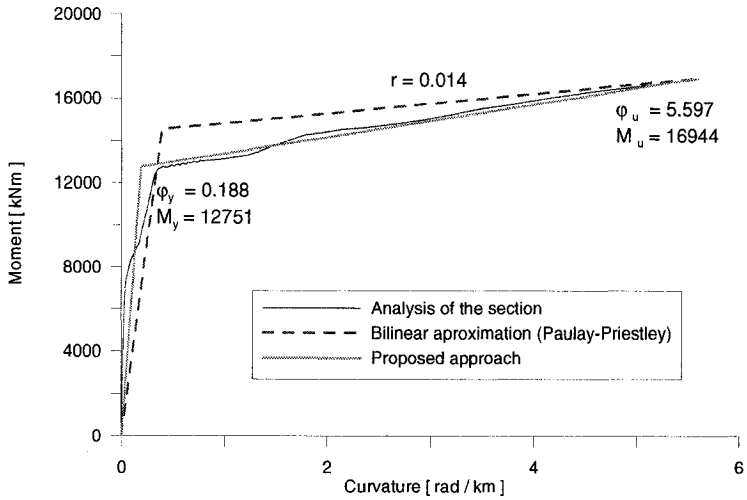

Figure 4.11 Moment-curvature: Vancouver - level 10

The comparison of the proposed model with the "actual" curve and the "Paulay-Priestley" approach shows that the proposed model leads to a better match with the actual response. This bilinear approximation is less accurate only in the first stage of loading, before yielding of the cross-section. Beyond that point, it follows very closely the actual response. Based on the above discussion, the proposed approach was retained for further use in this study.

B) Wall element

The second model used in this study is Model 4, or the "Structural-Wall" element as available in Ruaumoko. This model captures important parameters such as the material behaviour, the variation of the neutral axis along the wall cross-section during loading and unloading, the rocking of the wall, etc. The lack of information about the algorithm for this element was compensated by carrying out extensive preliminary validation studies. This parametric investigation was performed to study the response of the model under quasi-static, monotonic, cyclic, and dynamic loading. The parameters of the model have been calibrated against reliable experimental data.

Description of the model

The structural-wall member shown in figure 4.12.a was developed as the Taylor Wall element to represent the behaviour of reinforced concrete walls. This model uses several elements to represent a one-storey wall portion. As a result, a structural wall is represented by beam-column members with elastic shear deformations included. The properties of each section are evaluated by assessing the stresses and axial stiffness of a number of segments across the cross-section. At each section along the wall length, the central-line axial strain is computed and the curvature is determined as a function of the end rotation assuming that the cross-section remains plane, which permits to compute the longitudinal strain in each segment of the cross-section. For each of these segments in the cross-section, the concrete and steel stresses and tangent modulii are computed and the bending moment and axial force on the cross-section can then be obtained. A new effective cross-sectional area, second moment of area and location of the neutral axis is then computed. The section properties are integrated along the length using a Lobatto integration rule to get the member stiffness.

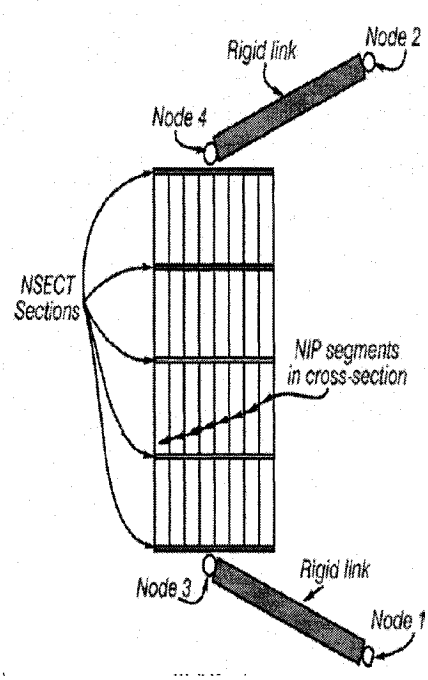

a) Wall member

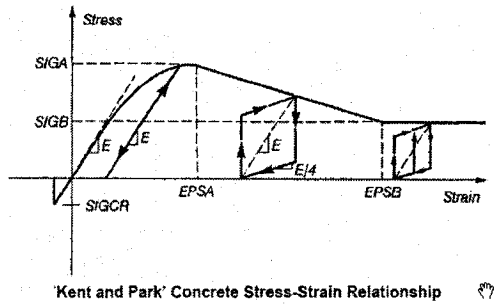

b) Kent-Park concrete rule

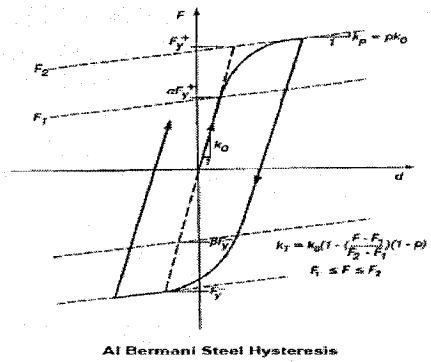

c) Al Bermani Steel Hysteresis

Figure 4.12: Structural-Wall element: a) Structural Wall Member; b) Concrete Stress-strain law; c) Steel stress-strain law (from Ruaumoko manual).

Hysteretic constitutive laws for confined concrete and reinforcing steel are incorporated into the model to define the stiffness and strength properties of the uniaxial elements. The axial stiffness of the elements is also based on the concrete and steel tributary area assigned to each element. The reinforcing steel stress-strain behaviour is described by either a simple bilinear hysteresis or the Al Bermani steel hysteresis shown in figure 4.12.c, which follows a Bounded Surface rule [Zhu 1995]. In the second model, the first plastic excursion is bilinear but the initial yield in subsequent cycles could be any fraction α of the input steel yield stress and the bilinear skeleton provides the plastic bounding surface.

The original Taylor element included only a very simple concrete stress-strain rule. Later, the Kent and Park hysteresis of Figure 4.12.b was introduced in the model. For the

analysis described herein, the monotonic envelope curve for the concrete in compression follows the Kent and Park model. The implemented concrete model describes the concrete stress-strain relation under an arbitrary cyclic strain history. The effect of the concrete confinement on the monotonic envelope curve in compression, the successive stiffness degradation, the effect of tension stiffening, and the hysteretic response under cyclic loading in compression and tension are incorporated in the model.

Validation of the model

A parametric study has been carried out to study the response of the model under quasi-static, monotonic, cyclic, and dynamic loading. The parameters of the model have been calibrated with reliable experimental data. To validate the Structural Wall element, the data from a large-scale test on a slender concrete wall conducted by Adebar and Ibrahim (2000) was used.

Description of the test

The 12.5 m tall cantilever concrete wall with a height-to-length ratio of 7.6 shown in figure 4.13, was constructed and tested in the horizontal position at the University of British Columbia (UBC). It had a flanged cross section and low percentages of vertical reinforcement: 0.65% in the flanges and 0.25% in the web. It was subjected to a uniform axial compression load that corresponded to $0.10f_c'A_g$ in addition to a reverse cyclic lateral point load applied at 11.33 m from the critical flexural section. The compressive strength of the wall concrete was measured to be 49 MPa. Tests on the 10M reinforcing bars indicated that the yield strength of the longitudinal reinforcement was 455 MPa and that the ultimate strength was 650 MPa. During the first four cycles of loading at each displacement level (see figure 4.14) , the lateral displacement was held constant at the peak value while the strains were measured over a 5 m height near the base, on both the compression and tension faces of the wall. Base rotation was observed in the test. Displacements measured at the base were used to estimate the rigid body motion at the top of the wall, and the recorded displacement at the top of the wall was corrected to

account for this effect. The lateral load was corrected for the friction force due to the Teflon bearings used to support the dead weight of the wall. This force was subtracted from the load recorded for each cycle.

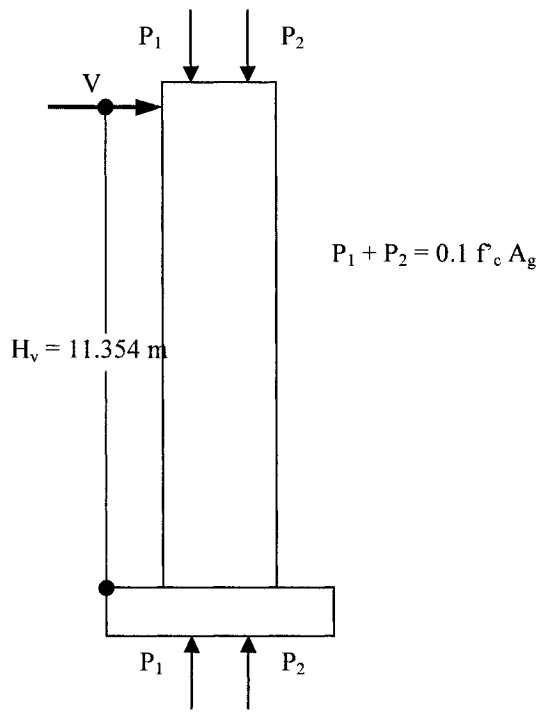

Figure 4.13: Schematic of the test setup

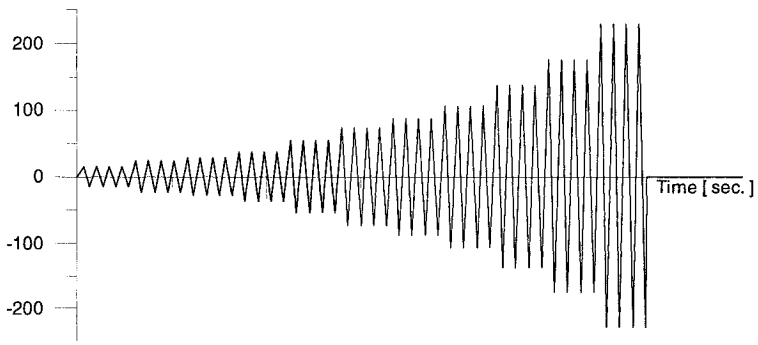

Figure 4.14: Sequence of imposed reverse cyclic lateral displacement at tip of the wall. (Adebar, P; Ibrahim, A.M.M.; 2000)

The corrected envelop of the load-displacement relationship shown in figure 4.17 and the experimental moment-curvature were used to validate the Wall element

Parametric study

For nonlinear analysis with Ruaumoko, the Taylor wall member was found to require smaller time step sizes than the model with frame element and concentrated plastic hinges to achieve acceptable results. A time step of 0.0001 s and five Newton-Raphson iterations for every time step were selected for the study, as recommended in the Ruaumoko manual. Based on a previous experience with Ruaumoko, the norm of 0.00001 of the out-of-balance force vector relative to the incremental force vector for the Newton-Raphson was chosen, which implied a tolerance of 0.1% in the residual vector.

Two types of loads were applied: cyclic and monotonic displacement at the top of the wall. It was found that the force-displacement envelopes were identical under both loading cases and it was decided that the remaining of the parametrical study would be continued with the application of the monotonic displacement only.

The first parameter studied was the number of Lombatto sections along the member, NSECT. It can be varied from 3 to 7. The study performed showed that the precision of the numerical solution was not dependant on NSECT. As a result an average value of 5 for NSECT was chosen.

The second parameter was the number of segments in the cross-section, NIP. In the Ruaumoko program, this parameter can be varied from 3 to 20. The influence of this parameter was examined by comparing the results of four push-over analyses. The wall was modeled with seven "Wall" members, with each member being made of ten integration sections, or fibres. The parameter NIP was given values of 5, 10, 15, and 20. The results are shown in figure 4.17. For this example, the variation of NIP had no significant influence on the response of the member. All computed responses are nearly

identical from the beginning of the loading until cracking of the section. From cracking to yielding of the flexural reinforcement, the responses are very much the same. The largest, although still small, difference in the results was observed after yielding with 5 NIP sections on one side and with 10, 15, and 20 NIP section on the other side,. The responses with 10, 15, and 20 NIP sections are essentially the same, and the maximum values for the base shear with these three values are respectively 147.2 kN, 147.3 kN and 147.6 kN. This can be explained by the fact that the flexural reinforcement was concentrated essentially at the both ends of the wall for this specific section, with a very small amount of distributed reinforcement. Another important issue is that the programme always assigns only one section for each flange. Hence, the concentrated reinforcement in all cases studied was assigned to one and always the same extreme section. Based on the above discussion, an average value of 15 was chosen for the NIP parameter to be used in further investigation of the responses of the "Taylor Wall" element.

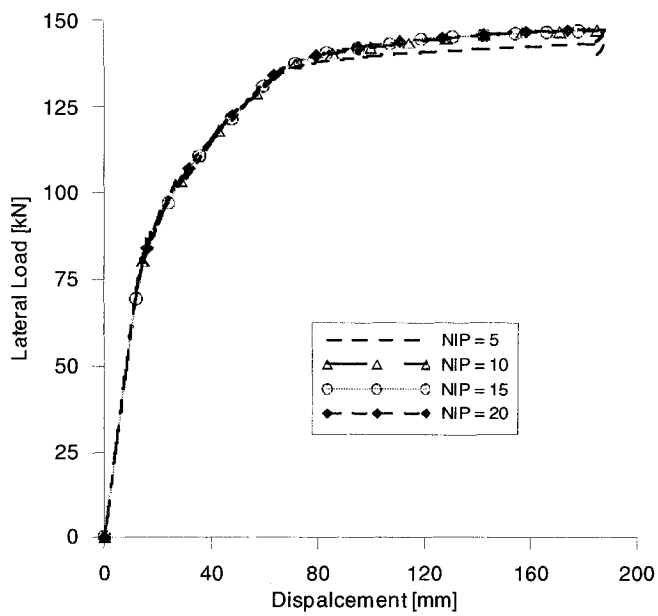

Figure 4.15: Influence of NIP on the lateral load-displacement response of the wall.

The third parameter was the height-to-width ratio of the elements. Because the height and the width were initially fixed, the number of elements representing the specimen was varied. Four cases were studied and compared: one, four, seven and ten elements, which represented height-to-width ratios of 6.97, 1.74, 0.99, and 0.70. In these analyses, the number of segments in the section (NIP) was 15, as discussed previously. The results are presented in figure 4.16. The response of the model with one member is completely different from the response of the wall modeled with more members. The responses obtained with four, seven, ten and twenty members are very similar. They follow the same tendency, with the shear force decreasing with an increase of the number of members. It could also be noticed that the responses obtained for ten and twenty members are almost identical and that the maximum shear force in both cases is the same, 141.60 kN and 141.20 kN.

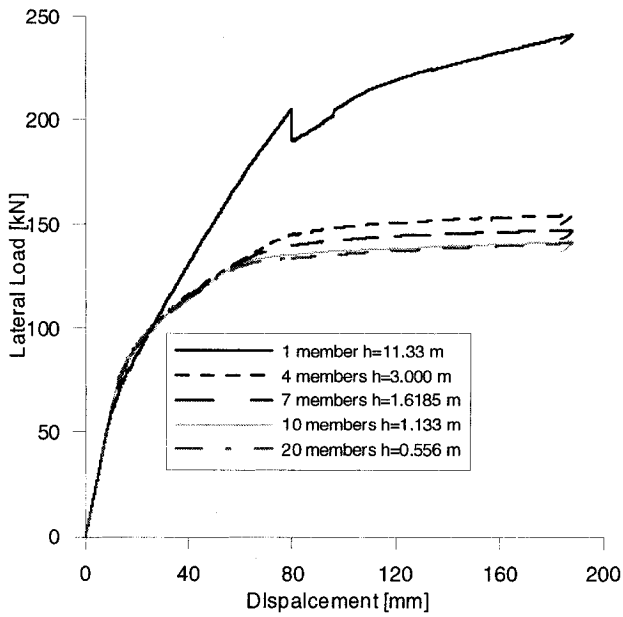

Figure 4.16: Sensitivity of the lateral load-displacement response of the wall to the number of members.

The final stage of the validation of the model was to compare analytical results obtained with "Wall" element to those obtained with the Response 2000 program and

from the physical test. Both the positive and negative envelopes obtained from the test results are plotted and compared with the analytical results. The results for twenty members are omitted herein because they are essentially the same as those with ten members. The prediction with the Response 2000 program matches well the test results until yielding starts, when the load V reaches approximately 90 kN. . The difference between Response 2000, on one side, and the "Wall" element, on the other side, can be explained by the fact that the reinforcement in the wall flanges in the "Wall" element is assumed to be distributed over the flange area. The flange is calculated as one section (fibre) in the analytical model. This is why the responses for different values of NIP and for different numbers of members for the "Wall" element are essentially the same and diverge from test and Response 2000 results after cracking up to first yielding. Once significant yielding has developed, the analytical results from the "Wall" element and Response 2000 are very similar to the test results. The best match is obtained with four elements, but this can be due to the numerical accuracy of the model. The solution converges when the number of members representing the wall is increased.

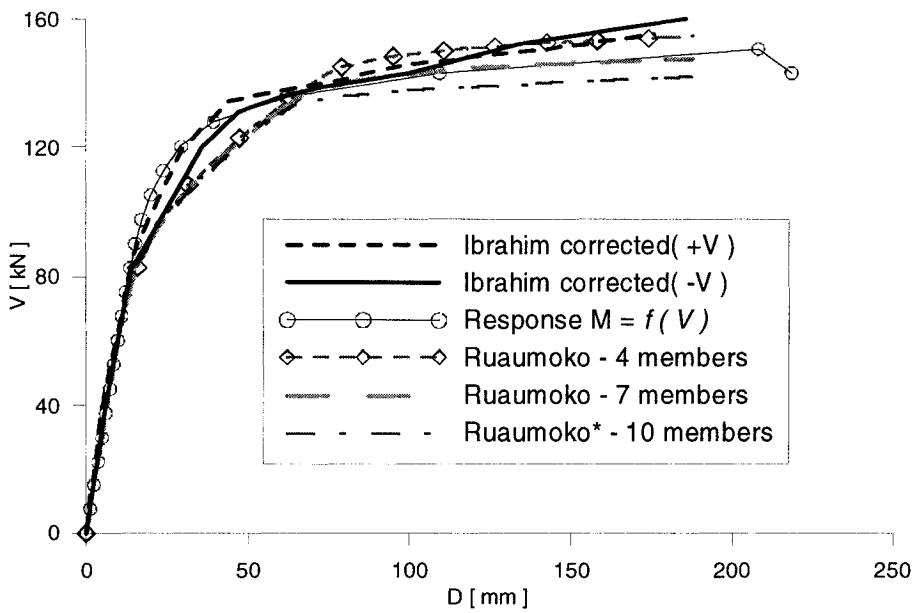

Figure 4.17: Influence of NIP on the lateral load-displacement response of the wall. (Note: the results for 10 and 20 members are essentially the same).

The difference between the analytical and test results can be attributed to the lack of data on the actual material properties and to the limitations of the material models used in both analytical programmes. The overall conclusion of this study is that the "Wall" element gives reliable results if a good set of parameters is prescribed. Hence, it can be used for further nonlinear investigation of the response of shear walls subjected to earthquake solicitations.

As was presented in Section 4.1 axial loading acting on a wall results in a pinched hysteretic response. The axial load contributes to returning the wall to its original un-deformed position at each cycle and adds an additional resistance to flexure. This effect is well represented with the Wall element and for the test wall when examining the cyclic moment-curvature response presented in figure 4.18.

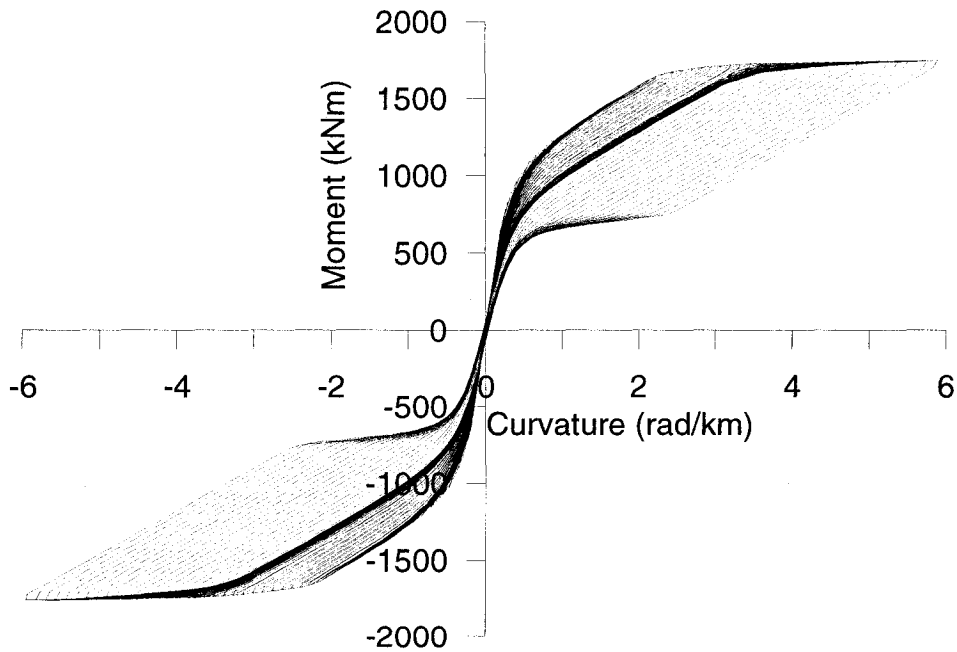

Figure 4.18: Influence of the axial load on the cyclic behaviour of RC walls

Concrete model

During the preliminary pushover analysis with the Kent and Park concrete model, a numerical instability of the response was noticed once the peak was passed. This motivated an additional comparative study on the two available concrete models.

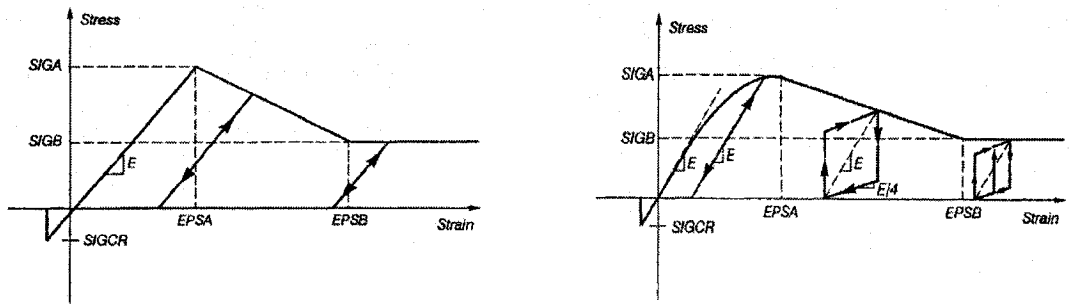

a) Taylor's Stress-Strain Relationship **b) Kent and Park Stress-Strain Relationship**

Figure 4.19: Available concrete models in Ruaumoko programme for Wall element

Both models are shown in figure 4.2.18. The Taylor model is a simple concrete model where the concrete elastic modulus is assumed to be constant until the maximum compressive stress is reached. The peak strain is assumed to be equal to E/f'_c. The Kent-Park model is a more refined model and gives a better representation of the concrete behaviour. It follows a quadratic rule until f'_c is reached and $\varepsilon_c = 2\ (f'_c/\ E)$. In spite of this, it may introduce a numerical instability during the integration and calculation of the forces. This is shown in figure 4.19, where a comparison is made for the section at the base of the wall in the five-storey building situated in Vancouver. Once the peak is passed on the concrete stress-strain curve, a sudden loss of the material stiffness occurs which leads to unbalance in the system. Before the tension cracking occurs, the K&P model provides a better fit with the Response 2000 curvature but the strength is lower (M_{max} = 20 940 kN-m with K&P model < $M_{Response\ 2000}$ = 21 235 kN-m), as shown in figure 4. 19. On the other side, the Taylor model provides less stiffness in the system but gives a higher strength (M_{max} = 21 340 kN-m).

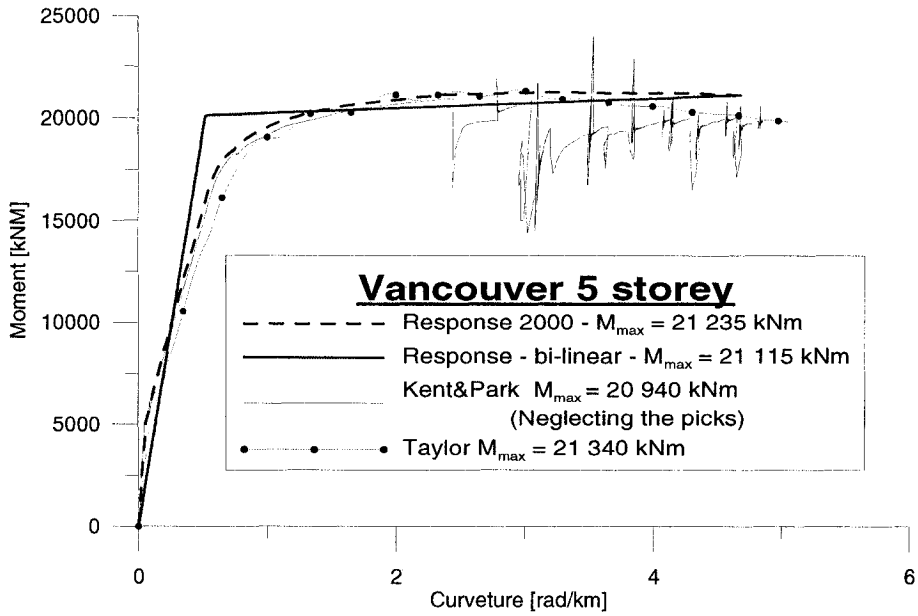

Figure 4.20: Comparison of the Taylor and K&P concrete models with Response 2000.

The difference between the two concrete models in terms of strength is less than 2%, which is acceptable. The Taylor's concrete model is closer to the Response 2000 results and it was chosen for subsequent use for the nonlinear earthquake analysis because of its greater stability and simplicity.

Influence of F_{cr}

During the evaluation of the results obtained with Ruaumoko, disagreement were found between the maximum shear force values reported in the output file and the peak shear forces in the recorded time history (in the .RES file). To find the causes for this disagreement, the response of the specimen was examined in detail at every 0.0001 s. Recording the response with this output step ratio showed a good agreement between the two types of output responses. Acknowledging that a time step of 0.0001 s, and even 0.01 s, has no real physical meanings for the earthquake event led us to the suspicion that there was a numerical momentous disequilibrium in the system. To find out the origin of this phenomenon, complementary analyses were run. In these analyses, we studied the base shear and story shear at the 17th floor of the 25-storey building located

in Vancouver when subjected to the simulated earthquake W65302 time history. That case was selected because of the greater difference that was observed between the two outputs. Figure 4.21 shows the plot of the shear force at the 17th storey. It can be clearly seen in the figure that large peaks developed in the response time history at 1.6, 1.8, and 2.0 seconds.

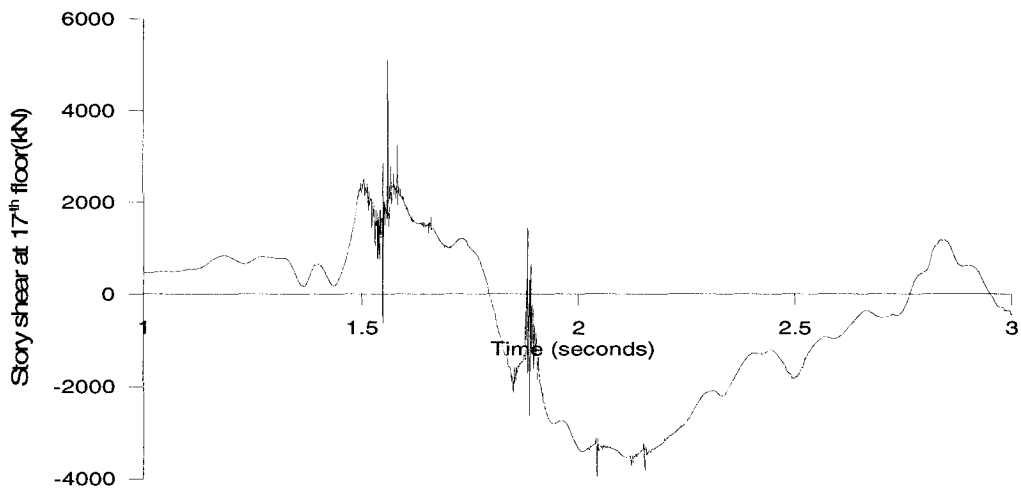

Figure 4.21: Storey shear at 17-th storey in the 25-storey building located in Vancouver under theW65302 ground motion

The following parameters were studied to explain this situation: the time-step, the "norm of the out-of-balance force vector", and the value of tensile strength of the concrete, F_{cr}. It was found that the tensile cracking stress had a significant influence on the results. The wall response values obtained from the output file are plotted in figure 4.22 for different values of F_{cr}: 0.175 MPa, 0.50 MPa, 1.075 MPa, and 1.75 MPa. The latter is the correct value.

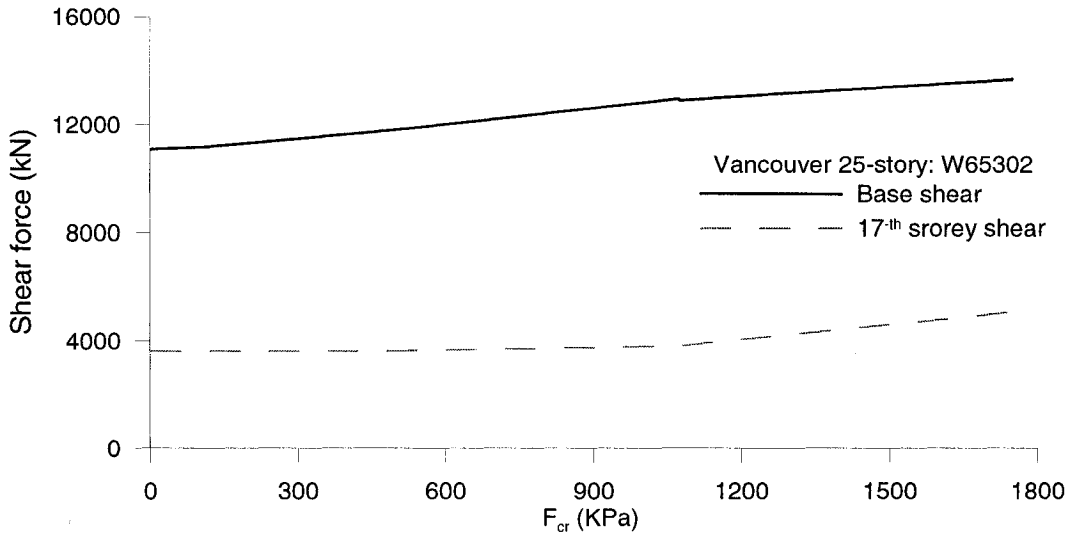

Figure 4.22: Maximum storey shear forces for different values of F_{cr} for the 25-storey building in Vancouver under the W65302 ground motion

The values of the maximum storey shear converge when the tensile strength of concrete is decreased. This is consistent with the results from time history output response files where several analyses for different F_{cr} values were ran. In figure 4.23, the base shear responses are plotted for the time period between 1.0 to 2.0 seconds. The storey shear at the 17^{th} floor is given for the time period between 1.0 to 3.0 seconds in figure 4.24. The time history of the effective stiffness relative to the gross stiffness for the case when F_{cr} = 1.75 MPa is also plotted in both figures. Both plots clearly show that during the first cracking of each section, at the time when the stress exceeds F_{cr}, the concrete section is no longer effective and the entire tensile force must be transferred to the steel fibre at this location. During this transfer, some disequilibrium is induced in the system and higher shear forces seem to be introduced to restore the force balance, which gives the observed peaks.

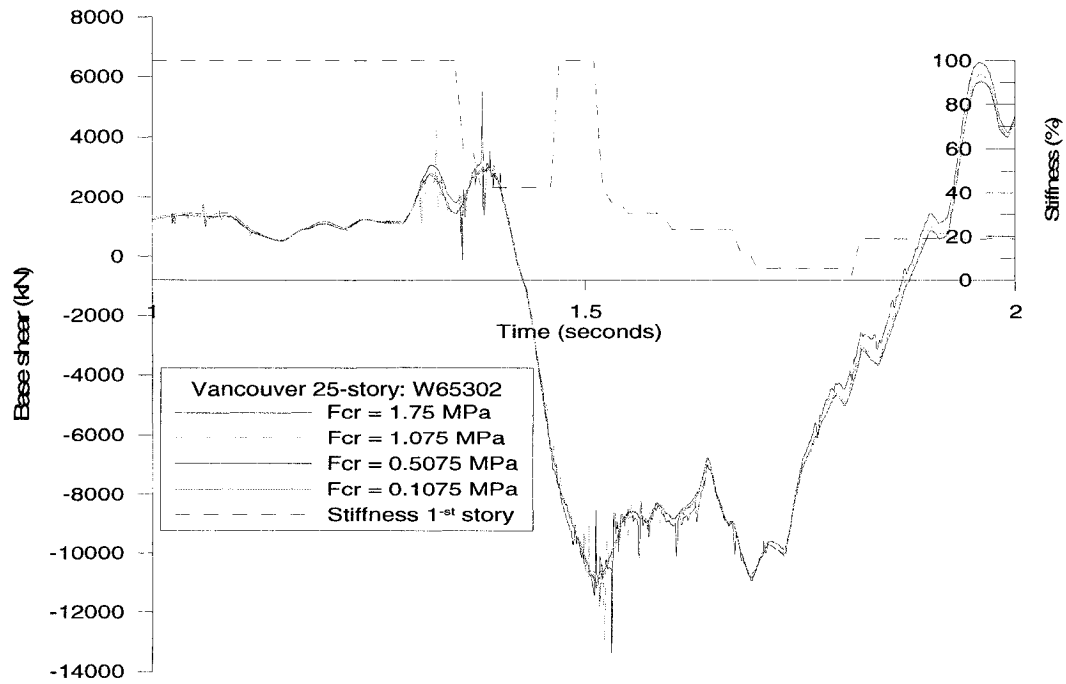

Figure 4.23: Base shear force time history for different values of F_{cr} for the 25-storey building in Vancouver under the W65302 ground motion

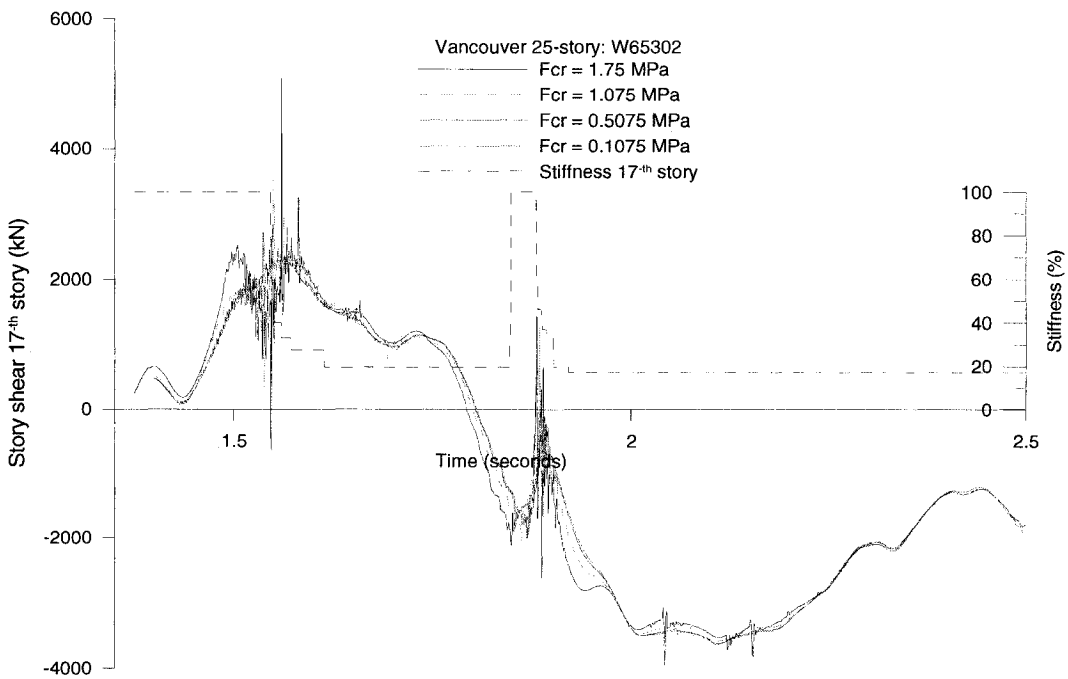

Figure 4.24: Storey shear force time history for different values of F_{cr} for the 25-storey building in Vancouver under the W65302 ground motion

The response from a complementary analysis performed with the artificial M7.0 72701 earthquake record was examined to confirm this finding and see the influence of the earthquake ground motion. The results are reported in figure 4.25 for the base shear and figure 4.26 for the story shear at the 17th storey. Both figures confirm the occurrence of instantaneous disequilibrium states upon cracking of the concrete section in tension and that the peak amplitudes tend to decrease when decreasing the tensile strength of the concrete. As shown, the three responses obtained with the three F_{cr} values are in phase and there is a slight shifting in time because of the shifting of the stiffness of the wall: a lesser value of F_{cr} leads to earlier cracking of the section, which leads to slightly different response of the wall.

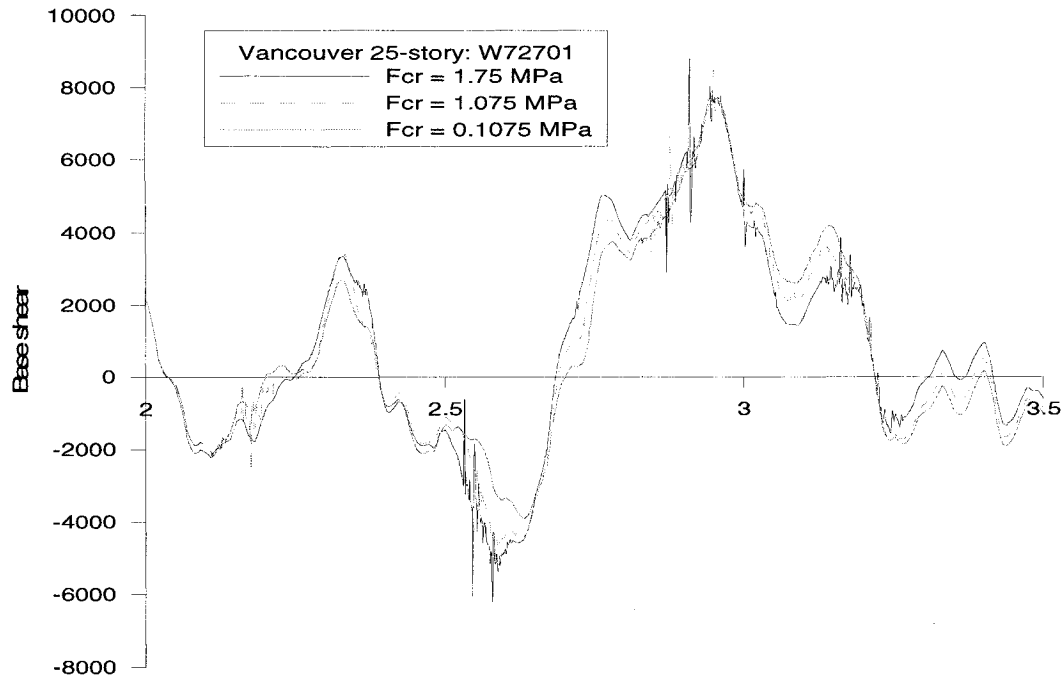

Figure 4.25: Base shear force time history for different values of F_{cr} for the 25-storey building in Vancouver under the W72701 ground motion

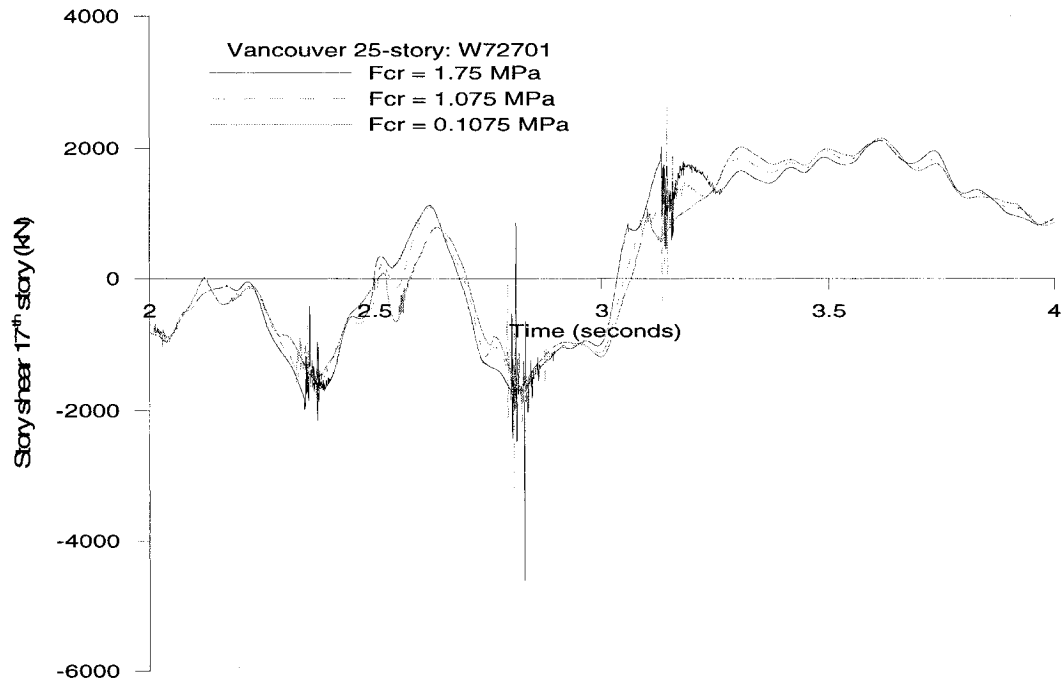

Figure 4.26: Storey shear force time history at 17th storey for different values of F_{cr} for the 25-storey building in Vancouver under the W72701 ground motion

Comparing the responses under both earthquakes, a similar instability was found during the tensional cracking of the concrete section and it could be concluded that the influence of the earthquake record and its magnitude are insignificant in terms of the convergence of the response and the introduction of the fictive "parasite" shear forces in the system.

It should be reminded that the shear wall studied herein has a C cross-section. The total length is 11 m and the flanges are 4.0 m wide and 0.3 m thick and, hence, a large portion of the concrete section is located at the extreme fibres. Even when the flange was divided into three sections, these sections were still much larger than the web sections. Furthermore, the reinforcement in the flanges is close to the required minimum, which means that the concrete carries relatively high tensile force at the time of cracking of the section. A large drop in resistance is therefore associated with the sudden cracking of the concrete for this wall. In order to study the influence of the shape of the wall and

the proportion of the concrete area located in the flanges, as well as to confirm the findings discussed above, the response of the ten-story building located in Vancouver with a simple wall shape with columns at both ends was examined. As described in Chapter 3, the length of the wall is 7.45 m with web thickness of 0.250 m, and the column dimensions are 0.45 m x 0.45 m. The wall was subjected to the same two earthquakes: W65302 and W72701. The analyses were carried out with three values of F_{cr}: 1.75 MPa, 1.075 MPa, and 0.1075 MPa. The results for the base shear and the 7^{-th} floor storey shear, i.e. at the same relative height compared to the 25-storey building (17/25 = 7/10), are presented in figures 4.27 and 4.28 for the W65302 ground motion and in figures 4.29 and 4.30 for the W72701 earthquake.

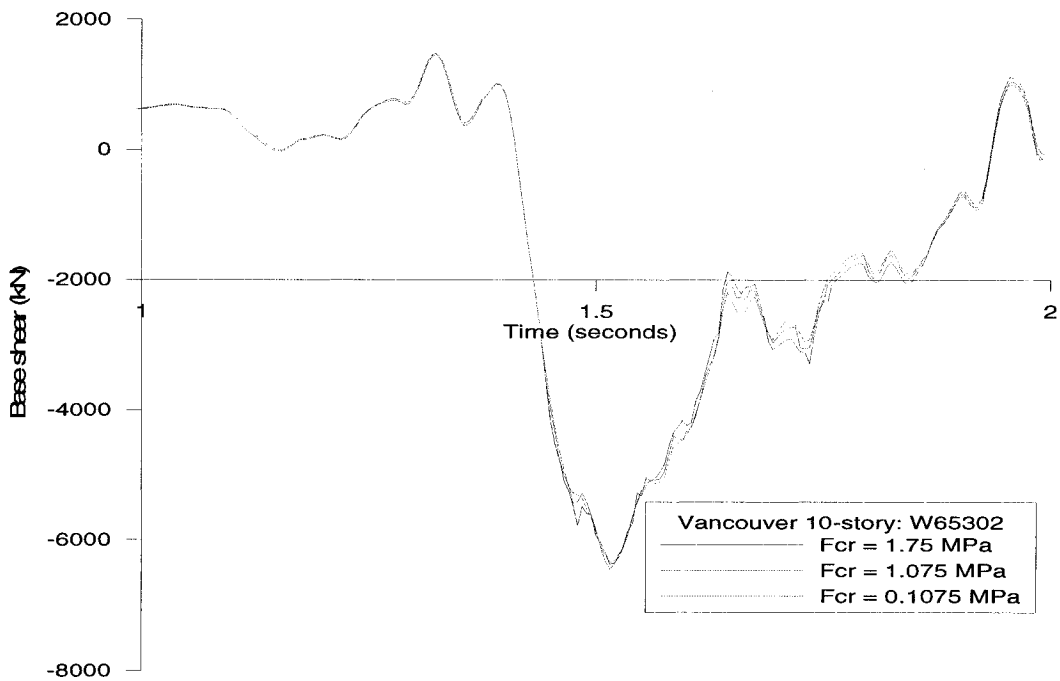

Figure 4.27: Base shear time history for different values of F_{cr} for the 10-storey building in Vancouver under the W65302 ground motion

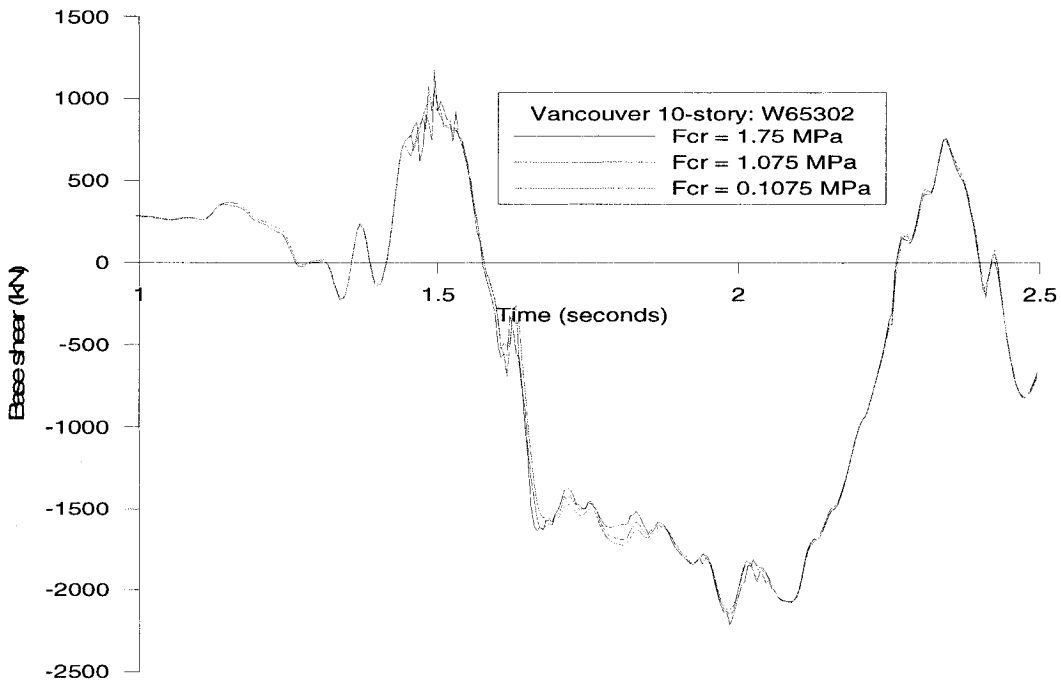

Figure 4.28: Storey shear force time history at 7th storey for different values of F_{cr} for the 10-storey building in Vancouver under the W65302 ground motion.

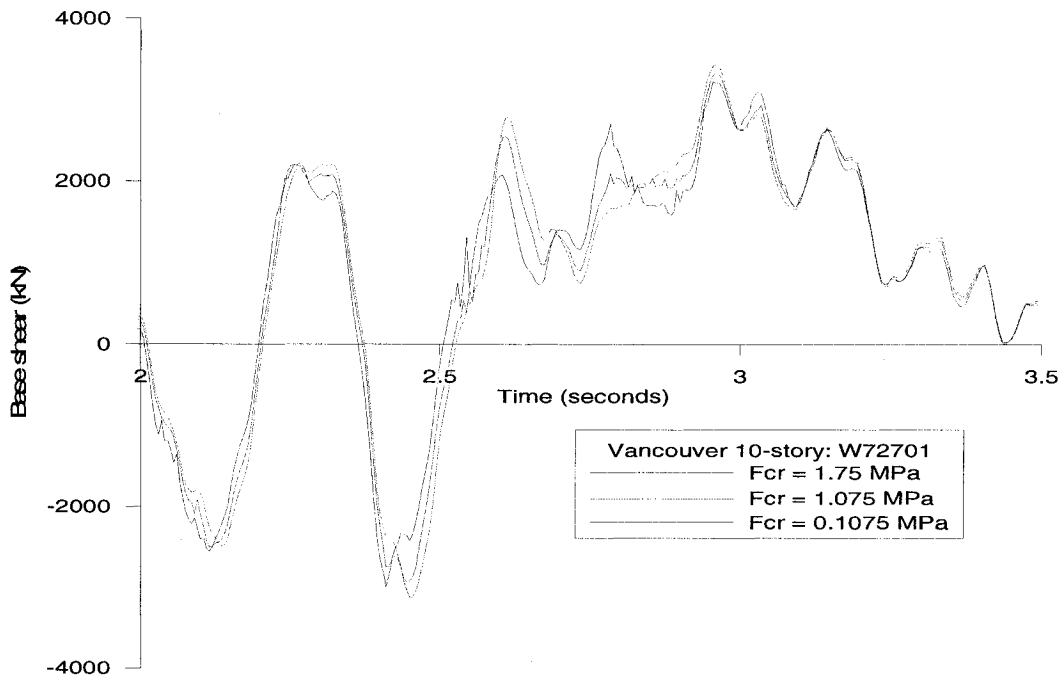

Figure 4.29: Base shear time history for different values of F_{cr} for the 10-storey building in Vancouver under the W72701 ground motion.

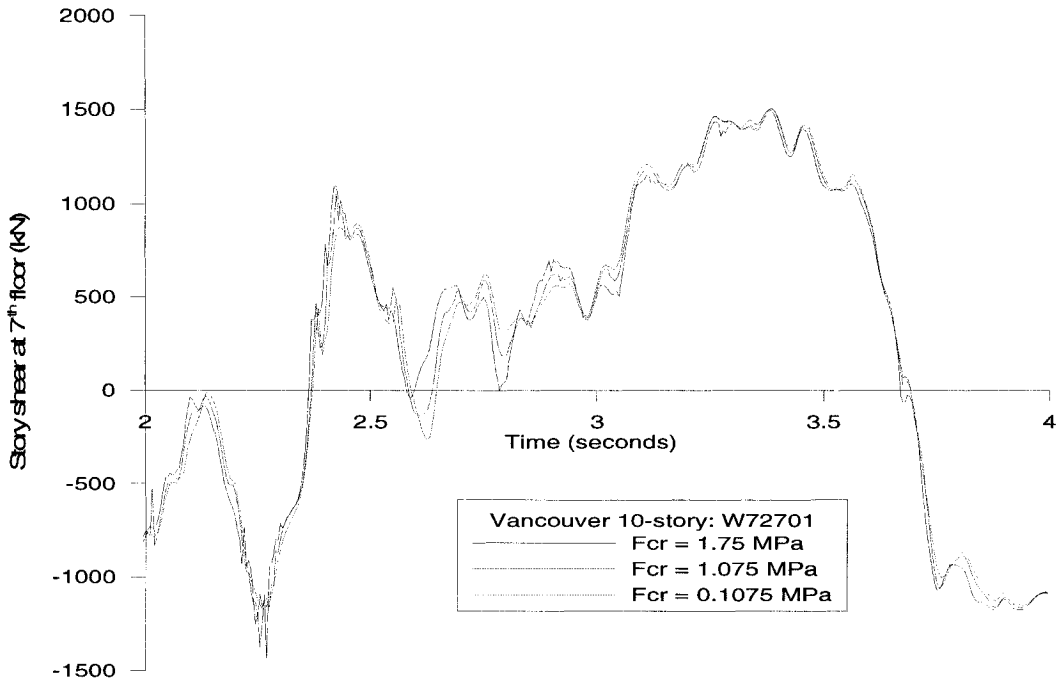

Figure 4.30: Storey shear force time history at 7th storey for different values of F_{cr} for the 10-storey building in Vancouver under the W72701 ground motion.

As can be noted, the responses are much more stable and are nearly identical at the base of the wall, except for the slight stiffening of the response. Some instability was observed at the 7th storey but they are relatively much smaller in amplitude and less pronounced compared to the case for the 17th storey in the 25-storey building. It should be underlined that minimum reinforcement design requirements governed the choice and the quantity of the steel reinforcement in the column at the 7th level of the 10-storey building.

In conclusion, it can be said that the stability of the solution for the shear forces in the reinforced concrete walls is sensitive to the tensile strength specified for the concrete. The value of F_{cr} has a significant influence on walls with large concrete sections and relatively small quantity of reinforcement. As the flange concrete area decreases and the steel reinforcement increases, the influence of F_{cr} is reduced and becomes basically zero for simple walls with high steel ratios for the concentrated

reinforcement regions. The effect of F_{cr} was the same regardless of the type and the magnitude of the earthquake record.

On the basis of these conclusions and on the fact that the maximum storey shear values are not sensitive to F_{cr} when the instability peaks are omitted, the decision was made to use a reduced concrete tensile strength F_{cr} = 0.175 MPa for the rest of the analytical study (all buildings at both sites) in order to avoid errors due to numerical stability problems.

4.3 Properties and parameters used for nonlinear analysis

As was explained above, two models were used for the nonlinear analysis: the standard Bar model and the Wall model. The 10-storey building located in Vancouver is used as an example to present the properties and characteristics used in the analysis. The models properties for all buildings are presented in Appendix B.

As explained in Section 2.2.1, the reduction in the seismic forces in NBCC 2005 is attributed to two factors: the ductility-related force modification factor R_d and the overstrength-related force modification factor R_o. The ductility-related factor R_d is accounted for by using nonlinear analysis. The overstrength-related force modification factor is a product of different factors, (see Section 2.2, equation 2.2). The analytical model reproduced the walls as designed and then included the contribution of R_{size}. A yield strength f_y equal to 420 MPa and strain hardening behaviour was included in the model such that the model included the contribution of R_ϕ R_{yield} and R_{sh}. For individual shear walls, R_{mech} is equal to 1.0 and has no effect. Hence, the walls as modelled were representative of actual walls as built and as was assumed in the formulation of the R_o factor in NBCC.

The mathematical representation of the structure for both models is the same: one element per storey, 3000 kN seismic weight per storey per wall, 504 kN axial gravity load per level. Integration time-steps of 0.001 s and 0.00002 s were used for the Bar and

Wall models, respectively. The P-delta effects were not included because they do not have a significant influence on the response for shear wall type of structures (Tremblay et al. 2000, Tremblay et al. 2006).

4.3.1 Bar element

At first, the common "Bar" or "stick" model of figure 4.30 was used to simulate the wall behaviour. In this model each storey was modeled as a single bar having the same flexural and axial rigidity as the wall section and carrying the seismic weight of the half of the building. In-plane torsion is accounted for in the ground motion amplitude, as discussed earlier. The cyclic flexural behaviour was approximated as bi-linear Modified Takeda degrading stiffness hysteretic model (Otani, 1974), figure 4.31, employing the method described in section 4.2.b. the moment curvature was calculated with Response 2000 program. To account for previous cracking, the tension stiffening parameter was set in the program equal to 0.3 (Vecchio 2004, personal correspondence - Bruno Massicotte[1], and Denis Mitchell[2]). We also used a stress blocks based on stress-strain curves with peak stress equal to $0.9 f_c'$ (27 MPa) to account for differences between the in-place strength and the strength of standard cylinders, as required in Clause 10.1.6 of CSA A23.3-04.

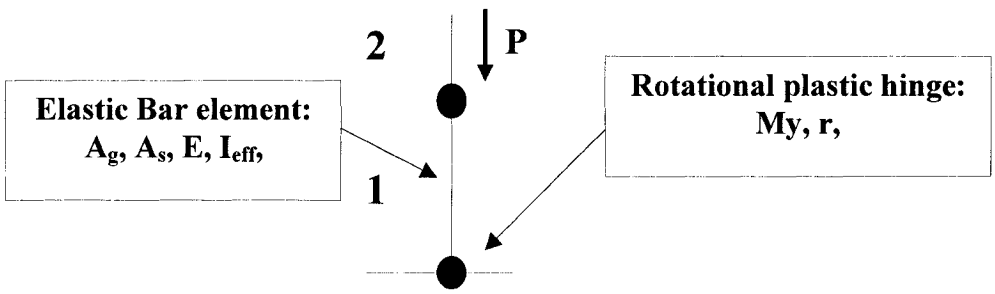

Figure 4.31: Analytical Bar models for shear walls.

[1] Professor at Ecole Polytechnique of Montreal
[2] Professor at McGill University

For 5- and 10-storey buildings we calculated the moment-curvature diagram for each storey. For the 15-storey buildings each storey of the bottom and middle parts were presented with a members having a properties characteristic for each storey. For the upper part of the building, where no significant yielding is expected, we used the same properties of moment-curvature model for every two storeys. For the higher buildings, of 20- and 25-storey, because of the negligible difference of member behaviour, every two storeys were characterized with the same moment-curvature hysteresis, calculated at the base of the bottom member.

For all member sections, the elastic modulus of the member is equal to the elastic modulus of concrete E_c = 25000 MPa and the shear modulus of concrete $G = G_c$ =10400 MPa. To account the total ductility demand at each storey the storey inelastic response was concentrated in one plastic hinge, located at the lower of each member and the plastic hinge length was set equal to the storey height. Bi-linear hysteretic response based on the bilinear approximation of the cross-sectional moment-curvature response, and following the Takeda hysteretic model shown in Figure 4.32. For analyses the unloading stiffness parameter, $\alpha = 0.50$, and the reloading parameter, $\beta = 0.25$.

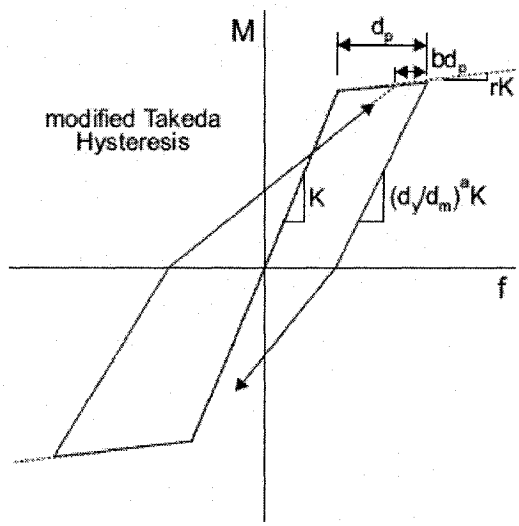

Figure 4.32: Takeda hysteretic model.

Table 4.1: 10-storey building Vancouver

Storey No	A_g m^2	A_s m^2	I m^4	r	M_y kNm	I/I_g
1	2.043	0.921	4.874	0.0062	37799	0.451
2	2.043	0.892	4.725	0.0105	35705	0.437
3	2.043	0.852	4.513	0.0113	34190	0.417
4	2.043	0.816	4.322	0.0131	32386	0.399
5	2.043	0.781	4.138	0.0135	30840	0.382
6	2.043	0.733	3.884	0.0148	29201	0.359
7	2.043	0.641	3.395	0.0134	23256	0.314
8	2.043	0.584	3.095	0.0156	21583	0.286
9	2.043	0.438	2.321	0.0135	14579	0.215
10	2.043	0.363	1.921	0.0165	12898	0.178

Example for member properties used as entry data for the 10-storey building located in Vancouver is shown in Table 4.1: gross area, A_g, steel area, A_s, effective moment of inertia (from K_0), I, and the bilinear ratio, r. Table 4.1 also gives, as additional information, the ratio of effective moment of inertia to the gross inertia moment.

4.3.2 Wall element

The full description of the Wall element is given in Section 4.2.b. and in figure 4.12. In this paragraph, we summarized the input values used to model the 10 studied buildings.

For the 5-, 10-, and 15-storey buildings, the cross-sections are represented by 10 fibres (NIP=10), as shown in figure 4.32.a, two for each column and six for the wall web. Because the 20- and 25-storey buildings have larger cross-sections, each storey was represented with more fibre elements: NIP=18, three for the flanges and twelve for the web (see figure 4.32.b).

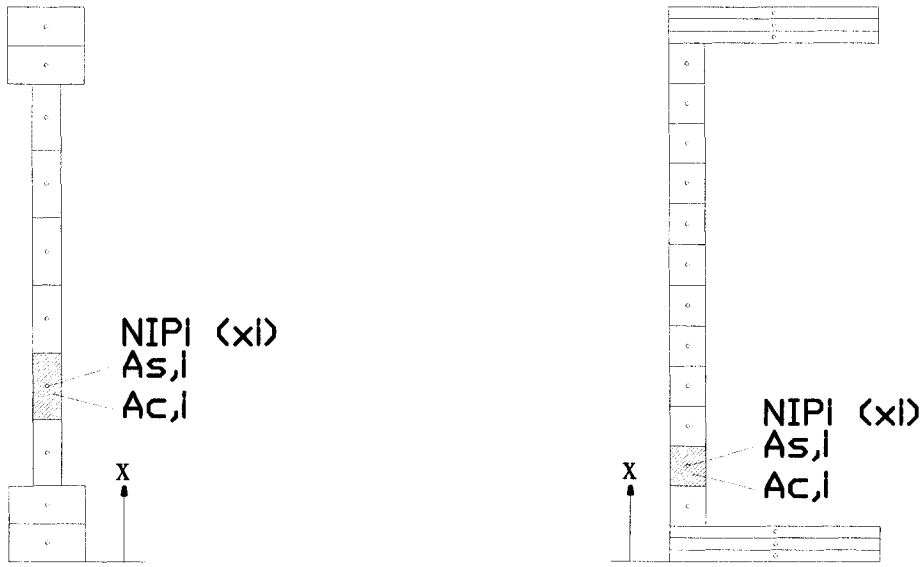

a) 5-, 10-, and 15-storey buildings **b) 20- and 25-storey buildings**

Figure 4.33: 10-storey building in Vancouver

To obtain the same deformation at maximum compressive stress, f'_c, as the base curve for the concrete material used in Response 2000 (Popovich-Thorenfeldt-Collins), which is similar to the Kent-Park concrete model, the input value of the concrete elastic modulus E_c was modified. For the Taylor concrete model in Ruaumoko (figure 4.18.a), $\varepsilon'_c = f'_c/E_c$, thus $E_c = f'_c/\varepsilon'_c$. Threfore, for $\varepsilon'_c = 0.00196$ from Response 2000, it is found that $E_c = 13800\ MPa$. As was discussed before, the maximum compressive strength of concrete was set equal to $0.9*f'_c$ = 27MPa,. The residual strength of the concrete, f'_{cu} corresponding to the compressive strength of concrete for deformations exceeding the ultimate compressive deformation $\varepsilon'_{cu} = 0.005$, was set equal to 10% of f'_c, or 2.7 MPa to reproduce nearly zero resistance at large deformations As also discussed above the tensile strength was modified from the original value and it was reduced to $0.175\ MPa$. The effect of concrete confinement is discussed later.

The steel reinforcement was modeled with bilinear elasto-plastic model with elastic modulus $E_s = 200\ 000\ MPa$, yielding stress $f_y = 420\ MPa$ and steel hardening factor r =

0.005. That ratio results in the ultimate strength $f_u = 550\ MPa$ being reached at an ultimate strain $\varepsilon_s = 0.130\ m/m$ (reinforcing steel CSA G30.16 400 MPa weldable).

Table 4.2 presents the input values used for modeling the 10-storey building located in Vancouver. For simplification, the total, gross area, of concrete sections is shown instead of the real value that was specified in the program, $A_{concrete} = A_g - A_s$.

Table 4.2: 10-storey building - Vancouver

Storey	Fibre	1	2	3	4	5	6	7	8	9	10
	Xi	0.113	0.338	0.996	2.088	3.179	4.271	5.363	6.454	7.113	7.338
Ag	Ac+As	0.1013	0.1013	0.2729	0.2729	0.2729	0.2729	0.2729	0.2729	0.1013	0.1013
As	1	0.0028	0.0028	0.0007	0.0007	0.0007	0.0007	0.0007	0.0007	0.0028	0.0028
	2	0.0028	0.0028	0.0007	0.0007	0.0007	0.0007	0.0007	0.0007	0.0028	0.0028
	3	0.0028	0.0028	0.0007	0.0007	0.0007	0.0007	0.0007	0.0007	0.0028	0.0028
	4	0.0028	0.0028	0.0007	0.0007	0.0007	0.0007	0.0007	0.0007	0.0028	0.0028
	5	0.0028	0.0028	0.0007	0.0007	0.0007	0.0007	0.0007	0.0007	0.0028	0.0028
	6	0.0028	0.0028	0.0007	0.0007	0.0007	0.0007	0.0007	0.0007	0.0028	0.0028
	7	0.002	0.002	0.0007	0.0007	0.0007	0.0007	0.0007	0.0007	0.002	0.002
	8	0.002	0.002	0.0007	0.0007	0.0007	0.0007	0.0007	0.0007	0.002	0.002
	9	0.001	0.001	0.0007	0.0007	0.0007	0.0007	0.0007	0.0007	0.001	0.001
	10	0.001	0.001	0.0007	0.0007	0.0007	0.0007	0.0007	0.0007	0.001	0.001

4.4 Choice of earthquake ground motions

The second parameter studied was the influence of the earthquake on the nonlinear earthquake response. The 2005 NBCC stipulates that the ground motion histories used in the Nonlinear Dynamic Analysis Method shall be compatible with the response spectrum constructed from the design spectral acceleration values S(T) at the site. Those spectral values are not the result of one single particular earthquake, but the combined effect of a number of different potential damaging events. It is impossible and unrealistic to use only the earthquakes which match the spectrum, especially when using historical records. Because of this, the approach used herein consisted in using of a number of records that matched the target spectrum for a selected building period range. Atkinson

& Beresnev (1998) and Tremblay and Atkinson (2001) showed that this could be adequately done using just two types of earthquakes: a lower magnitude earthquake to represent the short-period hazard, M6.0 for Montreal and M6.5 for Vancouver, and a larger magnitude, M7.0 and M7.2 to represent the long-period hazard. The hypocentral distances for those events are selected based on the contribution of the events to the seismic hazard at the site, a smaller distance for the short period part and a greater distance for long period part.

For this reason, a number of different time histories were selected. A total of fourteen earthquake records were chosen as input ground motions for the buildings located in Montreal, QC. Because of the absence of a variety of historical strong ground motion records representative for eastern Canada, only two historical ground motion records were chosen. To compensate this, twelve simulated time histories were used. Conversely, numerous historical data records are available for western Canada and a larger number of actual records were used. A total of fifteen earthquake records including seven historical and eight simulated motions were selected to represent the seismic hazard for the buildings situated in Vancouver, BC. All records were scaled to match the design code response spectrum for the specified sites. The description of the selected earthquakes and scaling factors are summarized in Table 4.3 for Montreal and in Table 4.4 for Vancouver. In those tables, the given PGA corresponds to the maximum ground acceleration of the ground motion before scaling.

Figures 4.34 to 4.36 show the response spectra of the scaled accelerograms of the chosen earthquakes used for the nonlinear analysis. The main characteristics of a time history record are the peak ground acceleration and the dominant frequency. As was explained earlier, the first factor was accounted for by applying the calibration (scaling) factor reported in the tables. The fundamental difference between the historical earthquakes for the eastern and western parts of Canada is that the ground motions in the west are characterized by a lower dominant frequency compared to those in the east. The

average value of the dominant frequency of the records used for the west is 3.3 Hz. It is equal to 16.6 Hz for the east, which makes a ratio f_W/f_E of 5.0. This difference is most significant, with ratio values reaching up to 12 when comparing the frequencies of the 1985 Nahanni and the 1989 Loma Prieta(direction 0°) records.

Table 4.3: Characteristics of the selected ground motions for Montreal

No	Time history	Trial Station	Magnitude [Ms]	PGA [g]	R [km]	Factor
E1	E60301 – simulated	1	M6.0	0.43	30	0.85
E2	E60302 – simulated	2	M6.0	0.52	30	0.85
E3	E60501 – simulated	1	M6.0	0.24	50	1.7
E4	E60502 – simulated	2	M6.0	0.19	50	1.7
E5	E70301 – simulated	1	M7.0	0.97	30	0.3
E6	E70302 – simulated	2	M7.0	1.05	30	0.3
E7	E70501 – simulated	1	M7.0	0.51	50	0.6
E8	E70502 – simulated	2	M7.0	0.63	50	0.6
E9	E70701 – simulated	1	M7.0	0.30	70	0.9
E10	E70702 – simulated	2	M7.0	0.29	70	0.9
E11	E701001 – simulated	1	M7.0	0.24	100	1.0
E12	E701002 – simulated	2	M7.0	0.26	100	1.0
E13	Nahanni (23/12/85)- Battlement Creek – 270°	S3	M6.9	0.19	21	3.0
E14	Nahanni (23/12/85)- Battlement Creek – 360°	S3	M6.9	0.19	21	3.0

Table 4.4: Characteristics of the selected ground motions for Vancouver

No	Time history	Trial Station	Magnitude [Ms]	PGA [g]	R [km]	Factor
W1	W60201 – simulated	1	M6.0	0.29	20	2.0
W2	W60202 – simulated	2	M6.0	0.42	20	2.0
W3	W65301 – simulated	1	M6.5	0.53	30	0.8
W4	W65302 – simulated	2	M6.5	0.54	30	0.8
W5	W72301 – simulated	1	M7.2	0.94	30	0.5
W6	W72302 – simulated	2	M7.2	0.65	30	0.5
W7	W72701 – simulated	1	M7.2	0.25	70	1.0
W8	W72702 – simulated	2	M7.2	0.26	70	1.0
W9	Western Washington Earthquake (13/04/49)– Olympia, Washington HWY Test Lab - 86°	S325	M7.1	0.28	76	1.6
W10	Western Washington Earthquake (13/04/49)– Olympia, Washington HWY Test Lab - 356°	S325	M7.1	0.16	76	1.6
W11	Morgan hill Earthquake (24/04/84) – Gilroy #6 - 90°	S 57383	M6.2	0.29	37	1.0
W12	Northridge Earthquake (17/01/94) –Old Ridge Route - 0°	S24278	M6.7	0.51	44	0.7
W13	Northridge Earthquake (17/01/94) – Old Ridge Route - 90°	ORR	M6.7	0.57	44	0.7
W14	Loma Prieta Earthquake (17/10/89) – San Francisco – Presidio - 0°	S58222	M7.1	0.10	100	1.4
W15	Loma Prieta Earthquake (17/10/89) — San Francisco – Presidio - 90°	S58222	M7.1	0.20	100	1.4

In addition to the scaling procedure adopted for spectrum matching, all ground motions were amplified further by 1.4 to account for in-plane torsional effects for

consistency with the design assumptions. This factor is not included in the spectra shown in figures 4.34 to 4.36.

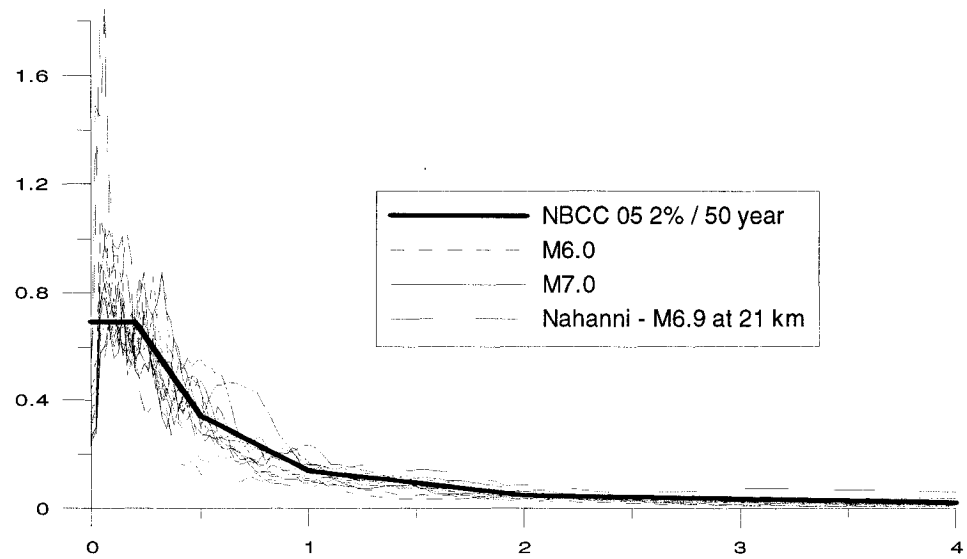

Figure 4.34: 5% damped response spectra for Montreal

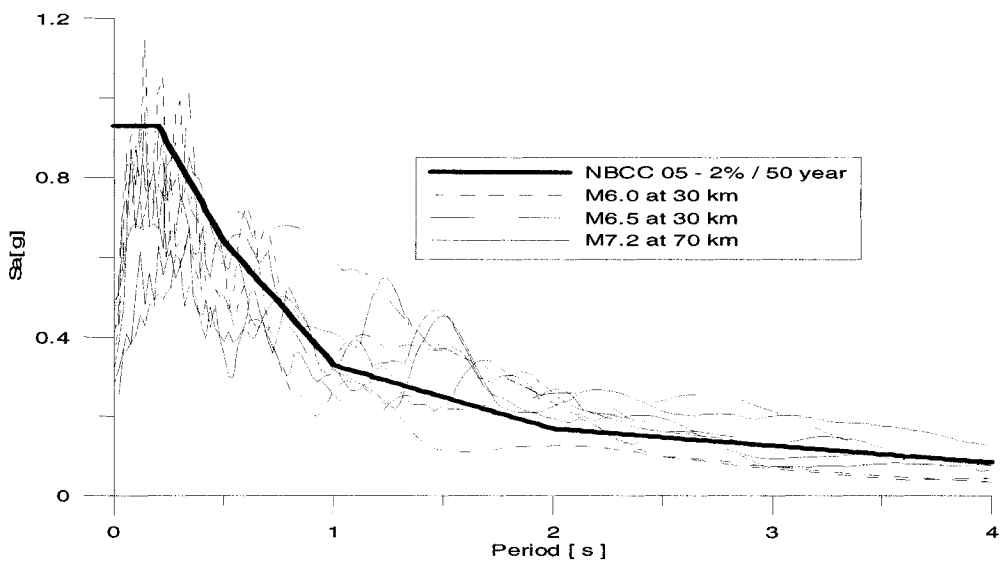

Figure 4.35: 5% damped response spectra for Vancouver – NBCC 2005 and simulated earthquakes W1 to W8

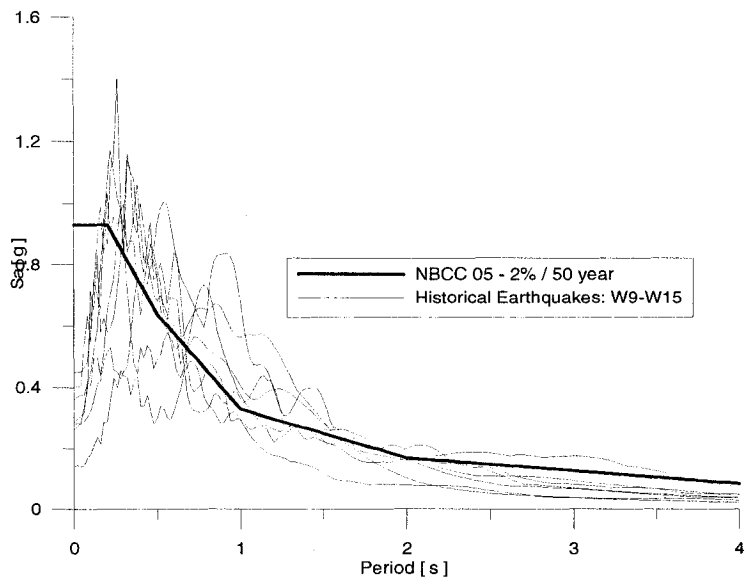

Figure 4.36: 5% damped response spectra for Vancouver – NBCC 2005 and Historical Earthquakes W9 to W15

4.5 Analytical results

The design spectra defined in NBCC 05 correspond to 50th percentile probability that the demand will be exceeded for the given return period (2475 years). Therefore, all commentaries and conclusions from this analytical study will be based on 50th percentile values of the analysis results obtained for the entire ground motion ensemble. However, to provide some insight into the variability of the results and give additional information on the results, the 84th percentile values are also presented herein.

To evaluate the reliability of the dynamic analysis models, we will present and compare the modal shapes and the period of vibrations of the buildings as obtained from the three mathematical models that were used: an elastic stick model with effective member properties according to CSA A23.3-04, the bar model with concentrated plastic flexural hinges at the member ends with a bilinear hysteretic response based on the bilinear approximation of the cross-sectional moment-curvature response, and following the Takeda hysteretic model, and the wall or "multi-fibre" element where both materials

are represented by stress-strain curves. The numerical data for the first for modes are reported in table 4.5.

Table 4.5: Computed building period (s) in the first four modes of vibration

Analysis	Site	Vancouver					Montreal				
	Mode	5	10	15	20	25	5	10	15	20	25
Ruaumoko Wall	1	0.662	1.390	2.082	2.316	2.804	0.800	1.795	2.418	3.001	3.818
	2	0.132	0.257	0.384	0.407	0.489	0.186	0.324	0.430	0.512	0.646
	3	0.061	0.109	0.162	0.164	0.195	0.082	0.134	0.179	0.201	0.250
	4	0.041	0.067	0.098	0.096	0.113	0.054	0.081	0.104	0.115	0.141
Ruaumoko bar	1	0.832	1.730	2.282	3.152	3.755	1.218	2.040	2.664	3.765	4.358
	2	0.180	0.341	0.446	0.602	0.716	0.246	0.403	0.514	0.713	0.828
	3	0.084	0.151	0.193	0.252	0.297	0.111	0.176	0.219	0.294	0.341
	4	0.058	0.094	0.118	0.149	0.175	0.074	0.109	0.132	0.171	0.194
Elastic CAN/CSA A23.3-04 SAP2000	1	0.645	1.320	1.737	2.131	2.577	0.943	1.605	2.148	2.675	3.196
	2	0.132	0.248	0.322	0.401	0.480	0.183	0.298	0.396	0.486	0.578
	3	0.061	0.107	0.136	0.171	0.202	0.082	0.127	0.166	0.201	0.237
	4	0.042	0.066	0.083	0.104	0.122	0.055	0.078	0.100	0.120	0.140

The differences in calculated periods arise from the different input stiffness values for each model. For the Ruaumoko Bar model, we used the effective inertia properties calculated by the bilinear approximation of the moment-curvature curve for each element. At the wall base, the stiffness varies from 0.376 to 0.507 of the gross cross-section stiffness. In the elastic model used in the modal analysis, the effective stiffness was calculated according to CAN/CSA A23.3-04 requirements. That stiffness varies from 0.65 to 0.70 of the gross stiffness. The Ruaumoko Wall model uses the gross section properties. It is noted that gross section properties do not affect much the seismic dynamic results because the effective section properties change with the load, as was explained in Section 4.1. However, the use of the Taylor concrete model, on one hand, requires using a smaller initial elastic modulus for the concrete, approximately equal to 0.55 times the "real" value. On the other hand, the Wall model accounts for the reinforcement in the section, which increases the gross stiffness by 5 to 12%, depending of the wall concrete area and reinforcement quantity. Combining both effects resulted in effective stiffness equal to 0.58 to 0.62 of the gross "concrete" stiffness used in other

models This is why the calculated modes with Wall model is between those calculated with Bar and CAN/SCA models.

The comparison of the normalized mode shapes allows seeing the relative influence of each mode of vibration on the total response for each element type. This is done in figures 4.37 to 4.46.

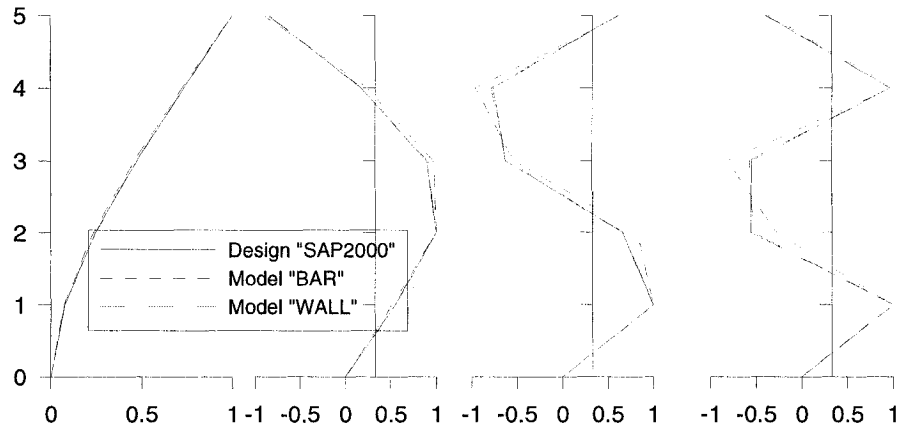

a) 1^{-st} mode **b) 2^{-th} mode** **c) 3^{-th} mode** **d) 4^{-th} mode**

Figure 4.37: Modal shapes of vibration: 5-storey building in Vancouver

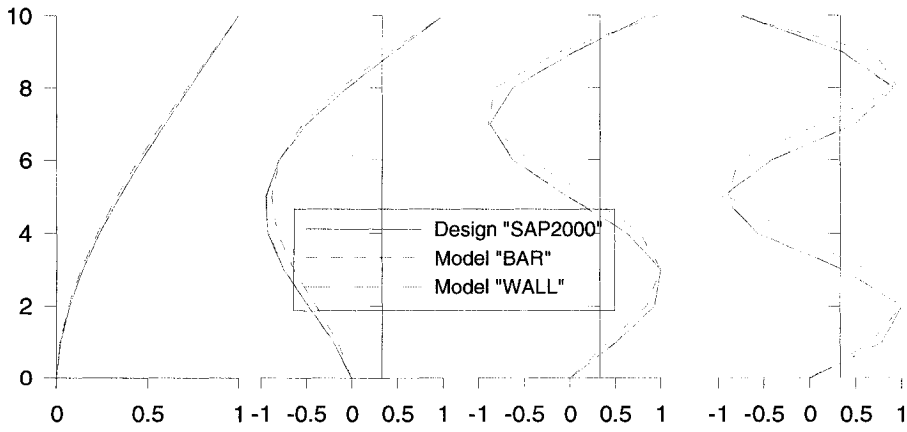

a) 1^{-st} mode **b) 2^{-th} mode** **c) 3^{-th} mode** **d) 4^{-th} mode**

Figure 4.38: Modal shapes of vibration: 10- storey building in Vancouver

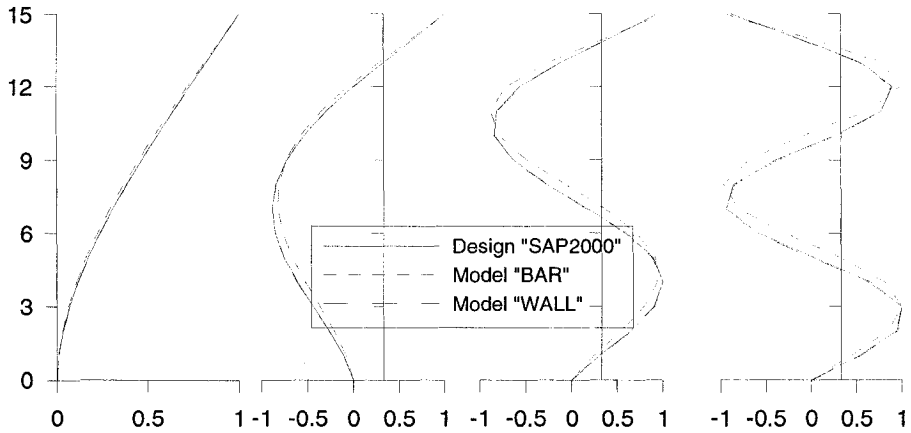

a) 1^{-st} mode **b) 2^{-th} mode** **c) 3^{-th} mode** **d) 4^{-th} mode**

Figure 4.39: Modal shapes of vibration: 15- storey building in Vancouver

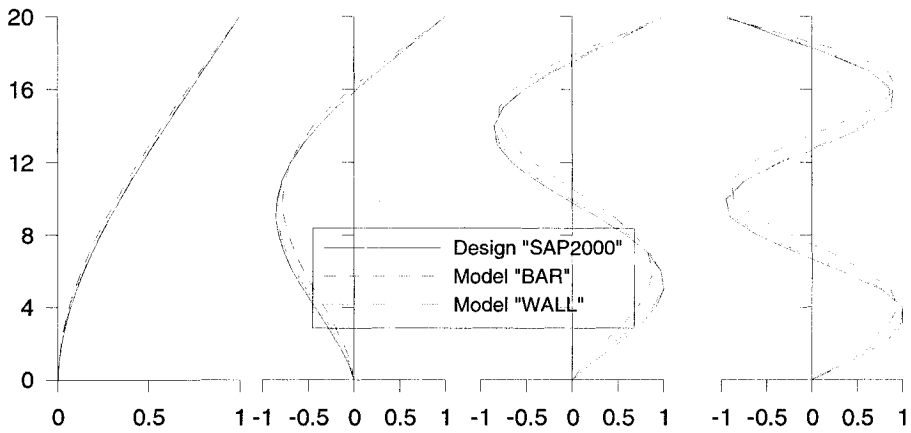

a) 1^{-st} mode **b) 2^{-th} mode** **c) 3^{-th} mode** **d) 4^{-th} mode**

Figure 4.40: Modal shapes of vibration: 20- storey building in Vancouver

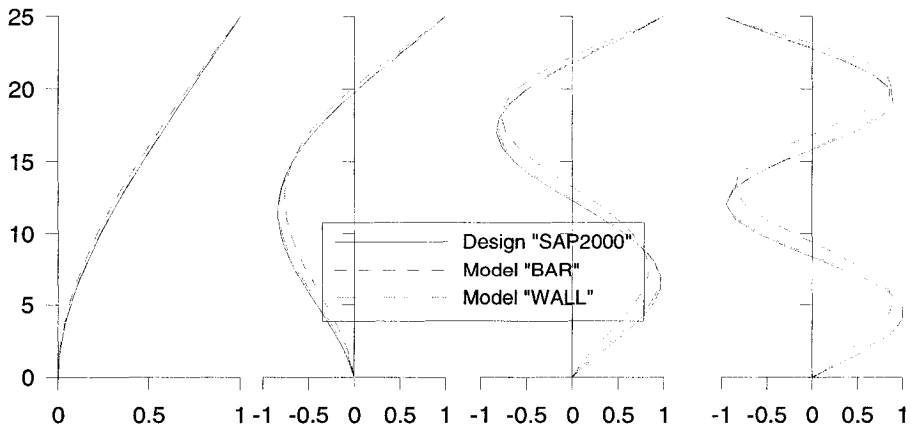

a) 1^{-st} mode **b) 2^{-th} mode** **c) 3^{-th} mode** **d) 4^{-th} mode**

Figure 4.41: Modal shapes of vibration: 25- storey building in Vancouver

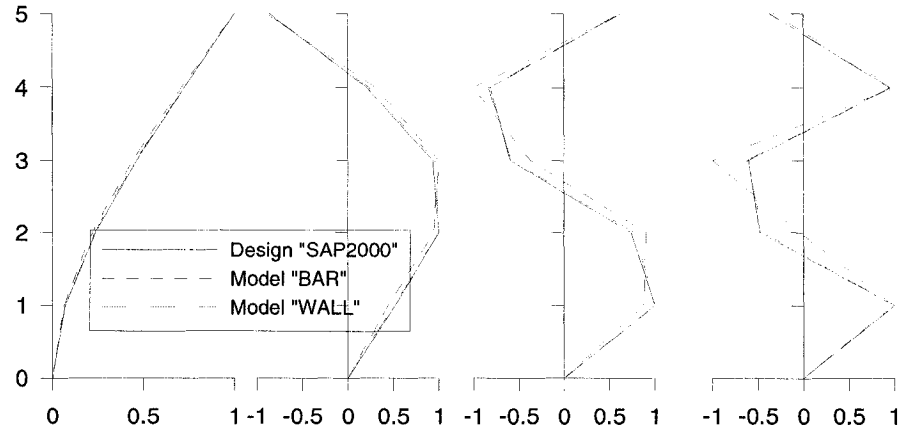

a) 1-st mode **b) 2-th mode** **c) 3-th mode** **d) 4-th mode**

Figure 4.42: Modal shapes of vibration: 5- storey building in Montreal

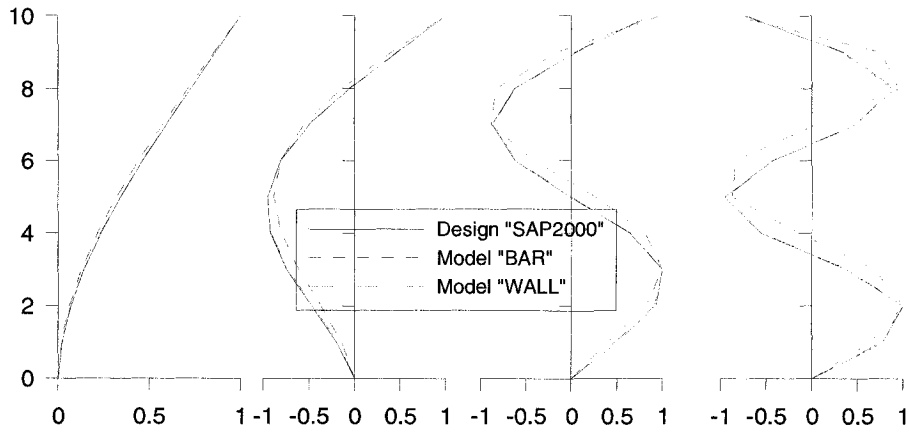

a) 1-st mode **b) 2-th mode** **c) 3-th mode** **d) 4-th mode**

Figure 4.43: Modal shapes of vibration: 10- storey building in Montreal

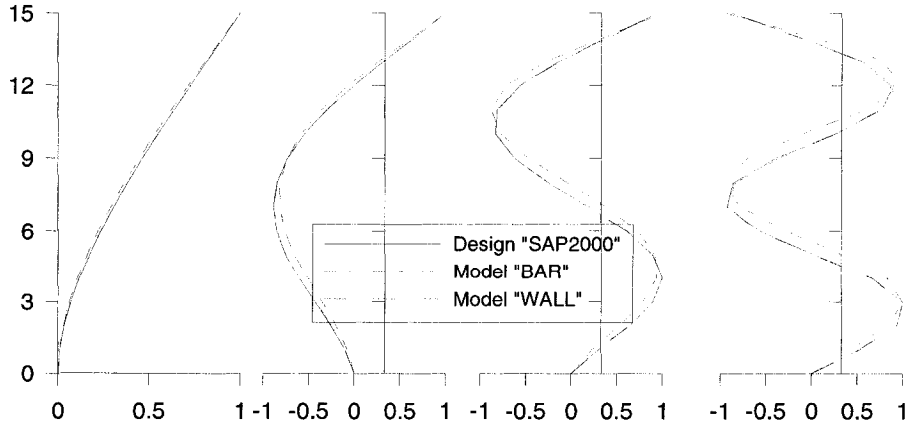

a) 1-st mode **b) 2-th mode** **c) 3-th mode** **d) 4-th mode**

Figure 4.44: Modal shapes of vibration: 15- storey building in Montreal

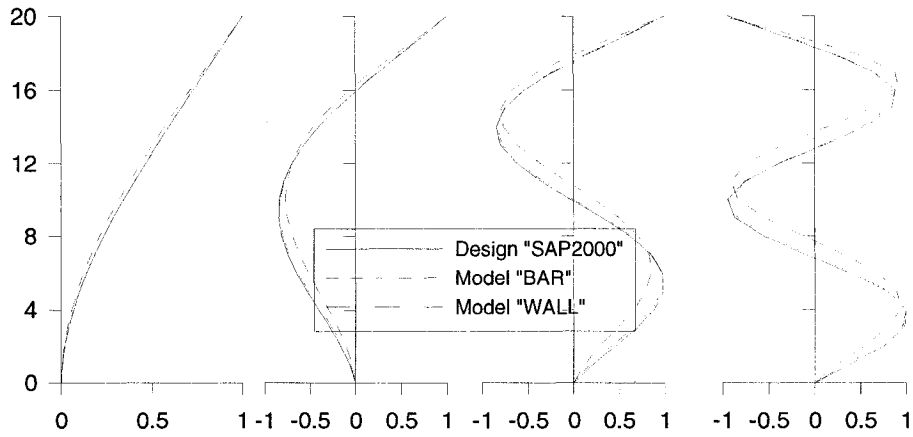

a) 1-st mode **b) 2-th mode** **c) 3-th mode** **d) 4-th mode**

Figure 4.45: Modal shapes of vibration: 20- storey building in Montreal

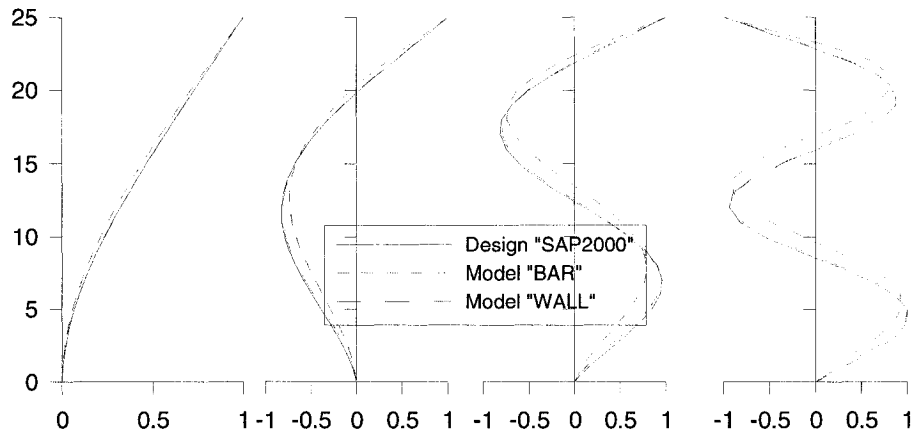

a) 1-st mode **b) 2-th mode** **c) 3-th mode** **d) 4-th mode**

Figure 4.46: Modal shapes of vibration: 25- storey building in Montreal

All three models led to very similar first mode shapes, and the Wall and SAP model practically give the same shapes for all first four modes. However the Bar model has slightly different second, third and forth mode shapes. The shape is somehow shifted towards the upper part of the wall. Comparing the mode shapes a larger participation factor can be expected for the higher modes for the Wall and Bar elements. However, as was explained before, the solution for the Wall elements is based on the elastic properties of the sections and is not representative of the nonlinear behaviour of the models during an earthquake, after cracking has taken place.

4.5.1 Comparison between elements "Wall" and "Bar"

A) Story displacements

Both elements are compared by examining the ratios of the peak horizontal storey displacements with respect to the ground for the 5-, 15- and 25-storey buildings located in Vancouver, which covers the short-, medium- and high-rise ranges of buildings. The ratios of the 50th and 84th percentile values of Δ_{wall} and Δ_{bar} are presented in figure 4.47.

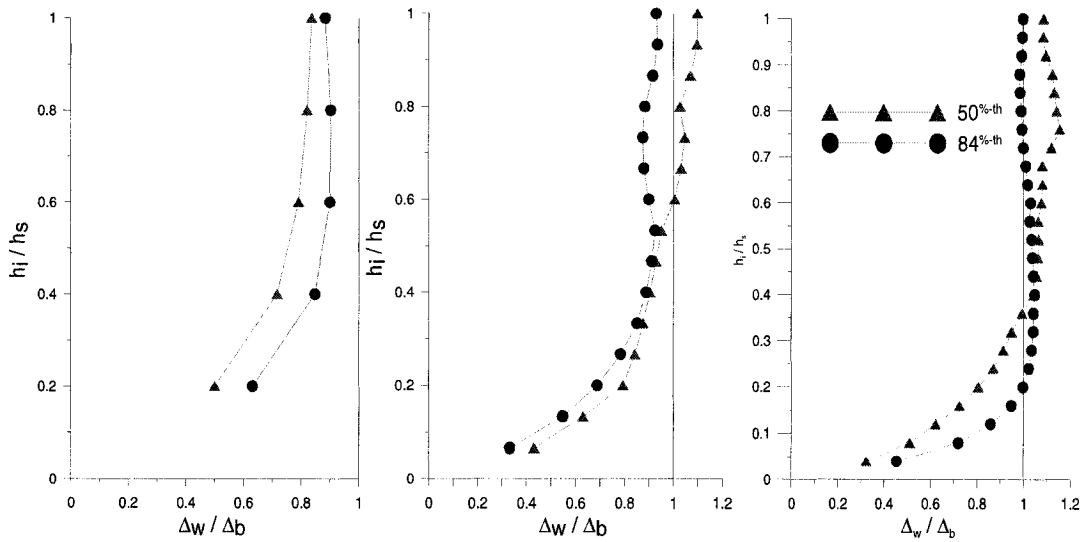

a) 5 story **b) 15 story** **c) 25 story**

Figure 4.47: Comparison of peak storey horizontal displacement from "Wall" and "Bar" elements (50^{th} Δ_{wall} / 50^{th} Δ_{bar}) for Vancouver buildings.

The displacements obtained with the "Bar" element at the base of the buildings are approximately twice as large as those obtained with the "Wall" element. The ratio Δ_{wall} / Δ_{bar} increases and tends to 1.0 in the upper floors. The trend is more pronounced with the taller building. For the 5-storey building (figure 4.47a), this ratio for the 50th percentile values is approximately 0.5 at the base and 0.8 at the top. The same tendency is observed for the 15- and 25-storey buildings in figures 4.47.b and 4.47.c. In the upper half of the building, the ratio even slightly exceeds unity for the 50th values.

The main conclusion that can be drawn from the ratios Δ_{wall} / Δ_{bar} is that the ratio increases with the elevation in the building: 0.5 at the base and 1.0 at the top. In addition, the maximum ratio increases with the increase of the height of the building, 0.9 for 5-storey building and 1.2 for 25-storey building.

No clear explanation could be proposed to explain the differences observed at the base. One possible reason for the larger displacements at the base for the "Bar" element compared with the "Wall" model can be attributed to the differences between the two computational models: the rotation of the "Bar" element is concentrated in one node at the bottom of the element whereas it is distributed over the height of the story for the "Wall" element (NSECT = 5). The rotational demand is higher at the base, so these differences are larger. With the height of the buildings, this concentration of the rotation in one node is compensated and very similar results are obtained.

The results obtained for the buildings located in Montreal are not presented here but are very similar to those for Vancouver.

B) Story shear

The second parameter studied was the peak storey shear forces. The results are presented as a ratio V_{wall} / V_{bar} for all buildings in Vancouver and Montreal and are shown in figure 4.48 and 4.49 respectively.

For all buildings, this ratio varies in the range of 0.8 to 1.25, but is generally close to one throughout the height of the walls.

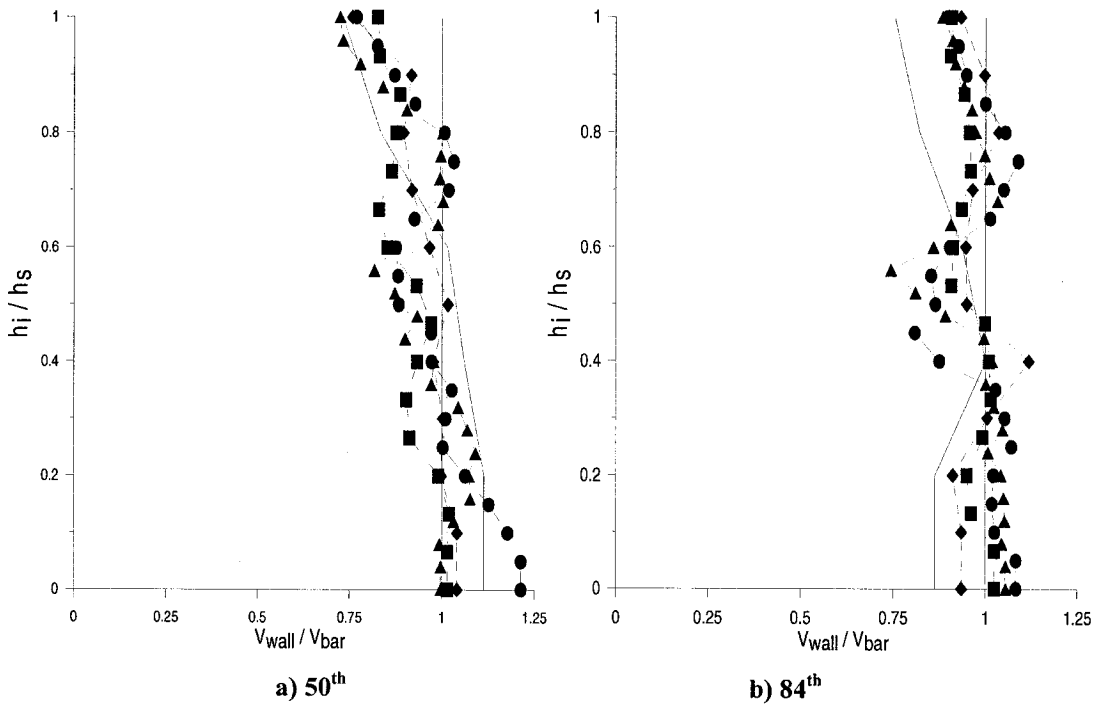

a) 50th b) 84th

Figure 4.48: Comparison "Wall"-"Bar" Vancouver: V_{wall} / V_{bar} Legend

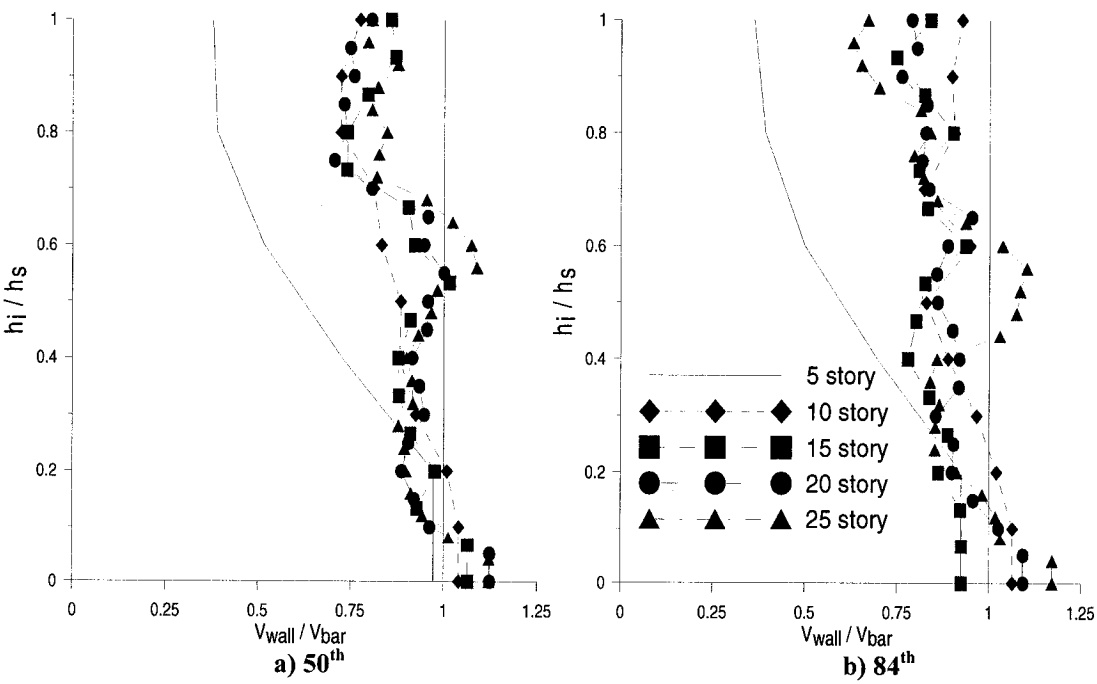

a) 50th b) 84th

Figure 4.49: Comparison "Wall"-"Bar" Montreal: V_{wall} / V_{bar}

The results cannot be generalized to distinguish groups of buildings having similar behaviour for both sites. In Vancouver, it seems that the difference at the base is more pronounced for the 5-storey and 20-storey buildings, but varies with the height. Conversely, in Montreal, this ratio tends to increase with an increase of the building height and this trend remains generally valid throughout the height of the walls. It could also be remarked that the ratios are smaller at the wall top compared to the bottom portion of the walls, in particular for the 5-storey structure One possible explanation for the differences is the larger apparent flexibility of the Bar element, as revealed by the larger deformations in Fig. 4.47: higher mode effects are more pronounced in a more flexible structure, which can result in higher shear forces in the top portion of the structure.

C) Top displacement, maximum ductility demand and inelastic ductility demand at the base of the wall

As explained in Chapter 3, the requirements for ductility capacity in CAN/CSA A23.3-04 are expressed in terms of inelastic rotational capacity and inelastic rotational demand (Clause 21.6.7). The results related with ductility properties of walls are presented herein in terms of curvature ductility, based on the same assumptions as in CAN/CSA A23.3-04. In the new code, the rotation is calculated assuming the formation of a plastic hinge at the base of the walls: all of the rotation takes place at the centre of the plastic hinge and the rest of wall remains elastic. The inelastic curvature capacity was assumed equal to the difference of the maximum curvature and the curvature at the yielding point. Assuming that the height of the plastic hinge is equal to the length of the wall in the buildings and a yielding curvature $\varphi_y = \varepsilon_y / (l_p/2)$, the maximum curvature, according to A23.3-04, can be approximated as $\varphi_{code} = \varepsilon_{cu}/c$, where c is the length of the compression zone and ε_{cu} is the ultimate compressive strain of concrete (figure 4.50). For unconfined concrete ε_{cu} is equal to 0.0035 m/m, and the curvature at yielding for standard reinforcement is calculated as $\varphi_y = 0.004/l_w$.

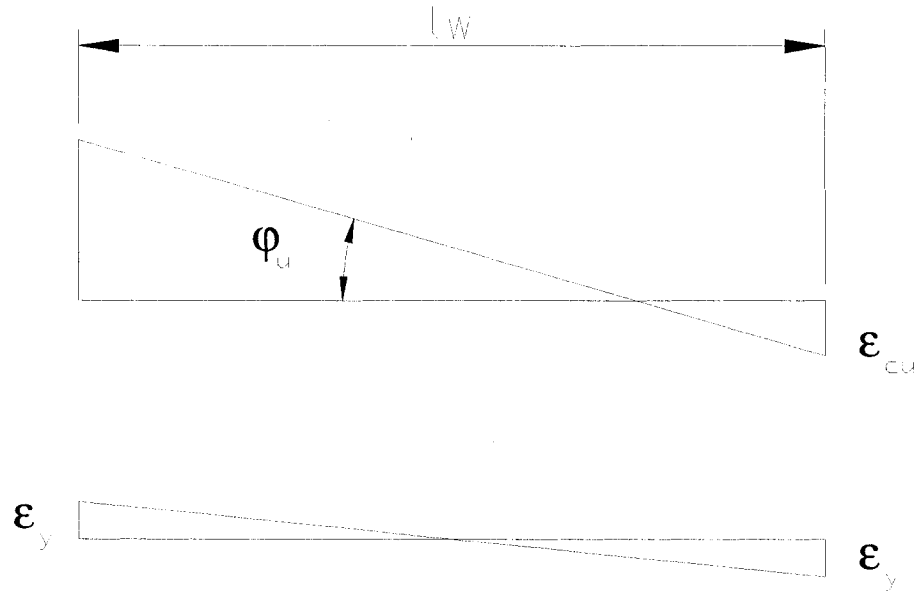

Figure 4.50: Definition of maximum permitted curvature and elastic curvature.

Figure 4.51 presents the statistics of the maximum roof displacement, Δ_{max}, and the maximum ductility calculated at the base of walls, φ_{max}. The values of φ_{max} are compared to the values of φ_{code}. The inelastic curvature ductility demand is calculated by subtracting the elastic curvature ductility, φ_y, from the total ductility demand (φ_{max} - φ_y) at the base. This value is compared to $\varphi_{d,code}$, the inelastic ductility demand calculated according to clause 21.6.7.2 of CSA A23.3-04 by employing the spectrum response method (as obtained in Chapter 3).

As shown in figure 4.51, the two elements give similar results in terms of maximum displacement of the top storey. They follow the same trend outlined in Section 4.5.1A, i.e. larger displacements with the "Wall" element for high-rise buildings and smaller values for the shorter buildings.

Both elements also give very similar values for the maximum curvature ductility demand at the wall bases for both sites and, as a consequence, similar inelastic demand values. The displacements and the ductility demand for the buildings located in Montreal

are approximately two times smaller than those observed in Vancouver. The differences in ductility can be explained by the different ductility-related force modification factors used in the design, 3.5 for Vancouver and 2.0 for Montreal, and the associated anticipated lesser ductility demand. The characteristics of the ground motions can also have contributed to the difference: the eastern Canada ground motions with higher frequency content are less likely to excite the building first vibration mode and, hence, lead to lower overall building lateral displacements and reduced rotational demand at the wall bases.

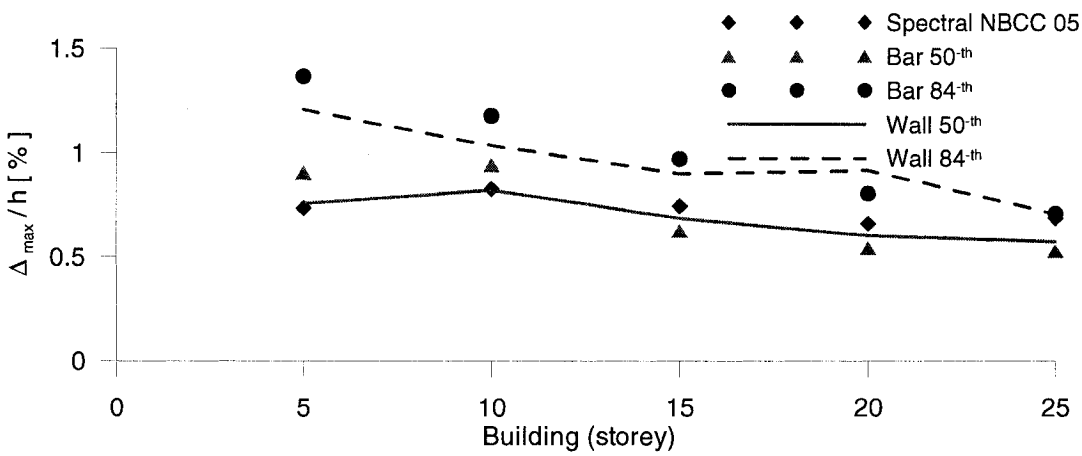

Vancouver

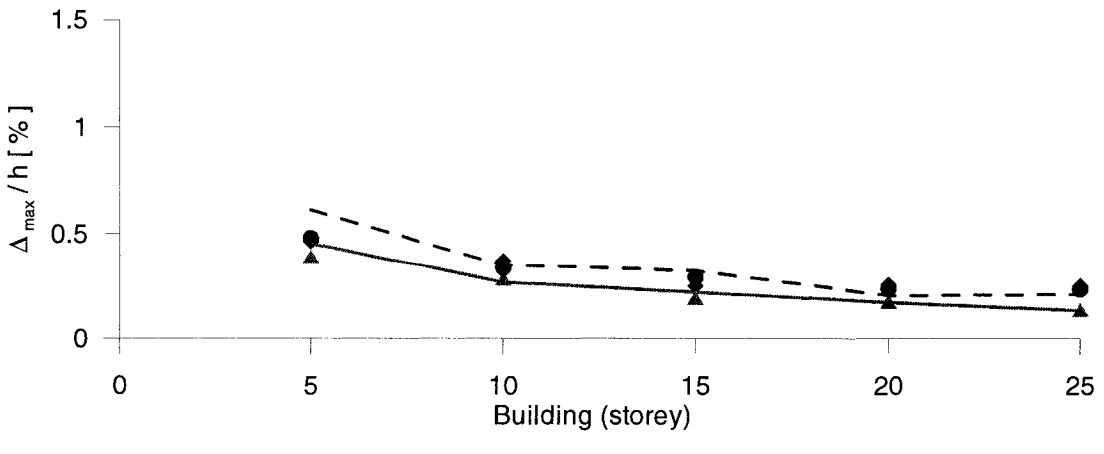

Montreal

a) Comparison Δ_{max}/h_w for elements "Wall", "Bar" and NBCC 05 spectrum analysis

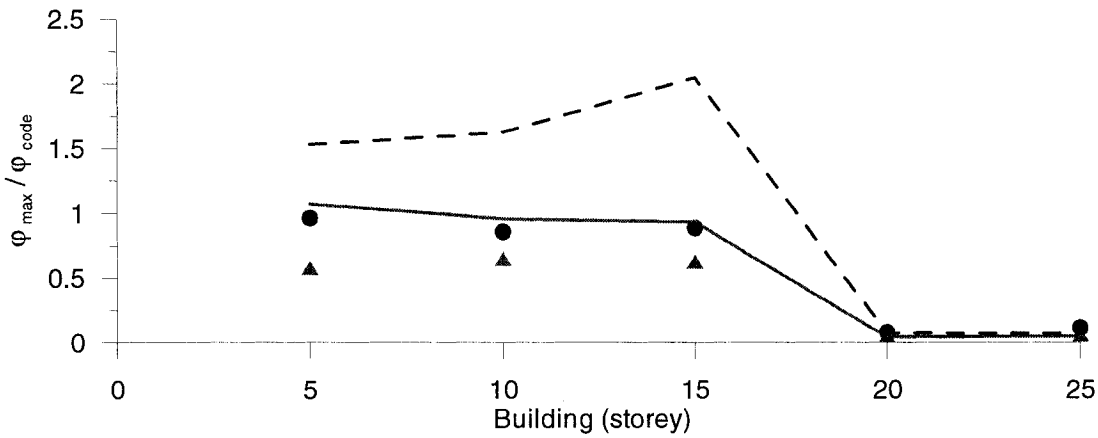

Vancouver

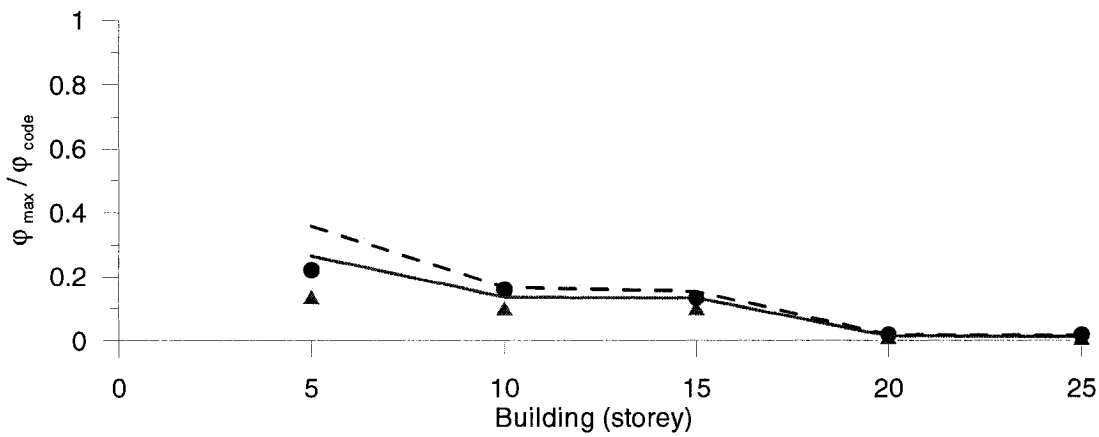

Montreal

b) Comparison Maximum ductility demand obtained with elements "Wall","Bar" and CSA – A23.3-04

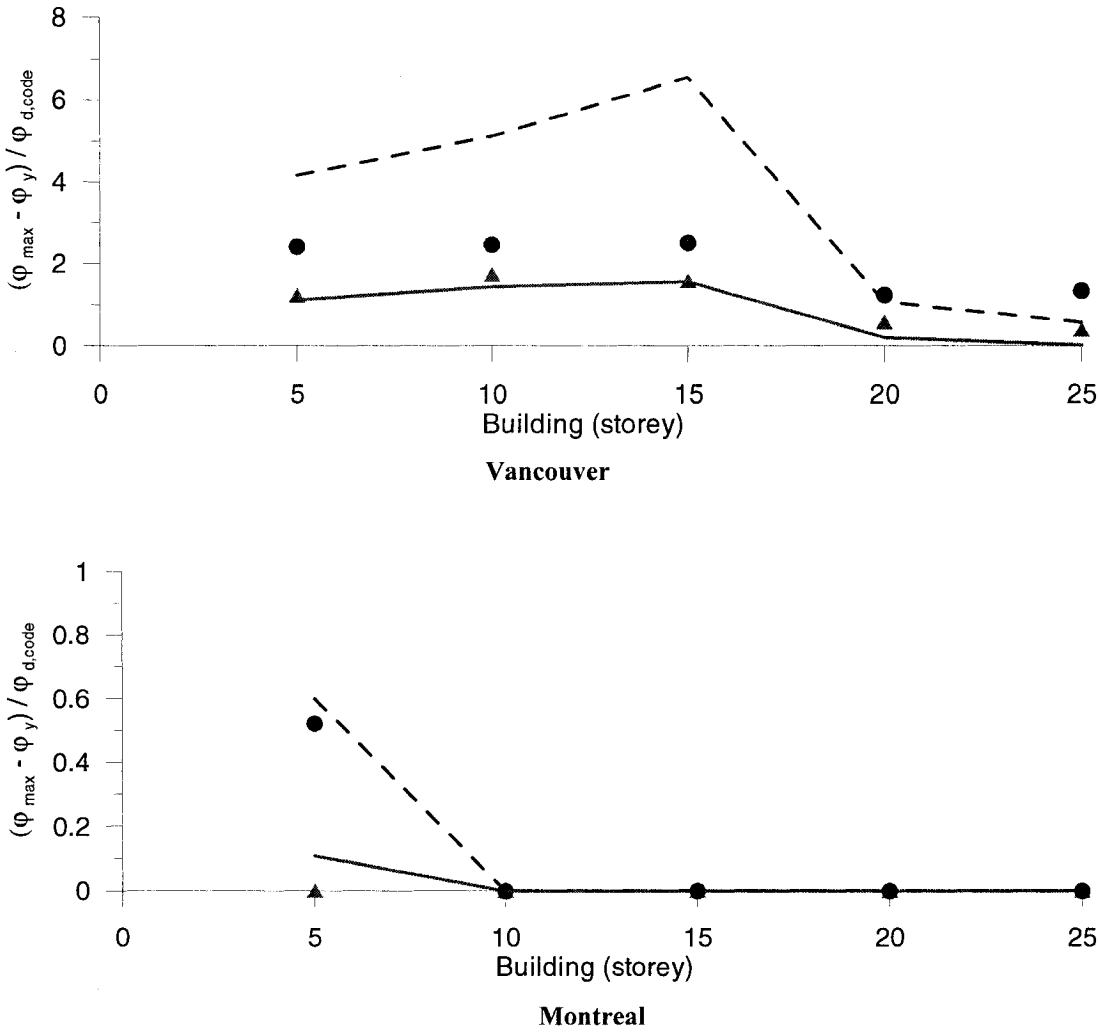

c) Comparison Maximum Inelastic ductility demand obtained with elements "Wall","Bar" and CSA –A23.3-04

Vancouver **Montreal**

Figure 4.51: Comparison "Wall"-"Bar": Δ_{top} / h_s; $\varphi_{max} / \varphi_{code}$; $\varphi_{inel.} / \varphi_{code}$

Conclusions and final choice

Based on the above results and discussions, a few conclusions can be drawn. Both elements give similar results for peak displacement, shear force, and ductility demand values. Because the "Wall" element better reflects the actual properties for the concrete

and steel materials and accounts for the variation of the section properties as a function of the flexural demand, it is believed that it gives a better representation of the behaviour of shear wall structures. Moreover, as discussed before, the use of the "Bar" model involves suggestive interpretation when determining the bi-linear approximation of the Moment-Curvature diagram of the element flexural behaviour. Based on this, the results obtained from the analyses with the element "Wall" will be discussed herein. For completeness, all results for all buildings for both the "Wall" and "Bar" elements are reported in Appendix C.

4.5.2 Results for Element "Wall"

A) Displacements

The results are compared with the two main design values of interest stipulated in NBCC 05 in terms of drift control: the maximum allowed inter-storey drift, which is limited to 2.5% of the storey height, h_s, and the elastic spectral design displacement.

Figure 4.52, gives the ratios between the analysis results and the code limit of 2.5% h_s.

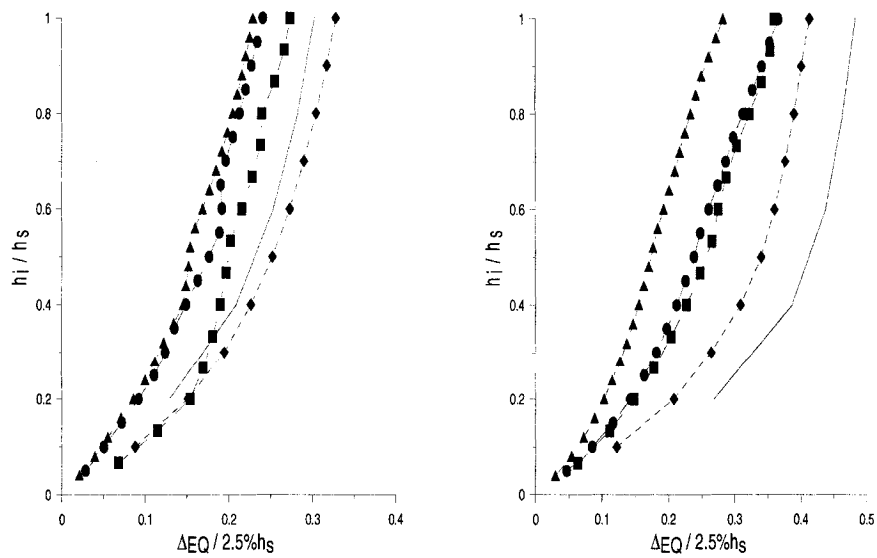

a) Vancouver 50$^{-th\%}$ **b) Vancouver 84$^{-th\%}$**

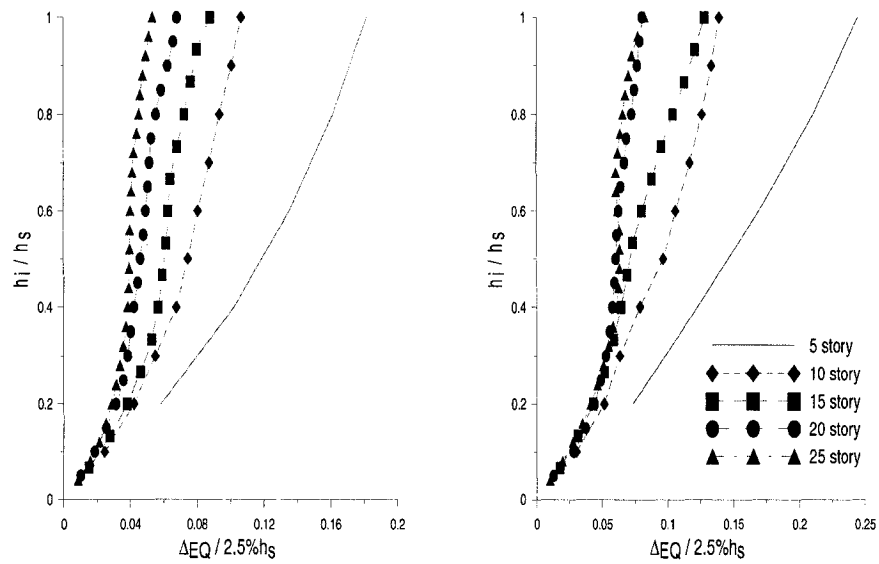

c) Montreal 50$^{-th\%}$ **d Montreal) 84$^{-th\%}$**

Figure 4.52: Maximum storey displacement: $\Delta_{wall} / \Delta_{code,max}$

It is clear that the maximum inter-storey drift angle values meet the code limit for all cases. It is noticed that for the shorter buildings, the ratio is larger than for the taller buildings. Another important result is that the ratio is approximately three to four times larger for the buildings situated in Vancouver compared to those located in Montreal. Two reasons are suggested to explain this difference. Firstly, the design spectral values for Vancouver are nearly two times those for Montreal for the periods longer than 0.5 s, which corresponds to the period ranges of all the buildings. The same tendency can be noticed when comparing the top displacements obtained with the spectral analysis according to NBCC 05 and reported in table 3.13 but not multiplied be R_dR_o. The ratios vary from 1.6 to 2.97.

The fact that the structures in Montreal were intentionally made more flexible than in Vancouver (the buildings in Vancouver have shorter first periods than those located in Montreal) likely also contributed in the differences in drift response between the two sites. The displacements are mainly influenced by the first mode of vibration, and the response in that mode is more pronounced for the Vancouver buildings. Another reason is the frequency content of the ground motions at both sites: the lower frequency content

in the west produces higher displacement demand than the high frequency ground motions in the east.

Figure 4.53 compares the maximum inter-storey drift angles from nonlinear analysis to the maximum elastic code predictions using dynamic spectrum method (the response spectrum values multiplied by R_dR_o). For the buildings located in Vancouver, the storey drift angles in the upper half of the buildings are close to those obtained with the response spectrum analysis. For the bottom half, they can be separated into two groups: the low- and medium-rise group which includes the 5- to 15-storey buildings, with lower deformation ratios, and the high-rise group with the 20- and 25-story buildings, with higher deformation ratios. This difference can be explained based on the basis of two facts: the actual effective flexural stiffness of the structures at any instant of time after cracking has occurred is smaller than the code prescribe values, and, secondly, cracking of the first group structures was found to occur over the entire building height while the upper part of the high-rise buildings remained generally elastic. However, the cracking does not occur simultaneously at each level. Hence finally, the displacements in the upper part of the buildings tend to approach those obtained using the code prescriptions (in the spectrum analysis, an effective stiffness corresponding to approximately 70% of the gross stiffness was assumed).

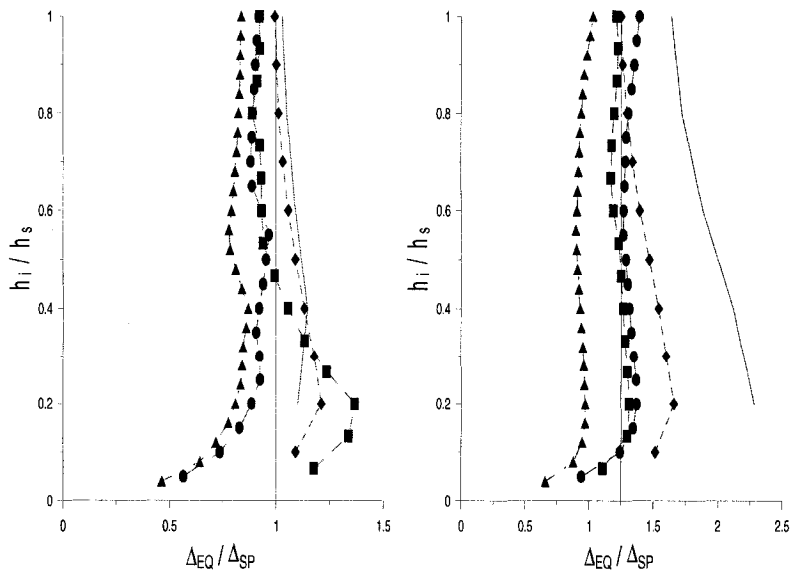

a) Vancouver 50$^{-th\%}$ **b) Vancouver 84$^{-th\%}$**

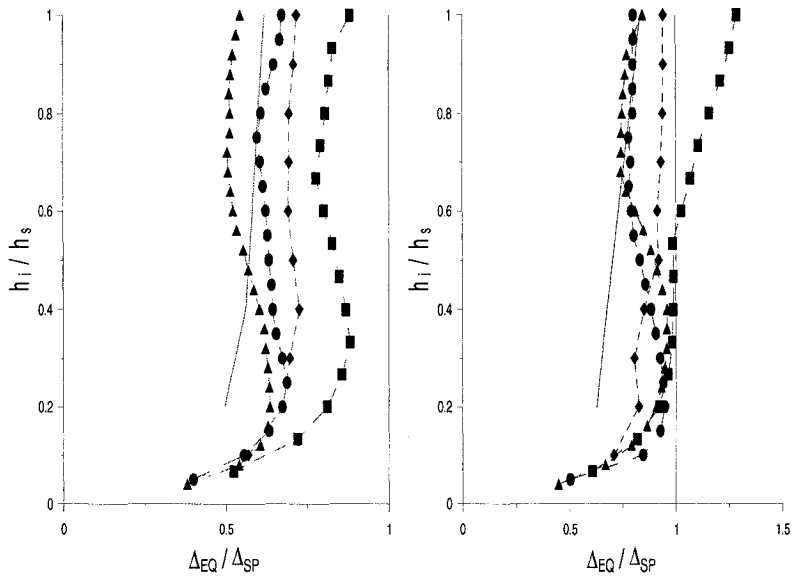

c) Montreal 50$^{-th\%}$ **d) Montreal 84$^{-th\%}$**

Figure 4.53: Maximum storey displacement: $\Delta_{wall} / \Delta_{spectral}$

Except for the 5-storey building, the same tendency can be observed for Montreal, with relatively larger displacements experienced by the shorter buildings. However, it is not possible to identify specific groups of buildings. What is common for all the buildings in Montreal is that the upper part remains elastic, similarly to the high-rise buildings in Vancouver, which can partly explain the smaller displacements obtained in this part of the structures.

B) Ductility demand

The results are presented in the form of curvature demand determined based on the same assumptions for yielding curvature, $\varphi_y = 0.004/l_w$, as in CAN/CSA-A23.3-04, and as explained in Section 4.5.1.C. The ductility demand is examined at the wall base, in the plastic hinge region, as well as above the plastic hinge region.

Figure 4.51b presents the ratio of the computed maximum ductility demand at the wall bases from nonlinear analysis to he code ductility values computed according to CSA A23.3-04 and based on spectrum analysis. For both sites, the buildings could be separated once again into the two groups described above with higher demand for the low- and medium-height buildings. For Vancouver the ratio is almost constant and equal to 0.6-0.7. For the high-rise buildings, it is very small, corresponding to approximately 10% of the code predictions. For Montreal, the ductility demand for the lower structures varies between 10% to 30% of the code prediction and is nearly zero for the taller walls.

Based on these results, it appears that the code provisions provide very conservative estimates of the anticipated ductility demand, especially for the Montreal site, where the computed values are much smaller than those determined in Vancouver. This can be explained by the fact that the calculation of the ductility demand at the base of wall according to CSA A23.3-04 is based on the first mode response. This is not the case for the more flexible buildings and/or high-rise buildings, for which higher vibration modes have larger contribution to the overall response of walls.

To complete the discussion on the ductility demand on walls, we plotted the maximum curvature ductility demand at the base of the walls and above the plastic hinge zone region. As shown in figure 4.54, the ductility demand in all cases is concentrated at the base of the walls, as intended in design. For both sites, the five-story buildings experienced the highest rotational demand compared to the other buildings. It can also be noted that the ductility demand generally decreases when increasing the building height.

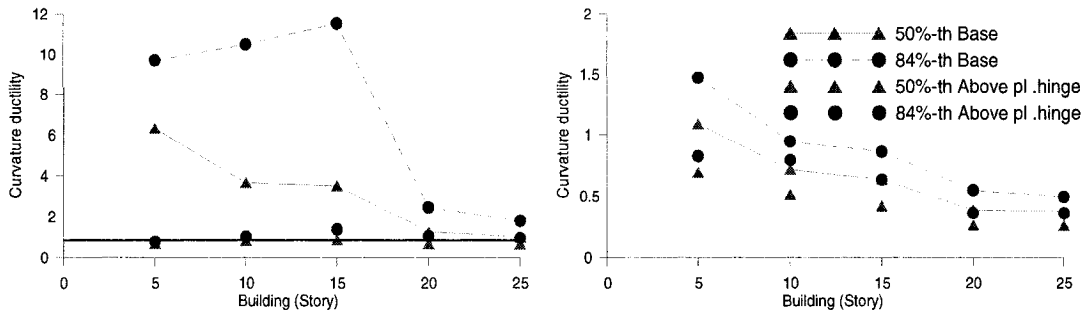

Vancouver **Montreal**

Figure 4.54: Curvature ductility at the base and above the plastic hinge

Figure 4.54 reveals another very interesting behaviour: all buildings located in Montreal and the 20- and 25-storey high-rise buildings in Vancouver remained essentially elastic during the earthquakes. In other words, they did not experience any yielding, contrary to what was anticipated based on NBCC 05 and CSA A23.3-04 provisions.

As could be expected, the ductility demand for walls in Montreal, designed as moderately ductile shear walls, is much smaller compared to that for the Vancouver structures designed as ductile shear walls. The ratio is approximately equal to six for the first group, as defined above, and to three for the two tallest buildings.

The 50th percentile numerical results for the computed maximum curvature ductility demand above the plastic hinge zone are presented in Table 4.6..

Table 4.6: 50th percentile of the curvature ductility demand above the plastic hinge

	5-storey	10-storey	15-storey	20-storey	25-storey
Vancouver	0.70	0.84	0.89	0.70	0.69
Montreal	0.69	0.50	0.40	0.30	0.30

For both sites, the walls remained elastic above the base hinge region, as was expected in design. As explained in Chapter 3, it should be reminded that conservative design assumptions have been applied for the buildings in Montreal in terms of the plastic hinge length (set equal to l_w) and design overturning moments above the plastic hinge region (taken equal to the moments from factored loads times the overstrength factor γ_h). CSA A23.3 does not include any specific requirements for these two aspects and the results seem to confirm that they would not be needed for moderately ductile walls located in eastern Canada.

We can summarise all the remarks made until now as follows: the buildings could be divided into two groups: low- and medium-height buildings up to 15 storeys and high-rise buildings having 20 and 25 storeys. The first group experienced higher inelastic ductility demand at the base while the second group remained elastic over their entire height. In addition, all buildings located in Montreal were found to remain elastic during the earthquakes, without even cracking in the top storeys of the high-rise buildings. The design aim to protect walls against undesirable yielding in the non-protected zone above the plastic hinge was achieved.

C) Forces

C1. Moments

The results for the base moment are presented in terms of the ratios of the peak base moment obtained in each of the nonlinear time-history analysis to the design base moment calculated by employing the spectral analysis procedure in NBCC 05. The results are presented in figure 4.55 for the Vancouver buildings. As expected from the base rotational ductility demand results, the 50^{th} percentile values of the base moments exceed the spectral values for these structures. Figure 4.56 shows the same ratios computed with respect to the probable moment capacity at the base of the walls, M_p. The results are close to unity and even slightly above.

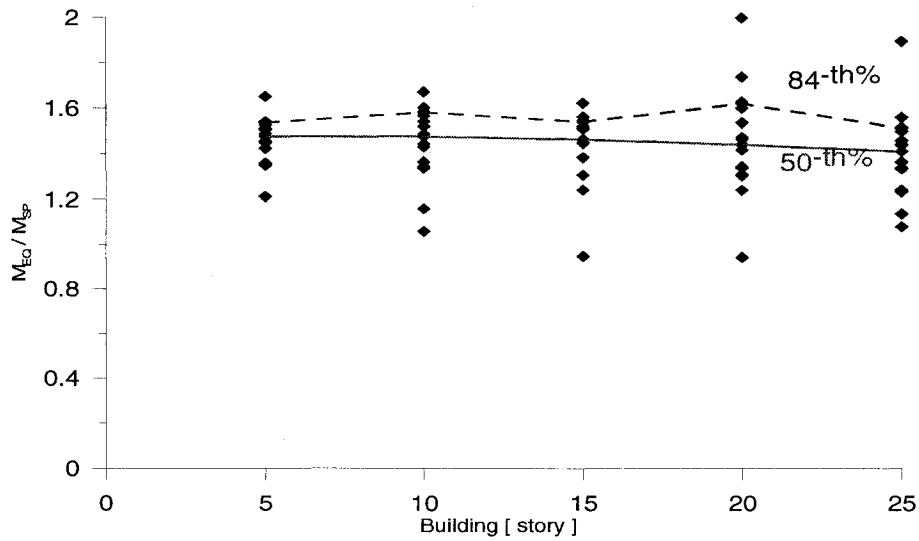

Figure 4.55: Base moments ratio for the Vancouver buildings: $M_{EQ}/M_{spectral}$

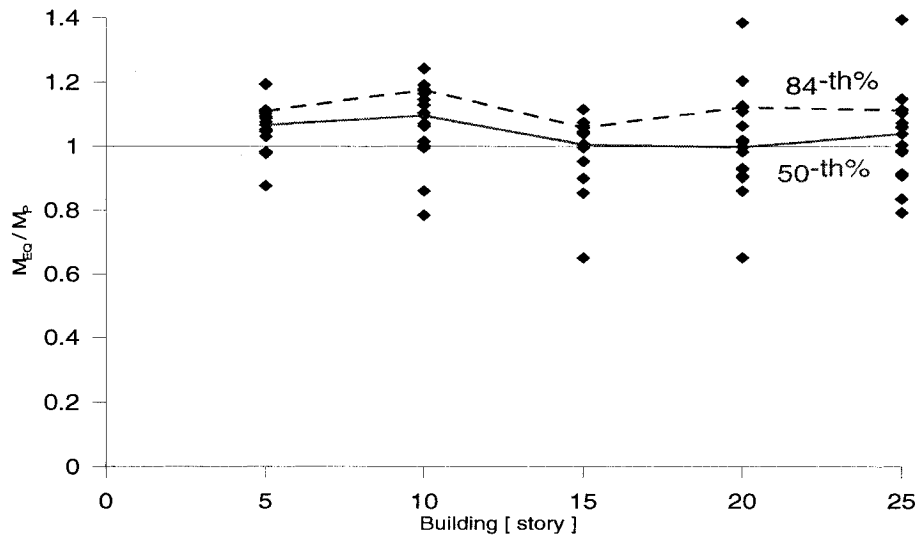

Figure 4.56: Base moments ratio for the Vancouver buildings: M_{EQ}/M_{p}

For the Montreal located buildings, figure 4.57 shows that the computed moments slightly exceed the moments computed with spectrum analysis. When compared to the nominal moment capacity M_n in figure 4.58, it is found that the 50th percentile of the

peak moment demand during the earthquakes did not reach the M_n capacity, except for the 5-storey building. Figure 4.58 shows shows that the ratio of the base moment to the nominal moment has the tendency to decrease when the building height is increased, which is consistent with the computed ductility demand. It also shows that the 25-storey building remains elastic during the all time histories.

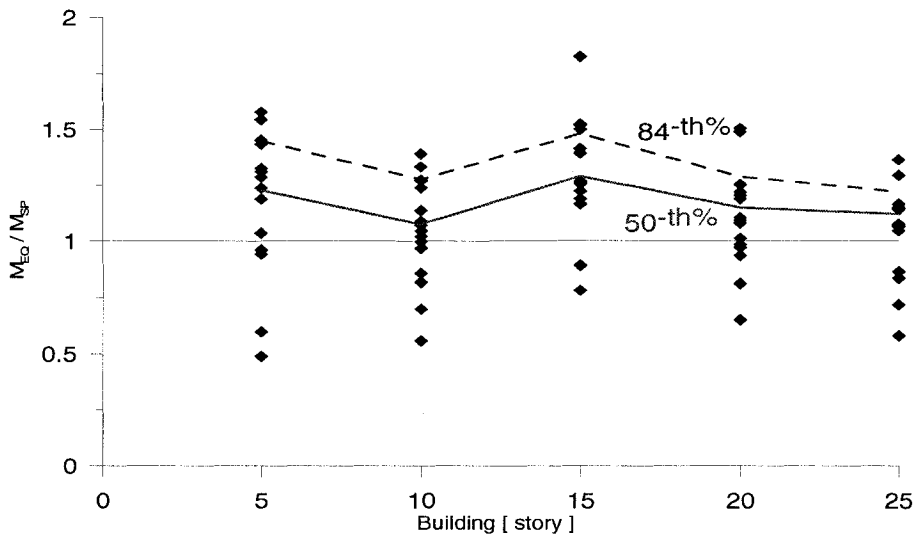

Figure 4.57: Base moments ratio - Montreal: $M_{EQ}/M_{spectral}$

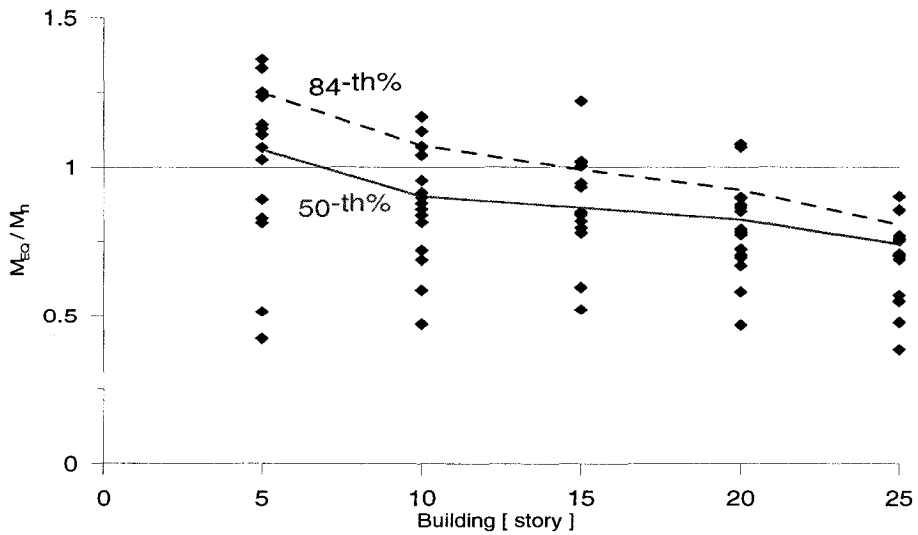

Figure 4.58: Base moments ratio - Montreal: M_{EQ}/M_n

C2. Shear forces

The results for the shear forces are presented into three steps, virtually following the design provisions for the shear resistance for shear walls. Firstly, figure 4.59 shows the results from non-linear analysis compared with those from the elastic spectral modal analysis divided by R_oR_d. For Vancouver, the ratio at the base varies from 2.2 for the 5-story building to 3.0 for the 20-story building and from 1.7 to 2.2 at the top of the walls. Similarly for the buildings in Montreal, the ratio decreases from 1.6 to 1.8 at the base to 1.0 to 1.5 at the top. Consistent results are generally obtained at both sites for all building heights.

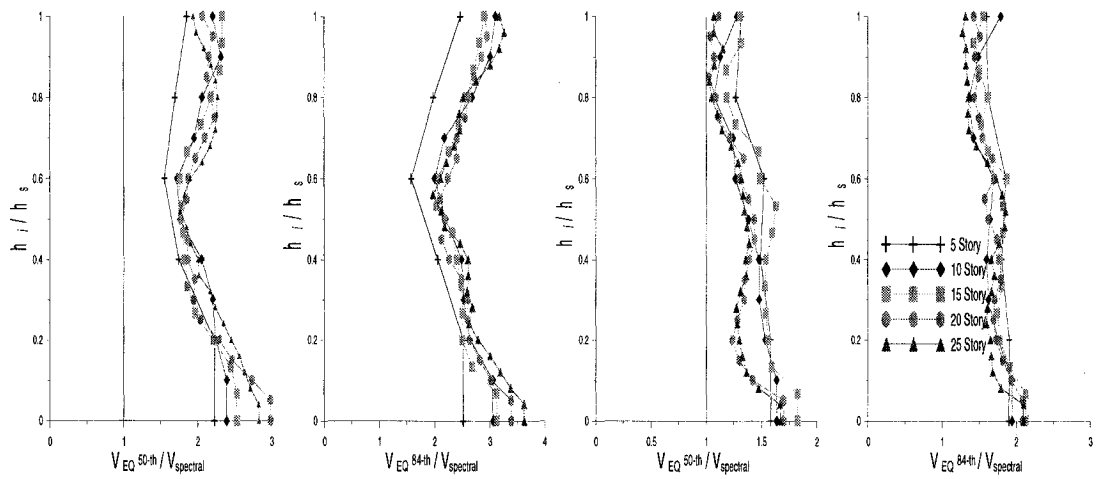

Figure 4.59: Shear forces: $V_{EQ} / V_{spectral}$

The next step corresponds to the development of the plastic hinge at the base of the buildings. Here, the non-linear results are compared to the shear corresponding to the probable moment capacity at the base of the walls, for the walls located in Vancouver and designed with R_d equal to 3.5, and to the development of the nominal moment capacity for the Montreal buildings designed for moderate ductility ($R_d = 2.0$). As shown

in figure 4.60, the nonlinear dynamic shear forces are again much larger than the design ones. The ratio at the base tend to increase with an increase of the building height for Vancouver. In Montreal, the inverse is true as the ratio tend to decrease when the height of the building is increased. The results plotted in figure 4.59 give the impression that the spectral analysis works slightly better for the short buildings located in Vancouver and for the higher ones located in Montreal, but fails to predict correctly the shear forces from non-linear analysis at the base of the buildings.

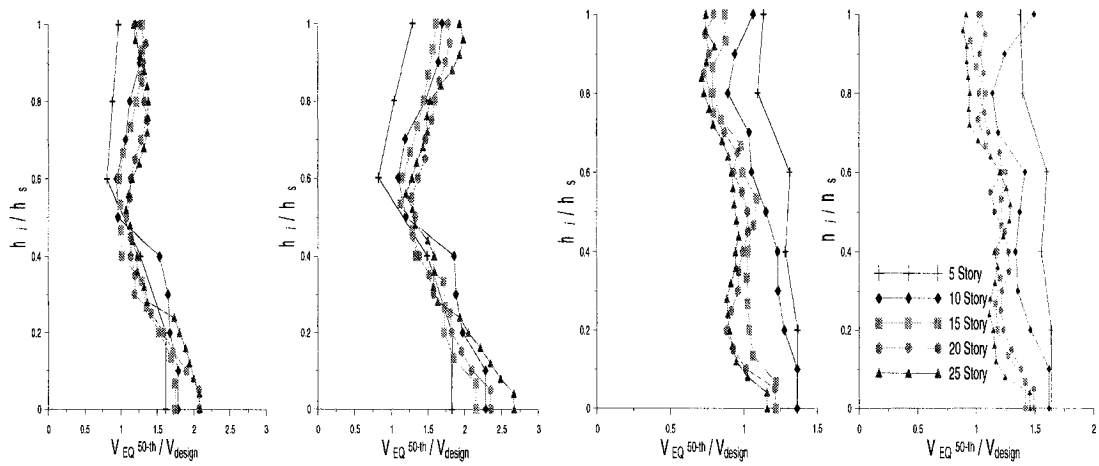

Figure 4.60: Shear forces: V_{EQ} / V_{design}

In the last step, the shear forces from nonlinear dynamic analysis are compared to the as-designed factored shear resistance of the walls following all requirements of CSA-A23.3-04. As can be visualized in figure 4.60, the walls as designed seem to exhibit sufficient shear strength in the upper half of the buildings, when compared to the 50th percentile shear seismic demand. In this part of the walls, minimum shear reinforcement requirements typically governed the design. However, the shear resistance in the bottom portion of the walls is insufficient. As a summary, Table 4.7 presents the ratios of the 50^{th} percentile shear force demand to the factored shear resistance, V_r, at the base of the walls, where the disagreement between both values is more pronounced. It is

noted that minimum steel requirement did not control the value of V_r at the wall bases. Therefore, V_r at the base closely matches the required design shear capacity, $V_f = \gamma_p V_{SP}$.

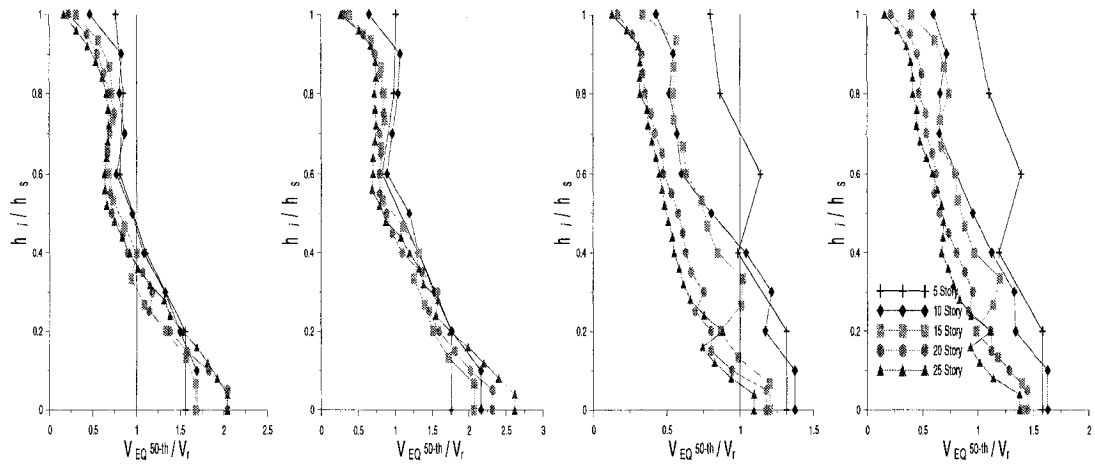

a) 50-th% b) 84-th% c) 50-th% d) 84-th%

Vancouver Montreal

Figure 4.61: Shear forces: V_{EQ} / V_r

Table 4.7: 50th percentile for V_{EQ} / V_r at the base of walls

	5-storey	10-storey	15-storey	20-storey	25-storey
Vancouver	1.56	1.69	1.68	2.04	2.04
Montreal	1.32	1.37	1.20	1.18	1.09

Figures 4.62 to 4.66 presents the ratios between the 50th and 84th percentile shear force demand values at the wall bases to the spectral and design shear force values for Vancouver and Montreal. Table 4.8 gives the ratios of the 50th percentile shear forces to the factored shear forces at the wall bases.

Comparing the results for the shear forces to those corresponding of the development of the plastic hinge at the base of the buildings, V_f, the nonlinear dynamic shear forces are again much larger than the design ones. The ratio at the base increases with the increase of the building height for Vancouver, varying from 1.61 to 2.08. The

opposite trend is observed for Montreal, with values varying from 1.37 for the shortest building to 1.1 for the tallest one.

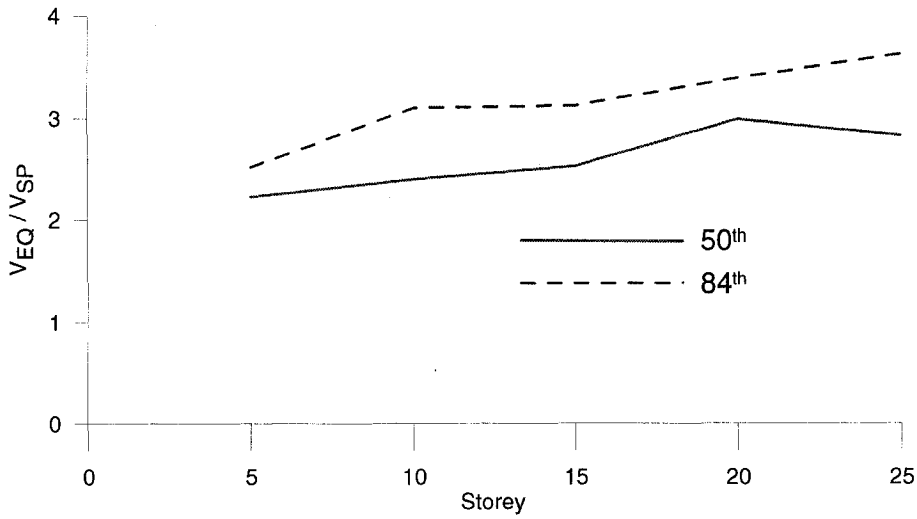

Figure 4.62: Base shear ratio - Vancouver: $V_{EQ} / V_{spectral}$

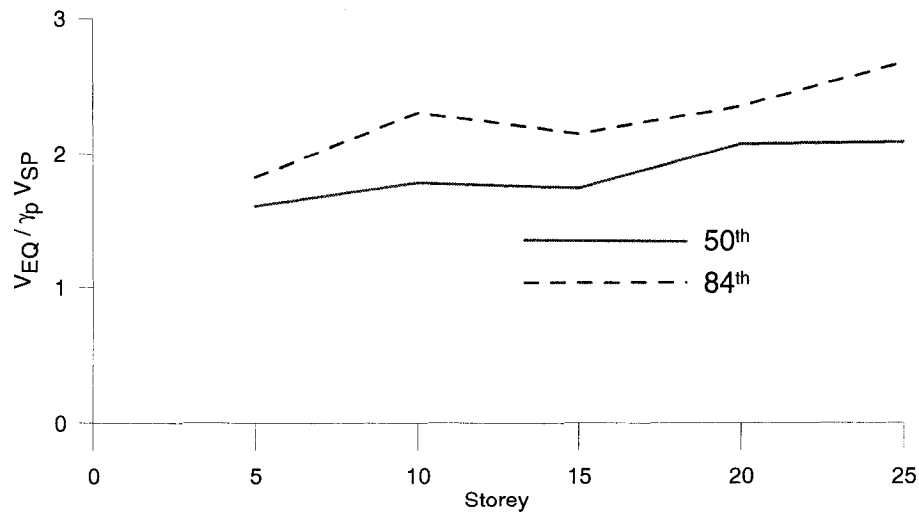

Figure 4.63: Base shear ratio - Vancouver: $V_{EQ} / \gamma_r V_{spectral}$

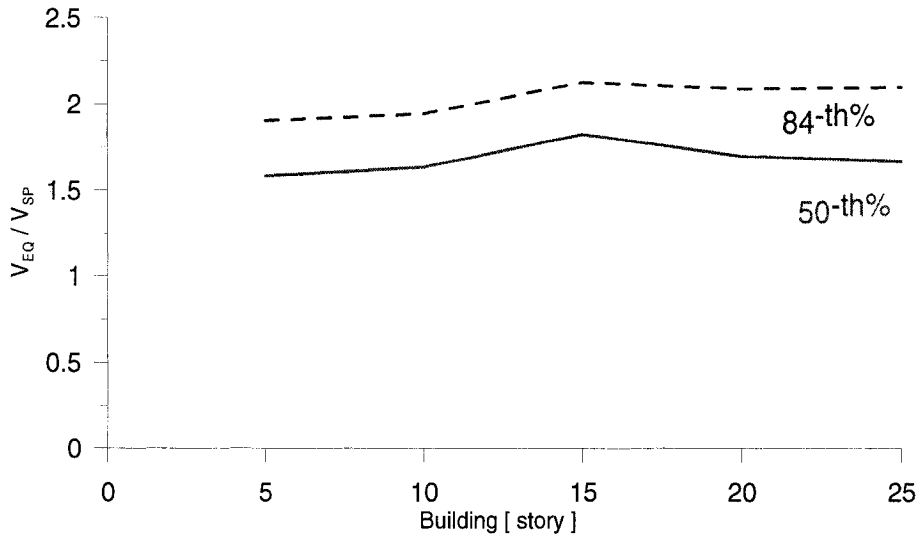

Figure 4.64: Base shear ratio - Montreal: $V_{EQ} / V_{spectral}$

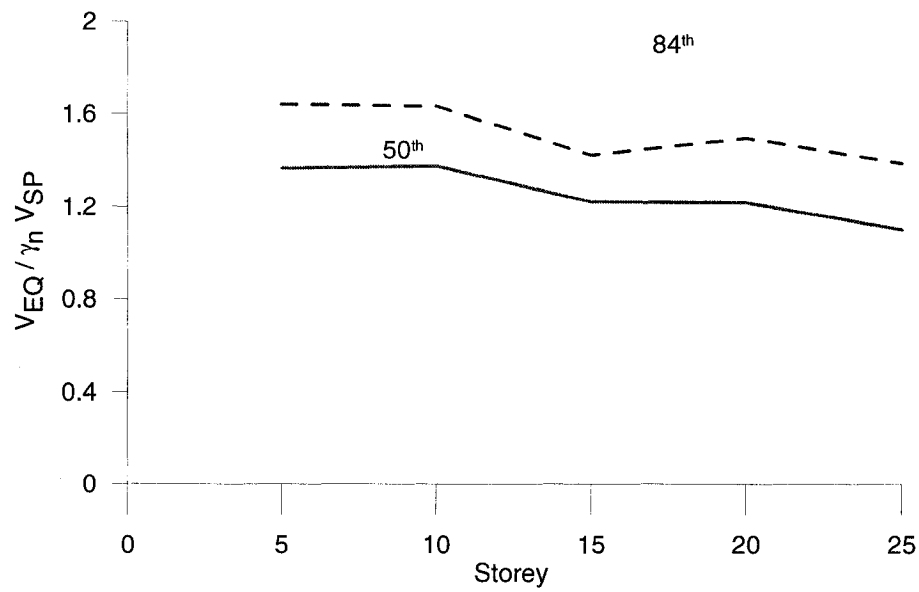

Figure 4.65: Base shear ratio - Montreal: $V_{EQ} / \gamma_n V_{spectral}$

These results clearly indicate that a shear amplification factor for dynamic response, γ_V, should be applied to the capacity design shear forces in the design of ductile and moderately ductile reinforced concrete shear walls. As proposed in other building codes and suggested by the trends observed in the results from this study, that

factor should vary as a function of the number of storeys, *n*. Two equations for this amplification factor are proposed for each site, one linear equation and one second order expression. The proposed amplification factors are compared to the obtained results in Table 4.9 and plotted in figures 4.66 and 4.67.

Table 4.8: Base Shears Ratio - $V_{EQ} / \gamma_p . V_{spectral}$ and $V_{EQ} / \gamma_n . V_{spectral}$

Building (storey)	Vancouver $V_{EQ} / \gamma_p V_{SP}$	Montreal $V_{EQ} / \gamma_n V_{SP}$
5	1.61	1.37
10	1.78	1.38
15	1.74	1.22
20	2.07	1.22
25	2.08	1.10

Table 4.9 gives the ratios between the shear dynamic amplification factors from the proposed equations and the shear demand to design ratios from analysis. The linear expressions at both sites represent well the 50th percentile results with errors varying between -5% and +8%.Similar deviations are observed when the second order expressions are used to predict the base shear force demand. The average values of these deviations are also reported in Table 4.9 and vary from 0 to 3%. Linear expressions are simpler to use in practice. However, the 2nd order equations seem to better reflect the trends observed for the taller buildings in Vancouver.

For Vancouver these equations are as it follows:

$$\gamma_v = 1.5 + n/40 \qquad (4.1)$$

$$\gamma_v = 1.5 + n/50 + (n/50)^2 \qquad (4.2)$$

For Montreal the correction factors have the following formulations:

$$\gamma_v = 1.4 - n/100 \qquad (4.3)$$

$$\gamma_v = 1.4 - n/140 - (n/140)^2 \qquad (4.4)$$

Table 4.9: Base Shears Correction Factors

Building (storey)	*Vancouver*					*Montreal*				
	$V_{EQ}/\gamma_p V_{SP}$	*Eq.4.1*	*%*	*Eq.4.2*	*%*	$V_{EQ} / \gamma_n V_{SP}$	*Eq.4. 3*	*%*	*Eq.4.4*	*%*
5	1.61	1.63	1.01	1.61	1.00	1.37	1.35	0.99	1.36	1.00
10	1.78	1.75	0.98	1.74	0.98	1.38	1.30	0.95	1.32	0.96
15	1.74	1.88	1.08	1.89	1.08	1.22	1.25	1.02	1.28	1.05
20	2.07	2.00	0.97	2.06	1.00	1.22	1.20	0.99	1.24	1.02
25	2.08	2.13	1.02	2.25	1.08	1.10	1.15	1.04	1.19	1.08
Average:			**1.01**		**1.03**			**1.00**		**1.02**

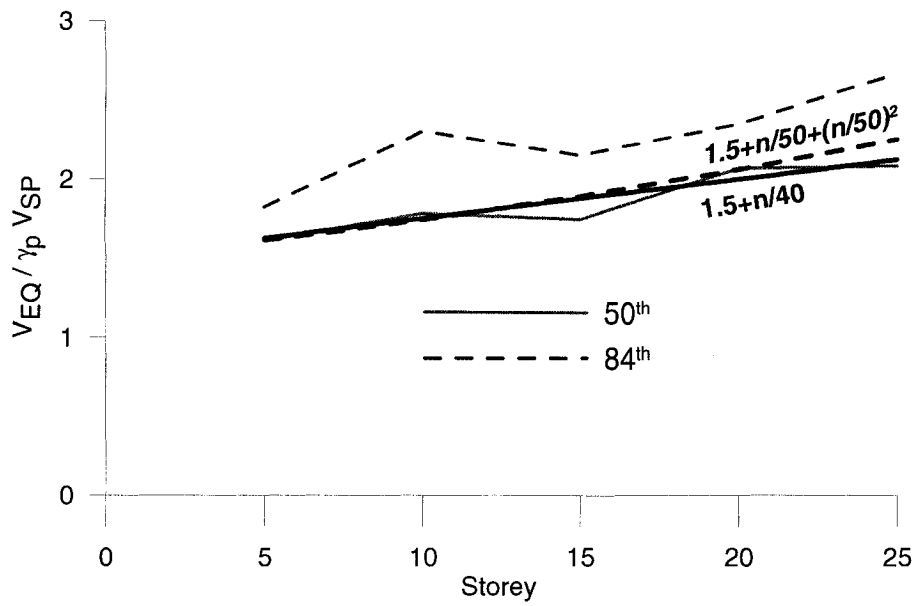

Figure 4.66: Correction base shear factors for Vancouver compared to $V_{EQ} / \gamma_p . V_{spectral}$

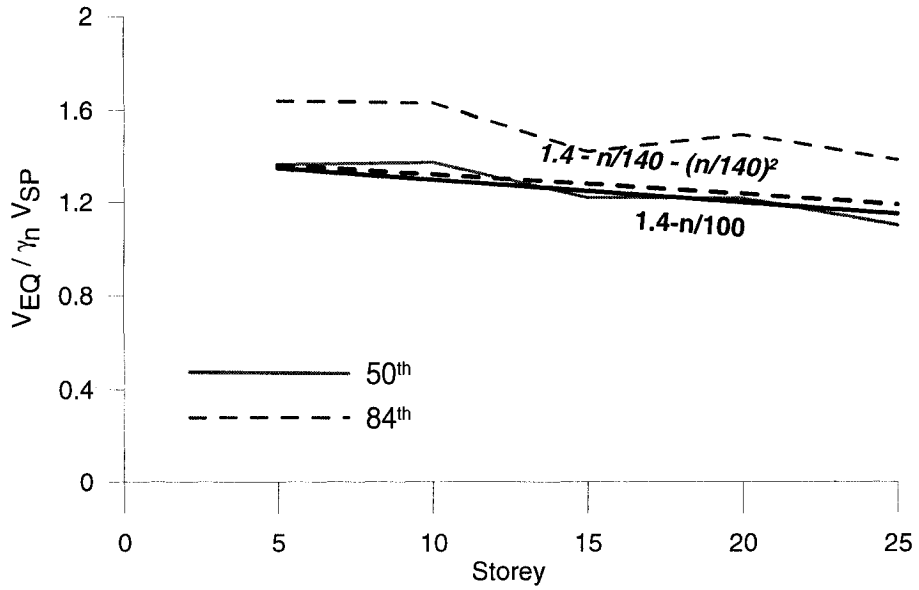

Figure 4.67: Correction base shear factors for Montreal compared to $V_{EQ} / \gamma_n \cdot V_{spectral}$

D) The influence of the concrete confinement

As described in Clause 21.6.7.3 of CSA A23.3-04 the ultimate compression strain of the concrete should be taken as 0.0035 for unconfined concrete, with a maximum stress equal to $0.9f'_c$. Clause 10.1.6 explains that the 0.9 factor accounts for differences between the in-place strength and the strength of standard cylinders.

In this section, we examine the influence on the wall responses of the confinement of the concrete in the compression zone of the walls. Clause 21.6.6.8 stipulates that the concentrated reinforcement shall be at least tied as in columns and that the ties must be detailed as hoops in regions of plastic hinging. The concentrated reinforcement shall also be tied with buckling prevention ties. The 5-, 10- and 15-story buildings at both sites with I shaped walls having columns at both ends were re-analysed with the assumption that only the concrete located in the concentrated reinforcement regions is confined as in columns and that the ultimate compression strain in the zone of distributed reinforcement is limited to 0.0035.

Various stress-strain models for confined concrete have been proposed in the scientific literature. The extensive experimental and numerical studies led to numbers of different models: Kent & Park (1971), Sheikh and Uzumeri (1982), Mander et al, (1988), Paultre (1993), Saatcioglu and Razvi (1993) Muguruma et al. (1980), etc. Equations are proposed for different cross-sections for columns and walls as a function of the unconfined concrete properties and the quantity and distribution of the confinement reinforcement steel. In this study, the models applicable for rectangular cross-sections were considered. The influence of the confinement was studied by comparing the Kent & Park and Taylor-Hoshikuma (1997) models and was adjusted for the Taylor concrete model used in the Ruaumoko program.

The comparison of the studied concrete models is presented in figure 4.68. Very similar results were obtained for the buildings at both sites.For simplicity, only the results for the Montreal buildings are presented herein. For completeness, the concrete model used in Response 2000 programme for the calculation of the moment-curvature sectional response for unconfined concrete is also plotted.

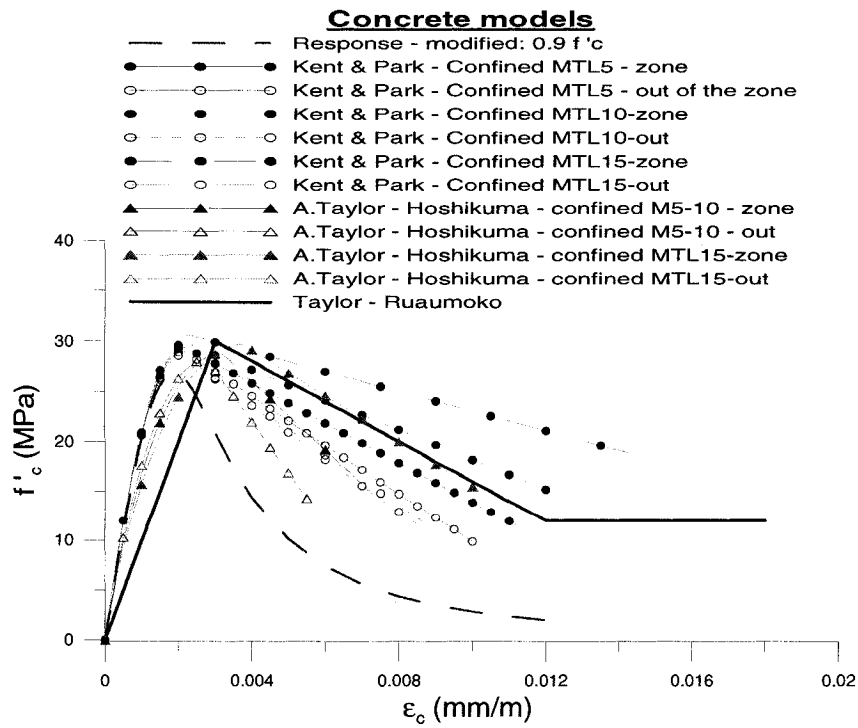

Figure 4.68: Concrete models - Montreal

In this figure the "zone" refers to the behaviour of the confined concrete according to the requirements for confinement of the plastic hinge zone and "out" refers to the response of the confined concrete according to the requirements for confinement and rebar spacing out of the critical zone.

Slightly different curves were obtained for the different models and for each cross-section. To achieve uniformity among all walls studied, the Taylor model was adjusted to represent a best-fit and a best representation of the confinement. The result is somehow between the concrete response for the confined (zone) and unconfined (out) regions. The resulting parameters for the Taylor model are: f'_c equal to $30MPa$, $\varepsilon'_c = 0.003$ and a post-peak residual strength equal to $50\% f'_c$ at $\varepsilon_{cu} = 0.012$.

The results of the nonlinear dynamic analysis of the walls with this confined Taylor concrete model are compared to those obtained with the unconfined concrete model. Three characteristics of the response of the walls are compared: peak displacement, peak bending moments and peak shear forces at each level.

When comparing the story displacements obtained for unconfined and for confined concrete models, figure 4.69, no uniform trend could be noticed over the height of the walls.

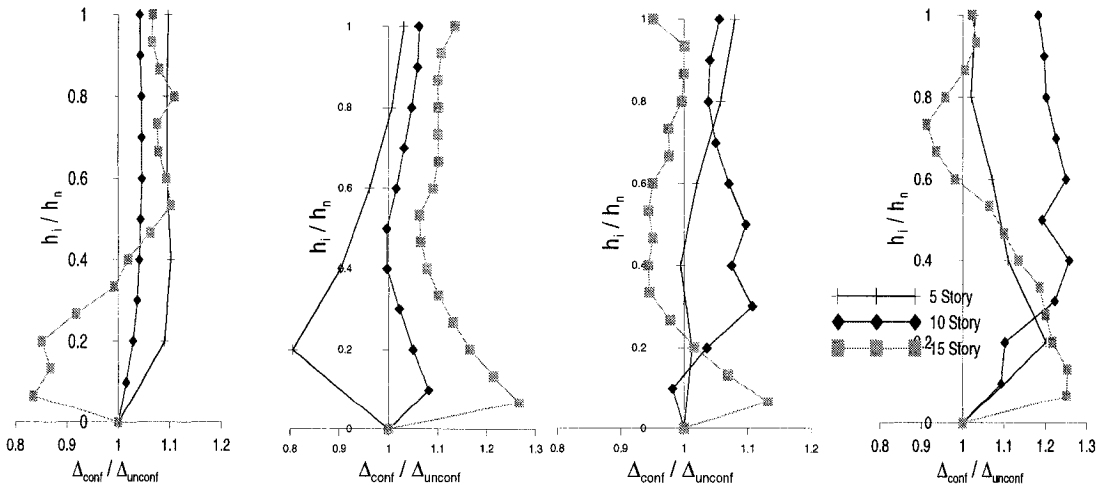

Figure 4.69: Comparison between confined and unconfined concrete models: $\Delta_{conf.} / \Delta_{unconf.}$

The displacements for the confined concrete model Δ_{conf} fall within ± 10% of the unconfined concrete model values, Δ_{unconf}. However, except for the 15-storey building in Montreal, the displacements at the top level is 5 to 10% larger when the confined concrete is considered, but the storey-drift angle values still remain smaller than the code limit of 2.5%.

The same variation was obtained for the storey bending moments, but the differences are slightly smaller, in the order of 2-3 % (maximum = 10% for 10-story building in Montreal), which was expected because the moments reached in the analysis depend much more of the reinforcement properties than the concrete material properties.

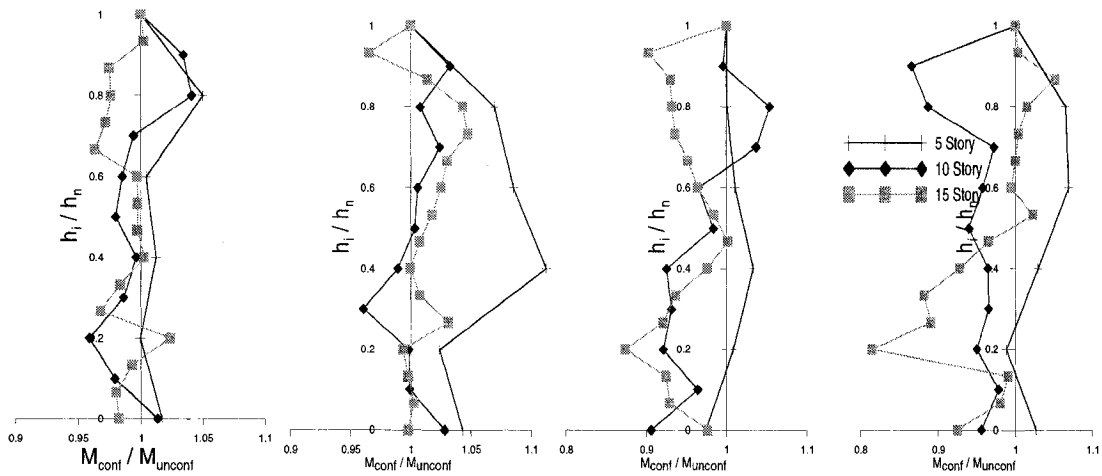

a) 50$^{-th\%}$ **b) 84$^{-th\%}$** **c) 50$^{-th\%}$** **d) 84$^{-th\%}$**

Vancouver **Montreal**

Figure 4.70: Comparison between confined and unconfined concrete models: $M_{conf.} / M_{unconf.}$

For the storey shears, the results are very similar to those obtained for the bending moments. In Vancouver, it can be noted that the variation at the base is smaller than in the upper part of the walls. The inverse is observed for the walls located in Montreal.

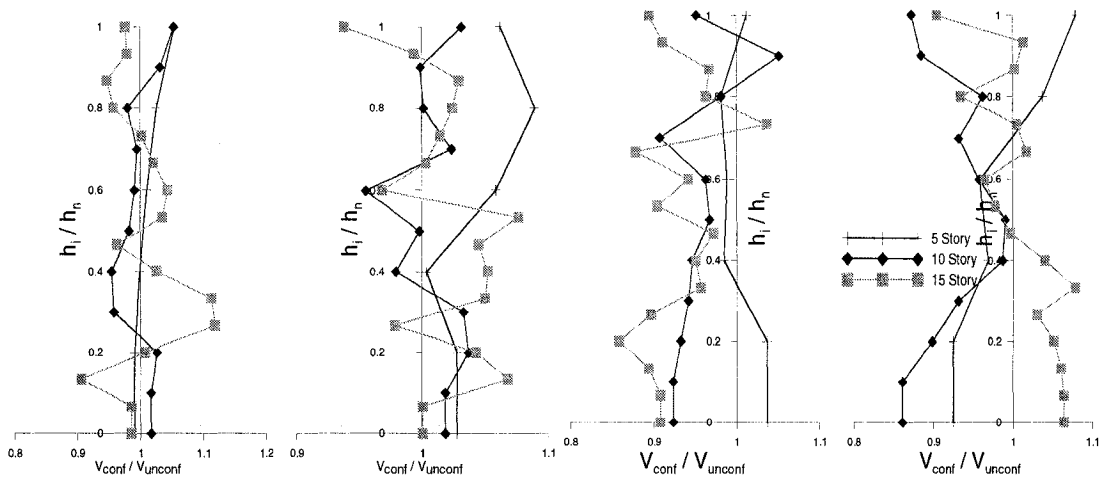

Figure 4.71: Comparison confined and unconfined model of concrete: $V_{conf.} / V_{unconf.}$

It can be concluded that accounting for the confinement of the concrete in the compression zone has a small influence on the overall response of the walls, with a 5-10% increase in the displacements in the top floors, and much smaller differences for the bending moments and storey shear forces. It seems that concrete confinement has a larger influence in the wall segments that remained elastic or experienced limited inelastic demand.

CHAPTER 5

DESIGN OF A WALL SPECIMEN FOR A SHAKING TABLE TEST PROGRAM

5.1 INTRODUCTION

To reduce the hazards associated with large earthquakes, it is essential to improve the reliability of earthquake resistance code provisions and reinforcement methods of the structures. Experimental techniques have always been an important part of engineering advancement. Whenever the theoretical knowledge reaches its limits, experiments provide alternative data and evaluation of the adequacy of the proposed design.

One of the difficulties with laboratory tests, especially dynamic laboratory tests, is model scale. For this purpose, failure mechanisms and collapse processes of full-scale structures must be investigated to alleviate any difficulties arising from physical limitations of the model. Considering the high cost of experimentation as compared to computer analysis, combined with the physical limitations as geometry of the models and capacity of the shaking tables and laboratory instrumentations, often the experimental work is carried out on scale models of elements and complete structures.

The main objective of the work presented in this Chapter is to propose a test specimen and reliable test set-up, which will serve later to verify the design assumptions and to obtain more detailed information about the influence of higher modes of vibration on the behaviour of ductile reinforced concrete shear walls designed according to NBCC 05 and CSA A23.3-04.

5.2 SIMILITUDE LAWS

The modeling theory of reduced-size testing is based on dimensional analysis. Dimensional analysis is an analytical method by which a dimensionally homogeneous equation, containing physical quantities and describing a physical phenomenon, is converted into an equivalent equation containing only dimensionless products of powers of the physical quantities. Dimensional analysis is based on the Buckingham PI Theorem, which states that a dimensionally homogeneous equation can be reduced to a functional relationship between a complete set of independent dimensionless products. The number of independent dimensionless products is equal to the total number of physical quantities involved minus the number of fundamental quantities needed to describe the dimensions of all physical quantities.

Several approaches have been considered to size the model walls. A summary of the shaking table studies and the relevant scaling laws was carried out by Moncarz (1981). According to his work, to describe the true response of reinforced concrete structures eight physical quantities are needed. They could be described with the following equation:

$$F = (a, g, t, L, M, \Delta, E, f_y, f'_c, E_c) \qquad (5.1)$$

where M, L and t are the fundamental quantities of the mass, length and time. The other quantities are acceleration, gravity, displacement, elastic modulus and elastic stress limit of materials. Applying the Buckhingam theorem we could write five independent dimensionless products:

$$G\left(\frac{a}{g}, \frac{\Delta}{l}, \frac{F_y}{E}, \frac{t^2 El}{M}, \frac{aM}{El^2}\right) \qquad (5.2)$$

The structural models of concrete structures can be divided in two fundamental groups: elastic models and ultimate strength models.

Considering that during the earthquake the shear walls work in its non-linear range an ultimate strength model is more convenient and reliable for representing the true response of the walls. The necessity of simulation of the behaviour of the prototype materials in its entire strength range significantly limits the potential model materials. In this case, the best choice for the materials for the models are concrete and reinforcement steel having the same strength and elastic modulus as those in the original prototype. It is important that the scaling of the concrete properties includes not only the appropriate scaling of the aggregate size but also scaling of the pore size in the gel, and void sizes in the aggregate. As for the reinforcement, a caution should be exercised in the use of the reinforcing bars with a form providing a proper simulation of the force transfer between concrete and the reinforcement.

The ratios in equation 5.2 give the relations between the prototype and the model responses. Those relations are in function of the scaling factor, which is ratio α between geometrical properties of the prototype and the model.

The most used similitude laws for the scaling of the engineering structures are called Acceleration similitude and Velocity similitude. The summary of the relations for the responses of interest is presented in "Structural study of seismic behaviour of buildings braced with shear walls" Chalah Ali (2004) from Ecole Polytechnique of Montreal.

The Velocity similitude allows bigger reduction of the used story dead weight, which is one of the biggest limitations for the dynamic shaking table test. Unfortunately this law implies a drastic increase of the frequency of the simulated ground motions, which is more critical for the earthquakes with higher frequency content, generally in the east of Canada. Because of this limitation the acceleration similitude is found more convenient for our purpose: to study the influence of the higher modes on the seismic behaviour of the shear wall structures.

Table 5. 1: Modeling parameters for Acceleration and Velocity similitude

Model type		Acceleration similitude	Velocity similitude
Scaling parameters	Prototype	Model	Model
Length wall	L	L/α	L/α
Thickness wall	E	E/α	E/α
Story height	H	E/α	H/α
Dead mass	M	M/α^2	M/α^3
Frequency	f	$f.\alpha^{0.5}$	$F.\alpha$
Time	t	$t/\alpha^{0.5}$	$t.\alpha$
Acceleration	a	a	$a.\alpha$
Weight stress	σ	σ	σ/α
Seismic stress	σ	σ	σ
Force	F	F/α^2	F/α^2

5.3 STUDIED BUILDING AND APPLICATION OF THE SIMILITUDE LAW

The choice of the studied building and the corresponding scale factor depend of many factors: geometrical restraints, capacity of laboratory equipments, the physical realisation of the model and at last but not the least the correspondence between the chosen model to the real prototype shear wall.

The first geometrical limitation is the available clear height for the construction, manipulation, instrumentation and instrumentation of the model. The Structural Engineering Laboratory at École Polytechnique of Montreal has a 10 m tall reaction wall, and a multi-purpose 12 MN load frame with 3 m wide x 8 m tall test space (Figure. 5.1). The clear height available above earthquake simulator is 10.7 m, in which we should fit the test specimen and its foundation, and 3.4 m x 3.4 m plan dimensions. The shaking table is mounted on four linear hydrostatic bearings, each with capacity of 175 kN.

The frequency range of the system is 0-50 Hz. It has maximum displacement of ± 125 mm, peak velocities of 1.0 m/s and peak accelerations ranging between 3.0 g and 1.0 g the capacity of the hydraulic jack and four supports limit the shear capacity and overturning moment resistances.

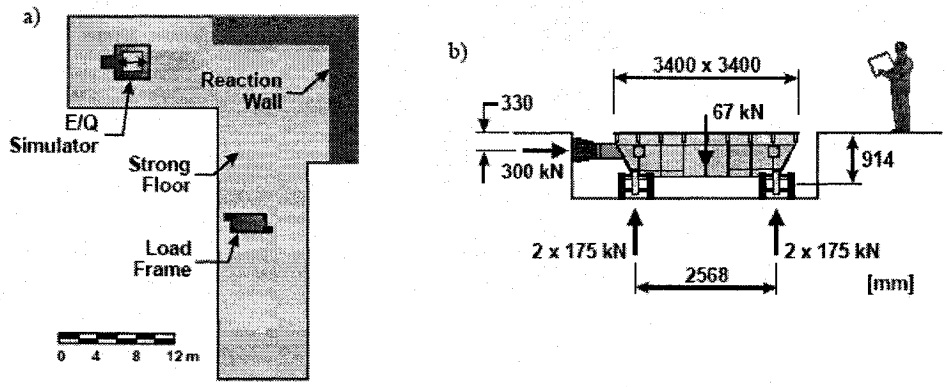

Figure 5. 1: Structural Engineering Laboratory at Ecole Polytechnique of Montreal: a) plan view of the new test area; b) characteristics of the earthquake simulator.

Another important restriction is the maximum applicable floor mass. According to the proposed set-up shown in figure 5.3, and the preliminary design, a maximum seismic weight of 60 kN per floor should be considered. Evaluating the concrete as the most performed (available, affordable and workable) material for manufacturing the dead loads, 2.5 m^3 of concrete per floor are needed. For simulating a dead load of a half of typical reinforced concrete building it requires 25 m^3 of concrete.

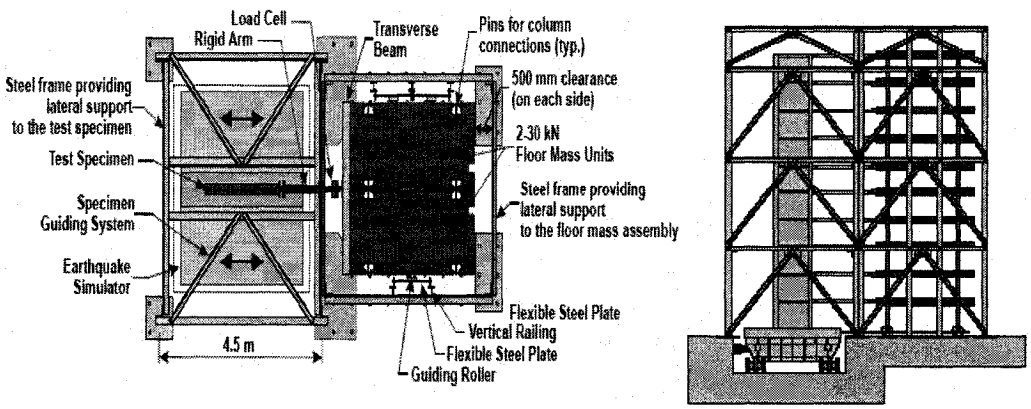

Figure 5. 2: Suggested test set-up: a) plan view; b) elevation view.

Based on the above remarks and on buildings already studied in chapters three and four, we have decided to base our model on a 30 x 30 m ten story building, with a fundamental period of 1.60 sec, located in Vancouver and designed with ductile shear walls, force modification factor, R_d, equal to 3.0. The building has a 6000 kN dead load per story and is braced with two simple shear walls in each direction. Torsional effects are neglected. The choice of the scale factor is based on the physical geometrical limits. The lower boundary is the maximum available height of specimen of 9.7 m, which requires a minimum scale factor of 3.09. The upper boundary is set by the minimum thickness of the specimen. Using the same materials for the specimen, concrete and steel reinforcement, a reasonable minimum thickness of 75 mm gives a maximum scale factor of 3.33. Obviously those bounds do not allow much flexibility in the choice of the geometrical scale factor. After a preliminary estimation a scale factor α set to 3.25. Applying the law of acceleration similitude, the story weight of the set-up for the simulated half of the building should the real weight reduced with a factor of α^2, or 278 kN per floor. Having an upper limit of 60 kN per floor and applying the acceleration similitude law, but using the inversed calculations, the prototype building, with the same fundamental period of vibration, should have a 17x17m plan dimensions, which is not quite realistic. To overcome this problem, another similitude law, called "modified acceleration similitude", is proposed herein.

To compensate the insufficient story dead weight, we will amplify the earthquake acceleration input with a factor β. The same material (concrete and steel) will be used for both the prototype and the model, which means that E_r = 1.0. From the dimensionless product $(t^2 E l_g / W)_p = (t^2 E l_g / W)_m$, and substituting $l_p = l_m / \alpha$ and $W_p = W_m / \beta$, it can be found that the relation for the time between the prototype and the model is now $t_m = t_p / (\alpha.\beta)^{0.5}$. Analogically, from the product $(aM/El^2)_p = (aM/El^2)_m$, and substituting $l_p = l_m / \alpha$ and $a_p = a_m / \beta$, it can be found that the relation for the seismic weight between the prototype and the model is $W_m = W_p / (\alpha^2.\beta)$. Because this model will not account correctly the stresses from gravity loads, they are β times less than required, the P-Δ effects would be underestimated

exactly with a factor of β. In the case of concrete shear walls those effects are in order of 2 to 5% (Tu, Tremblay and Leger, 2001) and they are practically negligible.

The choice of the new studied building and wall is schematically presented in Appendix E.

Applying this new factor a new building, with 24x24 m in plan dimensions and simple shear walls of 6.0x0.25, was found. The new prototype wall was designed according to NBCC05 and CSA 23.3-04. Dynamic spectral forces, design forces and vertical and horizontal reinforcement are reported in Table 5.2. There is also reported the yielding moment for the bilinear approximation of the moment-curvature diagrams use for Ruaumoko non-linear analysis.

Table 5.2 Design forces, reinforcement and Yielding moment approximation for Prototype

	Dynamic and Design forces (no torsion)						Vertical reinforcement		Horizontal reinforcement	M_y Takeda model
No	h_x	N	$V_{spec.}$	$M_{spec.}$	M_f	Vd^*k_d	Conc.	Distributed		
1	3.0	-1080.0	836.0	12145	**17063.7**	**1174.6**	6-25M	10M @ 250	10M @ 300	13901
2	6.0	-972.0	787.0	10186	**14311.3**	**1105.7**	6-25M	10M @ 250	10M @ 300	13626
3	9.0	-864.0	702.0	8506	**11950.9**	**986.3**	6-25M	10M @ 250	10M @ 300	13401
4	12.0	-756.0	603.0	7144	**11604.0**	**979.5**	6-25M	10M @ 250	10M @ 300	13134
5	15.0	-648.0	510.0	6043	**9815.6**	**828.4**	6-25M	10M @ 300	10M @ 300	12840
6	18.0	-540.0	446.0	5073	**8240.1**	**724.4**	4-25M	10M @ 300	10M @ 300	9900
7	21.0	-432.0	419.0	4096	**6653.1**	**680.6**	4-25M	10M @ 300	10M @ 300	9610
8	24.0	-324.0	409.0	3029	**4920.0**	**664.3**	4-20M	10M @ 300	10M @ 300	9354
9	27.0	-216.0	374.0	1882	**3056.9**	**607.5**	4-20M	10M @ 300	10M @ 300	9060
10	30.0	-108.0	260.0	781	**1268.6**	**422.3**	4-20M	10M @ 300	10M @ 300	8774

The relations between the prototype and the model, applying the new similitude law, called "Modified acceleration similitude" are summarized in table 5.3.

Table 5. 3: Modeling parameters for the proposed "Modified Acceleration Similitude"

Model type		Modified Acceleration similitude
Scaling parameters	Prototype	Model
Length wall	L	L / α
Thickness wall	E	E / α
Story height	H	E / α
Dead mass	M	$M / \alpha^2\beta$
Frequency	f	$f.(\alpha.\beta)^{0.5}$
Time	t	$t / (\alpha.\beta)^{0.5}$
Acceleration	a	$a.\beta$
Weight stress	σ	σ/β
Seismic stress	σ	σ
Force	F	$F / \alpha^2\beta$

5.4 ANALYTICAL VERIFICATION OF THE PROPOSED MODEL

Mathematical models

To verify the proposed model we conducted the non-linear analysis using the Ruaumoko program. The prototype and the model were modeled with element Bar and the flexural hysteretic behaviour was approximated with bi-linear Takeda model. The properties of the model were scaled applying the above-proposed factor. This verification has two main goals. First: verification of the proposed similitude and relations between the prototype and the model from one side, and second: feasibility of the proposed model specimen. The Prototype is model as a standard cantilever bar with lumped weights at each node. To achieve the second objective, the model specimen was modeled together with the seismic simulator. The schematics of mathematical models are presented in figure 5.3.b. in this model the seismic simulator is modeled as a rigid body with self-weight concentrated in two lumped weights. The foundation of the wall is also modeled as a rigid element, and is anchored to the table rigidly and moves with it as a unit. This model allows us to verify the horizontal and the vertical capacity of the seismic simulator during the test.

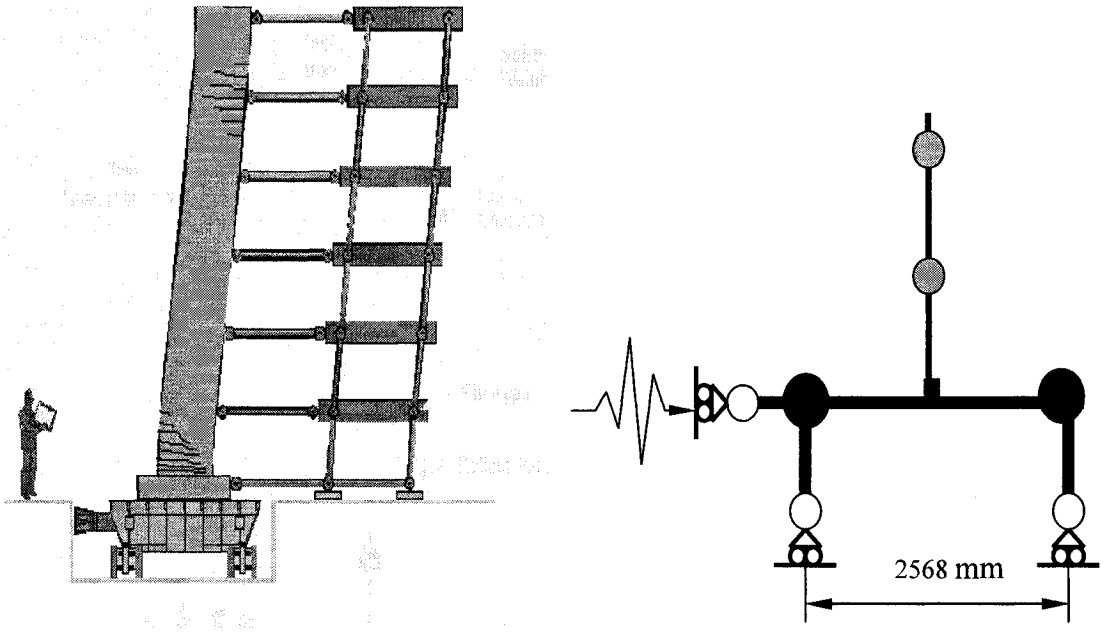

a) Set-up; **b) Mathematical modeling of the shaking table;**

Figure 5. 3: Proposed set-up and mathematical modeling of Model Wall specimen.

Analytical results

A) Verification of proposed Modified Acceleration Similitude

At first place we compared the global behaviour of the both walls, the maximum dynamic responses. As it is shown on figures 5.6 to 5.8 we obtained a very good fit between the Prototype and the Model. The difference of the responses is varying from 0% to 0.6%, which is practically negligible.

It is also plotted the spectral and design forces, according to NBCC 2005 and CSA 23.3-04. Dynamic shears, figure 5.4.b, from non-linear analysis exceed significantly the values prescribed by the code for design shear forces, which is coherent with the result reported in Chapter 4 herein.

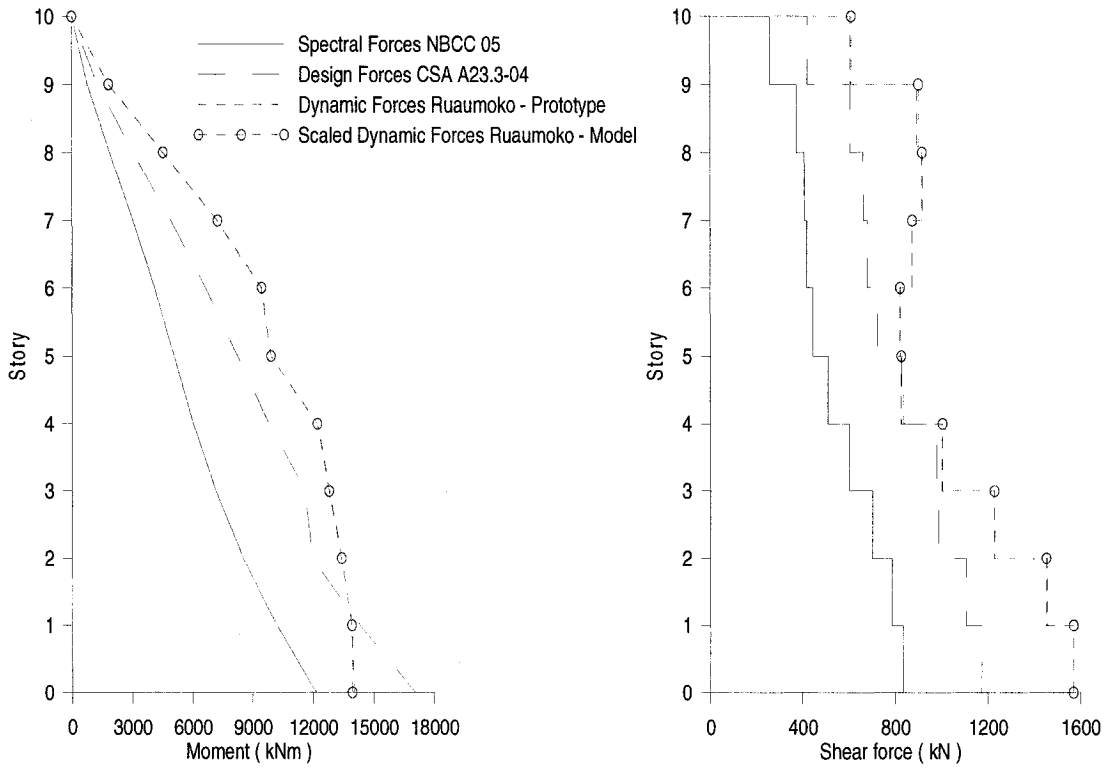

a) Dynamic Moments; **b) Dynamic Shears;**

Figure 5. 4: Comparison: Prototype - Model.

To verify similitude we compare also the local responses of Prototype and Model in time. In figure 5.5 is plotted the input ground acceleration for Prototype and Model. Applying the proposed scale factors, the acceleration for the Model is amplified by a factor of three and the time is reduced with 3.122, which is equal to $(3.25*3.0)^{0.5}$. It means that we reduce not only the duration of the input signal, but we reduced also the time step. As an input signal we used an artificial earthquake record W72701 with magnitude of M7.2 and epicentre at 70 km from the building.

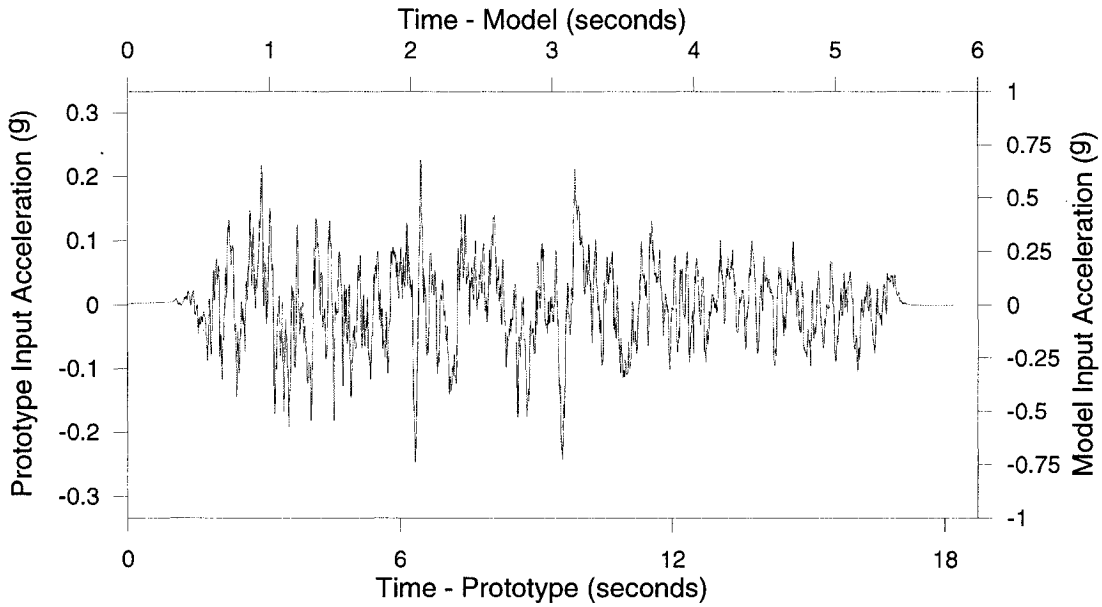

Figure 5. 5: Input ground acceleration W72701: Prototype - Model.

The first compared parameter is the top displacement. The results are presented in figure 5.6 as ratio of roof displacement to the total height of the wall, Δ_{top}/h_n. Both displacements are almost identical. The largest difference is in order of 0.6%, which is negligible and confirms that the influence of the axial force on effects of second order has small or negligible effect on the over-all behaviour.

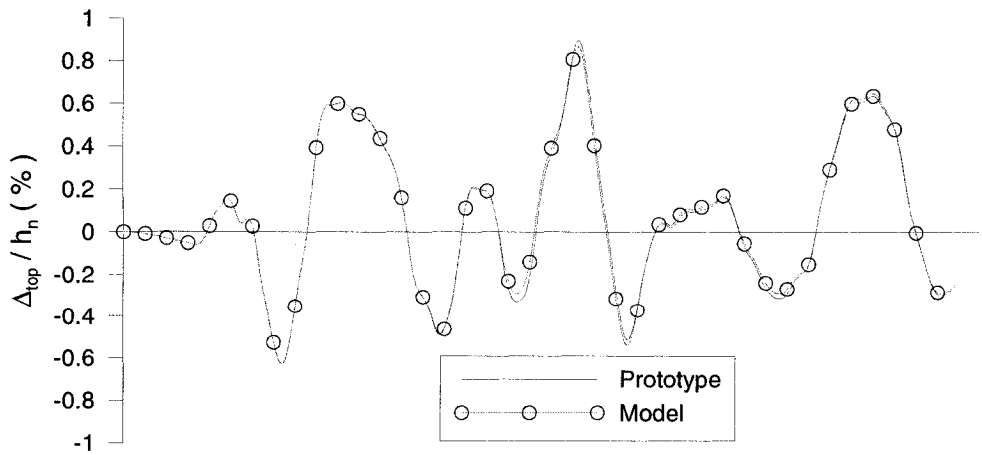

Figure 5. 6: Top displacement: Prototype - Model.

The next studied parameter is the base moment. Both responses are plotted in figure 5.7, where the time is scaled and the base moments are plotted in two different scales, representing the real values of the responses. Once again the maximum difference is in same order, about 0.6 %.

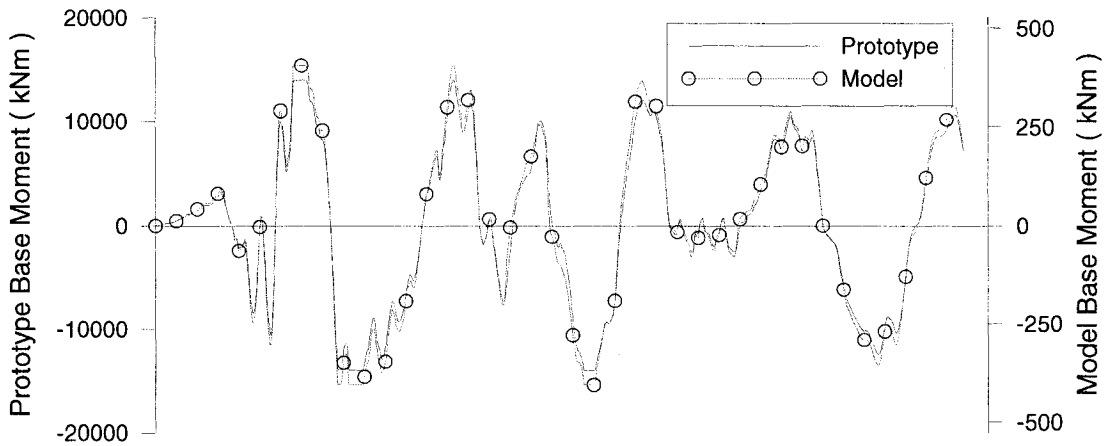

Figure 5. 7: Base moments: Prototype - Model.

The next studied parameter is the base shear. One more time the proposed similitude model gives a very good match of the responses for both walls. The results are plotted in figure 5.8.

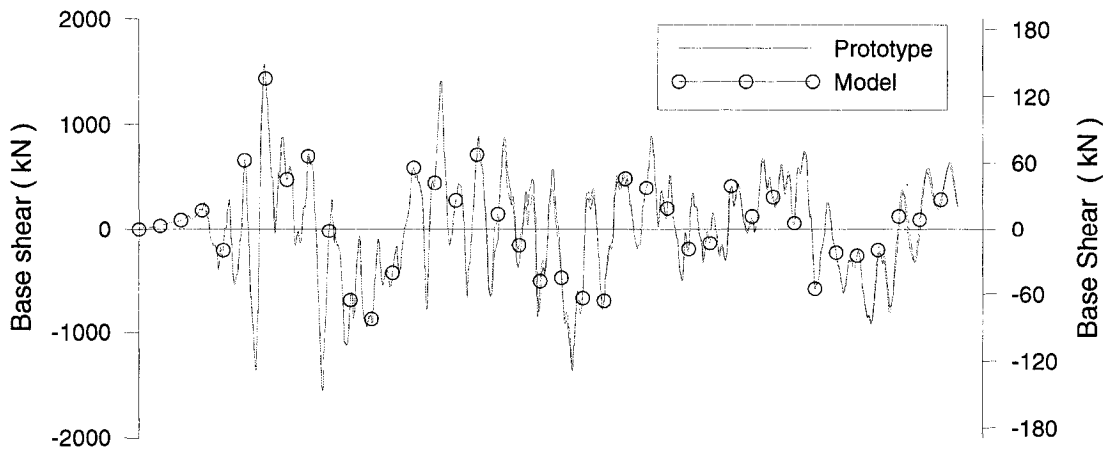

Figure 5. 8: Base shear: Prototype - Model.

B) Verification of capacities of the earthquake simulator

The second goal is to verify the capacity of the earthquake simulator. In the first place we verify the service capacity of the actuator. The history of the developed force in actuator is plotted in figure 5.9. The obtained absolute maximum force is 177 kN, which gives a safety factor of 1.7 for the actuator.

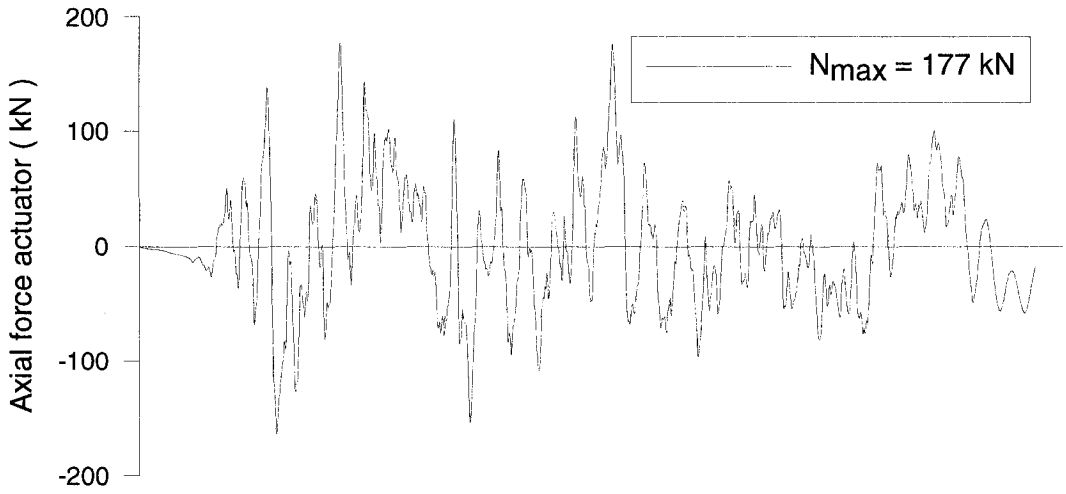

Figure 5. 9: Actuator axial force.

The second key element is the capacity of the vertical supports. The shaking table is supported by four linear bearings, each with capacity of 175 kN, or 350 kN on each side. The responses for each couple of bearings, left and right, is plotted in figure 5.10. The maximum obtained reaction is evaluated to 206 kN, which gives the same safety factor of 1.7 for the bearing supports.

The last studied parameter is the applied peak acceleration. As it is plotted in figure 5.5 the required peak acceleration for simulation of artificial earthquake W72302 and using a scale factor for acceleration of three is 0.73 g. It means that the simulator could develop its full payload capacity.

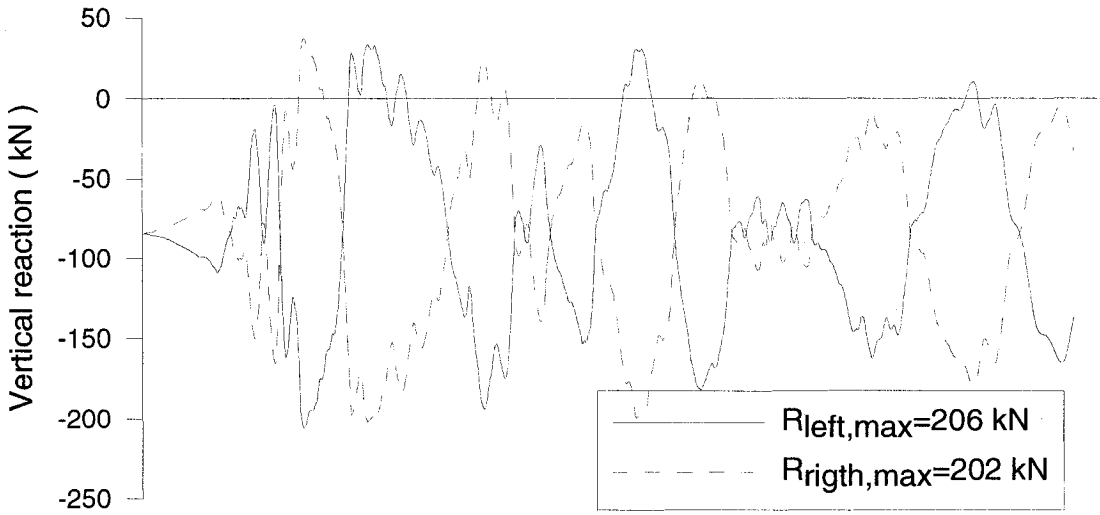

Figure 5. 10: Vertical reactions in the left and right supports.

5.5 CONCLUDING REMARKS AND RECOMANDATIONS

To study structural behaviour due to earthquakes, the most accurate way is to use a full-scale structural model and wait for earthquakes. But for the design purpose, it is absolutely impossible. If shaking table works as the loading equipments, full-scale model tests are still impractical for a very big shaking table will be needed and there are other problems such as the much higher cost and disposal after testing. Thus shaking table tests of scale models of structures are the best choices, taking into account, of course, economic, accuracy, and practical aspects of the test. However, the geometrical limitations and the limit choice of materials for simulation of reinforced concrete structures combined with the high bearing capacity of shear walls, make the common used similitude laws unpractical or unrealistic.

The proposed Modified Acceleration Similitude does not consider the exact influence of the gravity loads on the over-all response, however it gives satisfying results on structural systems not sensitive to the effects of second order. The analytical results show almost identical responses for Prototype and Model walls, with a largest difference of 0.6% for all studied values of interest.

The proposed test specimen and set-up are feasible and the induced forces do not exceed the capacities of the earthquake simulator. For this specimen and applied W72701 ground motion we found a safety factor of 1.7 for the actuator and for support bearings.

However, this analytical study is present only preliminary choice of test specimen and earthquake input signal. We recommend extending of this analytical study on test specimens, or buildings, with different first periods of vibration, varying from T_a, code prescribed period, to $3T_a$. The use of input ground motions with a different frequency content; covering the entire design spectrum is also highly desirable, specific for the West of Canada as well for the East.

CHAPTER 6

CONCLUSIONS AND RECOMENDATIONS

The main goal of this research was to evaluate the state-of-knowledge on the influence of higher modes on the nonlinear behaviour of reinforced concrete shear walls. That objective was achieved by employing two research tools. First, provisions from modern building codes from three different parts of the word were studied: North America – Canada (NBCC 2005) and USA (UBC97, NEHRP 2000), Australia and New Zealand - (NZS3101 and AC/NZS 1170.4), and Europe (EC8). An extensive review of the past research work concerning the higher mode effects and the dynamic amplification of shear forces reported in the scientific literature was performed as well. Second, ten shear wall buildings were designed according to National Building Code of Canada 2005: 5-, 10-, 15-, 20-, and 25-storey buildings located at two different sites, Vancouver in western Canada and Montreal in eastern Canada. Their seismic inelastic responses were examined through nonlinear dynamic analysis under several time history ground motions representative of the 2% in 50 years hazard level for each site, 15 records for Vancouver and 14 ground motions for Montreal.

Additional objectives included the development of a reduced-scale reinforced concrete shear wall model to be used in a shaking table test program. Two prototype models were designed and analyzed for verifying the practical applicability of the proposed scaling method.

A summary of the results and findings is presented below:

6.1 Codes comparison

All codes are based on the assumption that reinforced concrete shear walls will respond in the inelastic range during a strong ground motion, dissipating energy through inelastic rotation in flexural plastic hinges located generally at their bases, with the rest of the walls assumed to remain elastic. To prevent the formation of plastic hinges elsewhere in along the wall height and the possibility of brittle shear failures, all modern codes adopt a capacity design approach. The shear wall structures are regrouped in three different ductility classes: low, medium and high. The relative design loads for each ductility class shear walls in Canadian code generally compares well with the other codes. Among the different codes examined, NBCC 2005 prescribes the smallest design loads for the low ductility class walls, and the highest relative design loads for the moderate ductile shear walls. For the high ductility class, the NBCC loads are similar to those specified in UBC 97 loads when the redundancy factor is taken equal to one, and average the forces prescribed in the NZS and EC8 documents.

All studied codes, including the 2005 edition of the National Building Code of Canada, recognize dynamic analysis as the preferred procedure for obtaining the design forces and, in fact, makes such analysis mandatory for all irregular structures except those which have a low height or are located in zones of low seismicity.

When the equivalent lateral force method of NBCC 2005 is employed, the lateral loads used to calculate the shear forces and overturning bending moments are first magnified by the factor M_V to account for the dynamic amplification caused by higher mode response. In the bottom 60% of the wall height, the bending moments are then reduced using a reduction factor J. The value of M_V and J depend on the first mode of vibration and the shape of the acceleration spectrum for the site. The plastic hinge zone of the wall is first designed for flexural resistance. Then the design shear is calculated according to capacity design philosophy, based on the actual bending moment resistance

of the wall plastic hinge region. The EC8 and the New Zealand code use a different approach: the moment envelopes are calculated with non-magnified storey shear forces. The design shear forces are calculated by combining the capacity design approach with dynamic magnification for shear to account for higher modes effects on the shear forces.

6.2 Seismic loading, design forces and detailing requirements according to NBCC 2005 and CAN/CSA A23.3-04

A total of ten buildings, five situated in Montreal and five located in Vancouver, with a total height ranging from 15 to 75 m (five, ten, fifteen, twenty and twenty-five storey buildings), were designed according to NBCC 2005 and CSA A23.3-04. The fundamental periods of the buildings were fixed to be a multiple of the period T_a determined by the empirical equation given by the NBCC 2005: 2.0 times for the Vancouver buildings and 2.5 times for Montreal. The preliminary design for bending moments and shear forces at the wall bases led to following conclusions:

- For the buildings located in Montreal and designed with a ductility-related force modification factor of 3.5, the minimum requirements governed the choice of the flexural reinforcement. This, together with capacity design principles, led to a significant increase of the shear reinforcement, thus an ineffective utilization of the material, especially of steel reinforcement.

- The opposite conclusion was made for the buildings located in Vancouver. It was found that for the walls designed with $R_d = 2.0$, the shear area of the walls was insufficient as the computed shear stresses exceeded the maximum allowed values, and the wall thickness needed to be increased.

Based on these conclusions, the final choice of the sample buildings for the subsequent phase of complete designs and seismic analysis was: buildings designed with ductile shear walls *(R_d = 3.5)* for Vancouver, and shear walls with moderate ductility *(R_d = 2.0)* for Montreal.

The limited scope of the investigation does not allow conclusions of general validity to be drawn concerning the efficiency and accuracy of the design of shear walls according to NBCC 2005 and CSA A23.3-04. However, for structures having similar shear wall types and dynamic properties, the following findings are notable:

- The most important change in CSA-A23.3-04 is the explicit verification of the ductility of the wall, which is related to the inelastic rotation capacity of the wall. The inelastic rotational demand is associated to the design roof displacement whereas the inelastic rotation capacity is based on the wall properties in the plastic hinge region. For the calculation of the inelastic rotational demand, it is assumed that the displacement profile is similar to the first vibration mode and that the height of the plastic hinge is equal to half the length of the wall. This gives a conservative estimate of the inelastic rotational demand. All the buildings met the ductility requirement with inelastic rotational capacity exceeding the inelastic rotational demand, except for the 5-storey building located in Vancouver. For that particular building, the dimensions of the walls had to be changed in order to meet this requirement and the resulting dynamic period T_1 became equal to *1.70* T_a, instead of *2.0* T_a). The inelastic rotational demand tends to decrease with the height of the buildings designed with R_d = *3.5* in Vancouver. For all structures, the inelastic rotational capacity shows the opposite trend: it increases with the building height. For the taller buildings, it is approximately three times the inelastic rotational demand. As for the buildings located in Montreal and designed for R_d = *2.0* the rotational demand follows the same trend as for the buildings in Vancouver and is always governed by the minimum code requirement.

• Comparing the design base shear V_d obtained from Modal Response Spectrum Method with the limit of 80% of lateral earthquake design force from the Equivalent Static Procedure, the Modal Response Spectrum Method governed in all cases, except for the 25-storey buildings in Montreal for which the dynamic analysis results had to be increased such that the dynamic base shear matched the minimum value of 80% of the static base shear force V. Furthermore, for the longer period buildings in Vancouver (60m and 75m in height), the dynamic design base shear V_d was even larger than 100% of the static design force V.

• Another important change is the calculation of the design overturning moments and shear forces above the plastic hinge zone: the bending moments and shear forces in that part of the wall must be increased by the ratio of the factored moment resistance to the factored moment, both calculated at the top of the plastic hinge zone. This gives a value of design overturning moment above the plastic zone similar to the base design moment. This value combined with a lower axial compression force requires an increase of the flexural reinforcement just above the critical region, which has no practical justification. When this situation accured in this study, the amount of reinforcement used in the plastic hinge region was maintained over the plastic hinge region, without the increase required by the code.

• The CAN/CSA A23.3-04 is unclear for capacity design approach for type LD walls. In this study the height of the critical zone was calculated based on the Pauley-Priestley approach, i.e. the plastic hinge length was assumed equal to the length of the wall. The moment diagram shape above the plastic hinge zone was based on the linear distribution of moments assuming the development of nominal moment capacity in the plastic hinge zone.

6.3 Nonlinear dynamic analysis

The inelastic response of the buildings was studied using two different models: the Bar element and the Wall element. The first model represents the flexural behaviour of the wall section using beam-column elements with plastic hinges located at their ends. The main advantages of this modelling technique are its simplicity and the fact that it has been well studied and proven in past research. The second element is a multi-fibre element in which the cross section is modeled by meshes of concrete and steel fibres. In this element, both the concrete and the steel materials are represented with their respective stress-strain relationships and there is no need for the interpretation of the flexural and shear behaviour of the wall section at the macro scale. An extensive parametrical study of all parameters required to characterize the Wall element was conducted and values were proposed for these parameters. The validity of the results was verified by comparing the behaviour of the element with test results from a large-scale test on a slender concrete wall conducted by Adebar and Ibrahim (2000).

The results for both elements were compared in terms of displacements, shear forces and ductility demand at the wall base. In all cases the obtained values compared well. In view of these results, all the conclusions of the numerical study of the seismic performance of the walls in Montreal and Vancouver were based on the results obtained with the Wall element and these results led to the following conclusions:

- The maximum inter-storey drift angle values meet the code limit of 2.5% for all cases. The median estimates of the maximum values along the wall height are close to these calculated with the Modal Response Spectrum Method for the buildings located in Vancouver and between 0.50% and 0.88% for those in Montreal. The ratio of the results from nonlinear analysis to the 2.5% code limit is larger for the shorter buildings than for the taller buildings. This ratio is three to four times larger for buildings situated in Vancouver compared to those in

Montreal. Compared to the maximum elastic code predictions calculated using dynamic spectrum method, a good fit is obtained for the buildings located in Vancouver.

• The maximum ductility demand at the base of the buildings is smaller than the code predictions. For the low- and medium-height buildings in Vancouver, it is equal to about 0.6-0.7 of the code predicted ductility demand. For the high-rise buildings, it is even smaller, approximately 10% of the code predictions. For Montreal, the ductility demand for the lower structures varies from 10% to 30% of the code prediction and is nearly zero for the taller walls. This suggests that the CSA A23.3-04 code provisions give very conservative estimates of the anticipated ductility demand, especially for moderately ductile located in eastern Canada. The ductility demand in all cases was however concentrated at the base of the walls, as was intended in the design. For both sites, the five-story buildings experienced the highest rotational demand compared to the other buildings and the ductility demand decreases with an increase of the building height. The results revealed another very interesting behaviour: all buildings located in Montreal and both high-rise buildings in Vancouver remained essentially elastic during the earthquakes and did not experience yielding, as anticipated by the NBCC 2005 and CSA A23.3-04 provisions.

• The maximum base moments reached in the analyses for the Vancouver buildings are close to the probable moment capacity of the wall cross-sections and even slightly above. For the Montreal buildings, the computed bending moments were smaller than the nominal wall moment capacities, except for the 5-storey building in which case the moment demand reached xx times the wall nominal bending moment resistance. In Montreal, the ratios of the base moments to the nominal moments decreased with an increase of the building height.

• For all buildings, the shear forces from nonlinear dynamic analysis were found to be much larger than those corresponding of the development of the plastic hinge at the base of the buildings. The ratio between the two shear force values at the wall base increases with the building height for Vancouver, varying from 1.61 to 2.08. The opposite trend is observed for Montreal, with values varying from 1.37 for the shortest building to 1.1 for the tallest one. This indicates that a shear dynamic amplification factor, γ_V, must be applied in design to obtain realistic base shear force estimates when applying NBCC 2005 (with the dynamic response spectrum analysis method) and CSA A23.3 requirements. That amplification factor varies as a function of the number of storeys, n, and two expressions have been proposed for each of the two cases studied in this project: one linear equation and one second order expression. For ductile shear wall structures located in Vancouver, the shear force dynamic amplification factor, γ_V, could be obtained from either one of the two following expressions:

$$\gamma_V = 1.5 + n/40 \qquad (6.1)$$

$$\gamma_V = 1.5 + n/50 + (n/50)^2 \qquad (6.2)$$

For moderately ductile shear wall structures located in Montreal:

$$\gamma_V = 1.4 - n/100 \qquad (6.3)$$

$$\gamma_V = 1.4 - n/140 - (n/140)^2 \qquad (6.4)$$

• The influence of concrete confinement in the compression zone of the walls on the response of the 5-, 10- and 15-storey walls was examined. The analysis results were compared when specifying confined and unconfined concrete properties. The displacements with the confined concrete model were found to be slightly larger, less than 10%, but still smaller than the code limits. The changes in the storey bending moments are in the order of 2-3 % (10% for the 10-storey building in

Montreal), likely because bending moments essentially depend on the steel reinforcement rather than the concrete properties. The variations in storey shear forces were similar to those obtained for the bending moments. Overall, it can be concluded that the use of confined concrete models in the analyses, in lieu of unconfined concrete properties, has a small influence on the overall response of the walls and that the differences were small enough to be neglected.

6.4 Design of wall specimen for shaking table test program

A summary of the modeling theory was done and the different approaches for reduced-scale testing were reviewed. Past shaking table studies and relevant scaling laws proposed in the scientific literature were also reviewed and examined. The most important issues for scaling of the concrete and steel reinforcement were pointed out.

A test setup for dynamic shaking table test in the Structural Engineering Laboratory at École Polytechnique of Montreal was proposed. A shear wall specimen corresponding to a realistic prototype shear wall structure has been proposed considering the geometrical and physical constrains, the capacity of the laboratory equipment, and the physical realisation of a model. Two of the most commonly used similitude laws for the scaling of engineering structures, the acceleration and velocity similitude laws, were compared and pros and cons of each method were highlighted. Unfortunately, neither one of the two methods was practical for the particular application being studied. To overcome this shortcoming, a new similitude law called "Modified Acceleration Similitude", was developed for reinforced concrete shear walls. In the method, two different scaling factors are used: one for the length and one for the acceleration, allowing the fabrication of test models representing buildings with large floor seismic weights.

In the first place, the proposed model was validated by comparing the response of the Prototype and the scaled Model with non-linear dynamic analysis using the

Ruaumoko program. The global behaviour of the Prototype and the Model, including displacements, bending moments and storey shears, were found to be nearly identical: the differences between the responses varying between 0% and 0.6%. The local time history responses of the Prototype and Model structures for the top displacement, base moment, and base shear were also compared. Once again, the maximum differences were in the same order of magnitude (approximately 0.6 %), which is deemed negligible. The second verification that was conducted was to check that the demand on the earthquake simulator remained within the force capacity of the actuator, the vertical force capacity of the system horizontal hydrostatic bearings, and peak acceleration capacity of the equipment. All capacities were verified which confirmed the feasibility of the proposed scaled model shear wall. Three main conclusions can be drawn from this study:

- By combining two different scaling factors, one for the geometry and one for the acceleration, the proposed "Modified Acceleration Similitude" method gives more flexibility and freedom for the scaling of large shear wall specimens that meet typical geometrical and testing capacity limitations.

- In spite of the fact that the proposed model does not account correctly for the gravity load effects (P-delta effects), the "Modified Acceleration Similitude" gives essentially identical and realistic responses for the studied shear wall structure, because those structural systems are not sensitive to the geometric second order effects.

- The proposed test specimen and set-up are feasible and the induced forces do not exceed the capacities of the earthquake simulator.

6.5 Recommendations

Based on the results, current seismic design provisions for ductile and moderately ductile reinforced shear walls should be modified to include an amplification factor for the design shear forces.

It is important to extend the present study to include a wider ensemble of shear wall buildings having different geometries, dynamic properties, and ductility classes. The influence of the design seismic force demand should also be examined by studying additional sites and site classes.

More detailed analysis, such as nonlinear finite element analysis, and physical testing, such as shake table testing, should be conducted to look more closely at the at the shear force demand during inelastic response of reinforced concrete shear walls and confirm the findings of this study in terms of dynamic amplification of the shear forces. Shake table tests would also be particularly useful to validate assumptions and analytical results of this study, including damping, higher mode effects, and cracking response of concrete.

CHAPTER 7

BIBLIOGRAPHY

Amaris, M. A. D., June 2002, *DYNAMICS AMPLIFICATION OF SEISMIC MOMENTS AND SHEAR FORCES IN CANTILIVER WALLS*, a dissertation for master degree, Supervisor: Dr. Nigel Priestley.

Applied Technology Council for Building Seismic Safety and Federal Emergency Management Agency, NEHRP 2000 Edition, *Recommended provisions for seismic regulations for new buildings and other structures.*

Atkinson, G. and Beresnev, I. A. 1998, *Compatible ground-motion time histories for new national seismic hazard maps*, Can. J. of Civ. Eng.,25, 305-318;

Australia – New Zealand Standard, *Draft # DR PPCD8, Earthquake loading*, January 2003.

Blume, J., Newmark, N., & Corning, L., *Design of multi-storey reinforced concrete buildings for earthquake motions*, Portland Cement Association: Skokie, Illinois, 1961

Blakeley, R.W.G., R.C. Cooney & L.M. Meggett, *"Seismic sear loading at flexural capacity in cantiliver wall structure"*, Bulletin of the New Zealand National Society for Earthquqake Engineering, 1975.

BOCA, *The BOCA National Building Code, Building Officials and Code Administrators International*, Country Club Hills, IL, 1993, 1996, 1999.

CABO one & two family dwelling code / Council of American Building Officials. Homewood, Ill.: Building Officials and Code Administrators International, 1983;

CAN/CSA A23.3-04, December 2004, 5060 Spectrum Way, Suite 100, Mississauga, Ontario, Canada

CEN (2002) Comité Eropeen de Normalisation, Eurocode 8, Draft November 2002, *Design of structures for earthquake resistance*, Doc CEN/TC250/SC8/N335 Preliminary.

Chalah Ali, *Études structurales du comportement sismique des bâtiments contreventés à l'aide de murs de refend en béton armé*, 2004, École Polytechnique de Montréal, Québec, Canada.

COMITÉ EURO-INTERNATIONAL DU BETON, 1998, *Seismic design of reinforced concrete structures for controlled inelastic response*.

D'Aronco, D., Filiatrault, A., & Tinawi, R., rapport EPM/GCS -1993-13, *Evaluation of the shear forces in a ductile cantilever RC walls in Canada*, Ecole Polytechnique de Montreal, Quebec, Canada.

Eibl,J. and Kreintzel, E. *Seismic Shear Forces in RC Cantilever Shear Walls*, Proceedings, 9th World Conference on Earthquake Engineering. Paper 9-1-1, Tokyo-Kyoto, Japan, 1988 World Conference on Earthquake Engineering. Paper 9-1-1, Tokyo-Kyoto, Japan, 1988

El-Tawil S., & Hassan, M., *Inelastic Dynamic Behavior of Hybrid Coupled Walls*, ASCE, JOURNAL OF STRUCTURAL ENGINEERING ASCE / FEBRUARY 2004 / 285.

Freeman, Gilmartin, & Searer, *Using strong motion recordings to construct pushover curves*, 8th Canadian Conference on Earthquake Engineering – Vancouver-1999, p. 265-266.Geradin, M., & Negro, P. The European Laboratory for Structural Assessment (ELSA) and its Role for the Validation of European Seismic Codes.

Ghosh, S. K., *Update on the NEHRP Provisions: The Resource Document for Seismic Design*; PCI JOURNAL, May-June 2004.

Goel, Rakesh K., & Chopra, Anil K., *Period formulas for concrete shear wall building*, Journal of structural engineering, April 1998, p. 432.

Heidebrecht, Arthur C., *Overview of seismic provisions of the proposed 2005 edition of the National Building Code of Canada*, Can. J. Civ. Eng. 30: 241–254 (2003)

Hidalgo, P.A., Jordan, R.M., & Martinez M.P., *An analytical model to predict the inelastic seismic behavior of shear-wall, reinforced concrete structures*, Engineering Structures 24 (2002), p. 85–98.

Hiotakis, S., Lau, D.T. & Londono, N., *Research on seismic retrofit and rehabilitation of reinforced concrete shear walls using FRP materials.* http://www.ncree.org.tw/ 2004tcworkshop/pdf/3.pdf

Humar, J. M., Yavari, S., & Saatcioglu, M., (2003), *Design for forces induced by seismic torsion*, Can. J. Civ. Eng. 30: 328–337.

Ibrahim, A. M. M., & Adebar, P., August 2002, *Effective flexural stiffness for linear seismic analysis of concrete wall*, Earthquake Spectra, Vol. 18(3, pp. 407-426. Aug.)

Ibrahim, A. M. M., & Adebar, P., feb 2004, *Simple Nonlinear Flexural Stiffness Model for Concrete Structural Wall.*

ICBO, *Uniform Building Code*, International Conference of Building Officials, Whittier, CA, 1979, 1997.

Jianhua, Tu, April 2000, *P-Delta effects on the inelastic seismic response of reinforced concrete shear wall buildings*, Dissertation for master degree, Ecole Poletechnique of Montreal.

King, A., *Earthquake Loads & Earthquake Resistant Design of Buildings*, Structural Engineering Section Leader, Building Research Association of New Zealand(BRANZ). http://www.branz.co.nz/branzltd/publications/pdfs/cp55.doc

Kuenzli, Christopher M., El-Tawil S., & Hassan, M., *Pushover of Hybrid Coupled Walls. I: Design and Modeling*, P.E., M.ASCE1;, 1272 / JOURNAL OF STRUCTURAL ENGINEERING / OCTOBER 2002.

Lee, Tae-Hyung & Mosalam K. M., *Sensitivity of Seismic Demand of a Reinforced Concrete Shear-Wall Building*, Prof. of Ninth International Conference on Application of Statistics and Probability in Civil Engineering (ICASP 9), San Francisco, California, USA, July 6-9, 2003.

Mar, D., Panian, L., Dameron, R. A., Hansen, B. E., Vahdani, S., Mitchell, D., Paterson, J., *Performance-Based Seismic Upgrade of a 14-Story Suspended Slab Building Using State-of-the-Art Analysis and Construction Techniques.*

Mitchel D., Tremblay, R., Karacabeyli E., Paultre P., Saatcioglu M., & Anderason D., *SEISMIC FORCE MODIFICATION FACTOR FOR THE PROPOSED 2005 EDITION OF THE NATIONAL BUILDING CODE OF CANADA*, Canadian Journal of Civil Engineering, April 2003, 30, 2, p. 308.

New Zealand Standard, *Concrete Structures Standard, Draft Number: DZ 3101.2 rel. 1*, March 2004.

Nilson, A., Darwin, D., & Dolan Ch., *Design of concrete structures, 2004.*

Paterson, J., & Mitchell D., *Seismic Retrofit of Shear Walls with Headed Bars and Carbon Fiber Wrap*, JOURNAL OF STRUCTURAL ENGINEERING ASCE / MAY 2003.

Pannenton, M., Leger, P. & Tremblay, R., (2006), *Inelastic analysis of a reinforced concrete shear wall building according to the National Building Code of Canada 2005*, Canadian Journal of Civil Engineering, 33, 854-871

Paulay, T., *Seismic response of structural walls: Recent development*, Canadian Journal of Civil Engineering; Dec 2001; 28, 6; Wilson Applied Science & Technology Abstracts, p. 922.

Pautre, P. & Mitchell, D., Nouvelle Norme CSA A23.3-04 "Calcul des ouvrages en béton", *Presentation at Annual conference of ACI "Progrès dans le domaine du béton"*, Sherbrooke, Canada, 2004

Personeni, Arnold, Project rapport 2004, *SEISMIC BEHAVIOUR OF RC WALLS: EVALUATION OF NBCC 2005*, Ecole Polytechnique de Montreal.

Priesley, N., & Amaris, A., *Dynamic amplification of seismic moments and shear forces in cantilever walls*, European School for Advanced Studies in Reduction of Seismic Risk, Via Ferrata, 27100 Pavia, Italy.

RUAUMOKO, Carr, A.J. (2002) Inelastic Dynamic Analysis Program. Dept. of Civil Eng., University of Canterbury, NZ.

Reinhorn, A.M., Valles, R.E., Mattox, & Kunnath, S.K., *Seismic Damageability Evaluation of a Typical R/C Building in the Central U.S.*, The Quarterly Publication of NCEER Volume 10, Number 3, October 1996.

RESPONSE-2000, *Reinforced Concrete Sectional Analysis using the Modified Compression Theory*, Ver. 1.0.5, Bentz, E. and Collins, P., 2000.

Riva, P., Meda, A., & Giuriani, E., *Cyclic behaviour of a full scale RC structural wall*, Engineering Structures 25 (2003) 835–845.

SAP 2000, V7.40, Structural Analysis Program (2000), Computer and Structure Inc.

SBCCI, *Standard Building Code*, Southern Building Code Congress International, Birmingham, AL, 1994, 1997, 1999.

Seismic Design Methodology for Wall Systems, 8th Candian Conference on Earthquake Engineering – Vancouver-1999.p. 463-467.

Smith, R.S.H., & Tso, W.K., *Inconsistency of Force-Based Design Procedure*, JSEE: Spring 2002, Vol. 4, No. 1;

Tremblay, R., & Atkinson, G., *Comparative study of the inelastic seismic demand of eastern and western Canadian sites*, Earthquake Spectra, Volume 17, No 2, Mai 2001;

Vecchio, F. J., & Bucci, F., *Analysis of repaired reinforced concrete structures*, JOURNAL OF STRUCTURAL ENGINEERING / JUNE 1999.

Vecchio, F. J., Omar, A., Haro de la Pena, Bucci Ph., & Palermo D., *Behaviour of the cyclically loaded shear walls*, ACI Structural Journal, May-June 2002.

Wael Saad El Masri, Oct. 2001, *Earthquake design of shear walls in high-rise buildings: comparison between NBCC 95 and NBCC05*, a dissertation for master degree, Ecole Poletechnique of Montreal.

White, T. (2004), Doctorate thesis, *Seismic demand in high-rise concrete walls*, University of British Columbia.

W-SECT, Version 6.02, Softek Services Ltd.;

Yong Lu, *Seismic behaviour of multistory RC wall–frame system versus bar ductile frame system*, Earthquake engineering and structural dynamics, Earthquake Engineering Structural. Dynamics. 2002; 31:79–97 (DOI: 10.1002/eqe.99).

Appendix A

Shear wall building data reported in scientific literature

No	Author	Site	Building dimensions	No story / Height	W/story (kN)	w_{sismic} (Kpa)	I_{wall}	T_1 (s)	T_1 (s)
1	Wael Saad El Masri	Montreal	30x30	5	3700	8.22	27.5	0.30	
2			30x30	10	3700	8.22	34.1	0.83	
3			30x30	20	3860	8.58	47.1	2.52	
4	Filiatrault, D'Aronco & Tinawi	Montreal	30x45	3	3570	5.29	0.64	0.86	
5		Vancouver	30x45	3	3540	5.24	1.3	0.62	
6		Prince Rupert	30x45	3	3590	5.32	1.6	0.55	
7		Montreal	15x30	6	1238	5.50	0.7	1.51	
8		Vancouver	15x30	6	1230	5.47	1.6	1.01	
9		Prince Rupert	15x30	6	1233	5.48	1.6	1.01	
10		Montreal	27x42	10	3024	5.33	7.1	1.89	
11		Vancouver	27x42	10	3013	5.31	8.3	1.74	
12		Prince Rupert	27x42	10	3095	5.46	9.6	1.64	
13		Montreal	27x42	15	3082	5.44	13.7	2.91	
14		Vancouver	27x42	15	3200	5.64	14.4	2.87	
15		Prince Rupert	27x42	15	3320	5.86	19.2	2.54	
16		Montreal	40x40	25	4390	5.49	35.1	5.74	
17		Vancouver	40x40	25	8882	11.10	236.3	3.16	
18		Prince Rupert	40x40	25	9370	11.71	310.5	2.83	
19	Amaris & Priestley	Eurocode 8		2			0.7	0.34[1]	0.60[2]
20				4			1.6	0.796[1]	1.20[2]
21				8			3.8	1.878[1]	2.26[2]
22				12			5.4	2.721[1]	3.21[2]
23				16			6.8	3.392[1]	4.09[2]
24				20			7.3	3.649[1]	4.77[2]
25	Measured Periods	Palm Desert	60x80 ft	4				0.50	0.60[3]
26		C12284		50.2 ft					
27		LA - C24468	63x154 ft	8 / 127 ft				1.54	1.62
28	Goel & Chopra	San Bruno C58394	84x192 ft	9				1.20	1.30
29		San Bruno C58395		104 ft				1.00	1.45
30		Burbank	75x215 ft	10				0.60	0.56
31		C24385		88 ft				0.57	0.51
32		Pasadena	69x75 ft	10				0.71	0.52
33		N264-5		142 ft				0.98	0.62

34								0.97	0.62
35		San Jose	82x190 ft	10					0.75
36		C37355		124 ft					0.61
37									0.61
38		San Jose	64x210 ft	10				0.73	0.43
39		C37356		96 ft				0.70	0.42
40								0.65	0.43
41								0.63	0.41
42		LA ATC3	60x161 ft	12 / 159 ft				1.15	
43		LA N253-5	76x156 ft	12				1.19	1.14
44				161.5 ft				1.07	1.13
45		LA C24601	80x227 ft	17				1.18	1.05[3]
46				149.7 ft				1.00	1.00[3]
47	Mesured Periods	L8 Watsonville comercial building	22.9x21.6	4 / 20.1m				0.36	
48		M5 San Jose residential building	64x19.5	10 / 39.3m				0.80	
49	Y. Li & S. T. Mau	M6 LA office building	46.9x19.2	8 / 35.1m				1.50	
50		M7 San Bruno governement office	58.5x25.6	9 / 31.1m				1.20	
51		M8 Burbank residential building	65.5x22.9	10 / 26.8m				0.50	
52		M9 Walnut Creek comm. Building	45.1x31.7	10 / 29.3m				0.57	
53		H4 Oakland res. Building	64.3x23.8	24 / 66.8m				2.80	
54		Montreal		200 ft	36000 kips			2.00	
55		Vancouver		200 ft	36000 kips		R = 3.5	2.00	
56		Montreal		400 ft	72000 kips			4.00	
57		Vancouver		400 ft	72000 kips			4.00	
58		Montreal		800 ft	144000 kips			8.00	
59		Vancouver		800 ft	144000 kips			8.00	

60	Tu	Montreal	27x42	12	8000	7.00		1.58	NBCC95

(1) $I_{eff} = 0.5\ I_g$
(2) From Time-history
(3) Second principal direction

Appendix B – Element properties for nonlinear analysis

B.1 BAR Model

Table B.1 5-storey building in Vancouver

Storey No	A_g m^2	A_s m^2	Ief m^4	r	M_y kNm	I_{eff} / I_g
1	1.420	0.585	1.492	0.0000	21199	0.412
2	1.420	0.546	1.393	0.0020	20045	0.385
3	1.420	0.511	1.303	0.0080	18100	0.360
4	1.420	0.436	1.111	0.0084	12958	0.307
5	1.420	0.392	1.000	0.0060	7744	0.276

Table B.2 10-storey building in Vancouver

Storey No	A_g m^2	A_s m^2	I m^4	r	M_y kNm	I_{eff} / I_g
1	2.043	0.921	4.874	0.0062	37799	0.451
2	2.043	0.892	4.725	0.0105	35705	0.437
3	2.043	0.852	4.513	0.0113	34190	0.417
4	2.043	0.816	4.322	0.0131	32386	0.399
5	2.043	0.781	4.138	0.0135	30840	0.382
6	2.043	0.733	3.884	0.0148	29201	0.359
7	2.043	0.641	3.395	0.0134	23256	0.314
8	2.043	0.584	3.095	0.0156	21583	0.286
9	2.043	0.438	2.321	0.0135	14579	0.215
10	2.043	0.363	1.921	0.0165	12898	0.178

Table B.3 15-storey building in in Vancouver

Parameter Storey	A_g m^2	A_s m^2	I m^4	r	M_y kNm	I_{eff} / I_g
1	2.805	1.325	13.541	0.0043	68877	0.472
2	2.805	1.284	13.118	0.0046	66855	0.458
3	2.805	1.253	12.805	0.0078	64096	0.447
4	2.805	1.217	12.433	0.0084	61842	0.434
5	2.805	1.168	11.937	0.0101	59454	0.416
6	2.805	1.098	11.217	0.0106	57250	0.391
7	2.805	1.065	10.884	0.0114	54910	0.380
8	2.805	1.065	10.884	0.0114	54910	0.380
9	2.805	0.929	9.496	0.0119	43997	0.331
10	2.805	0.929	9.496	0.0119	43997	0.331

11	2.805	0.795	8.121	0.0118	35746	0.283
12	2.805	0.795	8.121	0.0118	35746	0.283
13	2.805	0.619	6.330	0.0166	28580	0.221
14	2.805	0.619	6.330	0.0166	28580	0.221
15	2.805	0.619	6.330	0.0166	28580	0.221

Table B.4 20-storey building in Vancouver

Parameter	A_g	A_s	I	r	M_v	I_{eff} / I_g
Storey	m^2	m^2	m^4		kNm	
1	4.710	1.719	21.528	0.0041	93319	0.365
2	4.710	1.681	21.058	0.0040	91202	0.357
3	4.710	1.633	20.452	0.0095	85688	0.347
4	4.710	1.624	20.339	0.0091	84120	0.345
5	4.710	1.568	19.640	0.0095	81946	0.333
6	4.710	1.517	18.997	0.0097	80065	0.322
7	4.710	1.470	18.407	0.0102	77860	0.312
8	4.710	1.470	18.407	0.0102	77860	0.312
9	4.710	1.351	16.918	0.0100	67418	0.287
10	4.710	1.351	16.918	0.0100	67418	0.287
11	4.710	1.219	15.274	0.0099	58758	0.259
12	4.710	1.219	15.274	0.0099	58758	0.259
13	4.710	1.092	13.677	0.0100	50685	0.232
14	4.710	1.092	13.677	0.0100	50685	0.232
15	4.710	0.941	11.792	0.0117	46286	0.200
16	4.710	0.941	11.792	0.0117	46286	0.200
17	4.710	0.807	10.107	0.0132	41950	0.171
18	4.710	0.807	10.107	0.0132	41950	0.171
19	4.710	0.682	8.538	0.0156	37415	0.145
20	4.710	0.682	8.538	0.0156	37415	0.145

Table B.5 25-storey building in Vancouver

Parameter	A_g	A_s	I	r	M_v	I_{eff} / I_g
Storey	m^2	m^2	m^4		kNm	
1	5.520	2.075	36.393	0.0083	129452	0.376
2	5.520	2.075	36.393	0.0083	129452	0.376
3	5.520	1.994	34.981	0.0086	124124	0.361
4	5.520	1.994	34.981	0.0086	124124	0.361
5	5.520	1.914	33.573	0.0092	118836	0.347
6	5.520	1.914	33.573	0.0092	118836	0.347
7	5.520	1.797	31.526	0.0092	113986	0.326
8	5.520	1.797	31.526	0.0092	113986	0.326
9	5.520	1.781	31.236	0.0087	105900	0.323

10	5.520	1.781	31.236	0.0087	105900	0.323
11	5.520	1.577	27.671	0.0091	90241	0.286
12	5.520	1.577	27.671	0.0091	90241	0.286
13	5.520	1.450	25.435	0.0091	83369	0.263
14	5.520	1.450	25.435	0.0091	83369	0.263
15	5.520	1.356	23.783	0.0101	77592	0.246
16	5.520	1.356	23.783	0.0101	77592	0.246
17	5.520	1.234	21.645	0.0112	72708	0.224
18	5.520	1.234	21.645	0.0112	72708	0.224
19	5.520	1.082	18.978	0.0112	67465	0.196
20	5.520	1.082	18.978	0.0112	67465	0.196
21	5.520	0.961	16.862	0.0136	62167	0.174
22	5.520	0.961	16.862	0.0136	62167	0.174
23	5.520	0.782	13.715	0.0158	54723	0.142
24	5.520	0.782	13.715	0.0158	54723	0.142
25	5.520	0.782	13.715	0.0158	54723	0.142

Table B.6 5-storey building in Montreal

Parameter	A_g	A_s	I	R	M_y	I_{eff} / I_g
Storey	m^2	m^2	m^4		kNm	
1	0.960	0.452	0.748	0.0064	12204	0.471
2	0.960	0.419	0.692	0.0125	12204	0.436
3	0.960	0.343	0.567	0.0108	12204	0.357
4	0.960	0.280	0.463	0.0105	12204	0.292
5	0.960	0.234	0.387	0.0123	12204	0.244

Table B.7 10-storey building in Montreal

Parameter	A_g	A_s	I	r	M_y	I_{eff} / I_g
Storey	m^2	m^2	m^4		kNm	
1	1.555	0.764	3.742	0.0052	24732	0.491
2	1.555	0.764	3.742	0.0052	24732	0.491
3	1.555	0.764	3.742	0.0052	24732	0.491
4	1.555	0.764	3.742	0.0052	24732	0.491
5	1.555	0.764	3.742	0.0052	24732	0.491
6	1.555	0.764	3.742	0.0052	24732	0.491
7	1.555	0.764	3.742	0.0052	24732	0.491
8	1.555	0.764	3.742	0.0052	24732	0.491
9	1.555	0.764	3.742	0.0052	24732	0.491
10	1.555	0.764	3.742	0.0052	24732	0.491

Table B.8 15-storey building in Montreal

Parameter	A_g	A_s	I	r	M_y	I_{eff} / I_g
Storey	m^2	m^2	m^4		kNm	
1	2.140	1.086	9.467	0.0021	41451	0.507
2	2.140	1.061	9.250	0.0025	39737	0.496
3	2.140	1.046	9.120	0.0031	37800	0.489
4	2.140	1.004	8.755	0.0038	35769	0.469
5	2.140	0.950	8.285	0.0043	33752	0.444
6	2.140	0.905	7.892	0.0048	31738	0.423
7	2.140	0.879	7.668	0.0041	30130	0.411
8	2.140	0.793	6.917	0.0043	26463	0.371
9	2.140	0.263	1.194	0.0037	25158	0.123
10	2.140	0.263	1.194	0.0037	25158	0.123
11	2.140	0.664	5.792	0.0062	20161	0.310
12	2.140	0.664	5.792	0.0062	20161	0.310
13	2.140	0.528	4.601	0.0080	15861	0.247
14	2.140	0.528	4.601	0.0080	15861	0.247
15	2.140	0.528	4.601	0.0080	15861	0.247

Table B.9 20-storey building in Montreal

Parameter	A_g	A_s	I	r	M_y	I_{eff} / I_g
Storey	m^2	m^2	m^4		kNm	
1	4.020	1.710	15.668	0.0019	58406	0.425
2	4.020	1.670	15.297	0.0021	56194	0.415
3	4.020	1.625	14.883	0.0046	52914	0.404
4	4.020	1.483	13.588	0.0048	49249	0.369
5	4.020	1.441	13.200	0.0047	47443	0.358
6	4.020	1.441	13.198	0.0050	47315	0.358
7	4.020	1.344	12.308	0.0054	45357	0.334
8	4.020	1.310	12.000	0.0054	43440	0.326
9	4.020	1.244	11.392	0.0059	41409	0.309
10	4.020	1.244	11.392	0.0059	41409	0.309
11	4.020	1.103	10.101	0.0063	37851	0.274
12	4.020	1.103	10.101	0.0063	37851	0.274
13	4.020	0.980	8.972	0.0071	33985	0.244
14	4.020	0.980	8.972	0.0071	33985	0.244
15	4.020	0.867	7.941	0.0085	30061	0.216
16	4.020	0.867	7.941	0.0085	30061	0.216
17	4.020	0.614	5.624	0.0118	24345	0.153
18	4.020	0.614	5.624	0.0118	24345	0.153
19	4.020	0.614	5.624	0.0118	24345	0.153
20	4.020	0.614	5.624	0.0118	24345	0.153

Table B.10 25-storey building in Montreal

Parameter	A_g	A_s	I	r	M_y	I_{eff} / I_g
Storey	m^2	m^2	m^4		kNm	
1	4.770	2.099	27.312	0.0018	84787	0.440
2	4.770	2.099	27.312	0.0018	84787	0.440
3	4.770	2.017	26.253	0.0042	78190	0.423
4	4.770	2.017	26.253	0.0042	78190	0.423
5	4.770	1.929	25.108	0.0041	73948	0.404
6	4.770	1.929	25.108	0.0041	73948	0.404
7	4.770	1.802	23.456	0.0048	68923	0.378
8	4.770	1.802	23.456	0.0048	68923	0.378
9	4.770	1.638	21.313	0.0046	64919	0.343
10	4.770	1.638	21.313	0.0046	64919	0.343
11	4.770	1.518	19.759	0.0054	59921	0.318
12	4.770	1.518	19.759	0.0054	59921	0.318
13	4.770	1.392	18.120	0.0058	55445	0.292
14	4.770	1.392	18.120	0.0058	55445	0.292
15	4.770	1.259	16.380	0.0066	50727	0.264
16	4.770	1.259	16.380	0.0066	50727	0.264
17	4.770	1.125	14.637	0.0074	46127	0.236
18	4.770	1.125	14.637	0.0074	46127	0.236
19	4.770	0.977	12.708	0.0084	41585	0.205
20	4.770	0.977	12.708	0.0084	41585	0.205
21	4.770	0.839	10.923	0.0095	37401	0.176
22	4.770	0.839	10.923	0.0095	37401	0.176
23	4.770	0.607	7.893	0.0134	30422	0.127
24	4.770	0.607	7.893	0.0134	30422	0.127
25	4.770	0.607	7.893	0.0134	30422	0.127

B.2 WALL Model

For element WALL used in Ruaumoko program the input requires the values for concrete and steel area for each fibre. Instead of giving those values, for simplicity, in the next tables we give values of the total (gross) section areas, which is the sum of the concrete and steel areas of the fibre section, and is always same for a given wall.

Table B.11 5-storey building in Vancouver

Storey	Fibre	1	2	3	4	5	6	7	8	9	10
	Xi	0.100	0.300	0.767	1.500	2.233	2.967	3.700	4.433	4.900	5.100
	Ac	0.078	0.078	0.182	0.182	0.182	0.182	0.182	0.182	0.078	0.078
1	As	0.0020	0.0020	0.0013	0.0013	0.0013	0.0013	0.0013	0.0013	0.0020	0.0020
2		0.0020	0.0020	0.0013	0.0013	0.0013	0.0013	0.0013	0.0013	0.0020	0.0020
3		0.0020	0.0020	0.0013	0.0013	0.0013	0.0013	0.0013	0.0013	0.0020	0.0020
4		0.0020	0.0020	0.0005	0.0005	0.0005	0.0005	0.0005	0.0005	0.0020	0.0020
5		0.0009	0.0009	0.0005	0.0005	0.0005	0.0005	0.0005	0.0005	0.0009	0.0009

Table B.12 10-storey building in Vancouver

Storey	Fibre	1	2	3	4	5	6	7	8	9	10
	Xi	0.113	0.338	0.996	2.088	3.179	4.271	5.363	6.454	7.113	7.338
Ag	Ac+As	0.1013	0.1013	0.2729	0.2729	0.2729	0.2729	0.2729	0.2729	0.1013	0.1013
As	1	0.0028	0.0028	0.0007	0.0007	0.0007	0.0007	0.0007	0.0007	0.0028	0.0028
	2	0.0028	0.0028	0.0007	0.0007	0.0007	0.0007	0.0007	0.0007	0.0028	0.0028
	3	0.0028	0.0028	0.0007	0.0007	0.0007	0.0007	0.0007	0.0007	0.0028	0.0028
	4	0.0028	0.0028	0.0007	0.0007	0.0007	0.0007	0.0007	0.0007	0.0028	0.0028
	5	0.0028	0.0028	0.0007	0.0007	0.0007	0.0007	0.0007	0.0007	0.0028	0.0028
	6	0.0028	0.0028	0.0007	0.0007	0.0007	0.0007	0.0007	0.0007	0.0028	0.0028
	7	0.002	0.002	0.0007	0.0007	0.0007	0.0007	0.0007	0.0007	0.002	0.002
	8	0.002	0.002	0.0007	0.0007	0.0007	0.0007	0.0007	0.0007	0.002	0.002
	9	0.001	0.001	0.0007	0.0007	0.0007	0.0007	0.0007	0.0007	0.001	0.001
	10	0.001	0.001	0.0007	0.0007	0.0007	0.0007	0.0007	0.0007	0.001	0.001

Table B.13 15-storey building in Vancouver

Storey	Fibre	1	2	3	4	5	6	7	8	9	10
	Xi	0.113	0.338	1.250	2.850	4.450	6.050	7.650	9.250	10.163	10.388
Ag	Ac+As	0.1013	0.1013	0.2733	0.2733	0.2733	0.2733	0.2733	0.2733	0.1013	0.1013
As	1-9	0.0028	0.0028	0.0011	0.0011	0.0011	0.0011	0.0011	0.0011	0.0028	0.0028
	9-10	0.0020	0.0020	0.0011	0.0011	0.0011	0.0011	0.0011	0.0011	0.0020	0.0020
	11-15	0.0015	0.0015	0.0011	0.0011	0.0011	0.0011	0.0011	0.0011	0.0015	0.0015

Table B.14 20-storey building in Vancouver

Storey	Fibre	1	2	3	4	5	6	7	8	9	10
	Xi	0.050	0.150	0.250	0.663	1.388	2.113	2.838	3.563	4.288	5.013
Ag	Ac+As	0.3545	0.3500	0.3545	0.2175	0.2175	0.2175	0.2175	0.2175	0.2175	0.2175
As	1-8	0.0050	0.0002	0.0050	0.0005	0.0005	0.0005	0.0005	0.0005	0.0005	0.0005
	9-10	0.0042	0.0002	0.0042	0.0005	0.0005	0.0005	0.0005	0.0005	0.0005	0.0005
	11-14	0.0036	0.0002	0.0036	0.0005	0.0005	0.0005	0.0005	0.0005	0.0005	0.0005
	15-20	0.0031	0.0002	0.0031	0.0005	0.0005	0.0005	0.0005	0.0005	0.0005	0.0005

Storey	Fibre	11	12	13	14	15	16	17	18
	Xi	5.738	6.463	7.188	7.913	8.638	9.050	9.150	9.250
Ag	Ac+As	0.2175	0.2175	0.2175	0.2175	0.2175	0.3545	0.3500	0.3545
As	1-8	0.0005	0.0005	0.0005	0.0005	0.0005	0.0050	0.0002	0.0050
	9-10	0.0005	0.0005	0.0005	0.0005	0.0005	0.0042	0.0002	0.0042
	11-14	0.0005	0.0005	0.0005	0.0005	0.0005	0.0036	0.0002	0.0036
	15-20	0.0005	0.0005	0.0005	0.0005	0.0005	0.0031	0.0002	0.0031

Table B.15 25-storey building in Vancouver

Storey	Fibre	1	2	3	4	5	6	7	8	9	10
	Xi	0.050	0.150	0.250	0.733	1.600	2.466	3.333	4.200	5.067	5.933
Ag	Ac+As	0.4000	0.4000	0.4000	0.2600	0.2600	0.2600	0.2600	0.2600	0.2600	0.2600
As	1-8	0.0058	0.0002	0.0058	0.0006	0.0006	0.0006	0.0006	0.0006	0.0006	0.0006
	9-10	0.0048	0.0002	0.0048	0.0006	0.0006	0.0006	0.0006	0.0006	0.0006	0.0006
	11-14	0.0041	0.0002	0.0041	0.0006	0.0006	0.0006	0.0006	0.0006	0.0006	0.0006
	15-25	0.0039	0.0002	0.0039	0.0006	0.0006	0.0006	0.0006	0.0006	0.0006	0.0006

Storey	Fibre	11	12	13	14	15	16	17	18
	Xi	6.800	7.667	8.533	9.399	10.267	10.750	10.850	10.950
Ag	Ac+As	0.2600	0.2600	0.2600	0.2600	0.2600	0.4000	0.4000	0.4000
As	1-8	0.0006	0.0006	0.0006	0.0006	0.0006	0.0058	0.0002	0.0058
	9-10	0.0006	0.0006	0.0006	0.0006	0.0006	0.0048	0.0002	0.0048
	11-14	0.0006	0.0006	0.0006	0.0006	0.0006	0.0041	0.0002	0.0041
	15-25	0.0006	0.0006	0.0006	0.0006	0.0006	0.0039	0.0002	0.0039

Table B.16 5-storey building in Montreal

Storey	Fibre	1	2	3	4	5	6	7	8	9	10
	Xi	0.100	0.300	0.667	1.200	1.733	2.267	2.800	3.333	3.700	3.900
Ag	Ac+As	0.0800	0.0800	0.1067	0.1067	0.1067	0.1067	0.1067	0.1067	0.0800	0.0800
As	1	0.0020	0.0020	0.0005	0.0005	0.0005	0.0005	0.0005	0.0005	0.0020	0.0020
	2	0.0020	0.0020	0.0005	0.0005	0.0005	0.0005	0.0005	0.0005	0.0020	0.0020
	3	0.0010	0.0010	0.0004	0.0004	0.0004	0.0004	0.0004	0.0004	0.0010	0.0010
	4	0.0006	0.0006	0.0004	0.0004	0.0004	0.0004	0.0004	0.0004	0.0006	0.0006
	5	0.0006	0.0006	0.0003	0.0003	0.0003	0.0003	0.0003	0.0003	0.0006	0.0006

Table B.17 10-storey building in Montreal

Storey	Fibre	1	2	3	4	5	6	7	8	9	10
	Xi	0.1125	0.338	0.929	1.888	2.846	3.804	4.763	5.721	6.313	6.538
Ag	Ac+As	0.1013	0.1013	0.1917	0.1917	0.1917	0.1917	0.1917	0.1917	0.1013	0.1013
As	1	0.0010	0.0010	0.0008	0.0008	0.0008	0.0008	0.0008	0.0008	0.0010	0.0010
	2	0.0010	0.0010	0.0008	0.0008	0.0008	0.0008	0.0008	0.0008	0.0010	0.0010
	3	0.0006	0.0006	0.0005	0.0005	0.0005	0.0005	0.0005	0.0005	0.0006	0.0006
	4	0.0006	0.0006	0.0005	0.0005	0.0005	0.0005	0.0005	0.0005	0.0006	0.0006
	5	0.0006	0.0006	0.0005	0.0005	0.0005	0.0005	0.0005	0.0005	0.0006	0.0006
	6	0.0006	0.0006	0.0005	0.0005	0.0005	0.0005	0.0005	0.0005	0.0006	0.0006
	7	0.0006	0.0006	0.0005	0.0005	0.0005	0.0005	0.0005	0.0005	0.0006	0.0006
	8	0.0006	0.0006	0.0005	0.0005	0.0005	0.0005	0.0005	0.0005	0.0006	0.0006
	9	0.0004	0.0004	0.0005	0.0005	0.0005	0.0005	0.0005	0.0005	0.0004	0.0004
	10	0.0004	0.0004	0.0005	0.0005	0.0005	0.0005	0.0005	0.0005	0.0004	0.0004

Table B.18 15-storey building in Montreal

Storey	Fibre	1	2	3	4	5	6	7	8	9	10
	Xi	0.125	0.375	1.183	2.550	3.917	5.283	6.650	8.017	9.125	9.075
Ag	Ac+As	0.1250	0.1250	0.2733	0.2733	0.2733	0.2733	0.2733	0.2733	0.1250	0.1250
As	1-9	0.0006	0.0006	0.0007	0.0007	0.0007	0.0007	0.0007	0.0007	0.0006	0.0006
	10-15	0.0004	0.0004	0.0007	0.0007	0.0007	0.0007	0.0007	0.0007	0.0004	0.0004

Table B.19 20-storey building in Montreal

Storey	Fibre	1	2	3	4	5	6	7	8	9	10
	Xi	0.050	0.150	0.250	0.608	1.225	1.842	2.458	3.075	3.692	4.308
Ag	Ac+As	0.3000	0.3001	0.3000	0.1845	0.1845	0.1845	0.1845	0.1845	0.1845	0.1845
As	1-20	0.0017	0.0001	0.0017	0.0005	0.0005	0.0005	0.0005	0.0005	0.0005	0.0005

Storey	Fibre	11	12	13	14	15	16	17	18
	Xi	4.925	5.542	6.158	6.775	7.392	7.750	7.850	7.950
Ag	Ac+As	0.1845	0.1845	0.1845	0.1845	0.1845	0.3000	0.3001	0.3000
As	1-20	0.0005	0.0005	0.0005	0.0005	0.0005	0.0017	0.0001	0.0017

Table B.20 25-storey building in Montreal

Storey	Fibre	1	2	3	4	5	6	7	8	9	10
	Xi	0.050	0.150	0.250	0.671	1.413	2.154	2.896	3.638	4.379	5.121
Ag	Ac+As	0.3002	0.3001	0.3002	0.2225	0.2225	0.2225	0.2225	0.2225	0.2225	0.2225
As	1-25	0.0019	0.0001	0.0019	0.0006	0.0006	0.0006	0.0006	0.0006	0.0006	0.0006

Storey	Fibre	11	12	13	14	15	16	17	18
	Xi	5.863	6.604	7.346	8.088	8.829	9.050	9.150	9.250
Ag	Ac+As	0.2225	0.2225	0.2225	0.2225	0.2225	0.3002	0.3001	0.3002
As	1-25	0.0006	0.0006	0.0006	0.0006	0.0006	0.0019	0.0001	0.0019

Appendix C – Results from nonlinear analysis

The following figures present the nonlinear dynamic analysis results obtained with the "Bar" and "Wall" elements. They also show the 50th and 84th percentile of the values of interest. The code limit for inter-storey drift is presented assuming 2.5% storey drift at every level.. In the moment diagrams for both models, the yielding moment value that is shown has been calculated according to the proposed bi-linear moment-curvature approximation, as explained in Chapter 4. The shear force diagrams show the design forces calculated according to NBCC 2005 and CSA A23.3-04 as well as the factored shear force resistance.

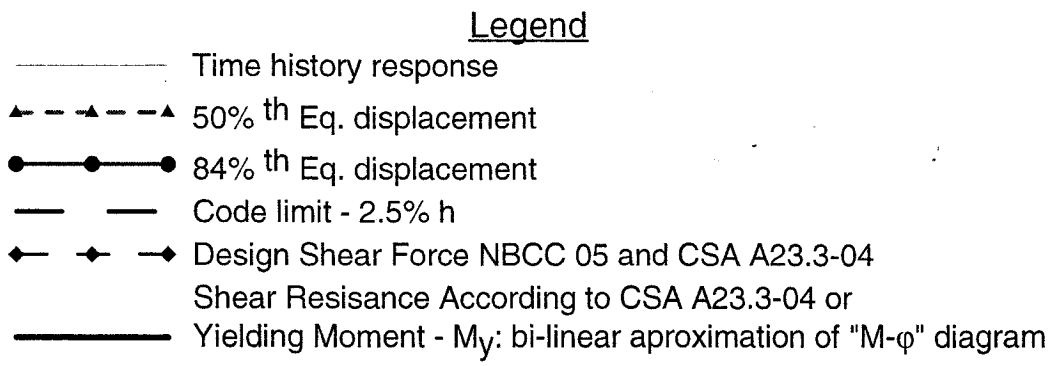

C.1 BAR Element

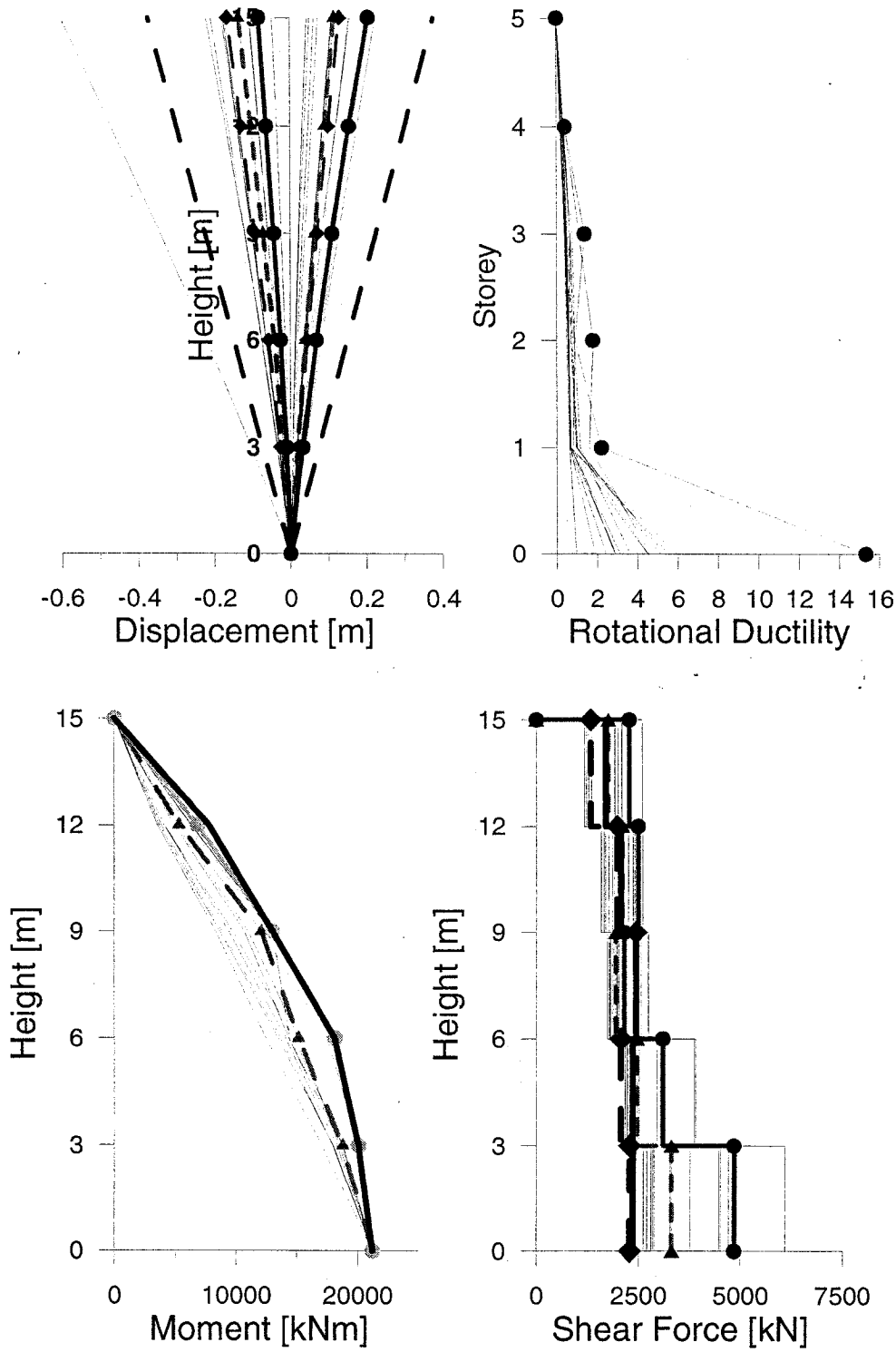

Figure C.1.1: Maximum storey responses 5-storey in Vancouver - "Bar"

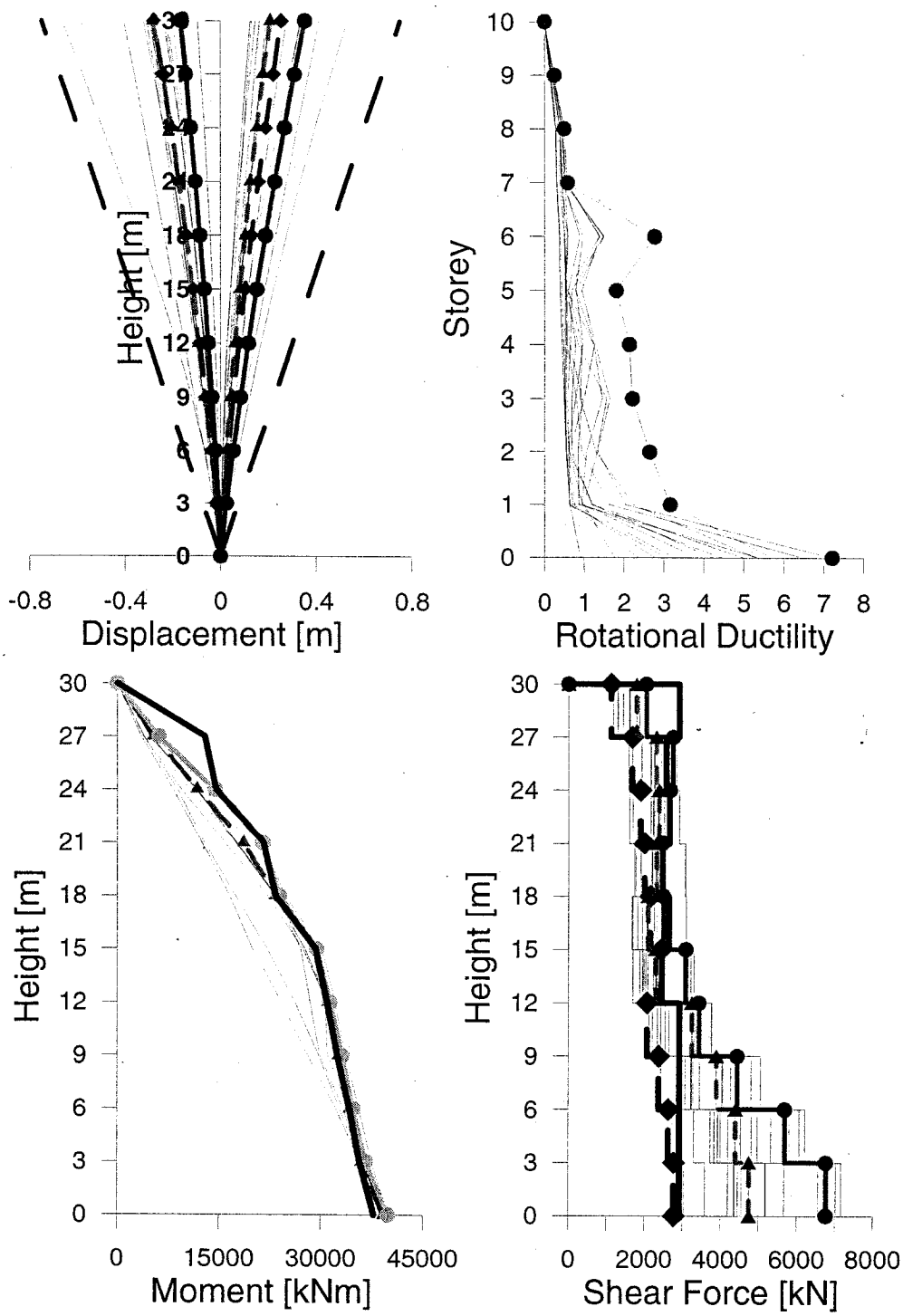

Figure C.1.2: Maximum storey responses 10-storey in Vancouver - "Bar"

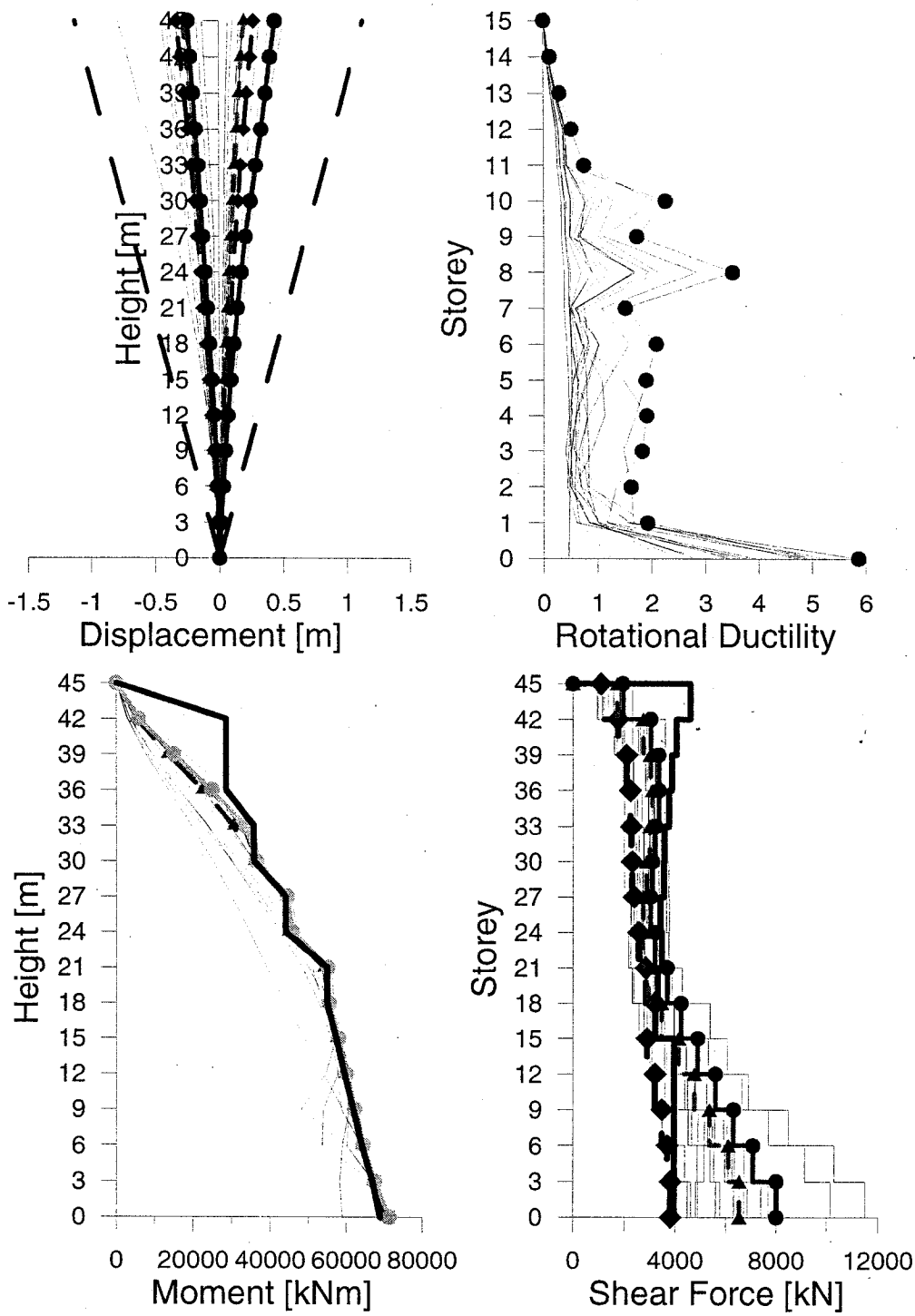

Figure C.1.3: Maximum storey responses 15-storey in Vancouver - "Bar"

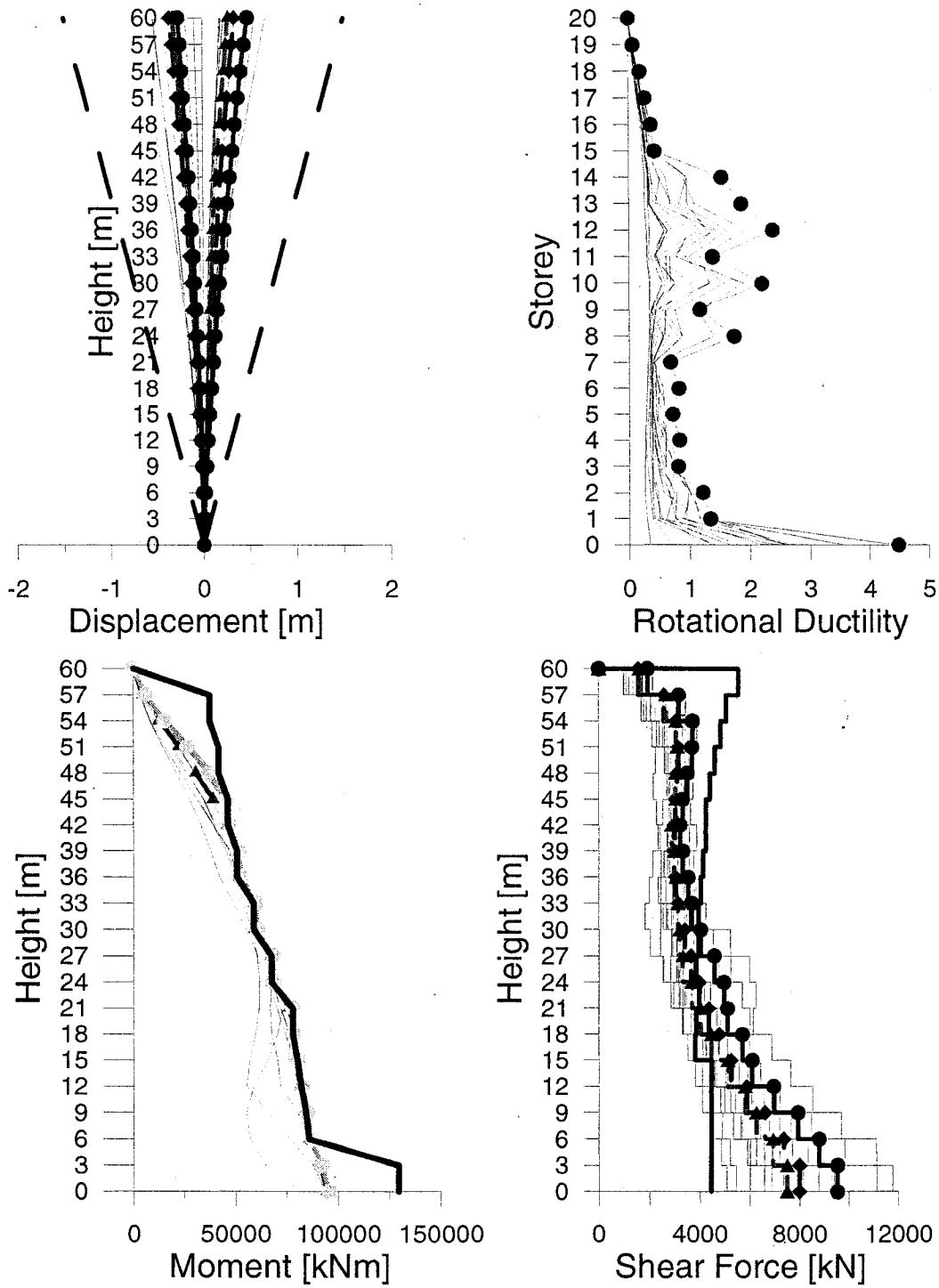

Figure C.1.4: Maximum storey responses 20-storey in Vancouver - "Bar"

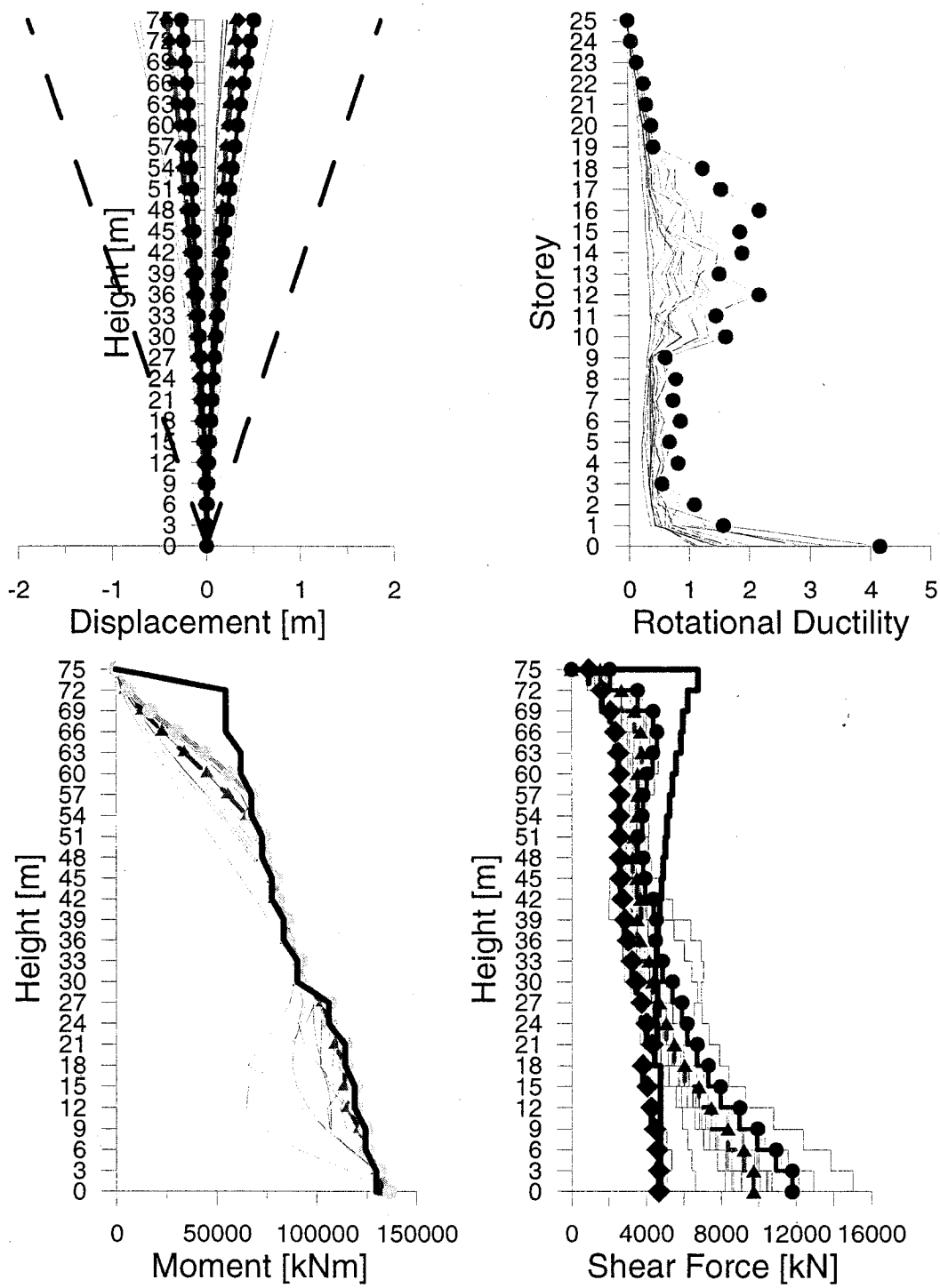

Figure C.1.5: Maximum storey responses 25-storey in Vancouver - "Bar"

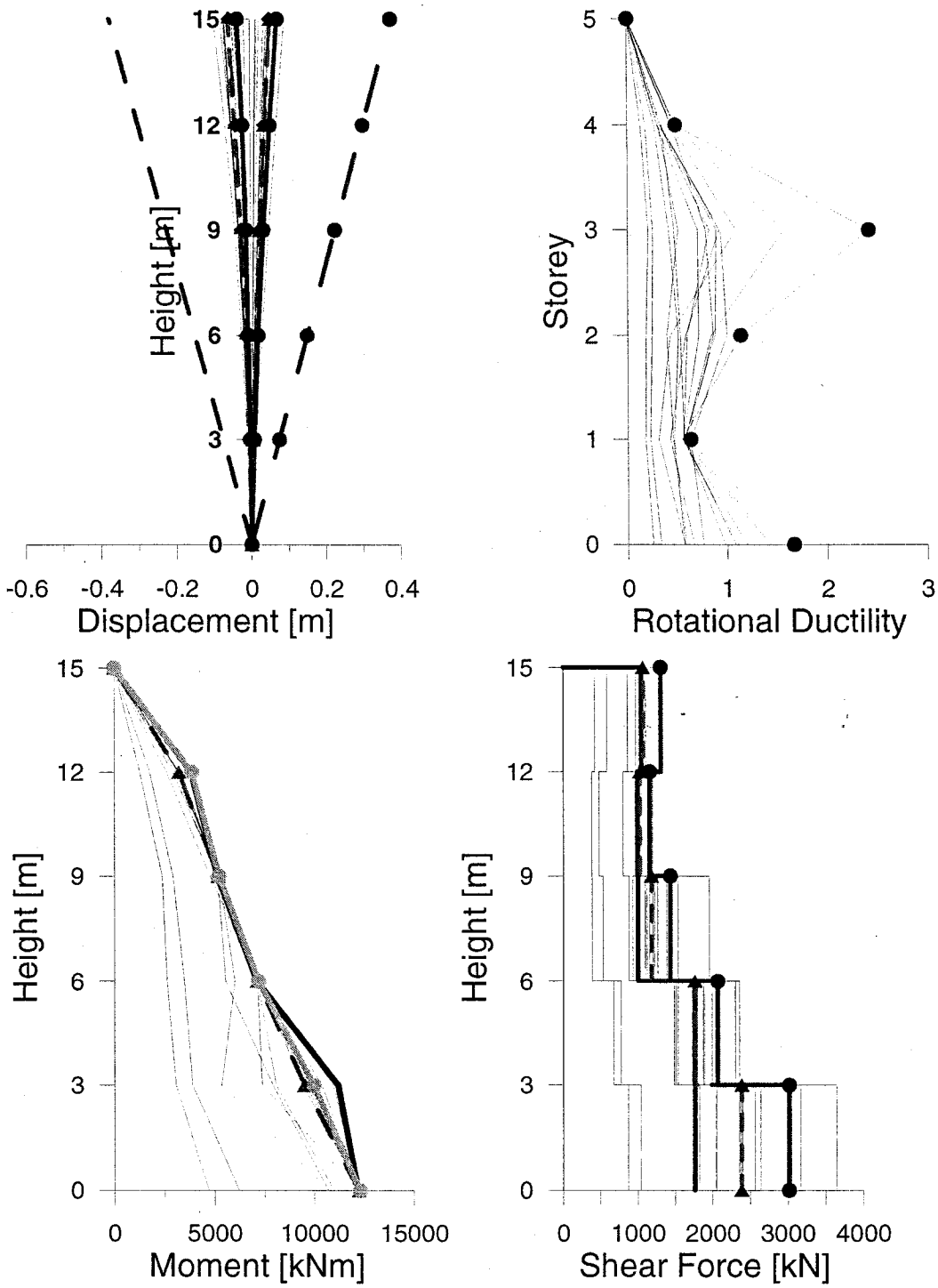

Figure C.1.6: Maximum storey responses 5-storey in Montreal - "Bar"

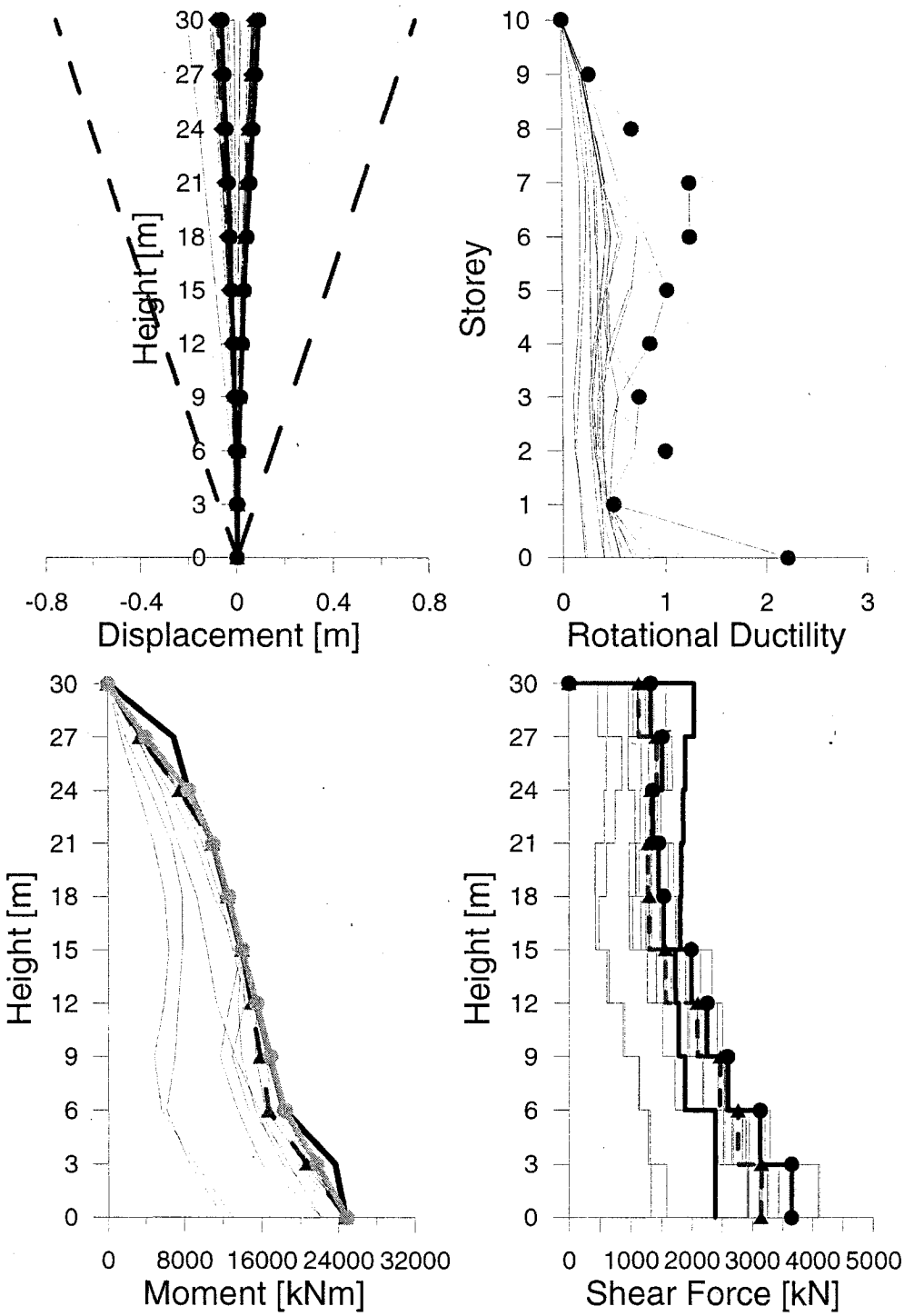

Figure C.1.7: Maximum storey responses 10-storey in Montreal - "Bar"

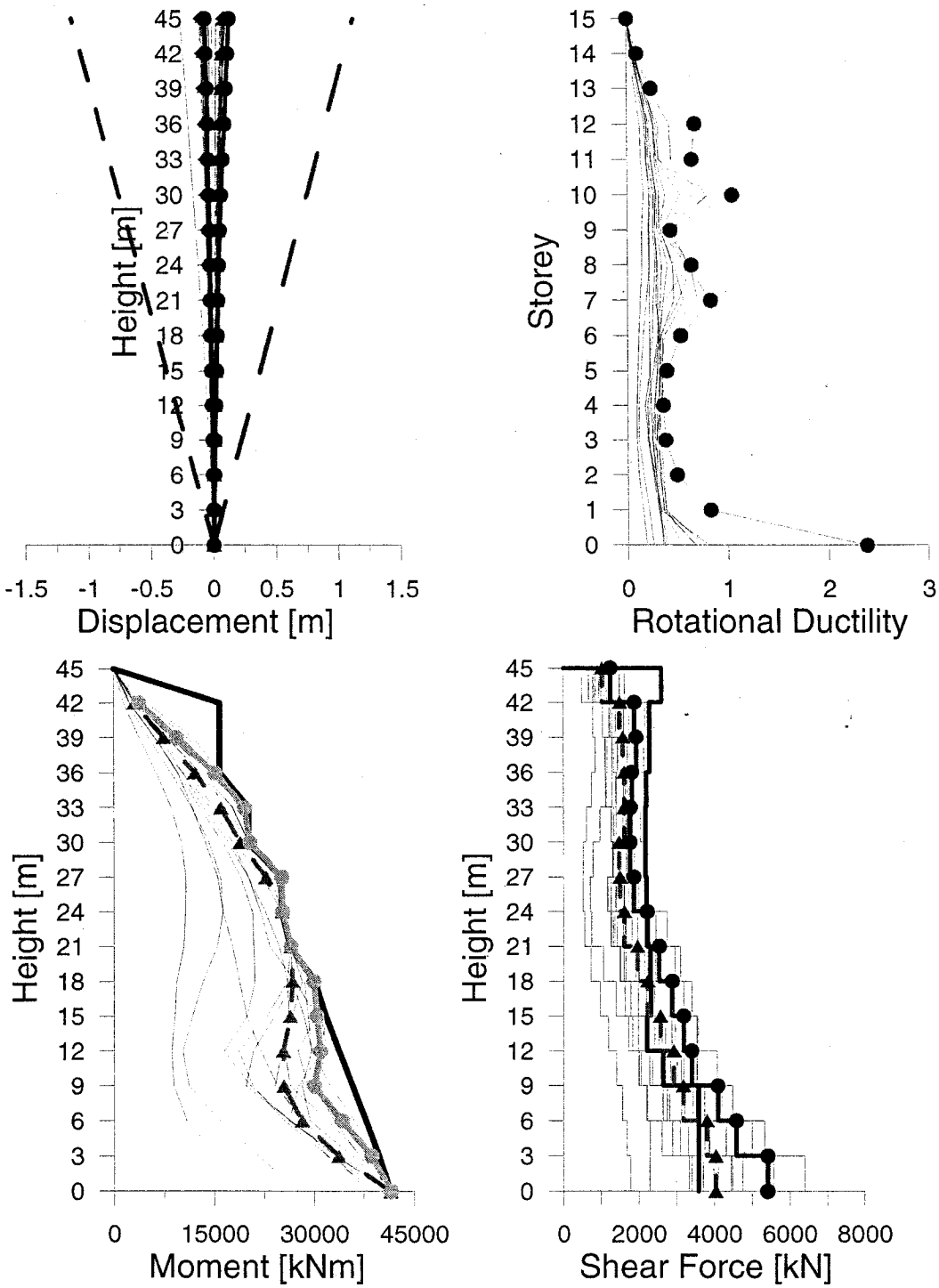

Figure C.1.8: Maximum storey responses 15-storey in Montreal - "Bar"

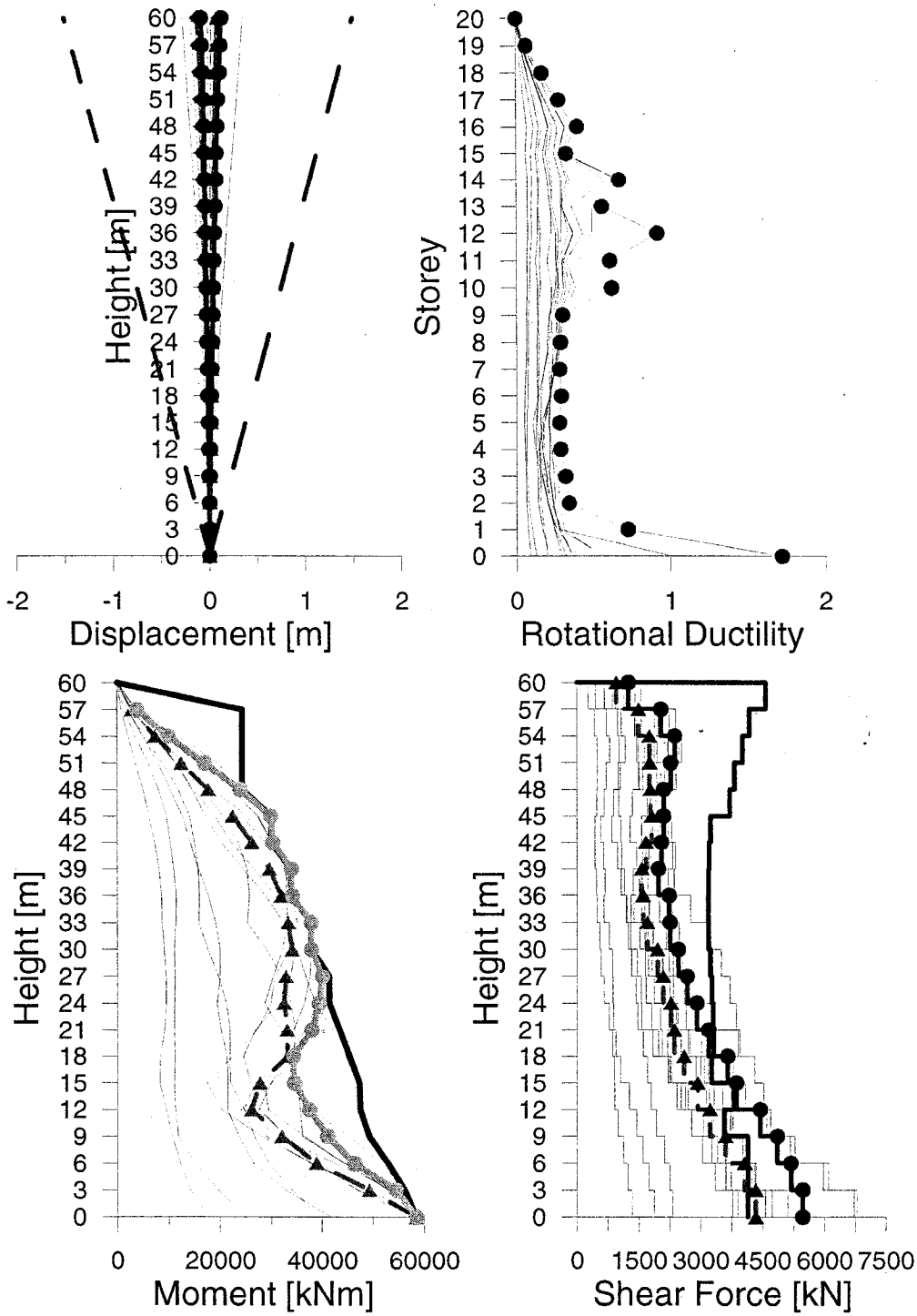

Figure C.1.9: Maximum storey responses 20-storey in Montreal - "Bar"

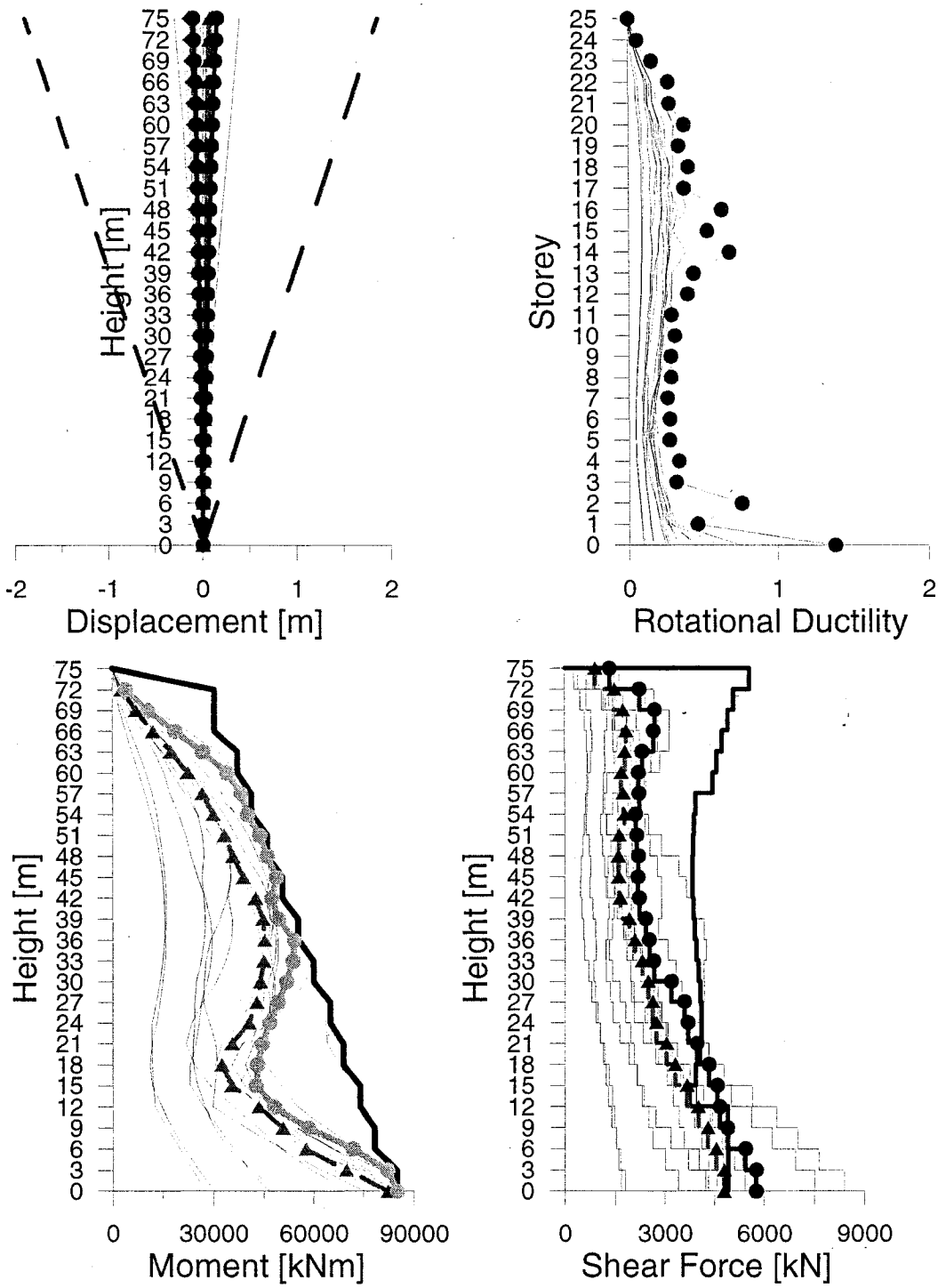

Figure C.1.10: Maximum storey responses 25-storey in Montreal - "Bar"

C.2 WALL Element

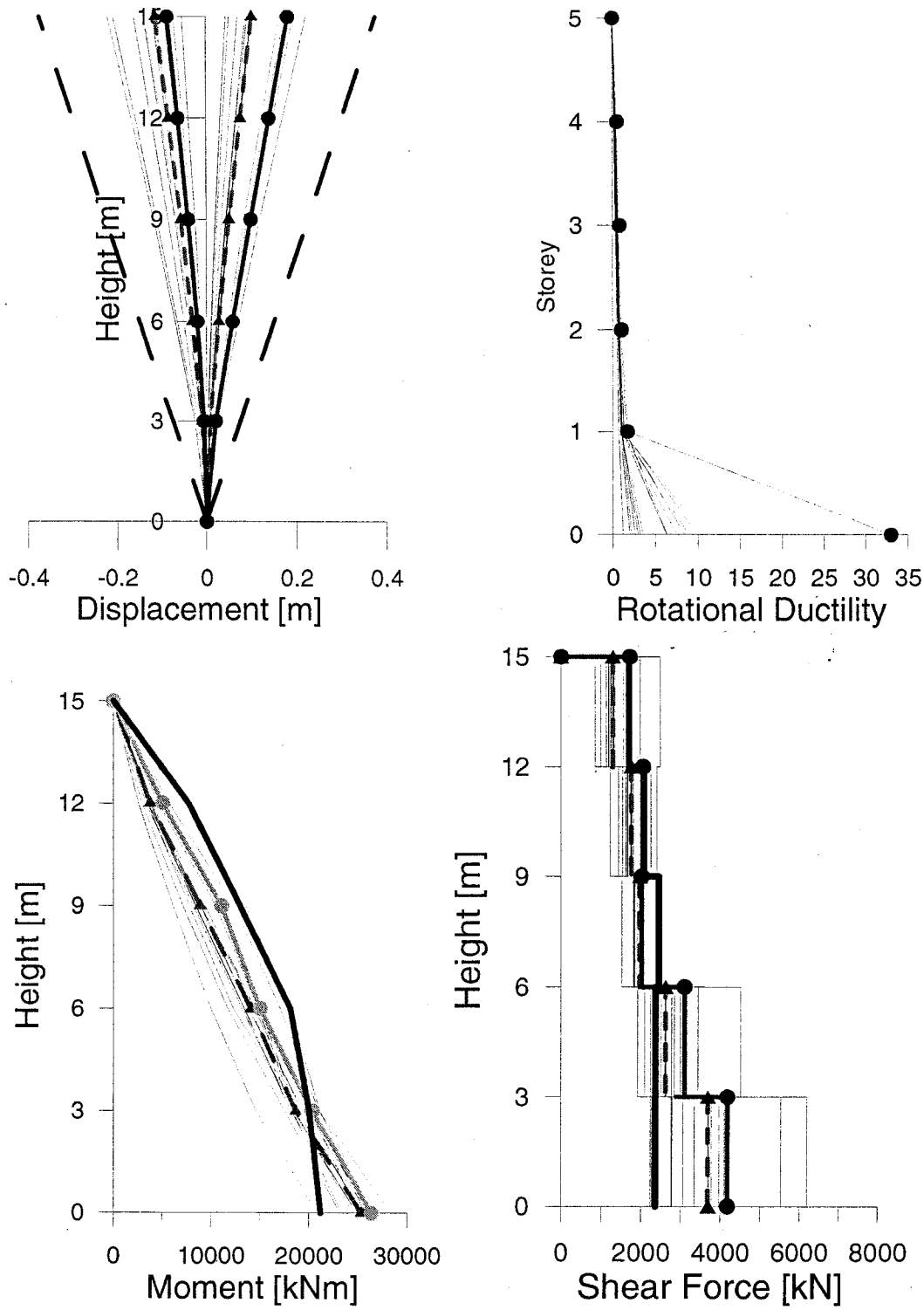

Figure C.2.1: Maximum storey responses 5-storey in Vancouver - "Wall"

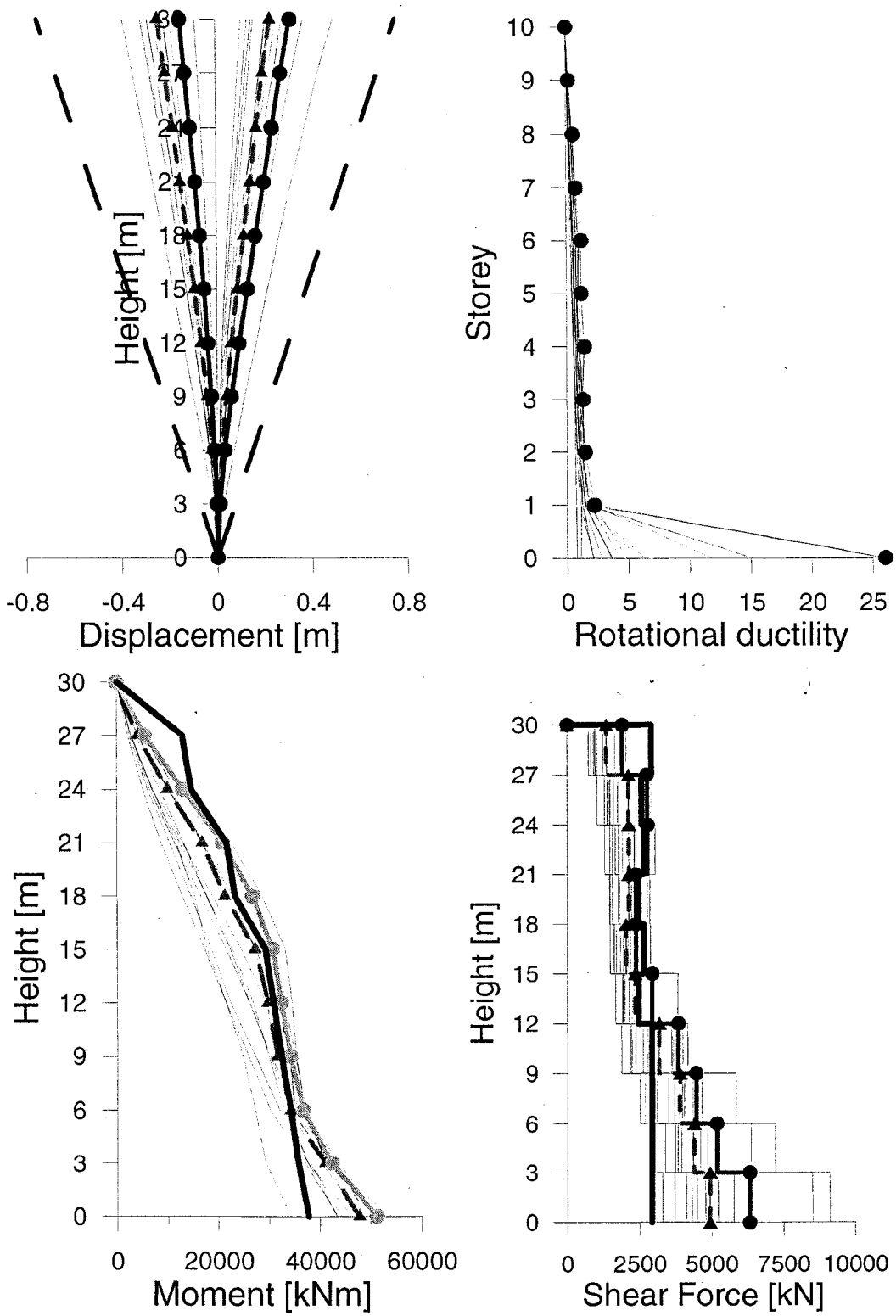

Figure C.2.2: Maximum storey responses 10-storey in Vancouver - "Wall"

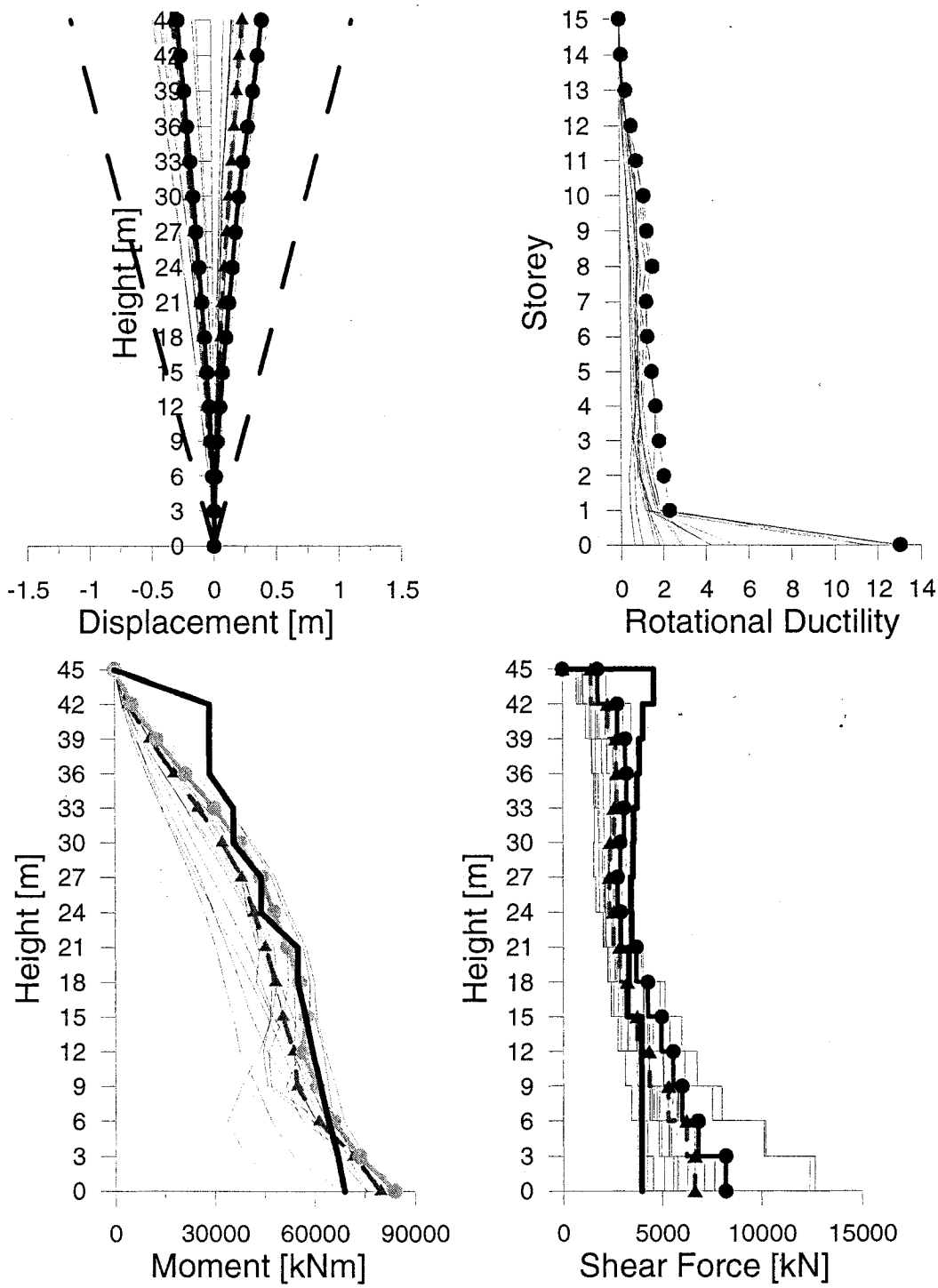

Figure C.2.3: Maximum storey responses 15-storey in Vancouver - "Wall"

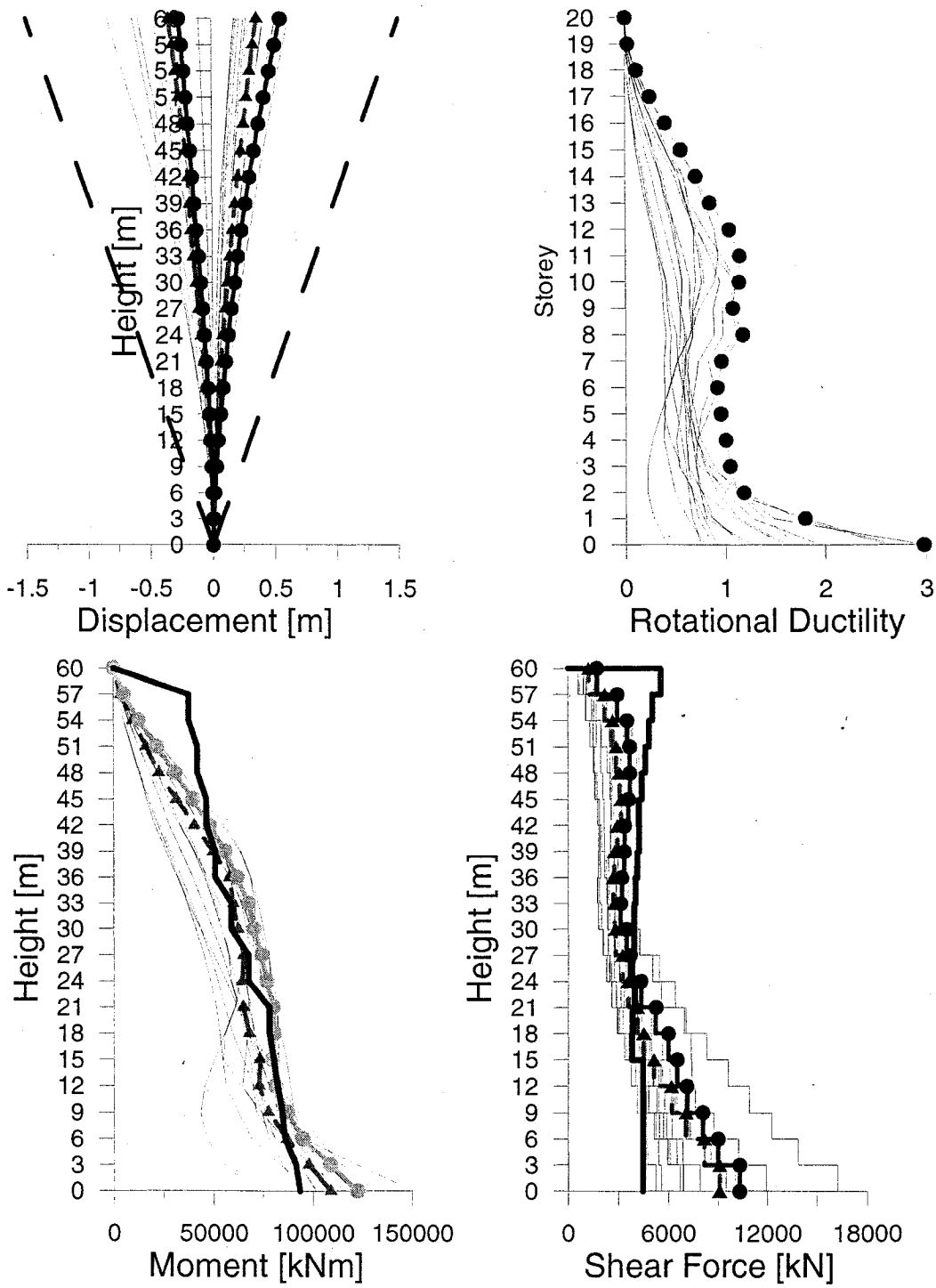

Figure C.2.4: Maximum storey displacement 20-storey in Vancouver - "Wall"

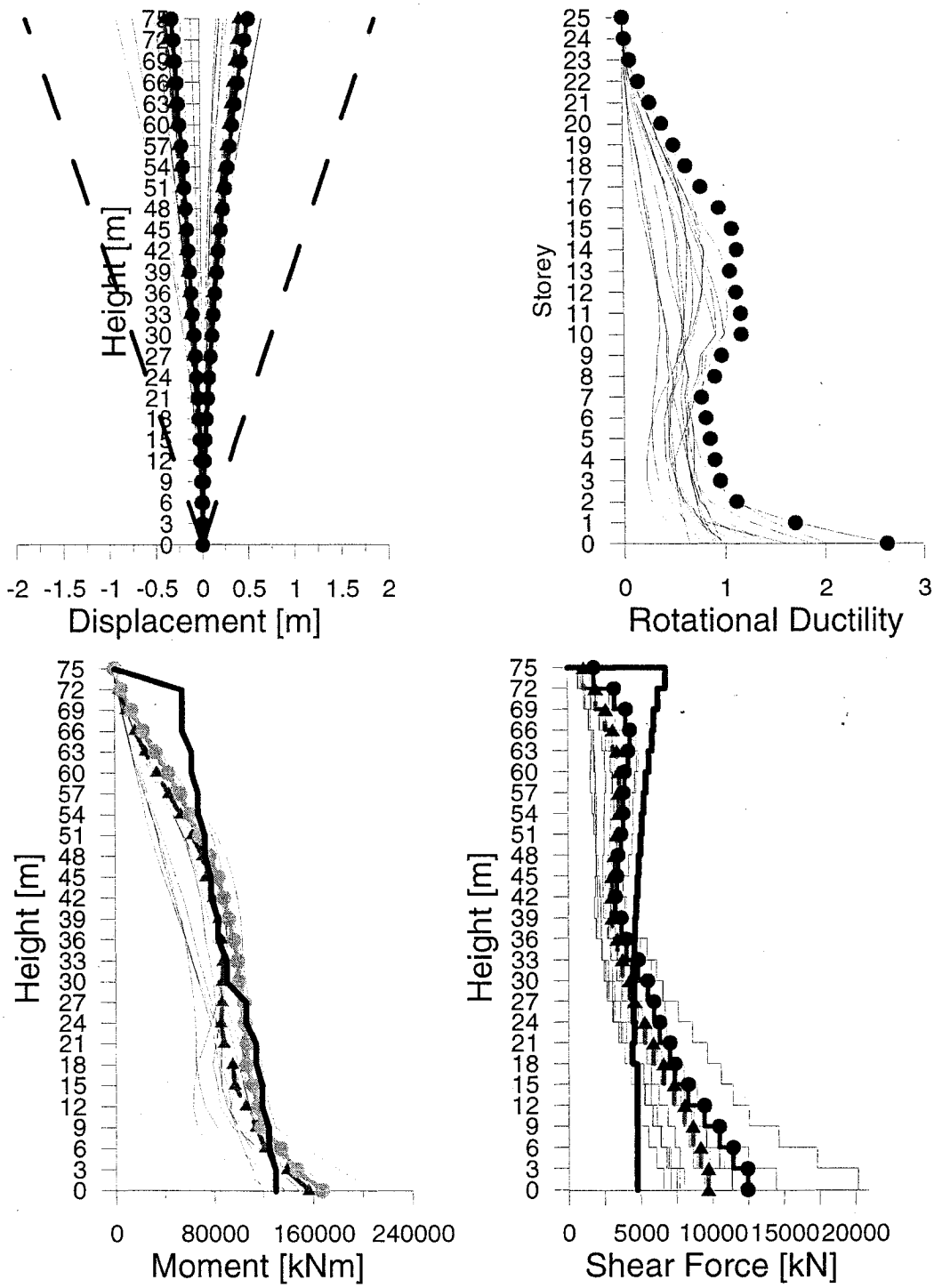

Figure C.2.5: Maximum storey responses 25-storey in Vancouver - "Wall"

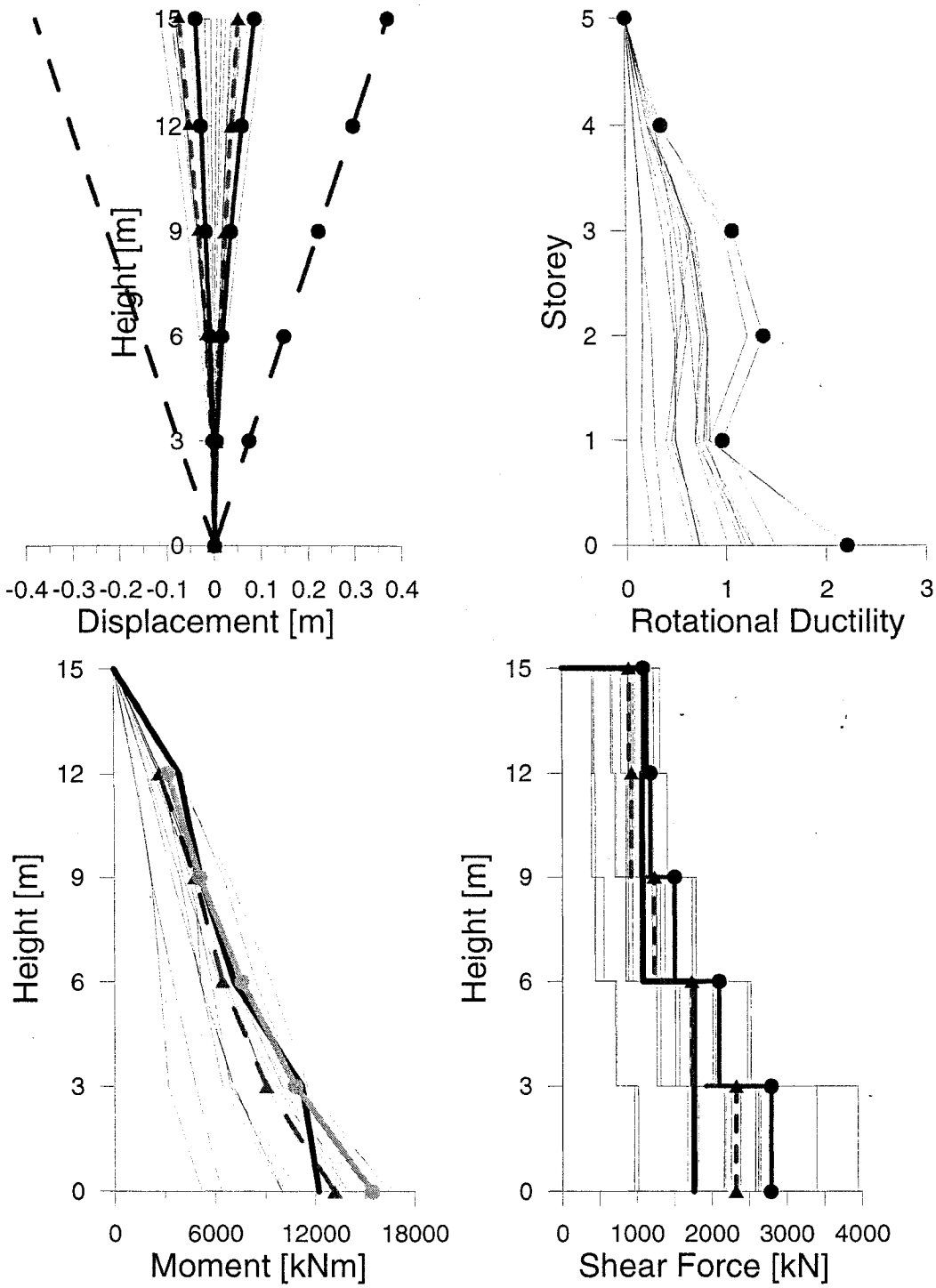

Figure C.2.6: Maximum storey displacement 5-storey in Montreal - "Wall"

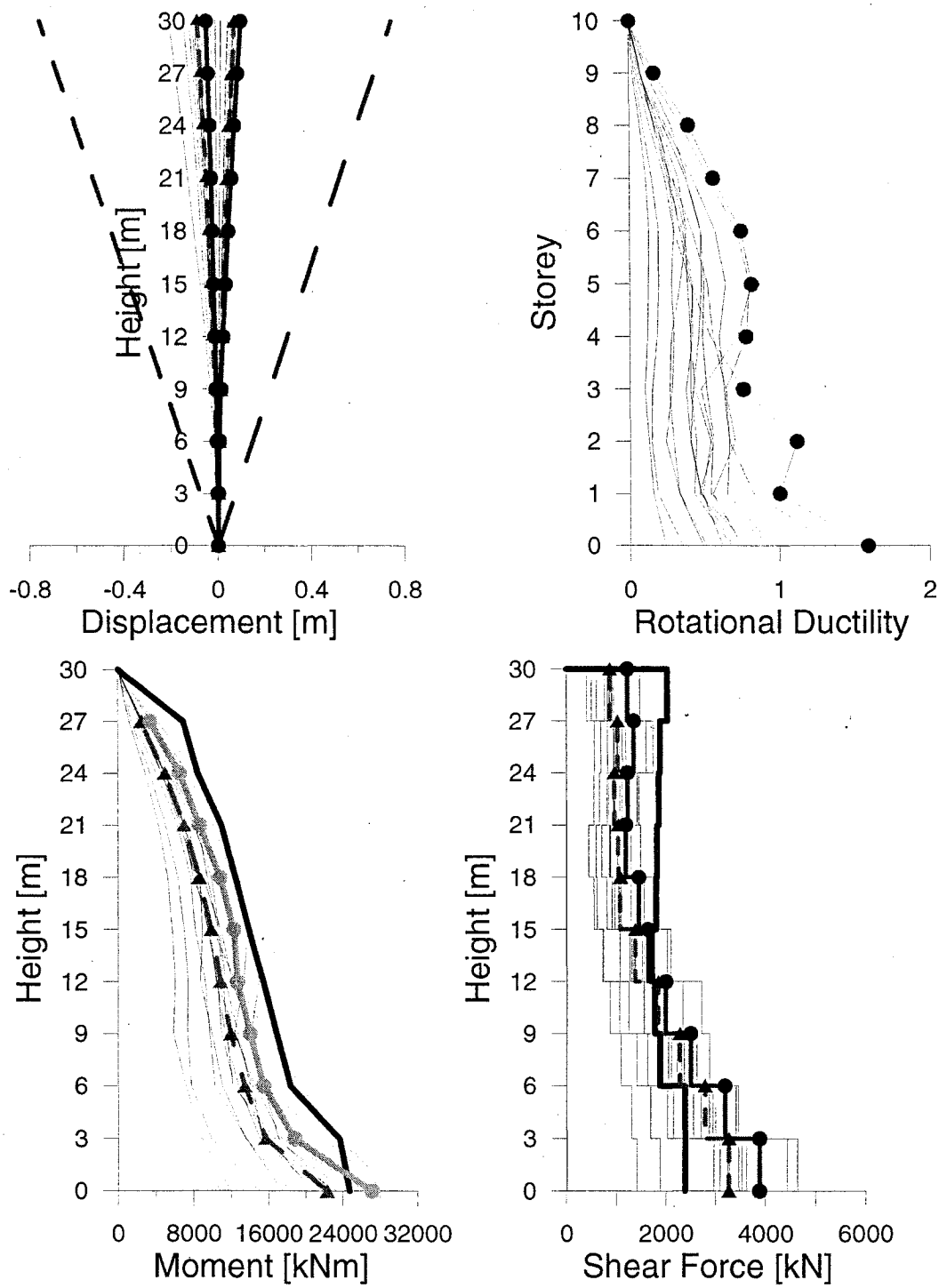

Figure C.2.7: Maximum storey displacement 10-storey in Montreal - "Wall"

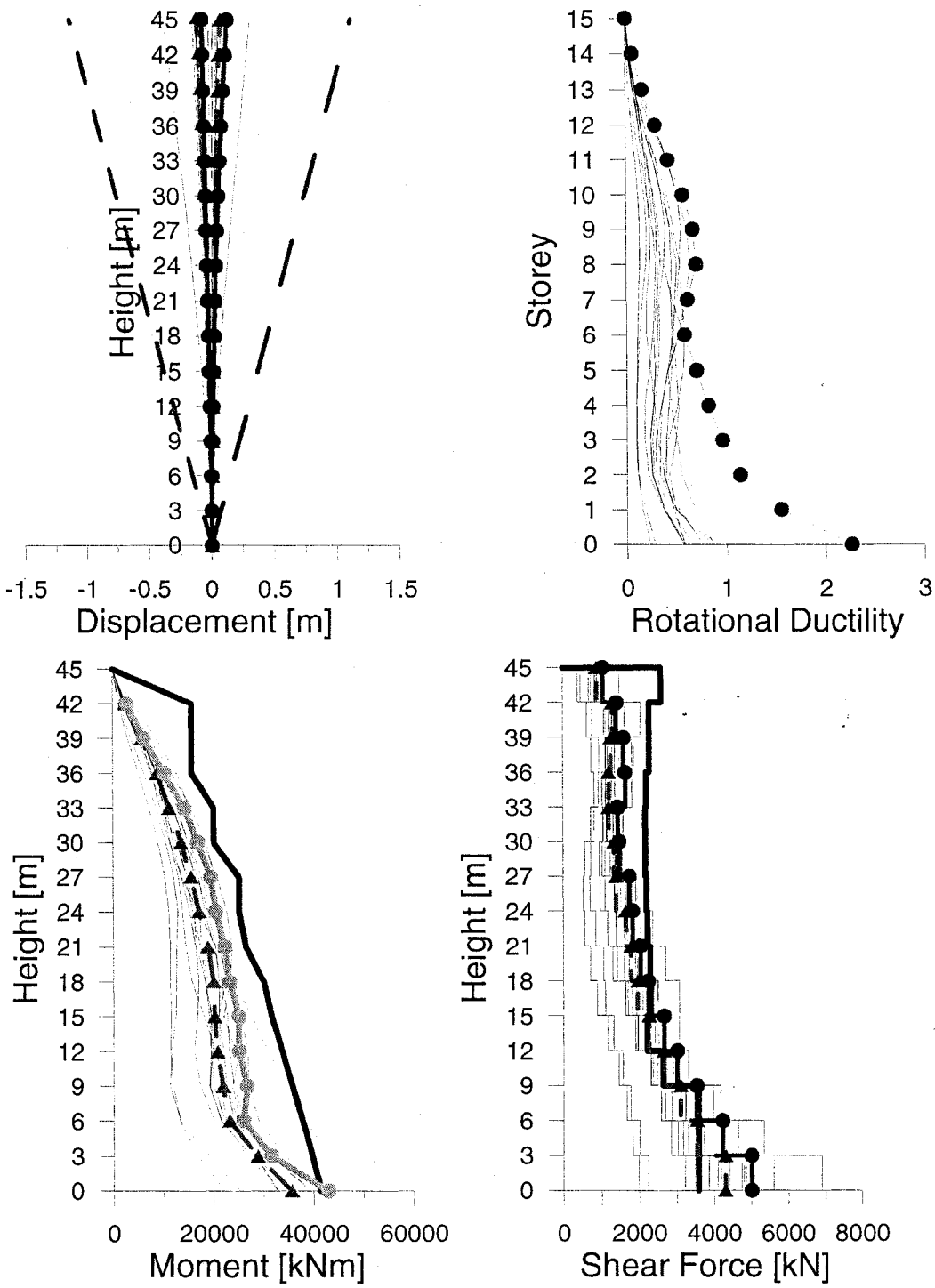

Figure C.2.8: Maximum storey responses 15-storey in Montreal - "Wall"

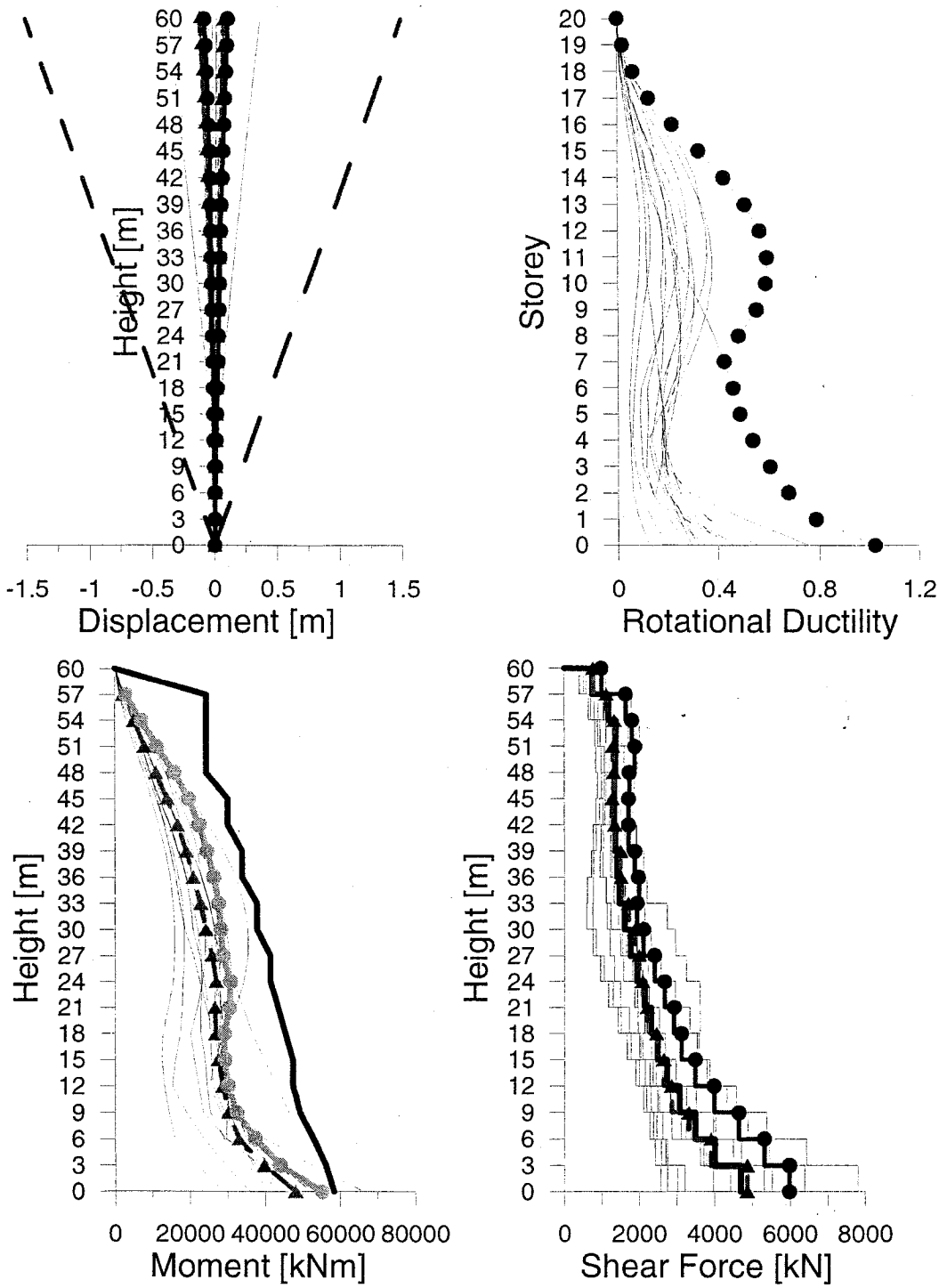

Figure C.2.9: Maximum storey responses 20-storey in Montreal - "Wall"

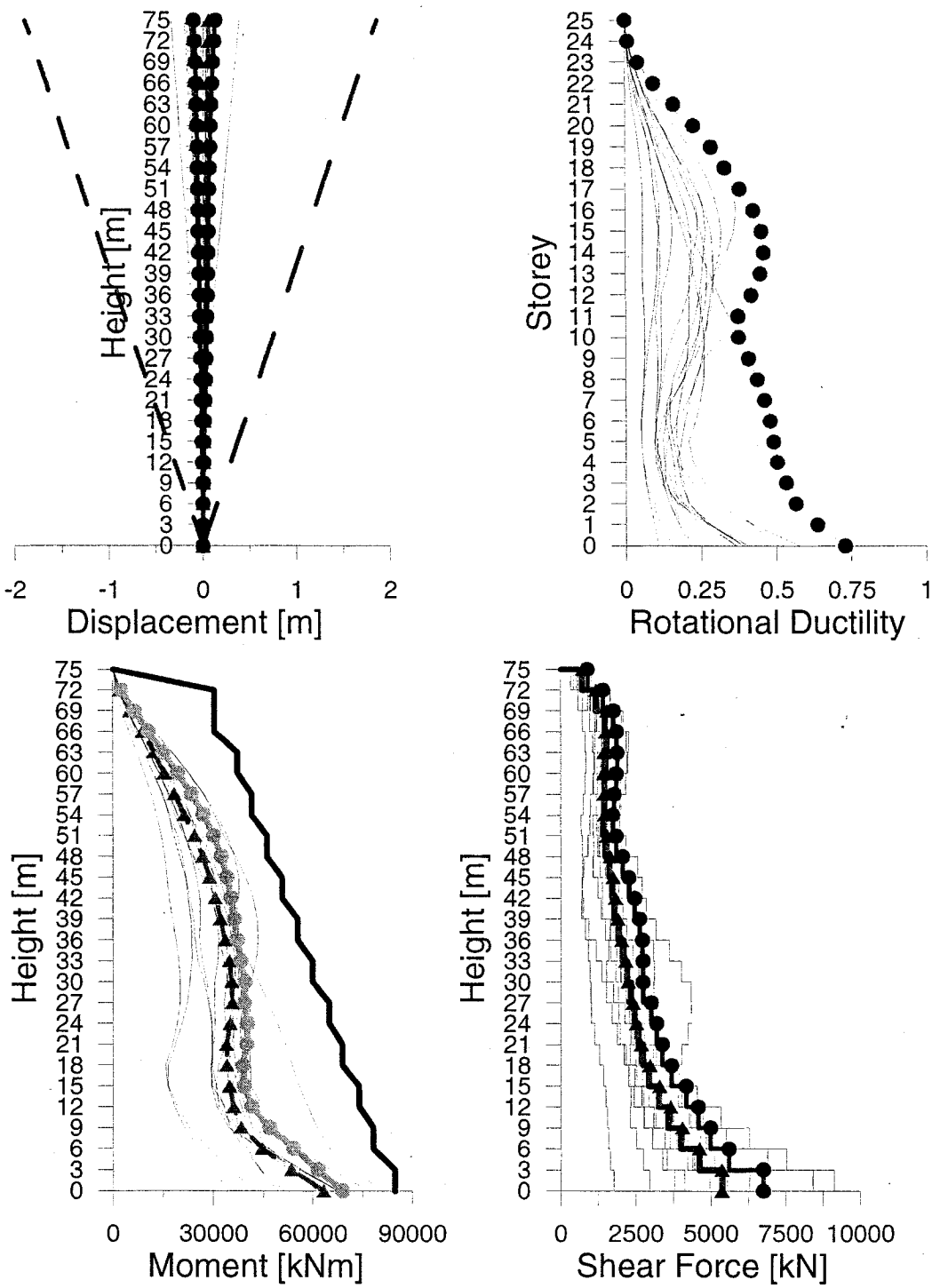

Figure C.2.10: Maximum storey responses 25-storey in Montreal - "Wall"

Appendix D

Ratios of the shear forces from nonlinear dynamic analysis to the shear resistance for the "Bar" and "Wall" elements

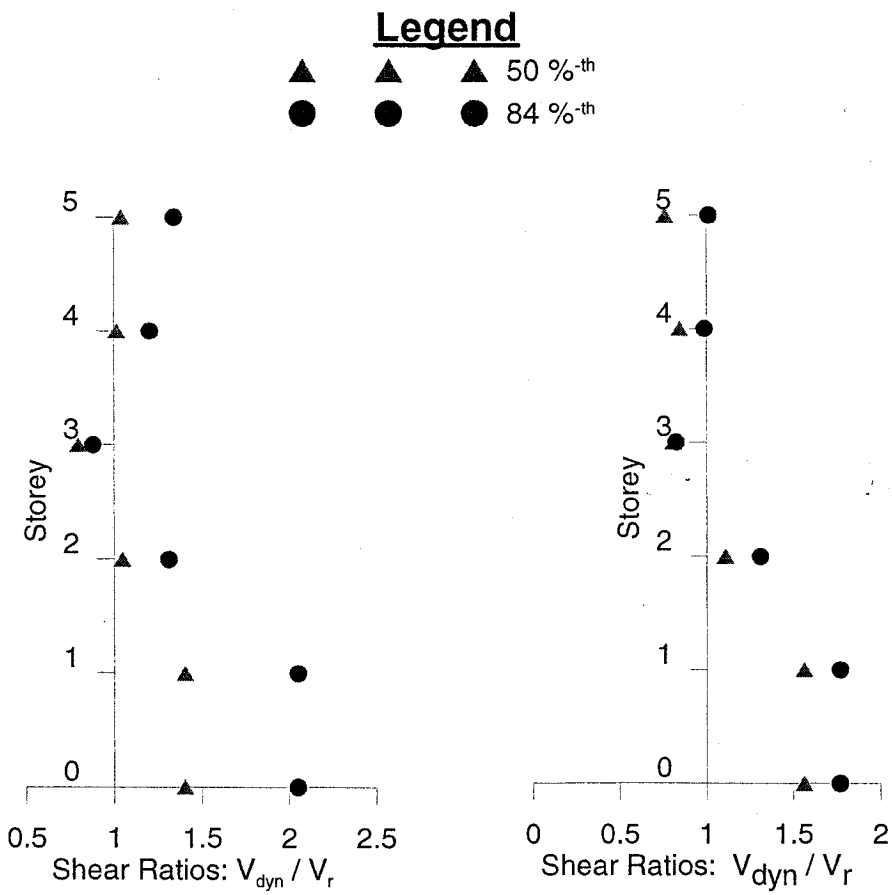

a) Bar element; **b) Wall element**

Figure D.1: Maximum storey shear responses 5-storey in Vancouver

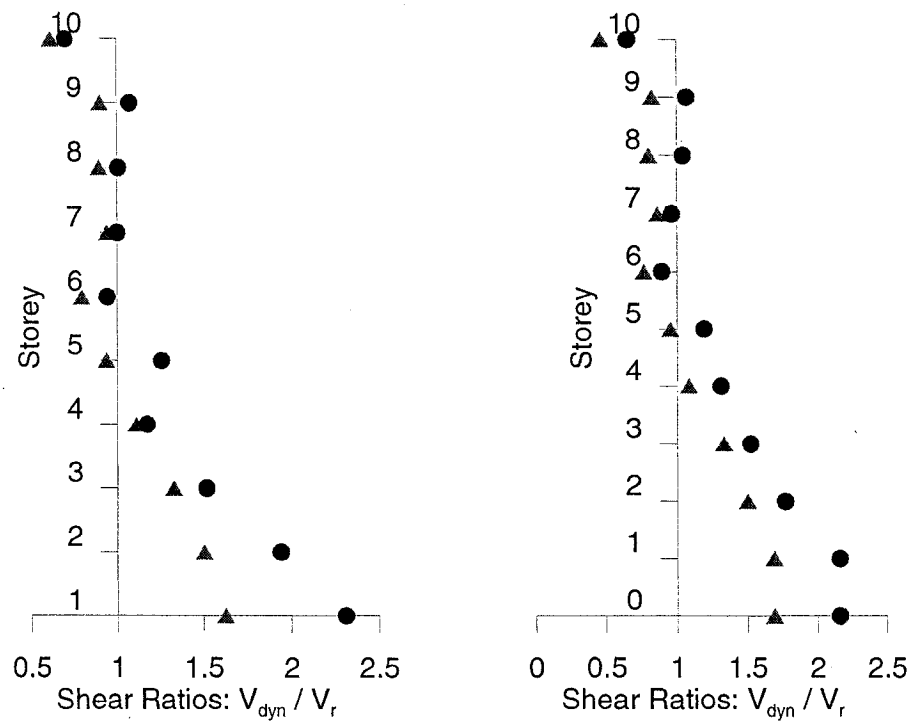

a) Bar element; **b) Wall element**

Figure D.2: Maximum storey shear responses 10-storey in Vancouver

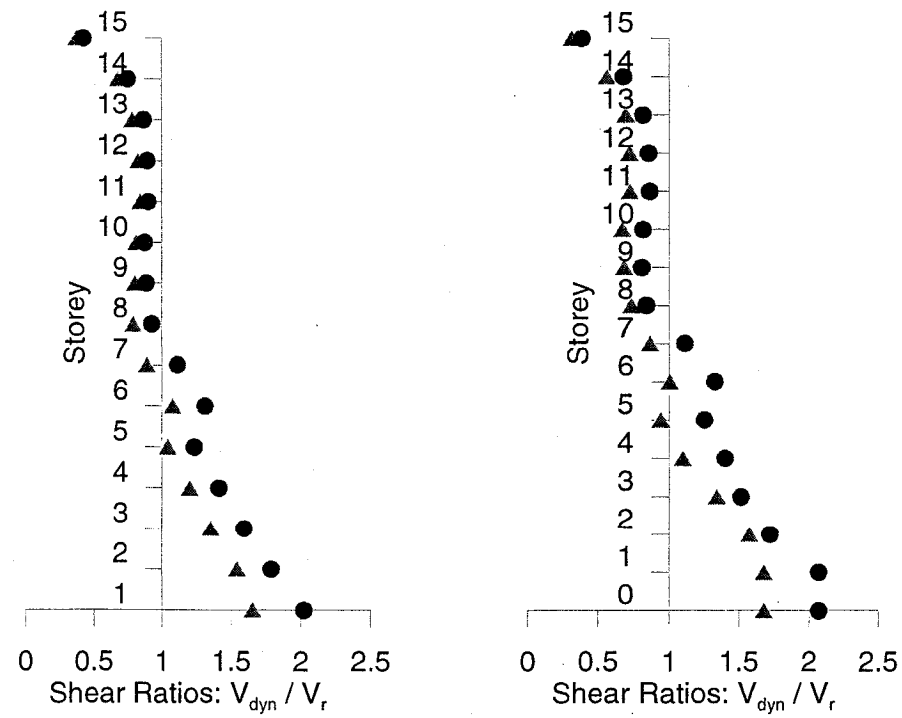

a) Bar element; **b) Wall element**

Figure D.3: Maximum storey shear responses 15-storey in Vancouver

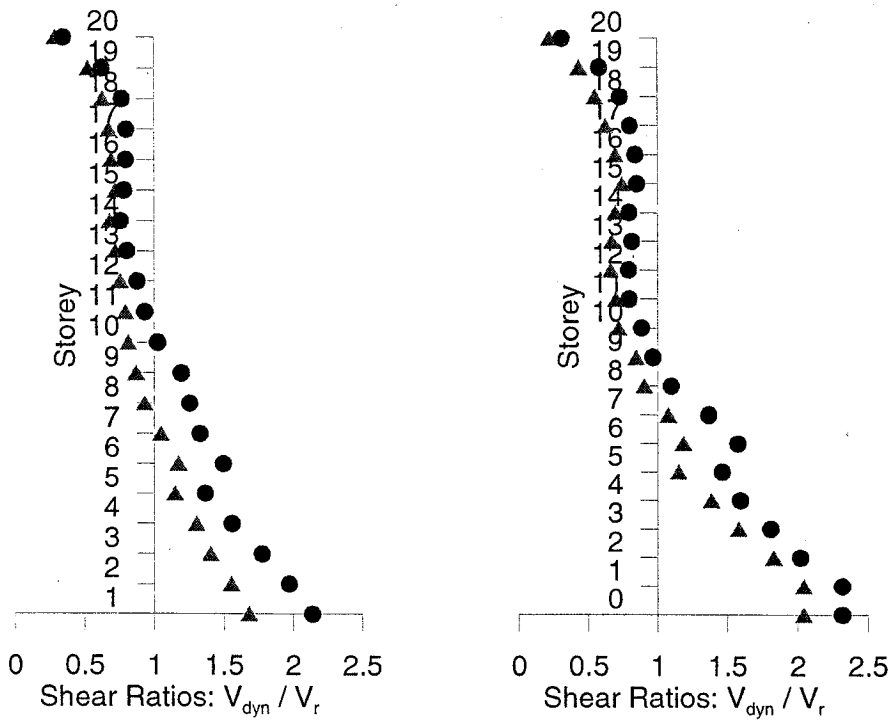

a) Bar element; **b) Wall element**

Figure D.4: Maximum storey shear responses 20-storey in Vancouver

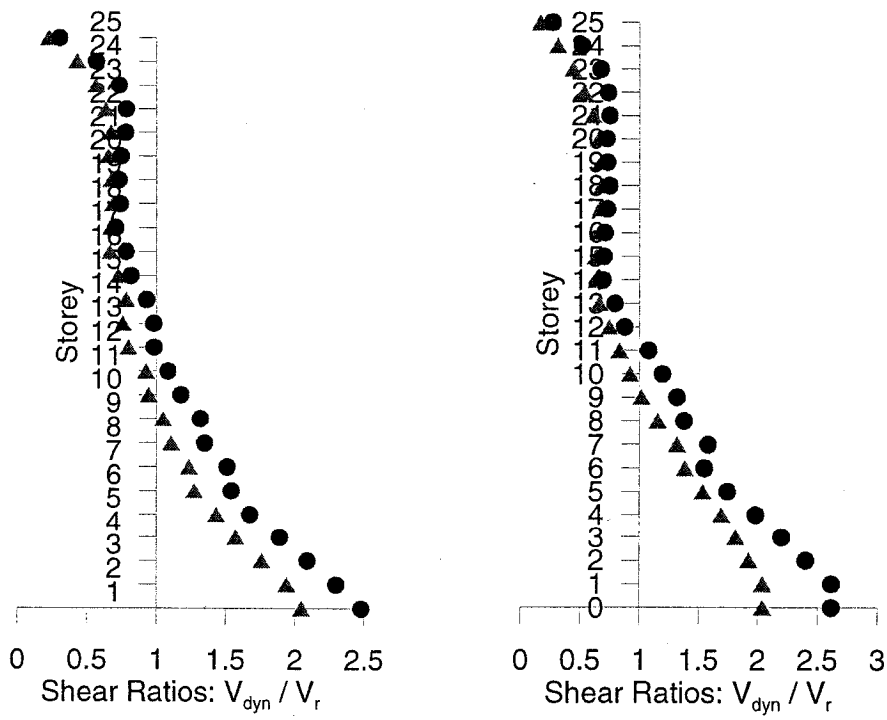

a) Bar element; **b) Wall element**

Figure D.5: Maximum storey shear responses 25-storey in Vancouver

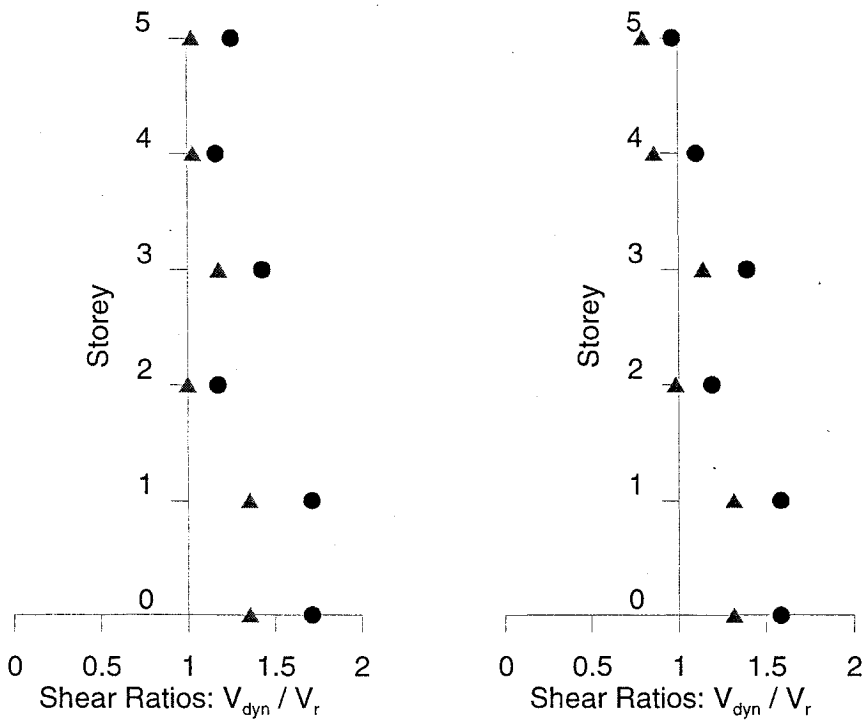

a) Bar element; **b) Wall element**

Figure D.6: Maximum storey shear responses 5-storey in Montreal

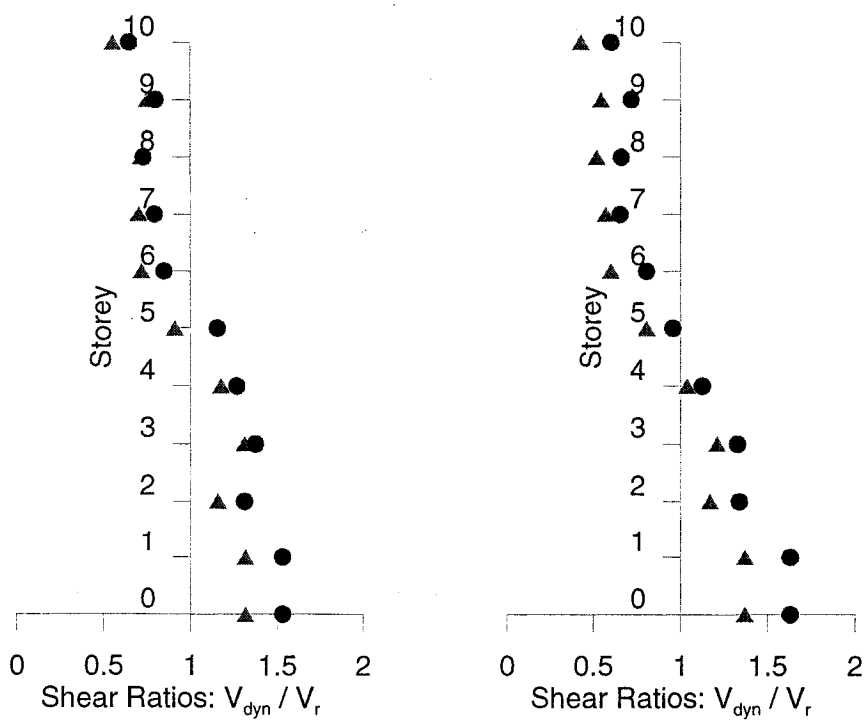

a) Bar element; **b) Wall element**

Figure D.7: Maximum storey shear responses 10-storey in Montreal

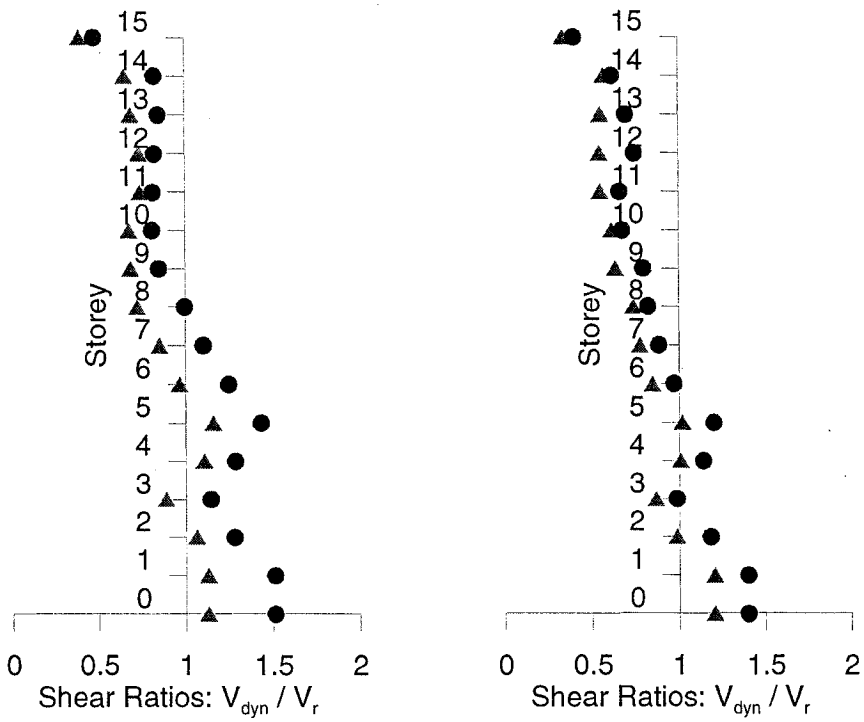

a) Bar element; **b) Wall element**

Figure D.8: Maximum storey shear responses 15-storey in Montreal

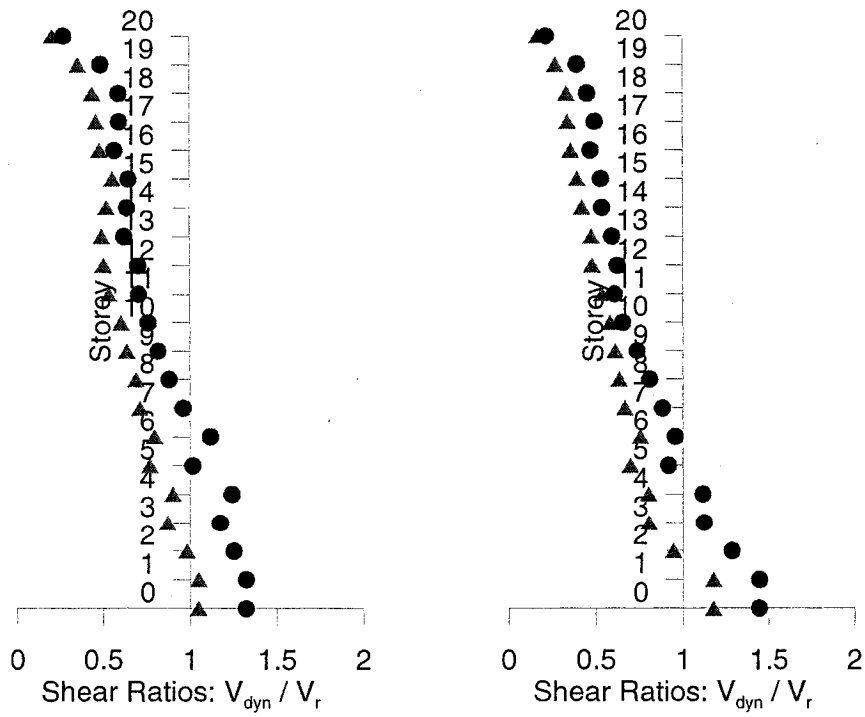

a) Bar element; **b) Wall element**

Figure D.9: Maximum storey shear responses 20-storey in Montreal

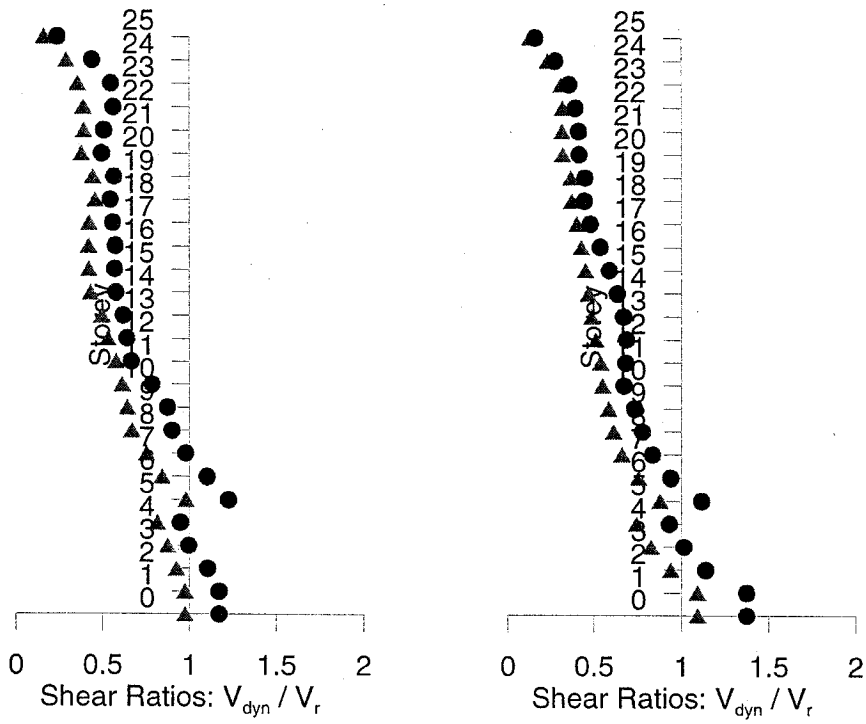

a) Bar element; **b) Wall element**

Figure D.10: Maximum storey shear responses 25-storey in Montreal

Appendix E: Development of "Modified Acceleration Similitude" law

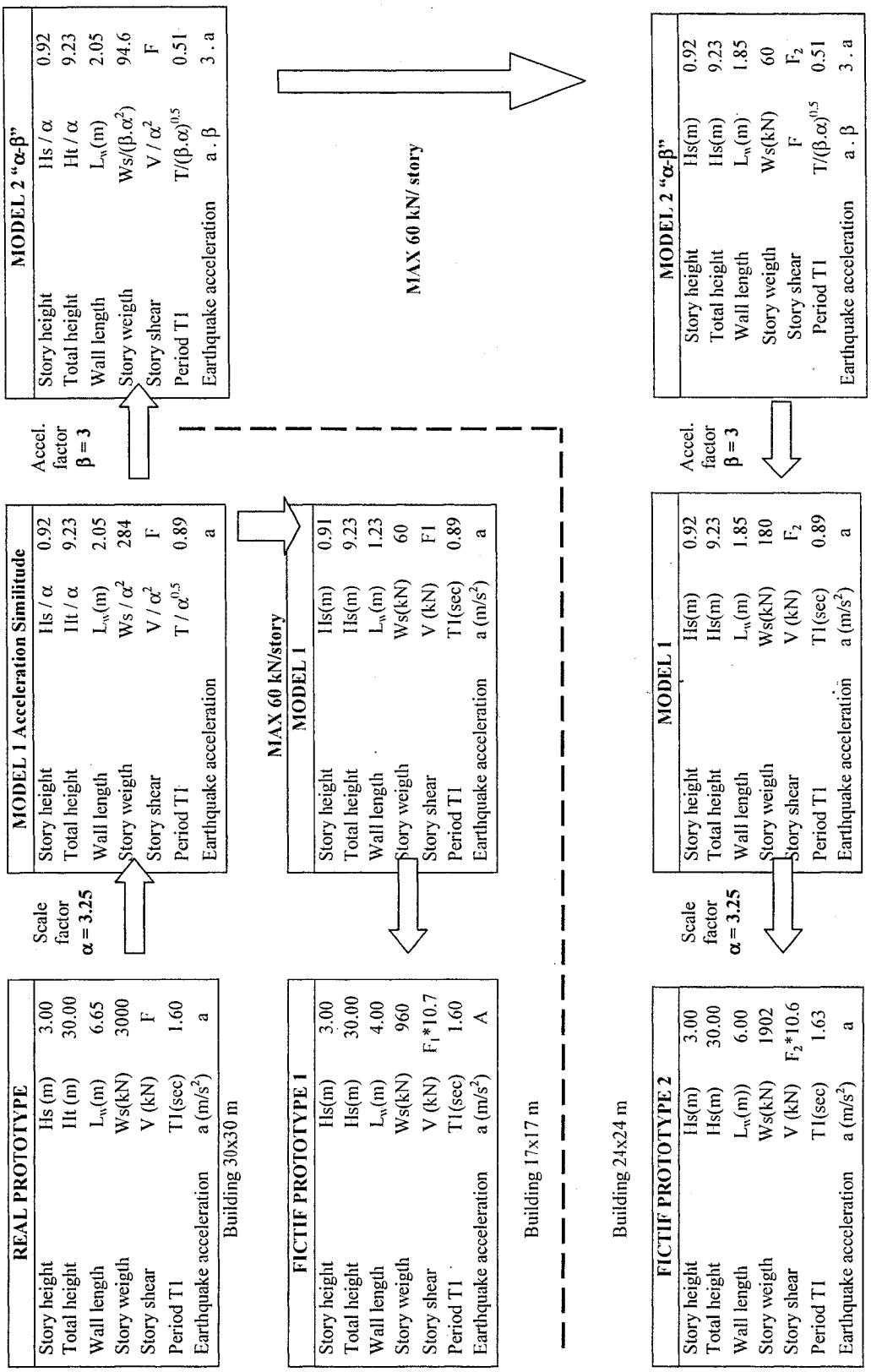

Appendix F

DESIGN OF THE SPECIMENS FOR SEISMIC TESTING OF SHEAR WALL STRUCTURES

F.1 Studied problem

To achieve a better understanding of the behaviour of shear wall buildings end to create a base for the future testing programme using an earthquake shaking table at Ecole Poletechnique a quasi-static testing programme was establish.

Objectives: The main aim of this work is to undertake an investigation of the seismic behavior of slender concrete shear wall in the non-linear range. Of particular interest are the shear resistance and the interaction of shear and flexion if the plastic hinge region

The first objective is to evaluate influence of the type of loading history. Two types of loading: monotonic and cyclic.

The second objective is to verify the proposed law of similitude for a scale factor $\alpha=2.37$: $F_m = F_p / \alpha_2$ and $\Delta_m = \Delta_p / \alpha$.

- Model validation;
- Analyses validation;
- Sophistication of numerical models;
- Calibration of the model for shaking table test program.

Methodology: The goals listed above will be achieved by testing four specimens: two with "real" geometrical sizes called "Prototype" and two "real replica" with scaled proportions – called "Model". First couple "Prototype – Model" will be subjected to monotonically increased controlled displacement, "Pushover", and the second – to cyclic increased control displacement.

F.2 Selection of wall to be studied

Original Wall

As it was discussed in Chapter 5 (Design of specimen for a shaking table test) a ductile cantilever shear wall from model building located in Vancouver was chosen for shaking table test. Because of that a ductile wall designed with $R_d = 3.5$ located in Vancouver was chosen for the quasi-static tests. Another reason is that for this type of wall it could be expected bigger inelastic demand and better behaviour at the ultimate state of loading (deformation).

Design of the wall was made using the Modal Response Spectrum Method as described in NBCC 2005 and CSA A23.3-04. The original wall, with dimensions L_w =7450 mm, b_w = 250mm and b_{col} = 450 mm, (in the building) was design with the dynamic forces and the existing axial forces from a dead load. As a result a concentrated reinforcement of 8-30M is needed in the columns, two curtains of distributed vertical reinforcement of 10M at 300 mm in the web and 10M at 150mm as a shear reinforcement which results in 96.9% shear utilization.

Choice of wall for quasi-static test program

Studied Wall

Because in the test program the axial force from gravity loads won't be in order to have the same behaviour, a wall similar to this but with slightly different geometry was chosen. The dimensions, L_w =7450mm, b_w = 200mm and b_{col} = 600mm, were chosen to obtain the same natural period of vibration according to the effective properties described in CSA A23.3-04, keeping the same length of the wall.

Using equation 21-2: $\alpha_w = 0.6 + \frac{Ps}{f'_c A_g}$,

We obtain $\alpha_w = 0.6$

With this effective property $I_{eff} = 0.6\ I_g$, the first period of vibration was evaluated to 1.31 seconds, v/s 1.32 seconds of the original wall.

The obtained spectral values for base moment and shear, including 40% for torsional effects, *M=32561 kNm* and *V = 2076 kN*, are slightly bigger than those for the original wall. This difference is because of the slightly bigger rigidity of the new wall and is found acceptable (negligible).

Design for flexure

The "lost" flexural resistance from the axial load was balanced by adding an additional flexural reinforcement. The distributed vertical reinforcement was changed to 15M at 300 mm which will helps later for the scaling of the specimens. The new concentrated reinforcement is evaluated to 14-30M to have the same flexural resistance as the "Original Wall". It should be mentioned that because of lack of the axial load and the bigger quantity of the reinforcement the probable overstrength, γ_p equal 1.47, is bigger than in the original wall.

Design for shear

Design for shear was made applying the provision of Clause 21.6.9.3 and 11.3.4. For the calculation of the shear resistance the general method was used. The values of ε_x was calculated by applying equation 11-13:

$$\varepsilon_x = \frac{M_f / d_v + V_f + 0.5N_f}{2E_s A_s}, \text{ where:}$$

for the values of M_f was used the probable moment and for V_f the shear corresponding of the development of the probable capacity of the section.

$$\varepsilon_x = \frac{48175/5.96 + 1.47 * 2076 + 0}{2 * (200 * 17800)}$$

The longitudinal strength at mid-depth was calculated to $\varepsilon_x = 1.57.10^{-3}$.

The value of β was determined from the following equation:

$$\beta = \frac{0.40}{(1+1500\varepsilon_x)} \frac{1300}{1000 + s_{ze}}, \text{ where } s_{ze} \text{ is equal to 300mm and the value of } b$$

was evaluated to 0.11. Applying Clause 21.9.6.3.b, and for inelastic rotational demand of 0.0074 the value of β for the calculation of V_c was found by interpolation to be 0.083.

$V_c = \phi_c \lambda \beta f'^{0.5}_c b_w d_v = 0.65*1.0*0.083*30^{0.5}*200*5960 = 352\ kN$

Calculation of V_s

$V_s = \phi_s A_v f_y d_v \cot\theta / s = 0.85 * 400 * 0.400 * 5960 * \cot 45^o / 300 = 2702\ kN$

The shear resistance V_r was determined to be 3054 kN by using 15M at 300 mm and the shear utilization was evaluated to be 99.9% of shear resistance.

As was mentioned previously a quasi-static set-up program would be conducted. This will helps us to reduce the height of the tested "real wall". In order to obtain the same efforts at the base of the wall, as in modal analysis, the position of application of the resultant lateral load was found by dividing the modal moment with modal shear force. The final height was calculated to be 15.68 m (= 32561 / 2076). It should be mentioned here that calculated in this manner is different from the height often assumed in the most common test programs where height for application of the resultant force is equal to *2/3* of the total height of the building (inverted triangular load), in this case 20.0m. In spite of that the wall is situated in west of Canada, in Vancouver, where the earthquakes have low predominant frequencies and the buildings respond mostly in their first mode of vibrations, the difference here is significant. For the same flexural capacity at the base of the wall the shear demand is 28% bigger in our case than the inverted triangular load pattern. The described procedure is illustrated if figure F.1.

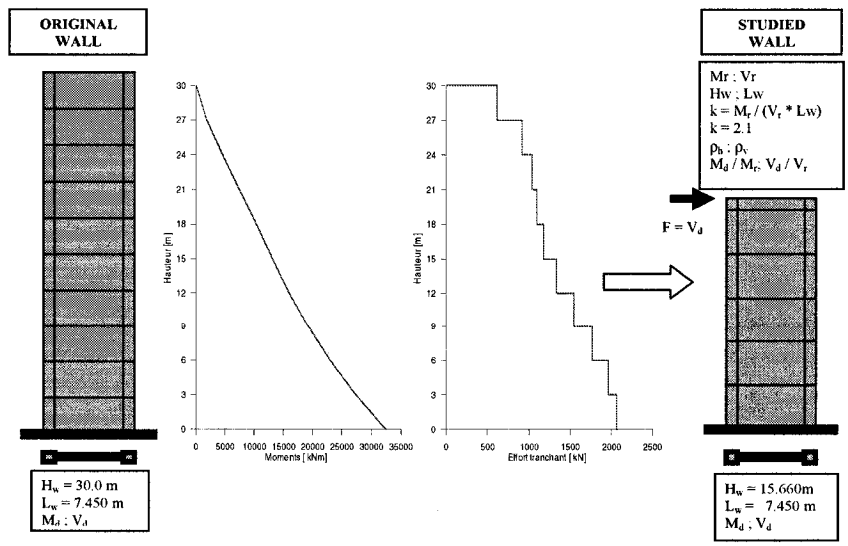

Figure F.1: "Studied" wall concept.

Test Specimens:

As it could be seen from the data above for the "Studied Wall" the geometry of the wall and the design resistance for flexure and shear require a huge amount of space, efforts complicated set-up and money. The geometrical limitations, the limits in the applied horizontal force and supports capacity needed a different solution. So, another rational engineering vision was found applicable and useful for our limited purposes.

The main conception could be resumed as follows: to find another shear wall which have smaller geometry properties and smaller flexural and shear resistances, but having at the same time the same flexural and shear behaviour as the "Original Wall" and "Studied Wall". A supplementary condition was imposed: the new wall, called "Prototype" should have the similar layout of shear and distributed vertical reinforcement, 15M at 300 mm for both reinforcements. The design properties for the "Prototype" are listed below:

- Same web thickness, 200 mm, and web reinforcement layout;
- The Prototype should have the similar ratios V_f / V_r, M_f / M_r, and the same nominal and probable flexural overstrength;
- To have the similar height to length ratio H_w / L_w.

Two different wall configurations were studied: a simple wall and a wall with columns. If the columns were added, their thickness would be at least 300 mm for a web of 200 mm. The shear deformations of the original, studied and prototype walls were compared to make the final form decision.

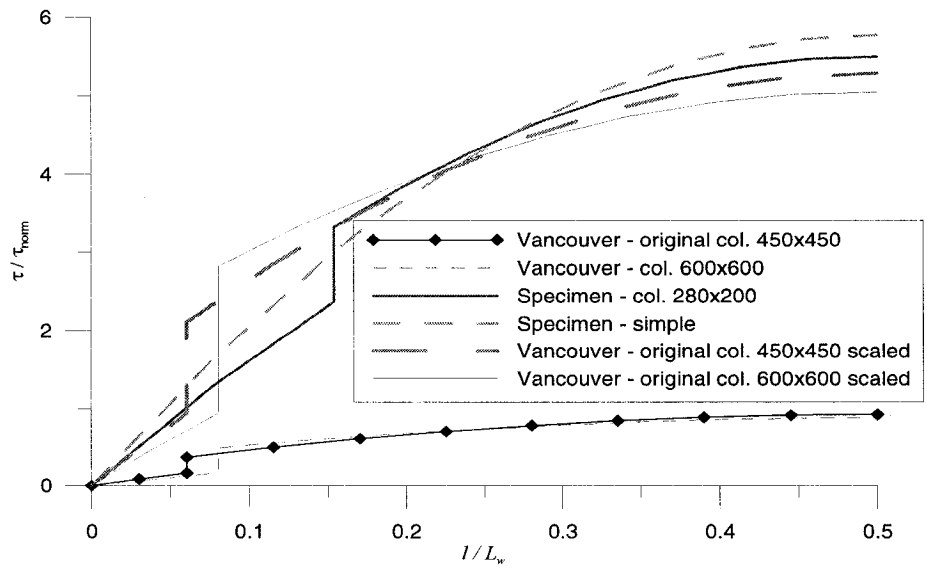

Figure F.2: Comparison between different wall configurations.

For the constructive reasons the "Prototype" needs to have at least three vertical bars which with horizontal reinforcement will form the web curtain reinforcement. This requirement leads to minimal length of 1200 to 1300 mm. Increasing the numbers of the vertical bars to four leads to bigger length, about 1500-1600 mm, which increase the moment capacity. For the same shear capacity this increases the height of the wall, which is undesirable. So it was decided to try a layout with three vertical bars and the length of the wall and amount of concentrated reinforcement will be found from the exigencies for M_f / M_r and V_f / V_r. Trying different lengths between 1200 mm to 1400 mm were used. Keeping in mind that the "Prototype" wall will be scaled using the similitude lows, specifically the similitude of the acceleration, (see chapter 6), the final proportions of both walls "Prototype" and "Model" would be obtained. The scaling procedure imposes a lot of constraints because of the limitation of the choice for a small deformed bar diameters at acceptable price. The smaller available bar is #3, a US designation, with diameter of 9.5mm and area of 71 mm^2. This impose the maximum scaling factor of 2-15M / #3, or $(400 / 71)^{0.5} = 2.34$. Using minimum of four bars for vertical reinforcement in the Model leads to 1600 mm for the concentrated reinforcement in the Prototype, or 2-25M and 2-20M, tied as a column. Applying the ratios for V_f / V_r, M_f / M_r, $M_f = H \times V_f$, H / L_w and the vertical and horizontal reinforcement describe above the final geometry

was found after few iterations comparing Studied, Prototype and Model wall, and using the method of "try and error".

The final length of the Prototype was found to be 1300 mm and the point for application of the force 2730 mm. The properties of the three walls are summarized in table F.1.

Property	Studied wall	Prototype wall	Model wall (scaled)
H	15680	2400	1030
L_w	7450	1300	548
H / L_w	**2.1**	**1.85**	**1.85**
M_f	32561	855	66.7
M_r	32664	856	66.8
M_f / M_r	**99.5%**	**99.9%**	**99.9%**
V_f	2067	357	61
V_r	3075	533	92
V_f / V_r	**67%**	**67%**	**67%**
M_n	38845	1019	79
M_p	48175	1262	98
γ_w	1.19	1.19	1.19
γ_p	1.47	1.47	1.47

Table F.1: Summary of the wall properties

The simple representation of the whole procedure is described on the figure F.3. It should the mentioned that this involves some iteration between the three walls.

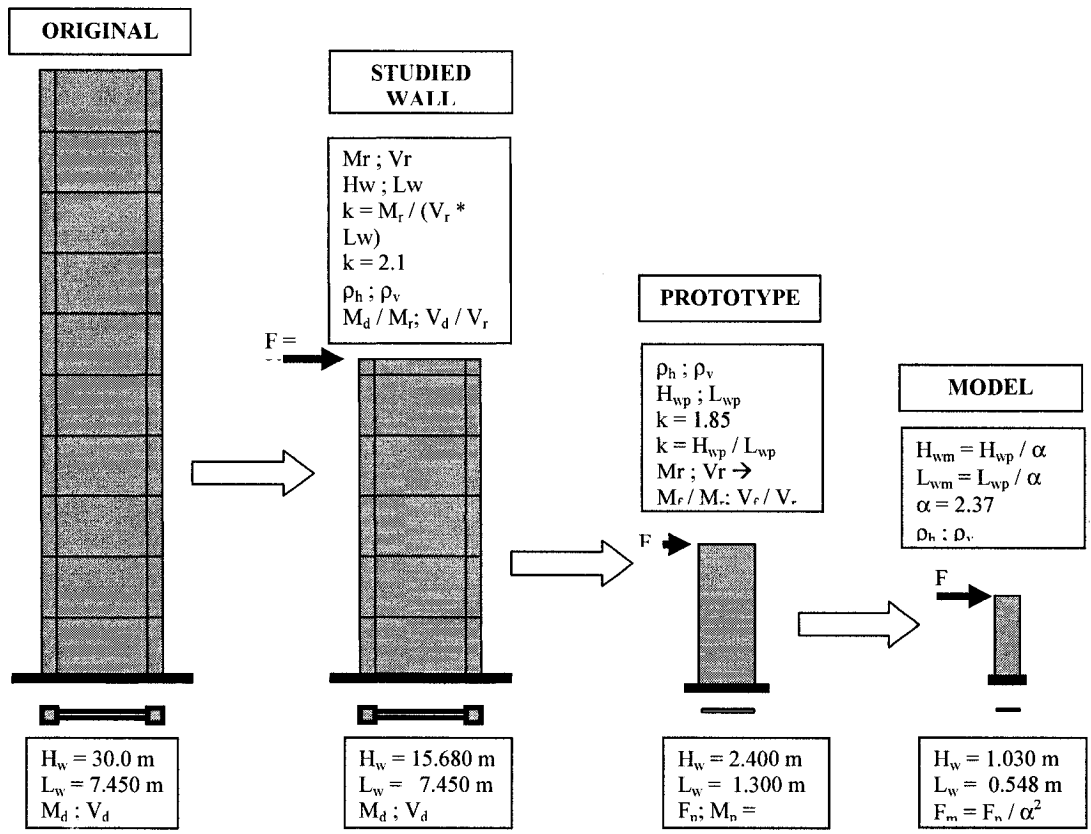

Figure F.3: "Prototype" and "Model" walls concept.

Validation of the proposed specimens

To validate the proposed specimens a complementary analysis were conducted using RESPONSE 2000. The member responses were compared using the nominal properties for the material behaviour. The three plots of Force – displacement at the top are plotted in figure F.4. The response quantities are normalized in order of comparison. As it could be seen in spite of huge geometrical difference between the "Studied" wall and the "Prototype", they both have very similar behaviour and the Prototype could successfully represent the earthquake behaviour of the "real" wall.

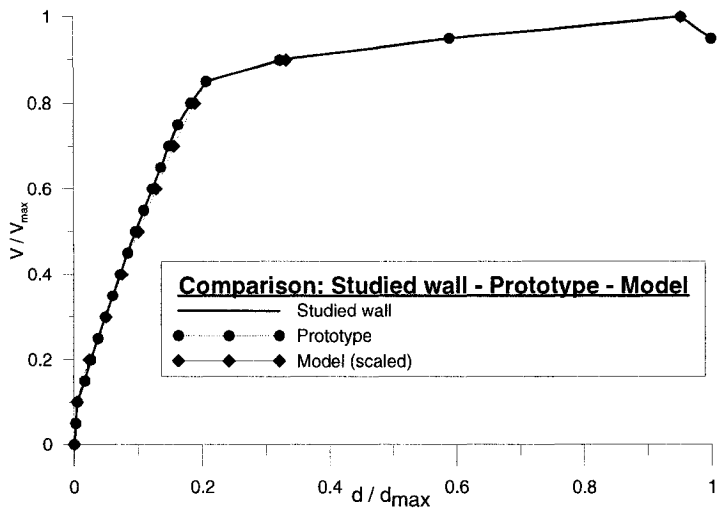

Figure F4: Normalized Force-displacement for Studied, Prototype and Model walls.

With the collaboration of Prof. Palermo, from the University of Ottawa, supplementary analyses were conducted. The results are presented in figures F.5 to F.8. in figure F.5 are presented the force-deformation responses of Prototype wall to monotonic and cyclic loading with different assumptions for numerical model of the base.

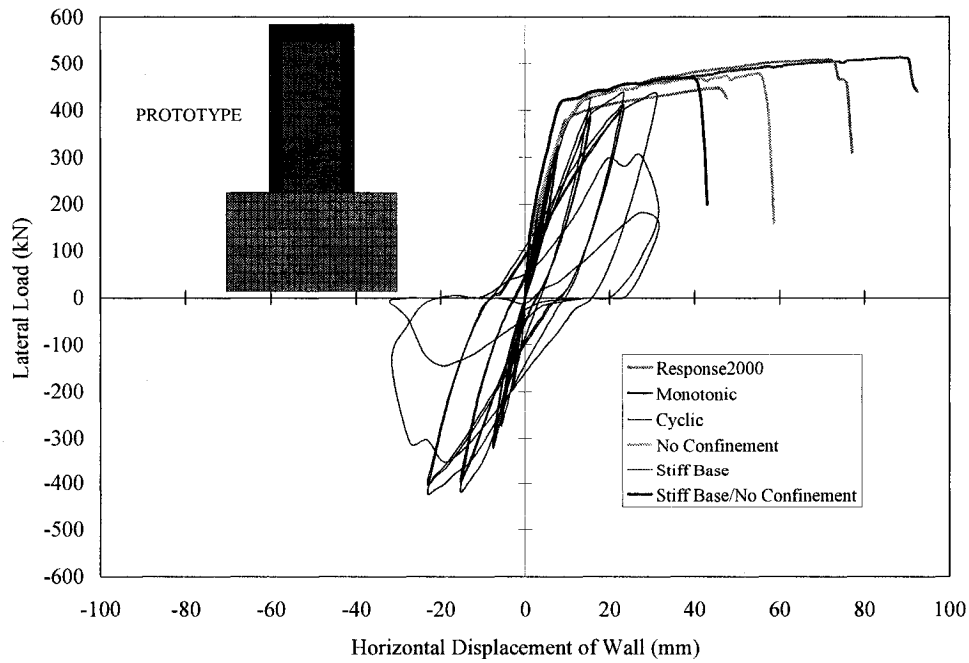

Figure F.5: Load-displacement response for Prototype wall

They are compared also to the Response 2000 results. The resulted crack patterns for monotonic and cyclic loading are presented in figure F.6.

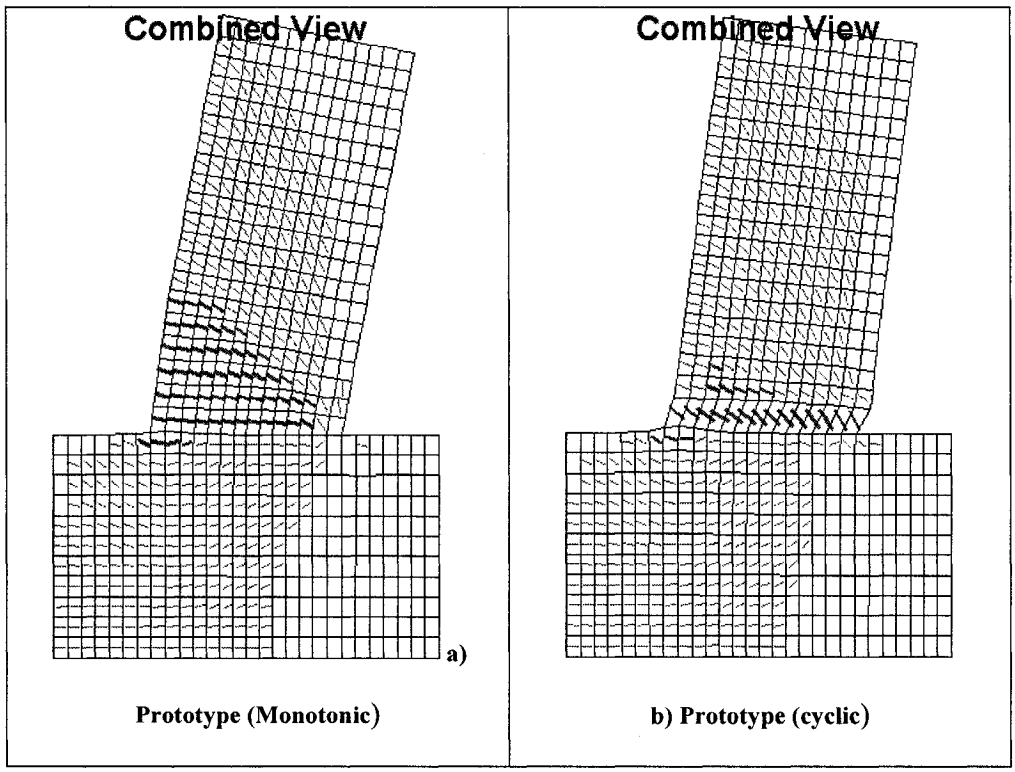

Figure F.6 Cracking pattern and displacements at the onset of failure for Prototype wall

The same analysis was conducted also for the model wall and very similar force-deformation curves and crack patterns were obtained, figures F.7 and F.8.

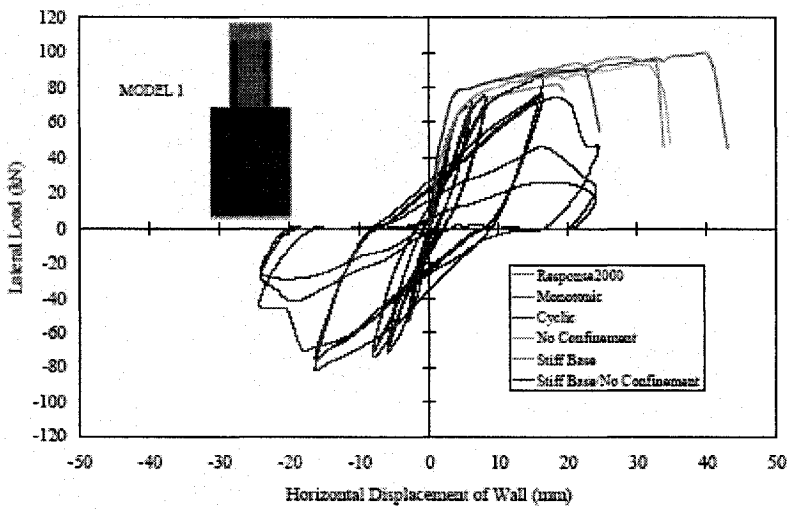

Figure F.7: Load-displacement response for Model wall

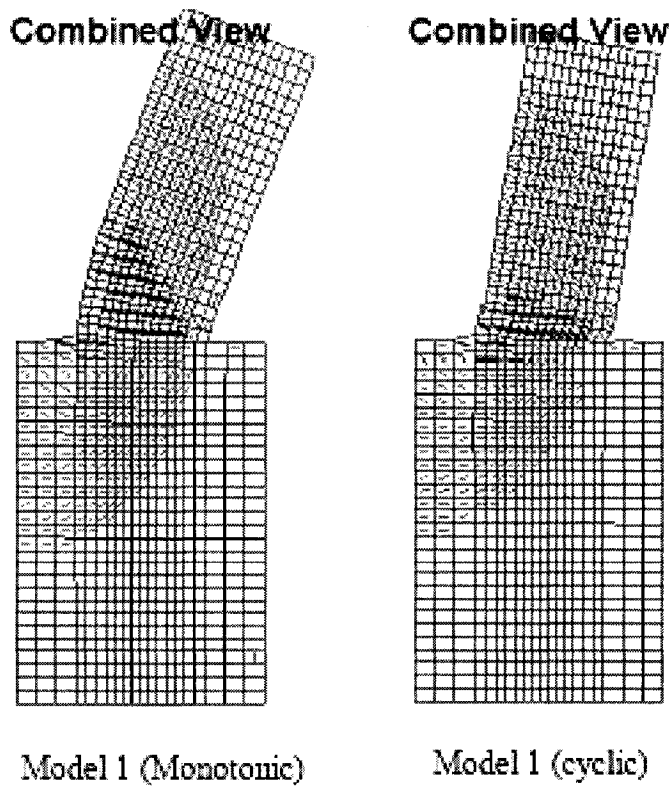

Figure F.8: Cracking pattern and displacements at the onset of failure for Model wall

The analytical result confirmed the reasonable expectations for the different behaviour of a ductile concrete shear wall under monotonic and cyclic loading. Two conclusions can be drawn:

- The obtained displacement ductility during a cyclic loading is smaller, about two times, than the one obtained during the monotonic pushover;
- The second and more interesting finding is the different failure modes for both types of loading. During the monotonic loading the wall fail in flexure with large cracks parallel to the base. Even the wall was designed as a ductile flexural RC shear wall during the cyclic loading it fails in sliding shear.

F.3 Alternatives of proposed specimens

As it is notted in Table F.1 the Proptotype wall is no exact replica of Studied wall. As it was explained we were looking for a similar behaviour, but not the exact replica. The Studied wall and Prototype have the same V_f / V_r, M_f / M_r, the same nominal and probable flexural overstrength, but not thee same height to length ratio H_w / L_w.

As an alternative to the propose prototype wall another Prototype wall or even Studied wall could be used. If we require the new prototype wall has the same M_f / M_r, the same nominal and probable flexural overstrength, and height to length ratio H_w / L_w a new V_f / V_r must be used. In this way we could either change the horizontal reinforcement ratio of the Prototype or either of the Studied wall. If we conserve the horizontal reinforcement in Prototype wall as 15M spaced at 300 mm, as a common construction practice, this requires, by employing backward calculation, changes in the Studied wall horizontal reinforcement.